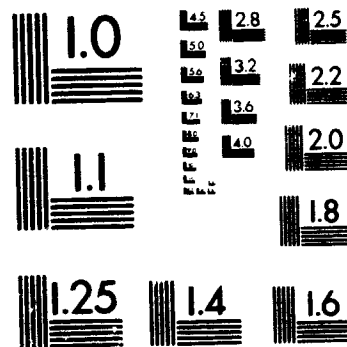


1 OF 2

N83-13065



MICROCOPY RESOLUTION TEST CHART
NATIONAL BUREAU OF STANDARDS
STANDARD REFERENCE MATERIAL 1010a
(ANSI and ISO TEST CHART No. 2)

NASA Contractor Report 166155

(NASA-CR-166155) PREDESIGN STUDY FOR A
MODERN 4-BLADED ROTOR FOR RSRA Final Report
(Sikorsky Aircraft, Stratford, Conn.) 176 p
HC A09/MF A01

N83-13065

CSCL 01C

Unclassified
G3/01 02039

Predesign Study For a Modern 4-Bladed Rotor For The RSRA



S. Jon Davis
SIKORSKY AIRCRAFT DIVISION
UNITED TECHNOLOGIES CORPORATION

CONTRACT NAS2 -10691
MARCH 1981

NASA

National
Aeronautics and
Space
Administration

PREFACE

This contract was managed by Mr. S. Jon Davis. The major technical contributors include:

T. Krauss, F. D'Anna, and R. Farley	-	Rotor Blade and Rotor Head Design
J. Kish, M. Raimondi	-	Transmission Design
R. Selleck	-	Blade Severance System
G. Sawyer, F. Carta (UTRC)	-	Instrumentation
R. Moffitt	-	Aerodynamic Analysis
C. Niebanck	-	Dynamics Analysis
R. Klingoff	-	Flight Controls and Stability and Control Analysis

Mr. Gerald Shockey was the NASA Technical Monitor for this contract.

PRECEDING PAGE BLANK NOT FILMED

TABLE OF CONTENTS

	<u>Page</u>
SUMMARY.....	1
INTRODUCTION.....	2
RESEARCH OBJECTIVE OVERVIEW.....	4
SELECTION OF ROTOR SYSTEM.....	8
ROTOR/RSRA INTEGRATION.....	11
Rotor Head Adaptation.....	11
Rotor Blade Adaptation.....	13
RSRA Transmission Modifications.....	15
Fuselage Vibration Level.....	17
Control Load Limits on Flight Envelope.....	18
Main Rotor Shaft Bending Load.....	19
Pitch-Flap/Lag Stability Analysis.....	19
Ground Resonance Stability Analysis.....	21
Coupled Rotor - Airframe Natural Frequencies.....	22
Stability and Control Considerations.....	25
PARAMETER CHANGE STUDIES.....	26
Airfoil Leading Edge Contour Modification for C_{LMAX} Enhancement.....	26
Blade Tip Modifications.....	27
Rotor Mast Height Variation for Study of Rotor-Body Interference	28
INSTRUMENTATION.....	29
Rotor Blade Pressure Instrumentation.....	29
Other Instrumentation.....	33
TECHNOLOGY PAY-OFF STUDIES.....	34
PROPOSED FLIGHT INVESTIGATION.....	38
DEVELOPMENT PLAN.....	42
Summary of Plan.....	42
Description of Work.....	42
Statement of Work.....	48
Work Breakdown Structure.....	52
Cost and Schedule Plan.....	58
DOCUMENTATION LIST.....	60
CONCLUSIONS	61

TABLE OF CONTENTS- (cont'd)

	<u>Page</u>
REFERENCES.....	62
TABLES.....	64
FIGURES.....	93
APPENDIX.....	160

SUMMARY

A predesign study was conducted to evaluate the feasibility of providing a modern four-bladed rotor for flight research testing on NASA's Rotor System Aircraft.

The objectives of the proposed tests are to acquire data (for correlation purposes) on the capabilities of a state-of-the-art rotor system and to quantify the contributions of key design parameters to these capabilities. Three candidate rotors were examined: the UH-60A BLACK HAWK rotor with and without root extenders and the H-3 Composite Blade rotor. It was concluded that the technical/cost objectives could best be accomplished using the basic BLACK HAWK rotor (i.e. without root extenders). Further, the availability of three existing sets of blade tip of varying design, together with a demonstrated capability for altering airfoil geometry should provide early research information on important design variables at reduced cost. For planning purpose it is estimated that the proposed rotor system could be available for testing in 24 months after authorization to proceed for a cost of \$6.098 million.

INTRODUCTION

The rotor Systems Research Aircraft (RSRA) provides a vehicle for filling the need for systematic experimental data on rotary wing systems. Validation of the technology base of current rotor systems and development of the experimental data base for extending their operating limitations is one of the most challenging technology problems facing the industry today. New rotary wing technology has developed at a faster pace than industry's ability to fully understand its fundamental foundations. In this respect, we are facing a technology gap between our efforts to improve existing flight hardware solutions and our knowledge of their detailed workings which will lead us to the next level of improvement. Although we depend heavily on analysis to bridge this gap, there are real limitations on analyses that can only be corrected by acquiring a strong parallel experimental data base. Once this data is obtained, methods can be correlated and designers can concentrate on evolving a new level of rotor technology. In addition to the need for baseline data, it is highly desirable that a test capability for varying important design parameters be available (at reasonable cost) to guide both future design and research efforts. Sikorsky believes that the adaptation of existing technology rotor hardware to the RSRA flight vehicle can significantly contribute to filling these needs.

The purpose of the study conducted was to define a new baseline rotor system providing a significant parametric capability. The focus was directed towards a cost effective design providing a balanced blend between the technology needs of the flight program and the cost of developing the hardware.

As part of the NASA program to provide and validate the helicopter rotor system technology required to improve the performance of current rotorcraft, a predesign study of a modern rotor for employment on the RSRA was initiated. For this study, an evaluation of three 4-bladed rotor system candidates was carried out. These were the:

- (1) Composite structure H-3 blades installed on a BLACK HAWK rotor head.
- (2) Standard BLACK HAWK blades and rotor head connected to an RSRA transmission with a modified gear ratio allowing operation at a higher tip speed.
- (3) Standard BLACK HAWK blades with radius extenders installed on a BLACK HAWK rotor head.

A comparison of the blade characteristics of candidates (1) and (2) is given in Table 1. Note that the blade characteristics of candidate (3) are identical to those of (2) except for the larger rotor radius obtained by the use of the extenders. Additional background technical information on these candidate systems is contained in the appendix. The final rotor system selection was based on a numerical score obtained by rating the candidates using six evaluation criteria, which were:

- (1) size suitability
- (2) technology level of baseline system
- (3) adaptability of rotor system to parametric changes
- (4) estimated costs for integration and parametric changes
- (5) integration hardware needs
- (6) future research capability

A rating of from one to five was assigned to each of the above categories for each rotor system. A rating of one indicated no major mission incompatibility or hardware development program required. A rating of five indicated major problems in either area. As shown in the rotor choice scoring chart, Table 2, the rotor system selected for further development as a replacement for the RSRA S-61 main rotor system is the BLACK HAWK rotor coupled to a modified RSRA transmission (configuration 2). This particular combination is the most suitable in terms of size, the most adaptable to parametric changes, costs the least to develop, and offers the greatest potential for future research capability.

After selection of the rotor system, detailed design investigations of the interface requirements of the rotor system and the RSRA were carried out. These were in the areas of:

- (1) Rotor head adaptation
- (2) Rotor blade adaptation
- (3) RSRA transmission modifications
- (4) Fuselage vibration level
- (5) Control load limits on flight envelope
- (6) Main rotor shaft bending loads
- (7) Rotor flap/lag pitch stability
- (8) Ground resonance
- (9) Coupled rotor/airframe natural frequencies

The performance and research capabilities of this rotor system were also defined in the areas of:

- (1) Instrumentation
- (2) Capability for rotor parametric configuration changes
- (3) Technology payoffs
- (4) Proposed flight investigations

The data thus obtained as a result of these investigations was then used to plan and estimate the cost and schedule of a proposed development/testing program for the RSRA/BLACK HAWK rotor system.

RESEARCH OBJECTIVE OVERVIEW

Selection and development of a replacement for the RSRA S-61 main rotor system will provide the helicopter industry with a strong technical data base that will guide advance rotor programs in the future. Successful completion of the project, however, requires careful attention to low cost hardware application tasks as well as astute definition of the specific research goals. With this in mind, Sikorsky has formulated a series of questions that formed the framework of the study conducted.

- . Are existing advanced 4-bladed rotor systems available which are properly sized for RSRA application and reflect current state-of-the-art design practices?

Yes, Sikorsky has two fully developed rotor systems which fill these needs. The BLACK HAWK rotor 16.36m (53.66 ft. diameter) and the H-3 composite blades 18.9m (62 ft. diameter) reflect state-of-the-art aerodynamics and dynamic technology. Each employs high non-linear twist distribution, second generation airfoils and swept tip technology. A third rotor variant is possible by using in-board extenders to increase the radius of the BLACK HAWK rotor blades. Photographs of the BLACK HAWK blade and the H-3 composite blade are shown in Figure 1. The primary design parameters of these rotor systems and the current S-61 rotor are contrasted in Table (1). A more complete technical description of the BLACK HAWK and H-3 composite rotor blades is provided in the appendix.

- . Why is there interest in acquiring a large experimental data base on an existing rotor system which has been previously tested?

Conventional rotor test techniques are designed to surface and correct developmental problems and seldom provide the type of systematic and detailed data required to validate the rotor technology base for research purposes. Data acquired with an advanced rotor configured RSRA should provide industry with sufficient performance, dynamic, acoustic, and handling quality data to define the mechanisms which constrain current operating limits. These limits, while identified in conventional flight test programs, are seldom examined in sufficient detail to understand fully the governing factors. As an example, rotor flight envelopes are often limited by an unacceptable build-up of control system vibratory loads. While the basic contributory mechanism of retreating blade stall is well known, detailed stall

processes are not fully understood. The basic stall mechanism is also influenced by such factors as contour quality control, blade dynamic response and loads associated with use of high blade twist rates, and periodic blade stall induced by local body and wake flow interference effects. It was the intent of this study to evaluate the suitability of available hardware within the context of a rotor research program sufficient in scope to allow investigations to examine in detail the factors contributing to various technical areas of interest. Once these factors are understood, new techniques can be developed to control the problem areas and permit further expansion of flight envelopes.

Why is it vital that the selected rotor system embody state-of-the-art technology?

Each new generation rotor system builds on the technical data base established by its predecessors. Since the primary intent of the established project is to aid the development of future rotor improvements, it is crucial that we solidify a data base that includes most, if not all, the emerging rotor technologies. If the needed experimental data base is not developed, advancement in that area will be impeded. A good example of this point is the development of advanced swept tip technology. Existing experimental data and analytical studies strongly indicate that use of swept tip rotor blades improves high speed rotor performance, improves blade dynamic stability, and reduces rotor acoustic detectability. Despite these known benefits, and their use on production aircraft, development of improved swept tip configuration is hampered by the lack of detailed knowledge of the 3-D lift environment at the blade tip. Inclusion of swept tips in the RSRA flight program would remove this obstacle. Likewise, exclusion of that technology would certainly extend the timetable for production use of more optimum second generation swept tips.

What will be the general objective of the planned research flight program?

Understanding the individual impact of rotor design parameters as they relate to performance, acoustic, vibration, and stability and control guides the overall program. Current rotor design practices have progressed to the point where each individual rotor design parameter, such as airfoil selection, must be evaluated in terms of its effect on all rotor operating characteristics. As a result of these multiple design goals, it is becoming increasingly difficult to find the best blend of the rotor design variables for a given mission. This task is being further compounded by emerging new technologies such as swept or anhedral tips and spanwise blade tailoring which greatly increase the designers options. The proposed study will systematically identify the hardware requirements which are necessary to eval-

uate the impact of specific rotor design technologies on the individual rotor characteristics.

Since the possible research areas are numerous goals need to be prioritized. Sikorsky selected the following rotor design parameters for evaluation in the technical development plan for the RSRA replacement rotor system.

- . Inboard airfoil $C_{L\max}$
- . Tip airfoil drag divergence
- . Blade tip sweep
- . Blade tip taper
- . Rotor tip speed
- . Rotor mast height

Can a low cost flight test program with high technical merit be fashioned from existing hardware?

Yes, the flight tested BLACK HAWK rotor systems, together with existing add-on hardware and inexpensive modifications form an excellent base for a low cost program. With little additional cost tip geometry, airfoil, and rotor-body interference effects can be studied.

A possible research program using the BLACK HAWK to attain specific research objectives is illustrated in Table 3. This provides brief insight into current hardware possibilities.

Why is blade airfoil change capability important?

Rotor flight envelope limitations are always affected, and often defined, by the build-up of adverse airfoil aerodynamic behavior at extreme operating conditions. When high advance ratio and/or high lift conditions are encountered, retreating blade stall and advancing side compressibility effects cause performance deterioration and excessive vibratory loads. Determining the impact of practical airfoil modification on these limits should be a high priority goal of the flight research project.

Two types of airfoil contour modifications should be considered. These are camber increases to elevate maximum airfoil lift capability and thin tip airfoil contours designed to retard advancing tip compressibility drag rise. Although existing rotor airfoil design studies have shown that increasing the airfoil $C_{L\max}$ and drag divergence Mach number simultaneously is not feasible, Sikorsky studies indicate that proper radial placement of separate high lift and transonic flow airfoils can effectively improve blade behavior on both the advancing and retreating sides. This concept is illustrated in Figure (2) which shows advancing and retreating side profile power loss distributions

for a full span high lift airfoil (SC1095-R8), a full span low compressibility drag airfoil (SC1095), and a blade employing the SC1095-R8 over the inner 85% of the blade radius and a SC1095 over the outer 15%.

The blade configuration combining the two airfoils retains the advancing side tip region drag reductions associated with the SC1095, but does not suffer corresponding retreating side penalties since the maximum lift requirement occurs in-board of the .85 radial station. Conversely the high lift SC1095-R8 airfoil does not experience high advancing side drag since the Mach number and angles of attack in-board of .85 radius do not exceed the SC1095-R8 drag divergence envelope.

In addition to assessing the effect of airfoil modifications on performance and blade dynamics, acquisition of companion acoustic data is also needed. Dramatic improvements in rotor acoustic "signatures" have been noted when stall tendencies are reduced and advancing side compressibility is reduced. Qualification of these gains will help identify low rotor noise technology required for the next generation of civil transport helicopters.

Why is blade tip design important?

There is much data that indicate the ability of blade tip design variables to influence many rotor attributes including performance, noise and vibratory load. Unfortunately detailed understanding of the complex aerodynamics in the rotor tip area is lacking and tip designs are by no means optimized. Added impetus to achieving such understanding has resulted from the new civil noise standards being proposed that will play an important role in the design of future commercial helicopters. As a result, technology must be validated that lowers the rotor noise signature without degrading other aspects of the aerodynamic and dynamic behavior. Existing experimental data indicates that both tip sweep, tip taper and thin tips are qualitatively effective. Quantitative data, however, is needed that will identify the noise savings over an extensive flight envelope and indicate associated changes in the main rotor flight characteristics. Figures (3) through (5) indicate three existing tip configurations which can be applied to a BLACK HAWK main rotor for this purpose.

The swept tip is the baseline configuration, while the double swept and double swept anhedral variants are new designs which to date have not been tested full scale.

Why is tip speed an important design variable?

Rotor tip speed variations allow the tradeoffs between the advancing and retreating blades to be studies so that the stall and compressibility limits for each area of the rotor can be defined. It is important that the baseline tip speed be properly selected so that a reasonable flight envelope is available for the study.

Does the current understanding of rotor-body interference effects warrant inclusion of rotor-mast height variation in the rotor system definition study?

Although previous analytic and experimental studies have identified high levels of fuselage vibratory excitation to be the result of fuselage flow interference, a detailed experimental data base is lacking. Data needs to be obtained that clearly indicates the flow interference effects on blade pressures. These results can then be used to correlate and improve analytic models of this complex interaction.

What concerns should dictate instrumentation requirements?

Data should be provided that measures the airload and dynamic rotor responses. Since correlation of existing analysis is an important step towards improving future designs, instrumentation planning should consider both response and greater understanding blade airload measurements to allow a cause and effect.

SELECTION OF ROTOR SYSTEM

Size Suitability

Hover performance (out of ground effect) for the three rotor configurations was calculated using Sikorsky Aircraft's CCHAP program. Maximum thrust available for hover was assumed to equal the thrust output of the main rotor at the power saturation limit of the RSRA transmission (2500 HP at 203 RPM), minus tail rotor, transmission, and system losses. Rotor size suitability for the three candidate configurations was evaluated in terms of hover capability. The hover criteria reflects the sensitivity of hover performance to rotor size and the fact that the high speed flight capability of the three rotor systems are equivalent. A comparison of high speed flight performance is presented separately under research capability.

Table (4) summarizes OGE and IGE maximum TOGW's for each configuration on a sea level standard day. The IGE condition corresponds to a 10 ft. hover wheel height. As noted, the standard BLACK HAWK configuration has less hover capability than the two larger rotors. This is due to the associated increase in disc loading. Despite this, the BLACK

HAWK rotor can initiate a mission with an OGE hover while carrying 200 lb of instrumentation and 1700 lb of fuel. Use of a 10 ft. wheel height IGE hover criteria increases the available fuel load to 3400 lb. This is clearly in excess of normal helicopter mode mission requirements.

Based on the OGE and IGE evaluation summarized in Table (4), the size suitability of the H-3 composite and extended BLACK HAWK blades were assigned a rating of 1 (no problems), while the standard BLACK HAWK rotor was assigned a 3 (adequate).

Table (5) illustrates RSRA research mission capability with a BLACK HAWK rotor and a 1.52m (5 ft.) wheel height hover take-off. The BLACK HAWK configuration is used in the illustrated mission since it has the more limited hover capability. The indicated mission radius of 2244km (139 mi) is again more than adequate and exceeds current RSRA flight practices. In practice, a BLACK HAWK rotor equipped RSRA would probably carry less fuel and transition to forward flight at a higher IGE wheel height.

Technology Level of Baseline

The technology level of all three rotor system configurations is of the same vintage. Table 1 provides a comparison of the BLACK HAWK and composite H-3 blades to the earlier technology S-61 rotor presently employed on the RSRA. Note that both the BLACK HAWK and composite H-3 blades employ the same high non-linear twist distribution and chord. Both utilize second generation airfoil sections (the SC-1095 on configuration 1 and the SC-1095 and 1095-R8 on configurations 2 and 3) and swept tip technology. Both utilize new technology blade construction techniques.

Adaptability of Rotor to Parametric Changes

The rotor system selected must be capable of easily being modified to test various parametric changes of a given rotor design. Areas of investigation which require this capability include:

- (1) the effect of airfoil contour changes on $C_{L_{MAX}}$
- (2) the effect of rotor tip geometry on rotor performance dynamic and acoustic characteristics.
- (3) the effect of rotor mast height on rotor/body interference.

Item (3) is common to all three rotor configurations. Thus its inclusion does not influence the selection of the rotor system. Table 6 illustrates the test objectives and the manner in which the various rotor configurations meet them. It can be summarized as follows:

- (1) The standard BLACK HAWK rotor coupled to a revised RSRA transmission (configuration 2) or with radius extenders and no changes to the transmission (configuration 3) can be modified to use the following already existing blade tips.

- (a) a tapered swept tip
 - (b) a tapered swept anhedral tip

Figures 3, 4, and 5, illustrate both these tips and the standard BLACK HAWK tip.

- (2) The standard BLACK HAWK rotor blade can be modified to incorporate airfoil contour changes simply by bonding a new leading edge to the blade.
- (3) The composite H-3 rotor requires fabrication of interchangeable tip fittings before the existing rotor tips can be used, requiring considerable design work.

Estimated Costs for Integration and Parametric Changes

Configuration (2), the standard BLACK HAWK rotor with a modified RSRA transmission is the lowest cost option. This can be seen from the summary of estimated costs contained in Table 7. The most costly option is seen to be the standard BLACK HAWK rotor fitted with radius extenders. The reason for this is the need to invest a considerable amount of effort in the design of the extenders themselves, plus tooling, fatigue testing, and design support. Likewise the composite H-3 rotor requires a considerable investment in effort to design and fatigue test root end fittings which adapt the blades to fit the BLACK HAWK hub. In addition, in order to meet the requirements for adaptability to parametric changes, added work must be done to produce interchangeable tip fittings which allow use of the already existing BLACK HAWK rotor tip configurations. The standard BLACK HAWK rotor with the revised RSRA transmission, on the other hand, requires no additional work to make it adaptable to parametric changes. In fact, the actual changes required to modify the RSRA transmission for operation at the higher RPM are small and relatively low cost, necessitating only a redesigned sun gear, pinions, and the use of assorted already existing parts.

Integration Hardware Needs

The integration hardware needs, above and beyond the common requirements for the integration of the BLACK HAWK rotor head with the RSRA transmission are approximately equal for configurations (1) and (2) and considerably more for (3). This reflects the fact that the fabrication and testing of blade radius extenders requires a considerable investment in resources compared to a revised transmission or fabrication of root end fittings for the composite H-3 blades.

Future Research Capability

In order to assess the performance capability of the various rotor system candidates, their flight performance was calculated using Sikorsky Aircraft's Forward Flight Data Bank (FFDB) analysis. Figure 6 provides a comparison showing the degree of correlation of this analysis to actual RSRA flight performance data.

The results shown in Table 8 show that all three configurations can attain higher power limited forward flight speeds than the S-61 rotor configured RSRA. Differences in the forward flight speed capabilities of the three candidates, however, are not considered to be significant.

ROTOR/RSRA INTEGRATION

The proposed BLACK HAWK rotor can be readily adapted to the RSRA. The following summarizes the new and relocated RSRA parts required.

1. New shaft adapter (Figure 7)
2. New stationary swashplate (Figure 7)
3. New rotating pitch control links (Figure 7)
4. New rotating scissor lower link (Figure 7)
5. RSRA spherical bearing raised 8.26cm (3.25 inches) (Figure 7)
6. Modified planetary stage of transmission (Figure 12)

Modifications to the existing blade severance system are also required as discussed in a subsequent section.

Rotor Head Adaptation

General

The modification of the RSRA to accept the proposed BLACK HAWK four-bladed rotor head incorporates a minimum of new components. Allowance has been made to match the amount of blade pitch presently available on the BLACK HAWK. The hub is mounted to the main rotor shaft through

a shaft extension which acts as an adapter to the S-61 shaft, and raises the rotor plane six inches above that of the baseline RSRA rotor. The swashplate assembly consists of a BLACK HAWK rotating swashplate and duplex bearing in conjunction with a new stationary swashplate and an S-61 spherical bearing. The proposed installation is shown in Figure (7).

Shaft Extension

The present BLACK HAWK hub design is readily adaptable to this objective because it is not an integral part of the main rotor shaft, but rather attaches to an intermediate shaft extension that allows the rotor head to be lowered for transportability of the BLACK HAWK vehicle. Therefore to mount this hub on a different shaft requires only a new shaft extension. The outside of the extension fits to the hub, while the inside is designed to fit the S-61 shaft. Since this shaft is similar in size to the BLACK HAWK shaft, the same wall thicknesses are incorporated into the new extension design. The extension provides clearance between the blade root end and the main rotor pylon fairing by raising the rotor plane six inches.

Swashplate Assembly

The new swashplate design introduces a slight amount of collective/cyclic coupling due to a 8.26 cm (3.250 inch) vertical offset between rotating and stationary swashplates. This offset is necessary because the RSRA servo input to the stationary swashplate is located at a 40.01 cm (15.75 inch) radius, and the BLACK HAWK pitch control rod location is at a 44.2 cm (17.40 inch) radius. These two dimensions would cause interference between the rotating and stationary controls in an in-plane swashplate design. The vertical offset eliminates this interference.

The rotor head control system, shown schematically in Figure (8), provides a negligible collective/cyclic coupling of .01 degrees per degree. This coupling is not expected to have a noticeable affect on handling qualities of the aircraft.

The swashplate assembly is designed primarily from existing parts except for the stationary swashplate. The S-61 spherical bearing is raised 8.26 cm (3.25 inches) to be in-plane with the rotating swashplate. The S-61 swashplate guide is used with a spacer installed to the upper transmission housing.

The location of the swashplate is dictated by the existing range travel provided by the servo/actuator system. The limiting factor is the forward servo which has the smallest range. The stationary swashplate is positioned such that the desired collective and cyclic range is centered within the forward actuator stroke.

The distance between the rotor plane and the rotating swashplate at high collective establishes the nominal length of the pitch control rod. The horn to control rod pick-up point is .203 cm (.080 inches) above the rotor plane for the blade to be in the high collective position. Adjustment of the control rod length is made upon final installation.

Rotor Blade Adaptation

General

Initially, it was planned to use the original set of four prototype BLACK HAWK blades for this program. A decision has been made, however - and will be discussed in more detail in a later section, to fully pressure tap a rotor blade for the proposed research program. The modifications required to the blade to do this are extensive enough to be more easily carried out using current production BLACK HAWK blades. Therefore, in order to avoid possible complications in blade balance and tracking which could result from using one current production blade (pressure tapped) in combination with three prototype BLACK HAWK blades, four current production BLACK HAWK blades will be acquired for the basic rotor and one additional current production blade will be modified for pressure taps. All costs and schedules will be estimated on this basis. Furthermore, it should be noted here that all of these blades (including the pressure tapped one) are capable of having their profile contours modified by the bonding on of leading edge shape modifications, as also discussed in a later section.

Rotor Blade Severance

The proposed modification to the blade jettison system for the 4-bladed BLACK HAWK rotor system significantly reduces the complexity of the pyrotechnic system, particularly with respect to the rotary transfer unit (RTU) that controls the sequencing and direction of rotor blade jettison from the aircraft. Only two cam thrusters and four firing pin assemblies achieve a fully redundant system (See Figure (9)) and provides sequential jettison of opposing blade pairs, laterally from the aircraft. Additionally, sequencers are unnecessary for the proposed system since the possibility of single blade imbalance (a potential blade jettison condition with the baseline 5-bladed system without sequencers) is avoided with a 4-blade jettison system. Figure (10) shows a layout drawing of the lower portion of the main rotor drive shaft and the placement of the elements of the rotary transfer unit.

Referring to Figure (10), the following changes are required in the rotary transfer unit and rotor shaft to effect change to the 4-bladed system.

Reduce number of cam thrusters from 5 to 2.

Reduce number of firing pin assemblies from 10 to 4.

Remove both sequencer assemblies.

Replace stationary plate with plate with new hole pattern.

Replace rotating plate with plate with new hole pattern.

Replace upper and lower housings.

Replace shaft extension.

Shim instrumentation plate, as required.

Reduce inert manifolds accordingly.

Plug unused holes in lower shaft manifold.

Reduce shaft shielded mild detonating cord (SMDC) lines from 10 to 4.

The cam thrusters in the rotary transfer unit are relocated to accommodate blade lag position and provide clearance of the blade over the tail cone with the tail empennage during jettison. Although eleven degrees is shown in Figure (10), this location will be reviewed during the design phase with respect to the maximum lag excursion possible using the BLACK HAWK four-bladed rotor. The 182 degree differential between opposing cam thrusters will be incorporated to effect initiation of the opposed firing pin assemblies within the same rotor rotation, thus increasing system reliability.

Figure (11), shows a layout of the pyrotechnic hardware at the rotor head area. Although the upper shaft manifold can be retained, its location will be changed to accommodate the new rotor configuration. This change will necessitate change in length only of the shaft SMDC lines.

The pyrotechnic configuration shown in Figure (11), includes 4-port manifolds for interconnect of the opposing blade severance assemblies. The reliability of the configuration shown, that employs the fourth port for crossover interconnect, will be evaluated during design against the use of three port inert manifolds and crossovers incorporated closer to the blade severance assemblies (BSA's) using additional 3-port manifolds.

Since the articulation characteristics of the BLACK HAWK rotor are similar to the baseline RSRA rotor system, re-qualification of the flexible confined detonating cord (FCDC) lines to meet the flexure requirements is unnecessary.

Development of a new blade severence assembly is the most significant change in the blade jettison system for the BLACK HAWK rotor. In the manner of the present RSRA BSA configuration, the new blade severing device consists of upper and lower halves containing chevron-shaped linear-shaped charges to sever the .15 inch thick titanium spar. However, the linear-shaped charge of the new BSA is significantly reduced in comparison with the present BSA that employ a 125 grain per foot linear-shaped charge to cut the thick aluminum blade spar. Prior titanium cutting tests conducted by Teledyne McCormick Selph indicate that reliable severance can be achieved with a linear-shaped charge of less than 100 grains per foot. Cutting charge sizing trials will be conducted early in the design phase using titanium spar sections. In addition, the reduced cutting charge requirement provides an opportunity to examine other linear-shaped charge materials that do not exhibit high temperature out-gassing, a potential characteristic of the lead CH-6 presently used in the BSA of the baseline rotor. Alternative materials and their resulting increase in charge size will be determined early in the design phase.

The application of a 4-bladed rotor on the RSRA provides a significant advantage to the overall emergency escape system beyond the reliability improvement gained from system simplification. Sequenced crew extraction coupled with sequenced (3-blade/2-blade) blade jettison of the baseline rotor system results in a minimum altitude operational restriction of over 200 feet above ground level. Due to the balanced, 2-blade/2-blade sequenced blade jettison of a 4-bladed rotor, the aircraft remains stable in pitch and roll, avoiding the lateral redirection of the crewman extracted last and thereby, eliminates the altitude restriction of the baseline system. The proposed changes to the pyrotechnic system for the four blade rotor system require requalification testing of the new BSA that includes developmental tests to select the most appropriate linear-shaped charge material and establish the required charge size to effect reliable spar severance.

Since no new pyrotechnic devices other than the BSA are required, only functional testing of the RTU to verify correct system operation and lot acceptance testing will be performed.

RSRA Transmission Modifications

General

The main gearbox of the RSRA aircraft is, basically, a S6135-22000-041 gearbox that transmits torque from two (G.E.) T-55-8 engines to the main rotor, tail rotor, and accessory section. An input engine speed of 18,966 rpm is reduced through a first stage spur gear reduction to 8,100 rpm. Power is then transmitted to the accessory section and through an over-running clutch to a helical gear second stage reduction which combines the power from the two engines into a single bevel pinion shaft operating at 3,195 rpm. The third stage bevel gear mesh

has a 3.4 to 1 reduction and supplies power to the tail rotor drive and accessory section located in the gearbox rear cover section, and to the planetary reduction stage. A 4.6296 to 1 reduction is accomplished in the planetary through a sun gear input and five planetary pinions reacting against a stationary ring gear to drive the main rotor shaft at 203 rpm.

Modifications

The proposed modification of the RSRA transmission to provide a higher output RPM (increased from 203 to 257 RPM) for the selected rotor system incorporates a minimum of new components. This is accomplished by a redesign of the planetary reduction stage to obtain a 3.6468 to 1 reduction ratio. Since the planetary is the last stage of gearing in the gearbox, all gears located between the engine input and planetary system remain unchanged. The power and torque ratings for these components also remain unchanged. Thus the accessories and tail drive systems do not require redesign with this approach.

In the planetary itself, the ring gear for the increased ratio system is the same as the ring gear for the conventional RSRA planetary having a diametrical pitch of 8 and 196 teeth. The ring gear is usually the most expensive component in a planetary to manufacture thus a cost savings is realized since the same ring gear is used. Since the ring gear is also a structural member which connects the open transmission cover to the main housing, these parts also remain unaffected. The connection between the upper planetary plate and the main rotor shaft is also the same thus the production RSRA main rotor shaft remains unchanged. New planetary components required include the sun gears, planet pinion, planetary bearings, bearing shafts, bearing shaft nuts, and upper and lower planetary plates. The plates have been designed in steel for cost savings. Minor modifications are required to redirect lubrication jets.

Table 9 lists the basic planetary stage data and provides a comparison between the proposed modification and the standard RSRA transmission. Figure (12) is a cross section of this section. Table 10 provides a weight comparison between the proposed and standard transmission. Note that the proposed transmission is slightly lighter, even though steel planetary plates are employed versus titanium planetary plates in the standard RSRA planetary.

Alternate Output RPMS

A wide range of output speeds is attainable simply by modification of this gear reduction stage. Table 11 lists these other possible gear ratios and the resulting output RPM's.

Fuselage Vibration Level

There are three approaches available to control n/rev vibration on the RSRA with the BLACK HAWK rotor installed. They are (1) a rotorhead bifilar absorber tuned to 3/rev, (2) the active isolation system (tuned appropriately to treat the required frequency range), and (3) a combination of the active isolation system and the bifilar. This third vibration control configuration would only be considered if the flight vibration with either options (1) or (2) was unacceptable. Vibration projections for the RSRA/BLACK HAWK rotor are acceptable based on available RSRA test data with the active isolation system installed or with the 3P bifilar alone.

Figure 13 presents vibration levels in the RSRA cockpit for the S-61 rotor with the active isolator functioning and locked out. These data have been taken from Reference 1. The only component of vibration which is significant is in the vertical direction and the isolation system provides 70% attenuation to a maximum level of about .15 g's. Since the BLACK HAWK rotor n/rev frequency is 17.2 Hz which is very close to the 17.6 Hz value for the S-61 (@104%N_R) the effectiveness of the isolation system as it is presently tuned can be expected to be equivalent. There may be a slight increase in hub loads because the contributing rotating system harmonics are one order lower (i.e., 3, 4, and 5/rev for the 4 bladed BLACK HAWK rotor versus 4, 5, and 6/rev for the 5 bladed S-61 rotor). This is not expected to increase vibration levels by more than 20%, however. For low RPM testing the isolation system may be retuned (by changing air pressure in the accumulators) to improve the vibration environment. Figure 14 shows flight data from the RSRA/S-61 configuration which suggests that a more optimum tuning may be desirable at lower rotor speeds.

The effectiveness of a rotorhead bifilar absorber on the RSRA is illustrated in Figure 15 which shows cockpit vertical vibration levels in the compound aircraft out to an airspeed of 315 km/h (170 kn). The bifilar absorber is centrifugally tuned and thus self-tuning with rotor speed.

A standard BLACK HAWK bifilar absorber will be used for the RSRA/BLACK HAWK rotor application. Figure 16 presents BLACK HAWK helicopter vertical and inplane hub vibratory loads determined from flight data by the methods described in Reference 2. Applying these loads to the RSRA using fuselage transmissibilities from shake test (inplane) and NASTRAN analysis (vertical) yields cockpit vibration levels shown in Figure 17. These compare well with the RSRA/S-61 vibration data shown in Figure 13. Addition of the BLACK HAWK bifilar absorber to the system reduces the vibration levels by about 80%, also shown in Figure 17 to an acceptable level in the vertical direction.

It is concluded that the RSRA Active Isolation System will provide acceptable vibration reduction with the 4 bladed BLACK HAWK rotor. A standard BLACK HAWK rotorhead 3P bifilar absorber is an effective alternative vibration control approach which should be included in the rotor integration requirements as a backup.

Control Load Limits on Flight Envelope

Methodology

The onset of rotor stall results in a rapid rise in rotor control loads, and the flight envelope of gross weight times load factor versus speed is generally limited to prevent excessive control system loadings.

An empirical technique has been developed to estimate these control load limits. The method uses accumulated data from flight testing of the UH-60 and SH-60B aircraft. As shown in Figure (18), non-dimensional vibratory control load (C_L/σ) is related to a corresponding non-dimensional factor $C_L/\sigma(1-\mu)^2$, whose value depends on flight condition. Figure (18) shows the envelope of UH-60A and SH-60B experience for steady turns and level flight.

For this pre-design study, it is assumed that the UH-60A rotor control system down to and including the swashplate is installed on the RSRA.

Non-dimensional load coefficients are determined using vibratory control load limits for a desired rotor speed and density. Figure (18) is entered with these values, and the upper boundary is used to determine the corresponding value of $C_L/\sigma(1-\mu)^2$.

Finally, at a given assumed flight condition, total rotor lift ($N_z \times GW$) is determined. For the assumed gross weight, N_z can than be determined corresponding to the control load limit.

Results

The control load limit boundaries for the selected baseline rotor speed (258 RPM) and two altitudes have been determined using the above described method. A gross weight of 8618 kg (19,000 lb) is assumed. It should be noted that these control load limit boundaries represent a conservative fairing of available flight test data, i.e., the upper boundary shown in Figure (18) was used.

The existing stationary link load limits for RSRA are also assumed, namely an endurance limit of $\pm 7562\text{N}$ ($\pm 1700\text{ lb.}$) and a do-not-exceed (DNE) abort limit of $+18683\text{N}$ ($\pm 4200\text{ lb.}$)

The effects of the increase in the radius of stationary link connection to the swashplate 40.01 cm (15.75 inches) on the RSRA versus 27.31 cm (10.75 inches) on UH-60A are assumed relatively small for the purposes of determining these control load limit boundaries.

Results are plotted in Figures (19) and (20), as load factor at 8618 kg (19,000 lb.) gross weight. A reasonable envelope of operation exists for the 258 RPM condition, since anticipated research missions involve steady flight conditions.

Main Rotor Shaft Bending Load

The UH-60A main rotor at design rotor speed (258 RPM) provides larger hub moment per degree of cyclic flapping than the S-61 rotor. Data and calculation supporting this are given in Table 12. In order to prevent shaft fatigue damage, a limit can be placed on cyclic flapping.

This limit has been initially set at 8.3 degrees for 258 RPM. This limit is modest, and is not considered a significant constraint to the research objectives. Nevertheless, this subject will receive further attention during the design phase of the 4-bladed rotor integration efforts.

Pitch-Flap/Lag Stability Analysis

Methodology

The rigid hinged blade analysis of Reference 3 was used to estimate the stability of single-blade flap-lag motions, with the existing (small) values of pitch-lag coupling present in the UH-60A rotor head. Preliminary studies indicate that changes on pitch flap coupling due to the shorter pitch link will be small. Data input to the analysis is given in Table 13 and in the captions of Figures 21 through 26.

Solutions were obtained for a range of airspeeds at three essentially constant levels of rotor lift, representing level flight and steady turns or other quasi steady maneuvers at 2g and 3g with 8618 kg (19,000 lb.) gross weight.

At each of the three levels of lift, flight at a maximum torque level (corresponding to 1864 kn (2500 HP) at 203 RPM) and a zero torque level were considered.

For each of the above conditions, pitch-flap-lag eigen solutions were obtained for $R = 220.9 \text{ m/sec}$ (725 ft/sec) tip speed (258 RPM).

For the 1g level flight condition, eigen solutions were also obtained for a range of lag damping values and a change of cyclic flapping values at a forward speed of 333.5 km/h (180 knots.)

While the method of Reference 3 does not consider blade flexibility nor aerodynamic stalling, it does consider blade flapping and coning and cyclic and collective pitch inputs. For this predesign study it provides an appropriate indication of the effect of reduced rotor speed on blade stability.

Results

The damping ratio of the lag mode versus airspeed is plotted in Figure 21 for powered flight at 1g, 2g, and 3g. The rotor power applied at 1g was that required for level flight up to a torque limit of 87694 Nm (64,680 ft. lb) (1864 kw (2500 HP) @ 203 RPM), with torque remaining constant for higher airspeeds, simulating a power descent. For the simulated quasi steady maneuvers at 2g and 3g, the full torque limit was assumed in the cases plotted in Figure 21. Lag mode damping ratio versus airspeed is plotted for zero torque (unpowered) flight at 1, 2 and 3g load factors in Figure 22.

All of the conditions of these figures considered a gross weight of 8618 kg (19,000 lb.) and a normal amount of lag hinge damping, 9039 N.m-sec (9039 N.m-sec (80,000 in-lb-sec), equivalent to 30 percent of critical damping at a rotor speed of 293 RPM.

Figure 23 shows the effect of various amounts of lag hinge damping for a full power dive at a speed of 333.5 km/h (180 knots.) A damping value of 9039 N.m-sec (80,000 in-lb-sec) is considered normal.

Figure 24 shows the effect on lag mode damping of various amounts of longitudinal flapping at a forward speed of 333.5 km/h (180 knots) and lift of 8437 kg (18,600 lb.) Tip path plane is held constant as flapping is varied. The lower rotor speed increases damping ratio sensitivity to flapping but not to a degree that would be troublesome.

Figures 25 through 28 present root-locus type plots corresponding respectively to Figures 21 through 24. On these figures, frequency is plotted on the vertical axis and stable convergence rate is plotted on the negative horizontal axis. The upper half-plane only of the complex conjugate solutions is shown, for both lag and flap modes. The solution values are non-dimensionalized by rotor rotational speed, so frequencies appear as cycles per revolution. Note that these are solutions of linear systems of equations with periodic coefficients for all forward speeds above zero. Therefore a solution frequency ω implies blade motions at frequencies $\omega+n$ and $\omega-n$ where n is any integer. In particular, the zero frequency solutions imply motion at harmonic frequencies.

Ground Resonance Stability Analysis

Methodology

The ground stability analysis considers the aero-mechanical stability of a rigid fuselage supported on spring-damper systems representing the landing gear oleos, tires, and landing gear-fuselage attachment structure. The analysis proceeds in two major phases: Calculation of rotor-off fuselage natural modes, frequencies, and damping; and coupled rotor-fuselage stability analysis.

The fuselage natural mode analysis considers 6 degrees of rigid body freedom. The rigid fuselage is supported by three series spring-damper systems representing the two main and tail landing gear oleos and tires. The linearized stiffness of the air spring of each oleo is calculated to be consistent with the landing gear static load for the particular condition being considered, as well as the landing gear-fuselage attachment structure stiffness. The consideration of the effect of static loadings on landing gear stiffness and damping includes the loss of oleo flexibility and damping that occurs when the landing gear becomes fully extended at high percent airborne conditions.

The coupled rotor-fuselage stability analysis uses the method of Reference 4. With the articulated rotor being considered, ground stability concerns involve the dynamic coupling of essentially rigid body blade motions about the flap and lag hinges with rigid fuselage natural modes whose frequencies are roughly coincident with 2/3 of the rotor rotational frequency.

Input data for the ground stability analysis is presented in Tables 14 through 17 for the fuselage and landing gears. Rotor data are as presented in Table 1². Additionally, back-up structure stiffness was adjusted in the math model to improve agreement of roll response with data from the ground shake test conducted at Sikorsky Aircraft between August 24 and October 3, 1977.

Results

The results of the stability analysis are presented in terms of the frequency and damping of the coupled rotor-fuselage modes. For the sake of clarity, only the two cyclic lag modes and fuselage pitch (or pitch-vertical) and roll modes are presented. These are the modes that could conceivably present unfavorable coupling effects if damping were sufficiently low. Note that the designation of the modes as pitch, roll, or lag describe the characteristic modal shape near the normal rotor speed of 258 RPM. The mode characteristic shapes vary as rotor RPM changes, but no attempt has been made to rename the various modal traces for high and low RPM's.

Figures 29 and 30 present data at 0% and 80% airborne versus rotor speed with blade lag damping as a parameter. The reference blade lag damping levels are those levels which give that damping ratio for the uncoupled lag mode at 258 RPM.

References 5 through 7 show that the lag damping ranges between $\zeta_{DR} = .35$ and $\zeta_{DR} = .50$, depending on harmonic damper motions induced by kinematic coupling with blade pitch inputs and the amplitude of transient subharmonic motions. The results in Figures 29 and 30 show that adequate damping margins exist over the entire range of operational rotor speeds. Damping minimums that are shown versus rotor speed are a result of coupling between the regressing lag mode and the pitch or lag modes.

Figures 31 through 33 present the variation of modal properties with percent airborne at three rotor speeds. Variations with percent airborne are due to changes in tire and oleo stiffness and damping as landing gear load varies. The variation in stiffness and damping that occurs as the main oleos become fully extended is a notable feature of the data in Figures 31 through 33.

Figures 34 and 35 are similar to Figures 29 and 30, but with rotor height variation above the present S-61 rotor location as a parameter. The sensitivity of ground stability to rotor height changes of the magnitudes being considered is seen to be small for the system modes of concern in the operational rotor speed range. In addition, stability is retained for an adequate rotor speed range over and above the operational speed range. It is therefore projected that raising the rotor shaft height over the distances being considered will not result in ground stability problems.

According to the analysis, ground stability will be adequate when the UH-60A rotor is installed on the RSRA helicopter and operated as planned.

Coupled Rotor-Airframe Frequencies

Methodology, Data

Coupled rotor-airframe natural frequencies were estimated by using the method of Reference 4. The method of Reference 4 is the Sikorsky Aeroelastic Rotor Stability Analysis, which is an eigen solution method considering a detailed representation of a flexible multi-blade rotor and elastic support or airframe. Blade stiffness, mass, inertia properties blade chord, and twist can have arbitrary distributions. Both aerodynamic and structural twist are represented. The blade pitch can be arbitrarily large. Center of gravity and aerodynamic center offsets from the elastic axis are represented. The airframe or support is represented by up to 10 sets of normal modes with corresponding hub motions. The rotor drive system is represented by a

system of springs and masses input to simulate the actual system. The rotor control system pushrods, swashplate, and servo stiffness are simulated. Blade aerodynamics are included as steady two-dimensional tabulated airfoil section data, with blade stall and Mach number effects included.

Fuselage modal data were obtained from the shake test of the RSRA helicopter configuration conducted at Sikorsky Aircraft between August 24 and October 3, 1977. A tabulation of these data are provided herein as Table 18. Control system stiffness data were obtained from Reference 8. A tabulation of the data extracted is provided herein as Table 19, along with control system geometric data. Drive system data were obtained from available RSRA files. Shaft stiffness was estimated from dimensions given in Sikorsky drawing S6137-23040. A diagram and tabulation of the drive system mechanical mathematical model and data are provided at Table 20. UH-60A main rotor blade data were obtained from current files, and is tabulated in Tables 21 through 23.

Results

Blade bending mode frequencies are plotted against the rotor speed range of interest in Figure (36). These data are plotted as seen from the rotating system to facilitate the evaluation of coupling with the fuselage and drive system, and the proximity of the various modal natural frequencies to harmonic forcing frequencies.

Consideration of fuselage flexibility, drive system, and control system flexibility results in significant differences in rotating system frequency for collective and cyclic rotor modes for the first edgewise and torsion blade modes. These differences are present but insignificant for the other blade modes considered.

Figure (37) presents the damping ratios of the coupled blade bending modes as functions of frequency. The damping ratio is based on modal frequency observed from the rotor system.

The significant fuselage mode frequencies (in the non-rotating frame of reference) are plotted against rotor speed in Figure (38), and compared with harmonic forcing frequencies. Also shown in Figure (38) are the coupled rotor flap-lag mod frequencies.

The damping ratios of the fuselage natural modes are plotted versus rotor speed in Figure (39), based on non-rotating system frequencies.

The damping ratios of the rotor flap-lag modes are plotted versus rotor speed in Figure (40), based on non-rotating system frequencies.

The following may be stated concerning the above data:

- . Blade mode frequency versus RPM is similar to the UH-60A, except for the torsion mode which is increased to 24 hz from 18.3 hz at 258 RPM. The increase is due to a stiffer control system on the RSRA.
- . The resonance of the 2nd flatwise bending with 5P near 260 RPM is similar to the UH-60A. No troublesome evidence of 5P magnification has been noted. This is probably due to relatively small aerodynamic forcing of this mode, and the presence of aerodynamic damping.
- . Resonance of the first edgewise bending mode at 5P is a potential impediment to operation at the lower rotor speeds.
- . Torsional resonance at 6P at 219 to 230 RPM will probably not be significant because of aerodynamic damping.
- . Resonance of the third flatwise bending mode at 8P at 250 RPM may be noticeable, but will probably not significantly impede operation near this speed range.
- . Resonance of the first edgewise collective mode is predicted above 310 RPM. Troublesome amplification at 4P would not be expected below 300 RPM.
- . Torsional resonance at 5P at 310 RPM would not be significant because of aerodynamic damping.
- . Once per revolution excitation of the first lateral fuselage mode will increase with rotor speed but is not expected to be troublesome below 285 RPM.
- . Principal RSRA fuselage mode frequencies are well below the 4 per revolution rotor blade passage frequency.
- . Two and three per revolution resonances will not be troublesome. The 4-bladed rotor normally has negligible force output at 2 and 3 per rev frequencies.
- . Coalescence of flap/lag mode frequencies with fuselage natural modes does not occur.
- . Damping of all coupled rotor-fuselage modes remains adequate throughout the rotor operating range of interest.

Analytical determination of coupled rotor-fuselage natural modes indicates that a useful range of rotor speeds can be investigated without troublesome resonances or instabilities. The analysis predicts a 5P first edgewise mode resonance at approximately 215 RPM, and a 8 third flatwise mode resonance at approximately 240 RPM. These resonances may result in high blade stresses or fuselage vibration which could impede operation at these rotor speeds.

Stability and Control Considerations

The installation of the BLACK HAWK rotor on the RSRA is not expected to present any significant problems in the stability and control area. Control power, control phasing, control rigging, blade clearance and autorotation characteristics must be considered. All have to be addressed in detail in an actual design but none are believed to present a problem as discussed below.

Control power with the BLACK HAWK rotor will increase despite the fact that the rotor diameter and the number of blades are lower than baseline S-61 rotor values. The reasons for this are the higher flap hinge offset, higher blade centrifugal force (due to higher tip speed) and the higher rotor position above the center-of-gravity. Preliminary analysis indicates the control power with the BLACK HAWK rotor will be about 50% higher at 100% N_R and about 25% higher at the low tip speed condition (91% N_R). This higher control power would be beneficial to the RSRA in pitch. If the roll sensitivity becomes a concern, a straightforward rigging change will be recommended.

The control phasing required for the BLACK HAWK rotor differs from that of the S-61 and thus would require an adjustment of approximately 11° against rotation. This adjustment, together with the small amount of collective-cyclic coupling present with the proposed swashplate can readily be accommodated by adjustments to the variable control phase analog system.

The higher twist of the BLACK HAWK rotor requires a collective rigging range change. This can be accommodated by properly selecting pushrod length.

Blade tip clearance relative to the fuselage is not expected to be a problem with the BLACK HAWK rotor due to the increased (15.24 cm(6")) height of the rotor and the reduced radius of the rotor. These should compensate for the reduced clearance that would otherwise result from the anhedral tip. For the same vibratory flap angle, as the S-61, these two factors increase the clearance over the tail by at least 15.24 cm (6"). Additional analyses would, of course, be performed in any detail design studies. Should any problem surface at that time flap envelope limits could be defined to control the situation.

Autorotation characteristics of the RSRA with the BLACK HAWK rotor at 100% N_R are expected to be slightly worse (but acceptable) than with the S-61 rotor because of slightly less (10%) energy in the rotor. The autorotative index for the RSRA/BLACK HAWK rotor on the RSRA is compared with the RSRA/S-61 rotor configuration and with the Sikorsky SEAHAWK in the table below.

Configuration	Autorotative Index $\frac{I_R}{(GW)(D.L.)}$
RSRA (S-61 Rotor)	36
RSRA (BLACK HAWK Rotor)	32
SEAHAWK (BLACK HAWK Rotor)	32

Parameter Change Studies

Definition of practical variation that can be applied to the selected baseline rotor system is essentially a cost/benefit tradeoff. The intent is to identify a set of parametric changes that allows flight evaluation of important rotor design variables without requiring major alterations to the blade substructure design. It should be clear that if modification of the blade substructure is required, costs will increase dramatically due to tooling, fabrication, and qualification needs. The BLACK HAWK rotor and airfoil modification techniques together with existing tip and airfoil modification techniques will permit a significant test program to be structured without major redesign or blade hardware efforts. For these reasons consideration of parametric changes that involve the blade structure (such as inboard twist and inboard planform modifications) were not considered.

Airfoil Modifications

Airfoil leading edge geometry modifications have been demonstrated to produce significant changes in the airfoil lift characteristics. The production BLACK HAWK main rotor blade incorporates an SC1095-R8 airfoil from 49.4% to 83.8% radium and an SC1095 airfoil inboard and outboard of this zone. Modification to the airfoil distribution, for example, full span R-8 airfoils can be made by bonding on leading edge shape modifications constructed of fiberglass. Such modifications were demonstrated during the prototype flight testing of these blades and are considered low risk and acceptable for limited time experimental flight testing. Life will be limited by erosion unless metal erosion strips are added. A layout drawing showing the leading edge modification for the RSRA is shown in Figure (41).

The leading edge modification applied to the original BLACK HAWK blades is illustrated in Figure (42). Figure (43) shows the dramatic increase in C_{LMAX} that resulted from this relatively simple and inexpensive contour change.

Design of the high lift inboard airfoil modification includes evaluation of rotor tip speed effects on the desired radial extent of the airfoil change. In practical terms, the need for a high airfoil C_L^{MAX} depends on the rotor design C_T/σ and hence the tip speed. As the rotor operating tip speed is decreased, extension of high lift airfoil contours towards the tip becomes feasible since advancing side compressibility penalties are decreased.

Two radial limits on the high-lift airfoil function have been examined. In the first, the use of the SC1095-R8 airfoil is extended to station 299 (.928R), which is where the swept tip cap begins. In the second, the SC1095-R8 is extended completely to the tip of the rotor blade. The performance of these configurations have been studied for several tip speeds and cruise flight conditions using a constant inflow, steady state aerodynamic method.

Initially, two main rotor tip speed ranges were also considered. One was based on using the unmodified RSRA transmission (100% $N_R = 203$ RPM). The other was based on the modified RSRA transmission (100% $N_R = 258$ RPM). Closer investigation revealed that operation of the BLACK HAWK rotor with the unmodified (lower RPM) transmission resulted in excessive push rod loads. This eliminated further consideration of its use in the research program. The tip speed range available with the revised RSRA transmission is from 92 to 110% N_R . Table 24 summarizes the tip speed/RPM ranges possible. Selection of the desired tip speed from this range is then a matter of research requirements constrained by the maintenance of the proper margins of rotor lift for safety of flight.

The effect on forward flight performance of extending the SC1095-R8 airfoil section to the tip (the selected configuration) is illustrated in Figure (44). Of special note is the increase in push rod limits relative to the standard BLACK HAWK blade. This is due to delayed retreating blade stall and the associated pitching moment divergence.

Blade Tip Modifications

The BLACK HAWK production main rotor blades incorporate tips which are swept back at 20 degrees over 6 percent of the blade span. Much of the sweep geometry is in the tip cap which is bolted onto the blade tip fitting. Because of the relatively large baseline tip cap, other tip geometries of similar length to the existing cap can be easily accommodated by the existing tip cap retention structure. Two such advanced tip geometry modifications have been designed and fabricated (see Figures 4 and 5). One is a swept tapered tip and the other a swept tapered tip with anhedral. The full aircraft sets of the 3 available tip geometries will allow immediate flight experiments on tip variations.

A layout sketch for adapting a 10% radius tip cap to the BLACK HAWK blades has been prepared and is shown in Figure (45). A preliminary structural analysis of the modification was performed. The design study was based on the assumption that the tip cap attachment location would remain the same as on the existing blades which means that the blade radius would be approximately 4% longer on the modified tip blades; this was the easiest and lowest cost approach. The extended cap was assumed to have the same sweep angle as the production cap. The extended cap design is constructed of fiberglass and honeycomb as shown on the drawing. Metal doublers are bonded to the attachment areas for strength. The higher attachment loads associated with the larger cap will require modifications to the existing attachment joint. Larger screws will be required and thus a modification to the tip block to which the tip cap attaches. Another critical area is the tip cap itself through its attachment area. The preliminary strength analysis indicates that sufficient life could be obtained to provide a reasonable flight program over the BLACK HAWK design flight spectrum by providing an increased thickness stainless steel doubler and the addition of an aluminum doubler at the joint area as shown in Figure (45). Based on the preliminary analysis it is felt that the reinforcement can be accomplished within contour by machining the tip block. More detailed analysis beyond the scope of the program is required to insure this. Table 25 compares characteristics of the production and extended tip caps.

Rotor Mast Height Variation for Study of Rotor-Body Interference

The effect of the RSRA airframe potential flow field on the selected rotor aerodynamic loading and dynamic response was analytically evaluated for two design mast heights.

The fuselage interference effect on the blade vibratory root shears was predicted with the methodology documented in Reference 9. This involved prediction of the fuselage potential flow velocities with the Sikorsky developed Wing and Body Aerodynamic Technique (WABAT). These velocities were then included in a vortex wake variable inflow analysis that solves for the total rotor downwash distribution due to the combined wake and fuselage flow effects. Use of the combined flow field in a normal modes aeroelastic rotor analysis yielded the required root shear prediction.

The two mast heights studied were the standard mast height 149.9 cm (59 in.) above the fuselage) for the proposed RSRA rotor (which is 15.24 cm (6 in) higher than the current RSRA rotor) and a mast 30.5 cm (12 in.) higher (180.3 cm (71 in.) above the fuselage). Figure (46) illustrates the azimuthal distributions of the vibratory flatwise stresses predicted for these mast heights. As can be seen, little difference is evident between the two configurations. Analysis of the azimuthal load distributions for the two alternate mast heights indicates that the fuselage upwash has stalled the in-board blade

sections over the aircraft nose. As a result, the impulsive blade loading did not develop due to low or negative static lift curve slopes. During actual aircraft flight, unsteady lift activity would prevent the stall and load variations would be higher than predicted.

Figure 47 shows the effect of mast height on calculated 4 per rev forces and moments. For each force or moment, results for mast extensions of 30.5 cm (12 in.) and 45.7 cm (18 in.) are compared to those of the baseline six in extension and those of an isolated rotor.

The relative insensitivity of the calculated forces and moments to mast extension reflects the previously mentioned static stall in the analytic model. Since angle of attack results indicate that significant levels of interference persist with both 30.5 cm (12 in.) and 45.7 cm (18 in.) mast heights, the 45.7 cm (18 in.) mast height has been selected for the alternate position. This will provide a larger change in the interference level than that achievable with a 30.5 cm (12 in.) alternate. Since the baseline BLACK HAWK rotor position is 15.24 cm (6 in.) above the S-61 rotor height, the 45.7 cm (18 in.) alternate position will require a 30.5 cm (12 in.) mast extension relative to the baseline BLACK HAWK rotor.

It should be noted that two additional vibration mechanisms, besides impulsive blade loading, will be influenced by the additional 30.5 cm (12 in.) extension of the rotor mast. These are fuselage canopy drumming due to vortex impingement and vibration transmittability due to changes in the rotor shaft impedance. Neither of these effects were included in the analysis.

INSTRUMENTATION

Rotor Blade Instrumentation

Rotor Blade Pressure Measurements

The decision to include airload measurements, and hence absorb the cost of a pressure tapped blade and associated flight testing, can be clearly justified in terms of merit to the flight research program. With airload measurement, three research approaches can be used that are not possible in the absence of airload data. These are: (1) separation of forcing function and blade dynamic response, (2) analytical identification of noise generating mechanisms, and (3), detailed study of blade pressure distribution as influenced by 3-D tip design and unsteady aerodynamics.

Without blade pressure measurements, baseline and alternate rotor configuration can still be evaluated for changes in flight characteristics, but the basic causes of differing attributes will probably be obscured. This will detract from the research aspect of the flying and tend towards the less demanding task of qualifying a second rotor

for flight on RSRA. In turns of research value per dollar spent, it is felt that the addition of the pressure instrumented blade is worth the expense. This is particularly true when one considers that the fractional cost to the program is small. In this case the total program cost is defined as costs associated with rotor integration plus the costs associated with data flying and data reduction.

Airloads will be measured using miniature pressure transducers recessed into the surface of one blade on the test rotor. The transducer type and the array in which they are installed must be optimized to yield the maximum accuracy in the integrated loads within the physical constraints imposed by the blade geometry and by the number of data channels available. The accuracy of each measurement, and hence, that of the integrated loads, will also be affected by the characteristics of the data acquisition and recording electronics. Details of these concepts, and the proposed methods to achieve the stated goals, will be discussed in the following paragraphs.

The United Technologies Research Center (UTRC) has had extensive experience in the use of miniature transducers to measure unsteady pressure phenomena. For example, measurements of the surface pressures on oscillating blades were made in cascade (Reference 10) and on the Sikorsky tunnel-spanning wing (Reference 11). Other unsteady measurements were made on rotating compressor blades subjected to an inlet distortion (Reference 12), and on turbine blades encountering wakes from an upstream blade row (Reference 13).

In all these tests UTRC developed measurement techniques and signal conditioning electronics compatible with the requirements of the experiments. (The turbomachinery tests, References (12) and (13), further required that these signal conditioning devices be placed on board the rotor and interfaced to the data system through slip rings.)

Although the state of the art in the manufacture of miniature pressure transducers is constantly improving, all current semi-conductor transducers exhibit measurable changes in sensitivity and zero offset with temperature. These adverse effects may be minimized with passive thermal compensation and all manufacturers use this technique. Customarily, the components required for thermal compensation are contained in a separate module which should be maintained at a constant temperature for proper operation. Alternatively, some transducers have compensation components built into the transducer housing such that the sensing element and the compensation components are always at the same temperature. The latter method entails a more complicated manufacturing technique, but is far easier to implement in a flight test, where there is no constant temperature region in which to locate a compensation module.

In addition, there is a slow, random drift in zero offset which cannot be compensated. This is usually accounted for by periodically taking zero pressure records.

In the past, drift problems were so severe that a typical test program at UTRC would use miniature pressure transducers only for unsteady measurements, and the time-averaged component of the pressure signal would be obtained by other means if required (e.g., pneumatic instrumentation). In current transducers the thermal and random drifts are sufficiently small that even the time-averaged portion of the pressure can be extracted from the signal. For the test of Reference (13), precise temperature calibrations and periodic zero reference records were employed to correct for any residual drift, and the entire pressure was successfully obtained.

Transducers can be obtained as either absolute or differential measuring devices. The absolute transducer has a sealed chamber behind the sensing element, whereas the chamber of the differential transducer is vented through a reference port. In wind tunnel applications, a low-range, differential unit with the reference port connected to test section total pressure is normally preferred for maximum sensitivity. However, in a rotor flight test there is no logical source for a reference pressure, nor is there a clear advantage to using a differential transducer. In fact, physical constraints dictated by the construction of the test blade, and the complicated reference plumbing requirements of multiple differential transducers may preclude their use in favor of the absolute transducers, whose installation is far simpler.

Structural integrity demands that neither the transducer nor its wiring penetrate the spar, and aerodynamic considerations require that the transducer not protrude above the local blade surface. It is desirable that the transducer be constrained within the existing skin without adding to the local blade thickness, and that transducer construction and installation be such that there is minimal sensitivity to local strain. Several candidate transducers will be evaluated to ensure that they can satisfy most or all of these apparently conflicting constraints. One method using proven equipment involves the addition of thin chordwise gloves (of limited spanwise extent) in which cylindrical transducers (.093" dia) would be soft-mounted into spanwise slots. These transducers are sufficiently rugged and stable to satisfy all measurement requirements for this test. If a transducer can be found which satisfies these requirements and also is thin enough to eliminate the need for the glove, it will be substituted for the cylindrical one.

Maximum accuracy in the integrated loads for a given number of transducers may be realized by using Gaussian quadrature techniques (References 11, 14, 15). The transducers will be placed in the locations prescribed by the segmented-Gaussian technique (Reference 14) in both the spanwise and chordwise directions, thus minimizing integration errors. This technique takes full advantage of prior knowledge of load distribution to concentrate transducers in regions of highest gradient. An array developed using this technique (Figure (48)) was used in the experiment reported in Reference 11. Here it was shown that integration of an analytically prescribed pressure distribution modelled after previously measured profiles yielded negligibly small errors in normal force and pitching moment, and an error less than 1% in chord force. In contrast to this, trapezoidal integrations of the same function yielded 0.5% error in normal force, 2.4% error in chord force, and approximately 2% error in pitching moment (based on a typical maximum value). It is anticipated that an optimum spanwise-chordwise array developed after the same manner will contain approximately 150 transducers and can be employed to determine the aerodynamic loads on the test rotor with errors of 2% or less. This array will automatically concentrate measuring stations in the tip region, facilitating the evaluation of different tip geometries.

The choice of transducers and the instrumentation array was dictated by the requirement to measure performance parameters (e.g. blade loads) which are low frequency phenomena. (For example, the 5° azimuth increments typically used for rotor performance predictions translates to a data rate of only 310 Hz for the proposed test rotor.) However, both the frequency response of the pressure transducers and the density of the chordwise arrays will also be adequate for the study of such transient phenomena as dynamic stall and blade-vortex interaction.

The addition of skin friction gages, if desired, would allow the study of transient surface flow phenomena such as laminar-to-turbulent transition and boundary layer separation. (UTRC has developed on-board electronics for making such measurements on rotating equipment.) The data rate required for the study of transient phenomena would be much higher than that required for performance measurements, perhaps as high as 10 kHz.

The accuracy of the final results will be intimately associated with the resolution of whatever system is used to acquire and record the data. Since the determination of blade loading involves a relatively small difference between the pressures on the opposing surfaces of the blade resolution of the load to a given accuracy may well require far greater accuracy in the resolution of the individual pressures. Experience at UTRC has shown that an effective resolution of 0.1% of full scale is adequate.

Other Instrumentation

Rotating blade instrumentation has been selected on the basis of two criteria. These are flight safety and satisfaction of research objectives. Although the BLACK HAWK rotor is a production system, RSRA interface modifies the control system dynamics and requires the presence of diagnostic data. Even without the control system changes, rotating strain guages would be required due to the large intended RPM range for the main rotor. The fact that blade tip geometries and airfoil contours will be changed during the research flight program also argues in favor of blade mounted strain guages as well as surface pressure transducers. Availability of both airload and blade bending response data will permit separation of aerodynamic and blade response effects. Stated differently, availability of both data types will show which improvements would accrue on a rigid blade, and which are due to the bending response of non rigid blades.

The following dynamic concerns were weighed during the rotating instrumentation specification.

- . Effects on ground and flight aeromechanical stability due to changes in rotor RPM and lag damping kinematics.
- . Effects on vibration of 4/rev force versus previous 5/rev .
- . Effects on engine/drive train stability due to increased RPM, associated gear ratio changes, and new lag damper kinematics.
- . Compatibility of test envelope and stress/load/stability boundaries.
- . Effects of airfoil shape and its spanwise variation on blade response (harmonic and non-harmonic).
- . Effects of control stiffness changes on blade and control load response.

The resulting instrumentation list (Table 26) is divided into eight categories. These categories generally refer to the physical location of the measurement guage. It should be noted that three types of blades are referred to in conjunction with the instrumentation. These are a master strain guage blade, additional blades, and a pressure tapped blade. A normal flight configuration will consist of the master strain guaged blade and three additional blades. Use of the pressure tapped blade is reserved for only those flights intended to gather airload data. This will limit the exposure of costly and fragile pressure transducers to fatigue damage.

TECHNOLOGY PAY-OFF STUDIES

General

Technology pay-off estimations are divided into four areas. These are: (1) comparison of baseline rotor OGE hover and level forward flight research envelopes with the existing S-61 envelopes, (2) assessment of envelope changes due to outboard extension of the SC1095-R8 high lift airfoil section, (3) assessment of tip modification effects on the research envelope, and (4), effects of rotor mast height on the flight envelope. The flight regime limits are defined for the pure helo configuration only. This is due to the specification of the active isolator configuration (which precludes the use of the wing).

Four Sikorsky developed analyses were used in the technology pay-off definition studies. All analytic OGE hover capability data was generated with the Circulation Coupled Hover Analysis Program (CCHAP). This is an isolated rotor hover analysis and results were accordingly corrected for RSRA vertical download. Figures (50) and (51) show correlation of the analysis with isolated rotor hover data from the Sikorsky whirltower. Baseline rotor and S-61 rotor power limited level forward flight envelopes were calculated with the Forward Flight Data Bank (FFDB). This is a semi-empirical energy based method that relies heavily on flight test data for definition of appropriate efficiency factors. Due to the large available quantity of BLACK HAWK and S-61 forward flight test data, the predicted envelopes for the two rotor systems are essentially accurate to within flight test measurement accuracy. Figure 6 correlates the method with existing pure helo RSRA forward flight test data. An assessed equivalent flat plate drag area of 2.12m^2 (22.8 ft^2) was used for these calculations.

Variations in the predicted forward flight test envelope were predicted with the Y201 normal modes aeroelastic analysis for the airfoil parameter change, the alternate tips, and the rotor mast height change. For the mast height change cases, body induced effects were assessed with the Wing and Body Aerodynamic Technique (WABAT). This method calculated inviscid fuselage potential flow interference velocities in the plane of the rotor. Changing the mast height varies the inter-rotor-body spacing and hence effects the level of interference velocities. These velocities normally have little effect on integrated rotor performance, but do have a distinct effect on higher harmonic hub shears and resulting fuselage vibratory excitation. Mast height changes can alter the dynamics of the coupled rotor/fuselage. Careful calibration is required to separate dynamic and aerodynamic effects.

Figures (52) and (53) compare dimensional and non-dimensional sea level standard day OGE hover performance for the RSRA configured with BLACK HAWK and S-61 rotor system. As indicated, use of the BLACK HAWK rotor decreases the OGE hover capability at the 1864 kw (2500 horse-power) transmission rating by about 408.2 kg (900 lb.) The loss in hover capability is due to the higher disc loading of the BLACK HAWK rotor system. In fact, the higher blade twist and newer airfoil sections on the BLACK HAWK rotor improve its hover efficiency (Figure of Merit) by about 9% relative to the S-61 rotor. This has largely offset the disc loading penalty and limited the loss in OGE hover gross weight capability to 408.2 kg (900 lb.) Although the non-dimensional OGE hover performance is presented for a standard day, the BLACK HAWK rotor is relatively insensitive to Mach effects and the curve can be effectively used for other temperature condition. The effect of rotor RPM on sea level standard hover capability is shown in Figure (54) as engine N_r is varied over the permissible range of 110% to 92%. It should be noted the in-ground-effect hover capability significantly increases the allowable take-off gross weight.

Forward flight research envelope limits for the BLACK HAWK rotor system are presented in Figures (55) and (56). For comparative purposes, equivalent S-61 rotor limits are illustrated in Figure (57) and (58). Each of these figures map limiting C_T/σ - advance ratio boundaries at 8708.9 kg (19200 lb) gross weight and a specified temperature altitude condition. Since the gross weight and density are fixed, the C_T/σ variation and associated varying advance ratio limits are the result of N_r changes. As with hover, the N_r variation range is 110% to 92%. Two types of limit lines are included on each plot. These are power limit lines and push rod load limit lines. The power limit lines effectively show the highest advance ratio that can be attained at a given N_r within the available power constraint. The C_W/σ and hover tip Mach number resulting from each N_r is shown on the vertical axis. The push rod limit lines express the C_T/σ - advance ratio boundary at which push rod loads will exceed endurance levels. These boundaries are derived from stress surveys obtained during the BLACK HAWK helicopter qualification testing.

Data is presented at two temperature altitude conditions, sea level standard and 1219.2 m (4000 ft) 95°, to illustrate the effect of ambient conditions on the limits. As indicated, the sea level standard flight envelope is primarily power limited. In contrast, 1219 m (4000 ft.) 95° operation is push rod load limited at tip speeds corresponding to less than 98% N_r . Since specified push rod load limits are defined at endurance level, it may be possible to exceed these limits for a brief period of flight.

Dimensional maximum level flight speed curves are presented in Figures (59) and (60) for sea level and 4000' - 95° conditions respectively. The second speed trend line shown for sea level conditions represents a constant 1864 kw (2500 hp) limit at all tip speeds rather than a constant gearbox torque limit. This curve shows that the peak rotor efficiency is achieved in the vicinity of the selected 100% N_r tip speed (220 m/sec (722 ft/sec)).

Effect of Airfoil Modifications on Research Envelope

Extension of the SC1095-R8 airfoil outboard to the tip cap is expected to primarily effect only high speed flight rotor characteristics. During hover, no significant impact is expected. The combination of relatively low tip Mach numbers, and the fact that profile power constitutes only 10 - 15% of total power in hover, should hold the effect to a loss of less than 45.3 kg (100 lbs) in hover capability.

During high speed forward flight, sea level standard conditions, the extended inboard airfoil will slightly decrease the maximum achievable advance ratio at 110% N_r tip speed (242 m/sec (794 ft/sec)). This performance penalty will decrease and become a performance gain as the N_r is lowered to 92% (203.6 m/sec (668 ft/sec)).

These changes, relative to the baseline BLACK HAWK envelope are depicted in Figure (44). It should be noted, as indicated, that the SC1095-R8 airfoil extension favorably moves the push rod limits at all operating N_r 's. This is to be expected since the extended high lift airfoil deters retreating blade stall and associated pitching moment divergence.

It is expected that all research flying with the extended airfoil blade will be conducted at the lower tip speed where an envelope expansion is indicated. This is the regime where good aerodynamic efficiency must be demonstrated to produce a practical low tip speed - low noise rotor, and also the regime that will yield unsteady aerodynamic blade pressures for near stall conditions.

Effect of Tip Geometry on Research Envelope

During hovering flight, only the mini-anhedral tip is expected to significantly affect the operating envelope. This effect is a 1.8% increase in OGE hover gross weight capability at constant power. Figure (61) compares non-dimensional hover performance for the BLACK HAWK baseline and BLACK HAWK mini-anhedral configuration. The indicated performance improvement for this tip geometry has been verified in both 1/6th scale model and full scale whirlstand tests. Based on this data, an increase of 158.8 kg (350 lb) in the sea level standard OGE hover capability is expected at the transmission torque limit.

The effect of the alternate tip geometries on forward flight performance and load characteristics is difficult to predict. This is due to the fact that, although current analyses can usually qualitatively predict tip effects on rotor behavior, they are not sufficiently precise to gauge the magnitude of these changes. This trend is well documented in Reference 16 that summarizes predicted and test results for four tip configurations tested full scale in the Ames 12m x 24m (40 x 80 ft) tunnel. Two of the four tested tips were similar to the standard BLACK HAWK and double swept tips proposed for test on the BLACK HAWK rotor configured RSRA.

Despite these acknowledged shortcomings, Table 27 summarizes predicted performance changes for the three alternate tip configurations for sea level standard conditions, 8708.9 kg (19200 lb) gross weight, and transmission torque limited power for the permissible engine N_t range. The level flight incremental speeds are identical for the double swept and mini-anhedral tips since the Y201 analysis does not currently calculate the aerodynamic or dynamic influence of spanwise anhedral droop. Also, as expected, the predicted performance benefits decrease as the rotor tip speed decreases, since sweep and planform taper are primarily effective under high advancing tip Mach number conditions.

Indications of expected tip modification effects on limiting push rod loads are available from experimental data obtained on 1/6th scale BLACK HAWK rotor blades tested in the NASA/Langley Transonic Dynamic Wind Tunnel (TDT). These tests were conducted in a Freon atmosphere simulating half scale Reynolds numbers. Figures (62) and (63) illustrate the favorable reductions in maximum vibratory torsion loads due to tip geometry modification. Figure (62) presents load trends as a function of C_L/σ for a constant advance ratio of .35, while Figure (63) shows the effect of flight velocity at a constant C_L/σ of .058. Of the four tips represented, the baseline, the mini-anhedral, and the swept tapered configurations are of particular importance to the four bladed RSRA program. The baseline, or BLACK HAWK tip, and the mini-anhedral are direct scale models of tips proposed for this program. The swept tapered tip is a 10% span configuration adaptable to the BLACK HAWK rotor with the proposed 10% span tip adaptor. It is noted that both the mini-anhedral and the swept tapered tip reduced critical control loads as a function of both rotor C_L/σ and rotor flight speed. Although the test conditions did not reach the critical combinations of C_L/σ and advance ratio that cause the full scale BLACK HAWK rotor to exceed control load endurance conditions, it is believed that the demonstrated favorable trends will extend to the more severe condition. Exploration of tip effects on control load flight envelope restrictions is, in fact, one of the flight program research goals.

Reduction of vibratory airframe excitation is an additional area that is expected to show a technological pay-off through advanced tip testing. As illustrated in Figure (64) both the mini-anhedral and the swept tapered tips reduced four per rev hub shear forces during the

Langley TDT tests. The 10% span swept tapered tip was particularly impressive in this respect, showing a 40% reduction in excitation level 1.

PROPOSED FLIGHT INVESTIGATION

General

The flight research program for a BLACK HAWK rotor configured RSRA is structured to provide an extensive experimental data base in three important areas of current rotor research. These are tip geometry effects, unsteady airfoil load characteristics and rotor-body interference effects. Whereas these areas have been previously addressed in analytical and model scale experimental studies, the investigations were inherently limited by incomplete analytical simulation and various compromises identified with model scale testing. To date, no comprehensive rotor analysis exists that effectively integrates three dimensional tip aerodynamics, wake inflow, unsteady aerodynamic loading, fuselage interference effects, and coupled rotor/fuselage dynamics. Data obtained through the model scale tests is subject to scale corrections in addition to being generally limited to steady state test conditions by the lack of body inertial relief. It should be noted that the selected research program does not include several important parameter variations that are not compatible with the basic BLACK HAWK blade structure and hence the cost objectives of the program. Examples of these are static twist variation, aeroelastic conformable dynamic twist tailoring, and inboard planform variation. These experimental studies are more appropriate for a later generation RSRA rotor program.

Rotor Tip Geometry Effects

The proposed rotor tip studies will evaluate the impact of four geometries on rotor performance, dynamics, acoustics, and handling qualities. Descriptions of these tips are available in the hardware section of this report. Three of the tip designs are currently available as flight worthy hardware. These are the basic 20° swept BLACK HAWK geometry, the double swept tip, and the mini-anhedral tip. Whereas these tip modifications effect only the outer 3 - 5% of the blade radius, available model scale forward flight data, and hover data obtained at model and full scale, suggest significant performance improvements and stress reduction have been achieved. The forward flight stress comparison data obtained in the Langley Transonic Dynamics Tunnel is documented in Reference 16 and summarized in Figures 62 through 64. Hover Figure-of-Merit comparisons for the baseline BLACK HAWK and mini-anhedral tips, obtained in Sikorsky sponsored 1/6th scale and full scale whirl tower tests, are presented in Figure (61). Forward flight performance data obtained in the test is not considered reliable due to repeatability problems.

The fourth tip allows for alteration of the outer 10% of the blade radius. This is accomplished by adding a structural fixture at the current tip cap junction and extending the blade radius an additional 4%. Figure (45) depicts the necessary blade structural changes in layout form. Although the aerodynamic design of the fourth tip is identified as a 20° swept SC1095 airfoil, the option exists to change the geometry prior to detail design as does the option to add more tip shapes to the study.

A primary purpose of the blade tip research flights will be the acquisition of blade airload data that delineates the mechanisms through which the altered tip geometries affect the rotor attributes—performance, noise, loads, etc. In order to prepare for the next generation of optimized tip design it is necessary to not only understand which parameters have a favorable effect, but to also understand why. As an example, improvements in rotor performance and acoustic traits for swept tip rotors may be due to advancing side shock attenuation, favorable aeroelastic blade bending, or enhanced retreating side tip lift under combined unsteady yawed flow. The selected blade pressure tap locations should ensure that adequate data is obtained for these diagnostic studies. Two chordwise arrays (95%R and 98%R) will be placed on the altered tip to directly monitor load levels and shock behavior. Five additional chordwise arrays over the remainder of the blade will provide changes in the spanwise load distribution caused by altered aeroelastic bending taken as a whole, the tip chordwise pressures, the blade spanwise load variation, and the resulting changes in the rotor characteristics, should provide a clear understanding of tip mechanics.

Acoustic signature of the RSRA will be obtained in hover and flyby for all four tip configurations. Measurements obtained during high speed flyby will be of particular interest since background noise normally compromises rotor noise measurements during wind tunnel testing. As such, little design information is currently available relating tip design parameters to forward flight acoustics. In addition to providing basic acoustic design data, the flight program will also produce companion airload data. This data can be used in current analytical models of rotor acoustic mechanisms for method validation and improvement. An example of such analyses is that developed by Farassat and documented in Reference 17.

Unsteady Airfoil Load Characteristics

Two types of data that are required to understand the effect of unsteady airfoil characteristics on rotor behavior will be provided by the flight research program. These are data that define the impact of high retreating side lift coefficient requirements on rotor behavior, and data that defines airfoil surface pressure response under the same condition. Since retreating side lift limits in an unsteady environment are not well understood, it is currently difficult for the rotor

designer to select the best spanwise airfoil distribution and rotor tip speed for meeting varied design requirements. Stated differently, selection of the proper rotor design C_L/σ for the best blend of performance, acoustic, and dynamic characteristics demands a greater understanding of the retreating side unsteady lift environment than is afforded by present research.

The trade-off between operating at a low tip speed with the associated high C_L/σ , and a higher tip speed that places less demand on retreating side lift coefficients, has taken on renewed importance in the light of pending stringent new civil noise regulations. From an acoustic standpoint, it is almost always desirable to lower the rotor tip speed. To do so, however, without substantially increasing the blade cost, vehicle weight, and vehicle cost, requires high operational retreating side lift coefficients. The following proposed investigation of rotor operation under high retreating side airfoil lift demands is intended to provide the data required to understand these lift limits.

The flight program consists of testing two rotor configurations, which differ in terms of retreating side lift capability at two distinctly different tip speeds. Each of the two rotor configurations will use an instrumented blade with sufficient pressure taps for mapping the unsteady lift response. The first configuration is the baseline BLACK HAWK blade that uses a high lift SC1095-R8 airfoil between 40% and 83% radius. The second configuration will be formed by extending the high lift SC1095-R8 section outboard to the blade tip. This approach is particularly attractive because the conversion of the outboard SC1095 airfoil to SC1095-R8 section dramatically increases the airfoil steady and unsteady lift capability at relatively low cost. The cost saving is due to the fact that the SC1095-R8 airfoil is a SC1095 with a modified drooped leading edge. The increase obtained in the maximum steady lift coefficient through the leading edge mod is illustrated in Figure (43).

Performance, acoustic, and dynamic data obtained with a given rotor configuration at the two tip speeds will investigate advantages and degradations that accrue, for fixed airfoils, as performance penalties are shifted from the advancing side to the retreating side. As RPM is lowered, the compressibility penalties on the advancing side will be reduced and the retreating side will experience problems related to stall. As previously mentioned, both the advancing or retreating side behavior require further detailed study to understand these impact on multiple design constraints. The availability of blade pressure histories for these flight conditions should clearly aid in defining flight boundaries for which the penalties become excessive on either side, and provide data for analytical correlation. Once the boundaries are understood and correlated, methods and procedures for moving the boundaries can be examined with greater confidence.

Flight investigation of the second rotor configuration, with the extended SC1095-R8 airfoil section, will probe the movement of the compressibility and stall boundaries as airfoil section drag divergence capability is traded for additional C_L^{MAX} margin. Obviously, this configuration will have extended capability at low RPM conditions and will probably incur relative penalties at the higher RPM. The intent of this phase of the flight research will be to determine if the low tip speed - high C_L^{MAX} blade is a superior approach for meeting current design goals. Again, the availability of blade pressure data can be used to contrast the effect of the airfoil contour change on the unsteady lift response and shock formation.

Rotor - Body Interference Effects

The dual mast height hardware will be used to explore effects of varying rotor body spacing and attending body on rotor and rotor on body interference. Briefly, two types of adverse interference are of concern. These are rotating system vibratory loads arising from the immersion of the rotor system in the potential flow field of the fuselage, and over pressure drumming on the airframe canopy due to close blade passage. Both types of interference have been studied analytically and in small scale tests. Full scale test data with a fully instrumented airframe, however, is lacking. As a partial result, only preliminary guidelines exist defining proper separation distances for acceptable flight characteristics in a variety of flight regimes. It should be noted that the development of such a criteria depends not only on the vibration characteristics of the airframe, but also on system weight and combined airframe, rotor shaft, and rotor head drag.

The selected mast extension will increase the minimum rotor pylon separation distance from 35.6cm (14 in.) to 66.0 cm (26 in). This corresponds to a non-dimensional increase from $(Z/R) = .043$ to $(Z/R) = .081$. For comparative purposes, the BLACK HAWK airframe hub-pylon separation distance is 53.3 cm (21 in).

In addition to the measured vibration and performance characteristics with the two mast heights, blade pressure and stress measurements will be obtained that detail the change in the resulting blade airload and response. Theoretically, the maximum change in blade airload due to airframe presence occurs in the vicinity of 40% radius and over the nose of the aircraft. The load change is almost impulsive in nature due to the abrupt potential flow upwash associated with flow acceleration over the nose and forward pylon. In the real world, the rotor wake can be expected to distort as it passes over the fuselage and the character of the interference may change accordingly. As such the calculated body on rotor interference levels, depicted in Figure (47), that were used to define the mast height variation are approximate. Comparison between these calculations and the measured data will be required to assess the modelling accuracy.

Canopy drumming due to blade passage over pressures can usually be detected from a spectral analysis of measured noise levels in the cockpit. In the case of significant activity, a spike will usually occur in phase with and at the blade passage frequency. As such, no special airframe instrumentation is required for detection.

DEVELOPMENT PLAN

Summary of Plan

The BLACK HAWK rotor configured RSRA development plan is concerned with the following major tasks presented in chronological order:

- a. Preliminary design and analysis
- b. Detail design and analysis
- c. Fabrication and procurement
- d. Ground test
- e. Delivery and installation
- f. Safety of flight review
- g. Contractor support of NASA flight test program
- h. Test in NASA/Ames 12m x 24m (40 x 80 ft) wind tunnel
(optional)

These tasks comprise the Statement of Work heading which define the development program recommended to provide the Government with a flightworthy BLACK HAWK rotor installed on RSRA. A Work Breakdown Structure (WBS) and associated cost estimates has also been developed.

The development program extends for a basic 24 month period culminating with the delivery and installation of the BLACK HAWK rotor system and related modifications to the RSRA flight vehicle. Beyond the basic development period, an additional support plan is presented. This is a sustaining 2 year Contractor support program for the NASA/Ames flight evaluation.

The development plan is presented in four sections. These are the Description of Work, the Statement of Work, the Work Breakdown Structure, and the Cost and Schedule Plan.

Description of Work

Preliminary design and analysis

The program plan starts with a review of all preliminary studies conducted during the feasibility analysis. The review will primarily focus on refining the conceptual blade and minimizing hardware qualification testing requirements. Whereas all hardware recommendations and analytical results reported in this contract will be subject to review, it is felt that the blade instrumentation (pressure tap arrays) and the ground test verification plan require further refine-

ment. Optimization of the pressure tap locations and installation technique is necessary for data accuracy assurance. Minimization of ground static and fatigue testing of the flight hardware is a difficult task to formulate since the deliverable rotor system is a mixture of previously qualified BLACK HAWK flight hardware and newly designed adaptation fittings.

The pressure tapped instrumented blade is currently laid out as a modified production blade with double Gaussian spanwise and chordwise tap arrays. As previously explained in the pre-design section, this technique greatly increases the accuracy of the pressure distributions that can be obtained with a given number of pressure sensors. The exact number of taps that should be used on each surface, as well as the juncture location between the fine mesh and loose mesh Gaussian distributions has not been determined. These will be fixed during the initial stage of the development program. The technique for installing the pressure taps in the blade skin will also be refined. Current plans call for the construction of a separate skin panel at each blade span station accepting a chordwise tap array. This skin, which replaces the production skin is slightly thicker, and must be feathered into the surrounding surface. Specification of the sensor holding skin thickness, width, and feathering rate will be defined. It is emphasized that the selection of the number of pressure taps and the minimization and control of contour distortion due to their presence will ultimately determine the accuracy of the flight pressure data.

The qualification testing plan, defined in the Statement of Work and priced in the WBS plan represents the current understanding of flight safety requirements. It is recognized, however, that further beneficial trade-offs may be possible regarding the definition of test systems. That is, the replacement of single component tests with tests of multiple part build-ups may offer an equivalent degree of safety assurance at a lesser cost. This aspect of the current development plan will be re-examined in detail prior to the test plan specification.

A third area which will receive major attention during the predesign review is the aerodynamic and dynamic specification of the 10% tip. Although a fixture design for mating the tip has been analyzed during the predesign effort, contour geometry was intentionally left nebulous. This was done to take advantage of several analytical and experimental research programs which are currently in progress and directly related to the 10% tip design goals. Included in these are advanced airfoil studies conducted by Sikorsky and model scale experimental studies in progress in the NASA/Langley Transonic Dynamics Tunnel. During the predesign review, the results of these efforts will be studied and a final flight test configuration selected. The selected design will likely incorporate planform taper and possibly anhedral in addition to sweep. If a new transonic airfoil section is

incorporated, transition between the new section and the SC1095-R8/SC1095 family will also have to be considered.

Detailed Design Study

The planned detail design effort will immediately follow the preliminary design review. During this period detailed design drawings will be prepared to effect the existing gear box modification, the BLACK HAWK rotor head adaption to the RSRA transmission shaft and existing fixed system control system, and construction of the pressure tapped instrumented blade hardware. In addition, detailed layouts will be prepared for the blade parametric change hardware. These consist of the 10% tip adaptation fitting, the 10% tip blade sections, and the spanwise extended SC1095-R8 airfoil leading edge modifications. As previously noted flightworthy blade tips already exist for the double swept and mini-anhedral tip geometries. As such, no further development work is required for these tips.

During detailed design, existing military specifications will be used where applicable. Where military specifications do not exist, specifications will be defined and documented from previous Sikorsky design practice. Critical loads will be calculated for new components inserted in existing high load paths. These will consist primarily of rotor head and control interface structures for the baseline rotor system and tip attachment fittings for the new extended tip. The critical load computation on the new rotating hardware will include the blade severence pyrotechnic package. These stress calculations will be augmented with fatigue life predictions based on the results of component final design geometries and physical properties. Weights estimates will be estimated and aeroelastic stability will be reviewed. Requirement for the latter will exist only if the total torsional stiffness of the blade-rotor head-control system deviates significantly from the predesign specifications. Finally, any new tooling associated with construction of the 10% tip, the leading edge modification, or the construction of the pressure tapped skin plies will be designed. The above design efforts implicitly include any facilities, systems, or components required for subsequent ground and flight qualification. Detail design drawings will be prepared for the new planetary components as well as minor integration requirements.

Fabrication

The fabrication phase of the program will be based on an experimental shop approach to minimize the development cost and schedule.

This approach entails:

- . Use of experimental type drawing for tooling and fabrication.

- Use of existing qualified RSRA components where possible.
- Use of soft tooling where possible; hard tooling will be used only where required from the standpoints of structural reliability cost or tolerances.
- Minimum machining rather than optimization of weight savings on interface hardwares.
- Machined metal components rather than use of shaped forgings.

As envisioned, the new tip caps will be primarily a composite-Nomex honeycomb structure with bonded in metal doublers where required. The two-half approach to construction of these caps has been demonstrated on other experimental caps (anhedral, etc) and is considered low risk despite the longer length. The modified tip retention block will be machined as required either from existing titanium forgings or from unforaged plate stock if forgings do not meet the dimensional requirements.

Airfoil leading edge modifications will be accomplished by hand contouring of a solid balsa wood core to the desired shape using templates. After checking of the balsa mass against required tolerances the core will be covered with fiberglass and polyurethane (for abrasion protection) and bonded to the spar leading edge using soft tooling. The technique has been demonstrated during the prototype completion flight test program and is considered low risk.

The pressure tapped blade as presently envisioned would start out as a basic production rotor blade except that appropriate instrumentation wiring and tubing would be bonded into the skin honeycomb aft fairing with leads terminating at the desired measurement stations. At these stations the skin and a portion of the core would be cut away in a chordwise strip. A pre-assembly pressure tapped module would be electrically attached to the leads and bonded into the cut away portion with over lapping at the edges for structural and contour continuity and the surface touched up as required to eliminate sharp discontinuities. The pre-assembled modules would be bench tested and qualified before installation to minimize the chance of having incorrectly functioning pressure instrumentation in the blade.

The control system will be assembled from purchased existing parts and new components which will be machined from plate stock.

Ground Test

Ground qualification testing will be performed on each component. Fatigue and static strength data obtained from these tests will then be used to calculate component fatigue life for use in reliability and maintainability analysis. For each separate test, appropriate test plans will be prepared describing test hardware, test techniques, and instrumentation and facility requirements.

The following component tests are currently planned. As previously noted, however, these may be altered during the pre-design review. These changes would be adopted only if qualification testing costs could be lowered without adversely affecting design verification.

- . Qualification testing of the modified main transmission assembly. The modified transmission will be qualified by 150 hours of sustained operation at up to 110% of design torque. Following successful completion of the prescribed test cycles, a partial tear down will be conducted to verify acceptable wear patterns on the modified components.
- . Fatigue testing of the modified swashplate assembly, one specimen will be tested.
- . Blade severance assembly (BSA) function verification. The BSA design, as reported in the pre-design section, has been modified to produce titanium spar severance. Verification of the modified design adequacy will consist of 6 pyrotechnic severance trials on representative titanium spar segments. Results of these tests will be reviewed to determine if a change in the linear charge size or stand-off distance is warranted. If design changes are made, additional test firings will be conducted to verify performance.
- . Fatigue testing under combined loads of the spar/tip fitting/tip cap attachment areas. Two specimens will be tested.
- . Fatigue testing of the rotor assembly with rotor mast height extenders. Load amplitudes will be based on calculated head moments for the new rotor on the RSRA. One of each specimen will be tested using a head and shaft test machine.
- . Calibration and testing of blade instrumentation. Installed pressure transducers on the pressure tapped instrumented blade will be checked for operational status. Calibration shifts due to installation procedures will be assessed. Defective gauges will be rephased to insure availability of a complete airload matrix.

Whirl Test

The purpose of the whirl test is to obtain qualification stress data on the two tip configurations which have not been previously whirled (the double swept and the 10% tip configuration), and to obtain general stress data on the pressure tapped blade rotor configuration. A secondary goal will be acquisition of performance data with the pressure tapped blade rotor configuration for comparison with baseline rotor performance. Although deterioration of aerodynamic sectional properties on the instrumented blade is not anticipated, verification of normal performance level is desired. Since the blades would be provided with the baseline airfoil configuration only this configuration would be whirled.

Prior to the whirl test, a detailed test plan will be prepared presenting run schedules, instrumentation requirements, and data requirements. Testing will be conducted on the Sikorsky 7457 kw (10,000 hp) main rotor whirl stand.

The basic rotor blades with three different tips will be dynamically and aerodynamically tracked and balanced before installation on the main rotor whirl stand. These procedures will be conducted on the 1491 kw (2000 hp) Sikorsky balance stand.

Safety of Flight Review

Prior to flight testing on the RSRA vehicle, the flightworthiness of the aircraft will be substantiated by a safety of flight review. In-house reviews will be initially conducted. Results of these informal reviews will be submitted to NASA for review prior to the formal review held with NASA personnel. Preparation for the review will include compilation of all data from previous ground tests and from structural, safety, and reliability analysis. Instrumentation and flight monitoring plans will be prepared. A flight test plan will be prepared for the initial shakedown flight program. Detailed safety and emergency plans will also be prepared and test pilot qualifications defined.

Each topic will be addressed in detail at the formal review. Upon approval of NASA, the shakedown flight program would be initiated.

Contractor Support of NASA Flight Test Activity

As requested by NASA/Ames, Sikorsky Aircraft will provide engineering technical support for a 2 year Government flight evaluation of the BLACK HAWK rotor configured RSRA. Since successful completion of the flight test evaluation requires multi-discipline support, coverage will be required in each of the following five disciplines. These disciplines are performance and power plants, structures, rotor dynamics, handling qualities, and instrumentation. It is assumed that

half time coverage in each of these areas will be adequate. This results in a 2 - 5 man-year effort for each of two years.

Whereas most of the support duties will be defined by the progression of the flight test program, specific tasks can be defined in certain areas. These are fabrication or procurement of spares required for the flight test program, definition of tasks required to implement the flight evaluation and preparation of maintenance and inspection manuals as related to new system hardware. In defining field operation tasks, plans will include logistics, operational support requirements, procedures, and equipment.

In addition to the effort described above, it is assumed that NASA will wish to conduct tests in which the in-board airfoil is extended onto the tip. To accomplish this, the blades would be returned to Sikorsky for installation of the modified airfoil. Only one set tips would be modified at that time the blades would be tracked and balanced on the 1491 kw (2000 hp) balance stand and returned to NASA. No whirl test is required for this modification.

AMES 40 ft x 80 ft Tunnel Test (Optional)

Sikorsky believes that a test of the BLACK HAWK rotor system in the Ames 12m x 24m (40 ft. x 80 ft.) wind tunnel is not required prior to testing on the RSRA vehicle. This is due to the maturity of the rotor system. Further, the issue of testing the entire RSRA vehicle in the Ames tunnel should probably addressed as a separate issue.

Statement of Work

A. Preliminary Design and Analysis

1. Perform preliminary stress, performance, and aeromechanical analysis of predesign components.
2. Conduct preliminary design reviews with related engineering discipline including aeromechanics, structures, and reliability, and manufacturing engineering to insure integrity of the integrated BLACK HAWK rotor system.
3. Update preliminary drawings based on results of design reviews and release for preliminary tool design of long lead time tools and conduct material planning.
4. Establish final aerodynamic configuration for 10% tip and perform related rotor stability analysis.

B. Detail Design and Analysis

1. Perform detail design and analysis of all new rotor and system components. Scope will include structural, dynamical, aeromechanical, performance stability and control, reliability and maintainability, handling qualities, weights.
2. Perform design of all tooling required for fabrication and assembly of system components.
3. Design all components required for ground and flight testing of systems or components.

C. Fabrication and Procurement

1. Establish schedule for parts and material procurement.
2. Procure parts and material.
3. Fabricate or procure required components for the rotor blades, the rotor head, the rotor head-RSRA control system interface, main transmission gear ratio change, blade severance, blade instrumentation, and blade modifications.
4. Assemble blade and rotor head assemblies for fatigue, static whirl, and flight test specimens.

D. Ground Tests

1. Component Tests

- a. Prepare structured test plans for the critical components. These tests will include at least.
 - (1) Head and shaft test of rotor head assembly under combined fatigue loads.
 - (2) Explosive severance tests of simulated titanium spare attachment section.
 - (3) Modified transmission qualification test.
 - (4) Simulated fatigue load test of 10% tip and attachment fitting.
 - (5) Head and shaft fatigue test of longer rotor height mast extender.
 - (6) Calibration and testing of rotor strain gauges.

- (7) Calibration of instrumented blade pressure transducers.
 - b. Assemble testing machines.
 - c. Instrument components as required.
 - d. Perform tests.
2. Whirl Test
 - a. Prepare whirl test plan for whirl qualification of two alternate tips. Plan shall include overspeed conditions of at least 110% of design maximum rotor speed.
 - b. Instrument the two modified blade tip configurations to monitor critical stress areas.
 - c. Install whirl test rotor on balance stand and adjust trim tabs, balance weights and pitch links to track and balance blade set.
 - d. Install one rotor and control system on whirl stand and perform whirl tests according to plan.
 - e. Remove rotor from stand after completion of testing.
3. Flight rotor instrumentation and blade tracking.
 - a. Prepare instrumented rotor blade for balance and tracking.
 - b. Install instrumented blade on balance stand. Balance and track the instrumented blade to same specification as non-instrumented blades.

E. Delivery and Installation of Four Bladed BLACK HAWK Rotor and Subsystems

1. Ship rotor and all related hardware (except modified outboard airfoil configuration) to NASA/AMES flight test facility.
2. Install rotor head, blades, and modified transmission on aircraft including blade severance system.

F. Safety of Flight Review

1. Analyze ground test data and review structural analysis to predict the flight characteristics of the RSRA with the baseline four-bladed BLACK HAWK rotor installed.
2. Define procedures for monitoring critical aircraft characteristics.
3. Prepare a 20 hour shakedown test program to demonstrate the airworthiness of the RSRA/BLACK HAWK rotor for future evaluation tests by the Government.
4. Submit safety of flight substantiation and shakedown flight test plan to the Government.
5. Hold safety of flight review with Government personnel, pilots, and other Sikorsky in-house experts.

G. Contractor Support of NASA Flight Test Activity

1. Provide a support crew to assist Government personnel during a 2 year Government flight evaluation. (2.5 men per year).
2. Provide qualified engineering assistance on an on-call basis during the flight tests.
3. Prepare a maintenance and inspection manual for an RSRA BLACK HAWK rotor as related to the Government evaluation test program.
4. Modify baseline blades with selected tip to extend in-board airfoil tip. Track and balance modified blades. Ship to NASA Ames.

Work Breakdown Structure

It should be noted that the Work Breakdown Structure (WBS) contained herein utilizes the numbering system contained in the WBS for the RSRA. This is done to provide consistency with previous RSRA documentation.

1.1.E.1.1	Mechanical Flight Controls Modifications	
1.1.E.1.1.1	Design	Design of new control system components. Preliminary stress and handling qualities analysis
1.1.E.1.1.1.1		Preliminary design review
1.1.E.1.1.1.2		Upgrade all preliminary design drawings based on results of design review
1.1.E.1.1.1.3		Perform design of all tooling required for fabrication and assembly by system components
1.1.E.1.1.2	Fabrication	
1.1.E.1.1.2.1		Establish schedule for parts and material procurement
1.1.E.1.1.2.2		Procure parts
1.1.E.1.1.2.3		Fabricate parts into assemblies for testing
1.1.F.1.1	RSRA Transmission Modifications	
1.1.F.1.1.1	Design	Preliminary stress and performance analysis
1.1.F.1.1.1.1		Preliminary design review
1.1.F.1.1.1.2		Upgrade all preliminary design drawings based on results of design review
1.1.F.1.1.1.3		Perform design of all tooling required for fabrication and assembly of system components
1.1.F.1.1.2	Fabrication	
1.1.F.1.1.2.1		Establish schedule for parts and material procurement
1.1.F.1.1.2.2		Procure parts
1.1.F.1.1.2.3		Fabricate parts into assemblies for testing
1.1.F.1.1.3	Testing	
1.1.F.1.1.3.1		Prepare structural test plans for the critical components

1.1.F.1.1.3.2	Run qualification test of modified transmission assembly
1.1.F.1.1.3.3	Partially tear down assembly, verify acceptable wear patterns
1.1.G.1.1	Rotor Hub Adaptation
1.1.G.1.1.1	Design
1.1.G.1.1.1.1	Preliminary stress and performance analysis
1.1.G.1.1.1.2	Preliminary design review
1.1.G.1.1.1.3	Upgrade all preliminary design drawings based on results of design review
1.1.G.1.1.1.4	Perform design of all tooling required for fabrication and assembly of system components
1.1.G.1.1.2	Fabrication
1.1.G.1.1.2.1	Establish schedule for parts and material procurement
1.1.G.1.1.2.2	Procure parts
1.1.G.1.1.2.3	Fabricate parts into assemblies for testing
1.1.G.1.1.3	Testing
1.1.G.1.1.3.1	Prepare structural test plans for the critical components
1.1.G.1.1.3.2	Test rotor head assembly under combined fatigue loads
1.1.G.1.2	Rotor Blade Adaptation (Blade Severance)
1.1.G.1.2.1	Design
1.1.G.1.2.1.1	Preliminary stress and performance analysis
1.1.G.1.2.1.2	Preliminary design review
1.1.G.1.2.1.3	Upgrade all preliminary design drawings based on results of design review
1.1.G.1.2.1.4	Perform design of all tooling required for fabrication and assembly by system components
1.1.G.1.2.2	Fabrication
1.1.G.1.2.2.1	Establish schedule for parts and material procurement

1.1.G.1.2.2.2	Procure parts
1.1.G.1.2.2.3	Fabricate parts into assemblies for testing
1.1.G.1.2.3	Testing
1.1.G.1.2.3.1	Blade severence assembly development testing
1.1.G.1.2.3.2	RTU functional testing
1.1.G.1.2.3.3	Lot acceptance testing
1.1.G.1.3	Airfoil Leading Edge Contour Modification
1.1.G.1.3.1	Design
1.1.G.1.3.1.1	Preliminary stress and performance analysis
1.1.G.1.3.1.2	Preliminary design review
1.1.G.1.3.1.3	Upgrade all preliminary design drawings based on results of design review
1.1.G.1.3.1.4	Perform design of all tooling required for fabrication and assembly of system components
1.1.G.1.3.2	Fabrication
1.1.G.1.3.2.1	Establish schedule for parts and material procurement
1.1.G.1.3.2.2	Procure parts
1.1.G.1.3.2.3	Fabricate parts into assemblies for testing
1.1.G.1.3.3	Testing
1.1.G.1.3.3.1	Install rotor on balance stand and track and balance blade set
1.1.G.1.4	Blade Tip Modifications
1.1.G.1.4.1	Design
1.1.G.1.4.1.1	Preliminary stress and performance analysis
1.1.G.1.4.1.2	Preliminary design review
1.1.G.1.4.1.3	Upgrade all preliminary design drawings based on results of design review
1.1.G.1.4.1.4	Perform design of all tooling required for fabrication

		and assembly of system components
1.1.G.1.4.2	Fabrication	
1.1.G.1.4.2.1		Establish schedule for parts and material procurement
1.1.G.1.4.2.2		Procure parts
1.1.G.1.4.2.3		Fabricate parts into assemblies for testing
1.1.G.1.4.3	Testing	
1.1.G.1.4.2.1		Fatigue test new 10% tip and attachment fitting
1.1.G.1.4.3.2		Prepare whirl test plan
1.1.G.1.4.3.3		Install rotor on balance stand and track and balance blade set for each of blade tip modification
1.1.G.1.4.3.4		Install rotor control system on whirl stand and perform whirl test for two sets of blade tips
1.1.G.1.5	Rotor Blade Fabrication	
1.1.G.1.5.1	Design	
1.1.G.1.5.1.1		Preliminary stress and performance analysis
1.1.G.1.5.1.2		Preliminary design review
1.1.G.1.5.1.3		Upgrade all preliminary design drawings based on results of design review
1.1.G.1.5.2	Fabrication	
1.1.G.1.5.2.1		Establish schedule for blade procurement
1.1.G.1.5.2.2		Procure blades
1.1.G.1.6	Rotor Mast Height Variation	
1.1.G.1.6.1	Design	
1.1.G.1.6.1.1		Preliminary stress and performance analysis
1.1.G.1.6.1.2		Preliminary design review
1.1.G.1.6.1.3		Upgrade all preliminary design drawings based on results of design review

1.1.G.1.6.1.4	Perform design of all tooling required for fabrication and assembly of system components
1.1.G.1.6.2	Fabrication
1.1.G.1.6.2.1	Establish schedule for parts and material procurement
1.1.G.1.6.2.2	Procure parts
1.1.G.1.6.2.3	Fabricate parts into assemblies for testing
1.1.G.1.6.3	Testing
1.1.G.1.6.3.1	Fatigue test rotor height mast extender
1.1.L.1.1	Rotor Blade Instrumentation
1.1.L.1.1.1	Evaluate various candidate transducers for task
1.1.L.1.1.2	Determine optimum spanwise and chordwise locations for pressure transducers
1.1.L.1.1.3	Design
1.1.L.1.1.3.1	Design skin panels to accept chordwise pressure tap array
1.1.L.1.1.3.2	Preliminary design review
1.1.L.1.1.3.3	Upgrade drawings based on results of design review
1.1.L.1.1.4	Fabrication
1.1.L.1.1.4.1	Establish schedule for parts and material procurement
1.1.L.1.1.4.2	Procure parts
1.1.L.1.1.4.3	Fabricate rotor blade for testing
1.3.2.1	Ground Testing
1.3.2.1.1	Calibrate and test rotor strain gauges
1.3.2.1.2	Calibrate and test blade pressure transducers
1.3.2.2	Whirl Testing
1.3.2.2.1	Prepare instrumented rotor blade for balance and tracking
1.3.2.2.2.	Balance and track the instrumented blade
1.3.3.1	Rotor System Test Program

1.3.3.1.1	Rotor/RSRA Flight Test
1.3.3.1.1.1	Delivery and Installation of rotor and subsystems
1.3.3.1.1.2	Shipment of rotor and all related hardware to NASA/Ames flight test facility
1.3.3.1.1.2	Transportation of engineering and shop personnel
1.3.3.1.1.3	Installation of rotor head, blades, and modified transmission on RSRA (including blade severance system)
1.3.3.1.1.2	Safety of Flight Review
1.3.3.1.1.2.1	Analysis of ground test data and structural analysis to predict RSRA flight characteristics with rotor installed
1.3.3.1.1.2.2	Determine procedures for monitoring critical aircraft characteristics
1.3.3.1.1.2.3	Prepare and submit 20 hour shake-down test program to demonstrate RSRA/rotor airworthiness to government
1.3.3.1.1.2.4	Hold Safety c: Flight review with government personnel, pilots, etc.
1.3.3.1.1.3	Contractor Support of NASA Flight Test Activity
1.3.3.1.1.3.1	Provide support crew to assist government personnel during 2 year government flight evaluation
1.3.3.1.1.3.2	Provide qualified engineering assistance during flight tests
1.3.3.1.1.3.3	Prepare maintenance and inspection manual for RSRA/rotor

Cost and Schedule Plan

Using the Contractor's Work Breakdown Structure as a framework, the funding plan for all phases of design, fabrication and contractor's testing up to delivery is presented in Table 28; the master phasing schedule is shown in Table 29.

Planning estimates were prepared by the responsible functional sections of the engineering and manufacturing departments based on: (a) the work statements for design, fabrication and test; (b) extent and complexity of designs; (c) predesign information defining the hardware (d) professional judgment obtained from experience on Simior and RSRA programs.

Material cost, that become part of the delivered aircraft end item, was estimated and adjusted to reflect hardware changes, complexity, size and weight differences of the RSRA. These costs are included in the manufacturing estimate; also included in the manufacturing estimates are the cost for material consumed in fabricating tools and aircraft parts consumed in testing. Material cost to set-up and perform tests is included in testing cost.

The assumptions used in the schedule and cost analysis are as follows:

- . NASA shall provide the test vehicle.
- . NASA shall retain control of the aircraft and support the aircraft with material, fuel, and technicians to maintain the aircraft in a flightworthy condition.
- . NASA shall provide the interface between the aircraft and the Sikorsky Aircraft designed hardware and will provide the labor for installation and test.
- . NASA shall provide office space and office furniture for Sikorsky Aircraft personnel in installation, test, and support phases for two years.
- . A UH-60A main rotor head for flight test and fatigue test will be provided as GFE to the project. The cost for this item is not included in the estimate.
- . The RSRA aircraft will fly in helicopter mode (wings will not be used).
- . Experimental type drawings will be used.
- . Experimental type tooling will be used.
- . Sikorsky Aircraft will provide at no cost the existing swept tapered tips and anhedral tips (assuming successful

completion of contract DAAK51-81-C-0011, "Flight Evaluation of Main Rotor with Anhedral Tips") for research testing by NASA. Installation costs for pressure instrumentation of these tips will be borne by NASA. Refurbishment, if required is not included.

- . Since start date is not definitized, price is subject to adjustments in calendar years in which work shall be performed.
- . Prices of certain goods and services to be provided to the contractor in the performance of this program are at best estimates and would change in the definitization of the statement of work and period of performance.

DOCUMENTATION LIST

The following Contractor reports will be required for design and safety of flight substantiation.

1. Design and Integration Report
2. Performance Report
3. Aeroelastic Stability Report
4. Instrumentation Report
5. Component Qualification Reports
 - . Rotor Head and Control System
 - . Transmission Modifications
 - . Blade Severence
6. Whirl Test Report
 - . All Tip Shapes
 - . Baseline and pressure Tapped Blades
7. Maintenance and Inspection Manual
8. Safety of Flight Report

CONCLUSIONS

1. Of the three rotor configurations evaluated, the UH-60A BLACK HAWK rotor system best meets the technical and cost objectives set forth by NASA because it is an advanced state-of-the-art rotor, that requires minimal RSRA adaptive hardware and readily lends itself to significant research studies.
2. The smaller diameter of the BLACK HAWK rotor requires a transmission modification to alter rotor RPM, but this was judged to involve less risk and cost than providing root extenders to increase the diameter.
3. The smaller diameter of the BLACK HAWK rotor does not compromise handling quality characteristics and permits an operating envelope sufficient to accomplish desired research objectives.
4. A research program that defines not only the baseline rotor characteristics but also the effects of such important design variables as outboard airfoil, tip speed, tip taper, tip sweep, tip anhedral and rotor-fuselage separation can be efficiently accomplished with the selected rotor system using three existing sets of tips and a proven airfoil modification technique.
5. For planning purposes, it is estimated that the BLACK HAWK rotor system could be available for testing four different tip designs, one outboard airfoil design and two rotor-fuselage separation distances in 24 months for a cost of \$6.098 million. A second modified blade configuration incorporating an altered out-board airfoil design could be made available within four months after completion of NASA baseline blade tests.

REFERENCES

1. Kuczynski, W.A., Madden, J. "The RSRA Active Isolation/Rotor Balance System," Journal of the American Helicopter Society, Vol. 25, No. 2, April, 1980.
2. Miao, W. and Mouzakis, T. "Bifilar Analysis Study" NASA CR-159227, Sikorsky Aircraft, August 1980.
3. Peters, D. A., "Flap-Lag Stability of Helicopter Rotor Blades in Forward Flight," Journal of the American Helicopter Society, October 1975.
4. Johnston, R. A. and Cassarino, S. J. "Aeroelastic Rotor Stability Analysis," USAAMRDL TR-75-40, U. S. Army Aviation Material Laboratory, Fort Eustis, Virginia, January 1976.
5. Marshall, J., and Miao, W. Revision 2 (5/10/78) to Sikorsky Engineering Report SER-70545, "UH-60A Aeroelastic Stability Analysis Report."
6. Niebanck, C., "SH-60B Aeroelastic and Mechanical Stability Report" Sikorsky Engineering Report SER-520105 November 7, 1979.
7. Blackwell, R.H., "YEH-60B Aeroelastic Stability Analysis Report" Sikorsky Engineering Report SER-70378 November 10, 1980.
8. Sikorsky Engineering Test Report ETR F1-0223.
9. Sheehy, T. W. "An Aerodynamic Analysis Technique for Arbitrary Rotorcraft/Aircraft Configurations," Sikorsky Engineering Report 50964, June 1976.
10. Carta, F. O. and St. Hilaire A. O., "Effect of Interblade Phase Angle and Incidence Angle on Cascade Pitching Stability. Transactions of the ASME, Journal of Engineering for Power, Vol. 102, No. 2, pp. 391 - 396, April 1980.
11. St. Hilaire, A. O., Carta, F. O., Fink, M. R., and Jepson, W. D., "The Influence of Sweep on the Aerodynamic Loading of an Oscillating NACA 0012 Airfoil. Vol. I - Technical Report. NASA Contractor Report 3092, May 1979.
12. Hardin, L. W., "An Experimental Study of the Response of a Turbomachine Rotor to a Low Frequency Inlet Distortion. North Carolina State University, Engineering Design Center Report EDC-78-6 (AFOSR-TR-79-0073), December 1978.

13. Dring, R. P., et al, "Experiment on Turbine Rotor-Stator Aerodynamic Interaction. Work in progress under AFAPL Contract No. F33615-80-C-2008. (to be published).
14. St. Hilaire, A. O., "The Segmented Gaussian Quadrature and its Application for Optimizing Airfoil Instrumentation Arrays. United Technologies Research Center Report UTRC76-150, October 5, 1976.
15. Milne, W. E., "Numerical Calculus, Princeton University Press, 1949, pp. 285 - 290.
16. Weller, W. H., "Experimental Investigation of Effects of Blade Tip Geometry on Loads and Performance for an Articulated Rotor System," NASA Technical Paper 1303, January 1979.
17. Davis, S. J. and Egolf, T. A., "An Evaluation of a Computer Code Based on Linear Acoustic Theory for Predicting Helicopter Main Rotor Noise," NASA Contractor Report 159339 July 1980.

<u>PARAMETER</u>	<u>BLADE</u>	<u>S-61</u>	<u>BLACK HAWK</u>	<u>H-3 COMPOSITE</u>
Radius ¹ m (ft)		9.449 (31)	8.178 (26.83)	9.449 (31)
Chord ² m (ft)		.463 (1.52)	.527 (1.73)	.527 (1.73)
Solidity ³		.0775	.082	.071
Twist		-8°	-16° non-linear	-16° non-linear
Airfoils		0012	SC1095 & SC1095-R8	SC1095
Swept Tip Extent		N/A	5.8%	5%
Sweep Angle		N/A	20°	20°
Root Cut Out ¹		18%	20%	20%
Blade Weight kg (lb)		150.4 (331.5)	95.25 (210)	122.5 (270)
Construction		Aluminum Spar, Nomex Pockets	Titanium Spar, Nomex Core, Fiberglass Skin	Composite Graphite Epoxy

- NOTES:
- 1) Referenced to original rotor head, BLACK HAWK or S-61.
 - 2) BLACK HAWK nominal chord for SC1095 portion of blade.
 - 3) $\frac{bc}{nR}$

TABLE 1. ROTOR CHARACTERISTICS COMPARISON

- 1 - DESIRABLE
 3 - ACCEPTABLE
 5 - MAJOR PROBLEMS

	COMP H-3 ROTOR	STANDARD B.M. ROTOR	STANDARD B.M. ROTOR EXTENDERS
	<u>XMSII CHANGE</u>		
TECHNOLOGY LEVEL OF BASELINE SYSTEM	2	1	2
INTEGRATION HARDWARE NEEDS	2	2	3
SIZE SUITABILITY	1	3	1
ADAPTABILITY OF ROTOR SYSTEM TO PARAMETRIC CHANGES	3-5	1	1
ESTIMATED COST FOR INTEGRATION AND PARAMETRIC CHANGES	3	1	3
FUTURE RESEARCH CAPABILITY	2	2	2
TOTAL	13-15	10	12

TABLE 2. ROTOR CHOICE SCORING

<u>Objective</u>	<u>Rotor</u>	<u>Data Required For</u>					<u>New Hardware Required</u>
		<u>Perf.</u>	<u>Dynamic</u>	<u>Acoustics</u>	<u>Stability & Control</u>	<u>Existing Hardware</u>	
Establish current technology data base	BLACK HAWK	X	X	X	X	Baseline BLACK HAWK rotor	BLACK HAWK head adaptation, transmission gearing change, blade severence
Define impact of low tip speed - high airfoil C _{LMAX} operation	Baseline with leading edge mod, altered tip speed	X	X	X	X	BLACK HAWK blades with and without leading edge change	None - testing can be conducted with current transmission speed and gearing change required for baseline
Define impact of tip geometry on rotor characteristics	Baseline and existing tapered swept tip	X	X	X	X	Tapered swept	None
	Baseline and existing swept tapered anhedral tip	X	X	X	X	Tapered swept anhedral tip	None
	Baseline and new thin airfoil tip	X	X	X	X		Fabrication of new tip
Define impact of rotor body separation of vibration	Baseline with high mast	X	X				Mast extender

ORIGINALLY CONSTRUCTED
OF POOR QUALITY

TABLE 3. POSSIBLE RESEARCH PROGRAM USING THE BLACK HAWK ROTOR

ROTOR SYSTEM WEIGHT BREAKDOWN	STANDARD BLACK HAWK ROTOR H-3 COMPOSITE	BLACK HAWK ROTOR WITH XMSN CHANGE	BLACK HAWK ROTOR WITH EXTENDERS
Weight Empty + Basic Instrumentation	7790.4 KG (17,175 lb)	7790.4 KG (17,175 lb)	7790.4 KG (17,175 lb)
Pilot	181.4 KG (400 lb)	181.4 KG (-400 lb)	181.4 KG (400 lb)
Increment in Weight Empty for Rotor Blades	-18.1 KG (-40 lb)	-181.4 KB (-400 lb)	-116.1 KG (-256 lb)
Additional Instrumentation	90.7 KG (200 lb)	90.7 KG (200 lb)	90.7 KG (200 lb)
Fuel for Mission	2016.7 KG (4,446 lb)	1508.2 KG (3,325 lb)	2016.7 KG (4,446 lb) (Max fuel)
Total	10061.1 KG (22,181 lb)*	9389.4 KG (20,700 lb)**	9963.2 KG (21,965 lb)***

ORIGINAL DESIGN
OF POOR QUALITY

- * 17.37M (57 ft) 1Gf hover at XMSN limit (SLS)
- ** 1Gf hover at SLS
- *** 14.63M (48 ft) 1Gf hover at XMSN limit (SLS)

TABLE 4. IGE MAXIMUM TOGW'S FOR THREE ROTOR CONFIGURATIONS

IGE HOVER @ SLS			
TOGW	9389.4 KG	(20,700 lb)	
5 Min Hover	-62.1 KG	(-137 lbs) fuel	
257.4 km (139 n.mi) Cruise @ V_{BR}	-578.3 KG	(-1,275 lb) fuel	
257.4 km (139 n.mi) Cruise @ 1864 kw (2500 HP)	-715.8 KG	(-1,578 lb) fuel	
Reserve (10%)	7881.3 KG	(17,375 lb)	

ORIGIN OF POOR QUALITY

TABLE 5. RSRA MISSION RESEARCH CAPABILITY WITH BLACK HAWK ROTOR

ROTOR	H-3 COMPOSITE ROTOR NEW HARDWARE REQUIRED*	BLACK HAWK ROTOR NEW HARDWARE REQUIRED*	BLACK HAWK ROTOR WITH EXTENDERS NEW HARDWARE REQUIRED*
ESTABLISH CURRENT TECHNOLOGY DATA	H-3 COMPOSITE BLADE ATTACHMENTS	BLADE ROOT END BASELINE B.H. ROTOR	TRANSMISSION GEARING CHANGE
EVALUATE TIP SPEED : AIRFOIL C MAX TRADES	H-3 COMPOSITE BLADE WITHOUT LEADING EDGE MODIFI- CATION	B.H. BLADES WITH LEADING EDGE CHANGE	B.H. BLADES EXTENSION OF INBOARD AIR- FOIL
DEFINE IMPACT OF TIP GEOMETRY ON ROTOR CHARACTER- ISTICS	TAPERED SWEPT TIP	FABRICATION OF INTERCHANGEABLE TIP FITTING (MAJOR REWORK OF BLADE)	LAYERED SWEPT TIP
	TAPERED SWEPT ANHEDRAL TIP	FABRICATION OF INTERCHANGEABLE TIP FITTING (MAJOR REWORK OF BLADE)	LAYERED SWEPT ANHEDRAL TIP
	NEW 10% TIP	FABRICATION OF NEW TIP, INTERCHANGEABLE TIP FITTING (MAJOR REWORK OF BLADE)	FABRICATION OF NEW TIP AND ASSEMBLY

OF POOR QUALITY

* B.H. ROTOR HEAD ADAPTATION, BLADE SEVERANCE COMMON TO ALL ROTORS.

TABLE 6. RESEARCH OBJECTIVES – HARDWARE REQUIREMENTS FOR VARIOUS ROTOR CONFIGURATIONS

ROTOR SYSTEM INTEGRATION MODIFICATIONS	COMPOSITE H-3		STANDARD B.H. ROTOR XSMN CHANGE		STANDARD B.H. ROTOR LXENDERS	
	ROTOR	-	-	-	-	-
BLADE ROOT END ATTACHMENTS	\$550K	-	-	-	-	-
MODIFIED RSRA XSMN PARTS	-	-	\$730K	-	-	-
ROTOR EXTENDERS	-	-	-	-	\$1100K	-
PARAMETRIC CHANGES TO ROTOR HARDWARE REQUIRED	INTERCHANGEABLE TIP FITTINGS	-	\$750K	-	-	-
TOTAL	\$1300K	\$730K	\$1100K	\$750K	\$1100K	\$750K

*ESTIMATED COSTS BASED ON 1981 \$ AND PRICES.

NOTE: B.H. ROTOR HEAD ADAPTATION, BLADE SEVERANCE NOT INCLUDED IN THESE COSTS AS THESE ARE COMMON TO ALL THREE ROTOR SYSTEMS.

TABLE 7. ESTIMATED COSTS FOR ROTOR INTEGRATION AND PARAMETRIC CHANGE HARDWARE

FORWARD FLIGHT ENVELOPE NOT SIGNIFICANTLY DIFFERENT FOR 3 ROTOR CONFIGURATIONS

ROTOR CONFIGURATION	H-3 COMPOSITE ROTOR	BLACK HAWK ROTOR WITH XSMN CHANGE	BLACK HAWK ROTOR WITH EXTENDER
ALT/TEMP	% INCREASE IN MAX FWD FLIGHT CRUISE SPEED OVER NOMINAL RSRA VALUES	% INCREASE IN MAX FWD FLIGHT CRUISE SPEED OVER NOMINAL RSRA VALUES	% INCREASE IN MAX FWD FLIGHT CRUISE SPEED OVER NOMINAL RSRA VALUES
SL, STD	3.1%	3.6%	1.2%
3000', STD	5.7%	4.4%	3.8%

ORIGINAL DATA
OF POOR QUALITY

NOTE: V_{MAX} OCCURS AT THE TORQUE LIMIT FOR THE RSRA XMSN (64674 FT-LB) OR
2500 IIP @ 203 RPM.

TABLE 8. COMPARISON OF FORWARD FLIGHT ENVELOPE OF VARIOUS ROTOR CONFIGURATIONS

CHART OF POOR CIRCUMSTANCES

Design HP	=	2220
RPM Sun	=	939
RPM Out	=	257
No. of Pinions	=	5
Pressure Angle	=	22 $\frac{1}{2}$ ^o
Diametral Pitch	=	8
Reduction Ratio	=	3.6468

SUN CM (IN)		PINION CM (IN)		RING CM (IN)	
No. of Teeth	74		61		196
Outside Diameter	24.1300	(9.5000)	20.0025	(7.8750)	61.5950
Pitch Diameter	23.4950	(9.2500)	19.3675	(7.6250)	62.2300
Root Diameter	22.7228	(8.9460)	18.5534	(7.3045)	63.0174
Face Width	6.6040	(2.600)	6.2230	(2.450)	7.3025
 PROPOSED					
No. of Teeth	54		71		197
Outside Diameter	17.7800	(7.0000)	23.1775	(9.1250)	61.5950
Pitch Diameter	17.1450	(6.7500)	22.5425	(8.8750)	62.2300
Root Diameter	16.3830	(6.4500)	21.7714	(8.5714)	63.0174
Face Width	8.7249	(3.435)	8.6360	(3.400)	7.3025

TABLE 9. BASIC PLANETARY STAGE DATA FOR MODIFIED RSRA TRANSMISSION

ON
OF POOR QUALITY

WEIGHT COMPARISON KG (LBS)

ITEM DESCRIPTION	UNIT WT	RSRA - S61		REQ.	QTY.	UNIT WT	TOT WT	PROPOSED
		UNIT WT	TOT WT					
Pinion	6.94	(15.30)	34.70	(76.50)	5	3.61	(7.95)	18.03
Bolts - NAS1309-80	.205	(.451)	2.05	(4.51)	10	NA	NA	NA
Bolts - NAS1309-76	.196	(.433)	.982	(2.165)	5	NA	NA	NA
O Ring - MS29561-251	.005	(.012)	.027	(.06)	5	NA	NA	NA
Nut - MS20365-9180	.030	(.066)	.449	(.99)	15	NA	NA	NA
Washer - MS9320-15	.012	(.026)	.295	(.65)	5	.0050	(.011)	.025
Roller Bearings	8.35	(18.40)	41.73	(92.00)	5	3.97	(8.75)	19.84
Plug - 56136-20679	.12	(.27)	.612	(1.35)	5	NA	NA	NA
Thrust Washers	.20	(.45)	2.04	(4.50)	10	.177	(.39)	1.77
Set Screw S6135-20693-1-2	.002	(.005)	.045	(.10)	20	NA	NA	NA
Washer - S6135-20195	.0018	(.004)	.181	(.04)	10	.0018	(.004)	.018
Spacer - S6135-20196	.0099	(.022)	.099	(.22)	10	.0099	(.022)	.099
Buffer Plate S6135-20125	.091	(.20)	.907	(2.00)	10	NA	NA	NA
Seal S6135-20059-4	.014	(.03)	.014	(.03)	1	.014	(.03)	.014
Spacer S6135-22014-1-2	.109	(.24)	1.633	(3.60)	15	NA	NA	NA
Plates, Match Set	14.61	(32.20)	14.61	(32.20)	1	39.64	(87.40*)	39.64
Collector Ring S6135-20126	.635	(1.40)	.635	(1.40)	1	.635	(1.40)	.635
Nut - S6135-20675	.426	(.94)	4.26	(9.40)	10	NA	NA	NA
Bearing Shaft	NA	NA	NA	NA	5	2.20	(4.86)	11.02
Nut, Bearing Shaft	NA	NA	NA	NA	5	.454	(1.00)	2.27
Bearing Spacer	NA	NA	NA	NA	10	.209	(.46)	2.09
Bolt NAS 1309-14	NA	NA	NA	NA	5	.070	(.154)	.349
Bolt NAS 1309-66	NA	NA	NA	NA	20	.172	(.38)	3.45
Nut SS 5086-9	NA	NA	NA	NA	25	.027	(.06)	.68
Spacer	18.96	(41.80)	18.96	(41.80)	1	18.96	(41.80)	18.96
Ring Gear S6135-	6.21	(13.68)	6.21	(13.68)	1	6.695	(14.76)	6.695
Sun Gear S6135-						Net Wt.		
Planet Assy	Net Wt.	130.27	(287.19)			Net Wt.	127.13	(280.27)

*Proposed Planetary uses Steel Plates vs. Titanium for Current Models.

TABLE 10. WEIGHT COMPARISON BETWEEN PROPOSED AND STANDARD TRANSMISSION

~~OPTIONAL~~
GEAR REDUCTION RATIOS

<u>Reduction Ratios</u>	<u>RPM</u>
4.629 (production S-61)	203
4.062	231
3.882	242
3.648 (chosen)	257
3.45	272
3.33	282
3.279	286
3.130	300

NOTE: Above ratios all utilize the same 196 tooth ring gear with 8 diametral pitch teeth.

TABLE 11. POSSIBLE ALTERNATE RPM'S AND GEAR REDUCTION RATIOS

TABLE 12. UH-60A AND S-61 MAIN ROTOR HUB MOMENT CAPABILITY

DATA	UH-60A	S-61
RPM	258	213
Blade Moment of Inertia KG - M ³ (ft-lb-sec ²)	2053.3 (1516)	2053.3 (1516)
Offset m (ft)	.381 (1.25)	.381 (1.25)
Blade First Moment of Mass kg-sec ² (lb-sec ²)	39.39 (86.83)	39.39 (86.83)
Number of Blades	4	4
Hub Moment/Cyclic Flapping Angle kg-m/deg (ft-lb/deg)*	382.4 (2765)	260.6 (1884)
		265.9 (1923)

$$*\frac{\partial M}{\partial \dot{a}_1} = \Omega^2 e s_B \frac{n}{2} \frac{\pi}{180} FT-LB/RAD$$

CHART 12
OF POOR QUALITY

<u>Description</u>	<u>Units</u>	<u>Value</u>
Rotor Radius R	cm (in.)	817.9 (322)
Rotor Solidity $bc/\pi R$	-	.0821
Lock Number $2\pi\rho CR^4/I_B$	-	8.84
Hinge Offset e	cm (in.)	38.1 (15)
Blade Moment of Inertia about Hinge	kg-m^2 (in.-lb-sec ²)	2053.2 (18191)
Blade First Mass Moment about Hinge	kg-sec^2 (lb-sec ²)	39.39 (86.838)

TABLE 13. UH-60A ROTOR BLADE DATA FOR PITCH-FLAP LAG ANALYSIS

**ORIGIN OF
OF POOR QUALITY**

ITEM	UNITS	VALUE
Main Rotor Station	cm (in)	762 (300)
Main Rotor Water Line	cm (in)	767.1 (302)
Main Landing Gear Station	cm (in)	607.1 (239)
Main Landing Gear Butt Line	cm (in)	± 165.1 (± 65)
Main Landing Gear Contact Water Line	cm (in)	325.1 (128)
Tail Landing Gear Station	cm (in)	1854.2 (730)
Tail Landing Gear Contact Water Line	cm (in)	325.1 (128)

TABLE 14. RSRA AIRCRAFT GEOMETRIC DATA GROUND STABILITY ANALYSIS

RSRA AIRCRAFT MASS DATA FOR GROUND STABILITY ANALYSIS
 (ROTOR OFF) (8346.1 kg (18,400 lb.) G.W.)

ITEM	UNITS	VALUE
Weight	kg (lb)	7615.8 (16,790)
Center of Gravity Station	cm (in)	750.8 (295.6)
Center of Gravity Water Line	cm (in)	568.5 (223.8)
Roll Moment of Inertia	kg-m ² (in-lb-sec ²)	8787. (77849.)
Pitch Moment of Inertia	kg-m ² (in-lb-sec ²)	130023. (1152000.)
Yaw Moment of Inertia	kg-m ² (in-lb-sec ²)	125846. (1115000.)

CONTINUE ON PAGE 74
 OF POOR QUALITY

TABLE 15. RSRA AIRCRAFT MASS DATA FOR GROUND STABILITY ANALYSIS

ORIGINAL DATA
OF POOR QUALITY

<u>ITEM</u>	<u>UNITS</u>	<u>MAIN OLEO</u>	<u>TAIL OLEO</u>
Pressure x Volume of Oleo Gas	N·M (lb-in.)	4027 (35640)	2237 (19802)
Preload	kg (lb)	1225 (2700)	488 (1075)
Static Nominal Load	kg (lb)	3674 (8100)	954 (2100)
Static Nominal Deflection	cm (in.)	22.35 (8.8)	22.86 (9.0)
Adiabatic Exponent	-	1.34	1.34
Damping	$\frac{\text{N}\cdot\text{sec}}{\text{m}}$ (lb-sec/in.)	4903.6 (28)	6129.4 (35)

TABLE 16. RSRA AIRCRAFT LANDING GEAR DATA FOR GROUND STABILITY ANALYSIS

ORIGINAL
OF POOR

RSRA AIRCRAFT TIRE STIFFNESS DATA FOR GROUND STABILITY ANALYSIS - 8346.1 kg (18,400 lb) G.W.

CONDITION	MAIN TIRE				TALL TIRE			
	Load kg (lb)	Lateral Stiffness 10^5 N/M (lb/in)	Vertical Stiffness 10^5 N/M (lb/in)	Fore-Aft Stiffness 10^5 N/M (lb/in)	Load kg (lb)	Lateral Stiffness 10^5 N/M (lb/in)	Vertical Stiffness 10^5 N/M (lb/in)	
0% AIRBORNE	3688 (8131)	8.23 (4700)	18.65 (10650)	15.41 (8800)	969 (2136)	6.30 (3596)	10.86 (6200)	
20% AIRBORNE	2968 (6543)	7.36 (4200)	18.65 (10650)	14.54 (8300)	741 (1633)	6.35 (4628)	10.16 (5300)	
40% AIRBORNE	2248 (4955)	6.48 (3700)	17.34 (9900)	13.66 (7800)	513 (1131)	6.43 (3670)	9.11 (5200)	
50% AIRBORNE	1887 (4160)	5.95 (3400)	15.94 (9100)	13.13 (7500)	399 (879)	6.47 (3693)	8.41 (4630)	
60% AIRBORNE	1527 (3366)	5.43 (3100)	14.19 (8100)	12.35 (7050)	285 (628)	6.51 (4720)	7.44 (4250)	
65% AIRBORNE	1346 (2968)	4.99 (2850)	13.75 (7850)	11.91 (6800)	228 (502)	6.54 (3735)	7.01 (4090)	
70% AIRBORNE	1167 (2572)	4.73 (2700)	12.96 (7400)	11.56 (6600)	171 (377)	6.57 (3749)	6.65 (3800)	
75% AIRBORNE	987 (2175)	4.38 (2500)	12.26 (7000)	10.95 (6250)	114 (251)	6.59 (3765)	6.13 (3900)	
80% AIRBORNE	806 (1777)	3.85 (2200)	11.56 (6600)	10.33 (5900)	57 (125)	6.62 (1781)	5.60 (3200)	
90% AIRBORNE	474 (1046)	2.98 (1700)	10.33 (5900)	8.93 (5100)	0 (0)	0 (0)	0 (0)	

TABLE 17. RSRA AIRCRAFT TIRE STIFFNESS DATA FOR GROUND STABILITY ANALYSIS - 8346.1 kg (18,400 lb) G.W.

Mode No.	Description	$\frac{kg}{Hz} \left(\frac{lb \cdot sec^2}{in.} \right)$	ϵ_x (in.)	ϵ_y (in.)	ϵ_z (in.)	MOTOR HEAD SHAPE			ϵ_u (in.)	ϵ_v (in.)	ϵ_w (in.)
						ϵ_1	ϵ_2	ϵ_3			
1 Rigid body roll		0 (19.90)	0 (0)	2.54 (1)	0 (0)	- .00632 (0)	0 (0)	.00016 (.0004)	-.00005 (-.0008)	-2.11 (-.831)	.656 (-.259)
2 Rigid body pitch		0 (555.9)	2.54 (1)	0 (0)	-2.997 (-1.18)	0 (0)	.0001 (.0006)	0 (0)	-1.40 (-1.31)	0 (0)	.11 (2.01)
3 Rigid body vertical		0 (21.4)	2.54 (1)	0 (0)	-5.34 (-2.24)	0 (0)	-.0013 (-.0032)	0 (0)	3.54 (1.392)	0 (0)	.23 (-2.648)
4 Rigid body fore-aft		0 (42.16)	2.54 (1)	0 (0)	.968 (.389)	0 (0)	.0007 (.0018)	0 (0)	2.92 (.736)	0 (0)	.68 (1.661)
5 Rigid body lateral		0 (26.74)	0 (0)	-2.54 (-1)	0 (0)	-.00213 (.0054)	0 (0)	.0011 (.0026)	-.121 (-.0416)	-2.06 (-.611)	.22 (.0913)
6 Rigid body yaw		0 (74.66)	0 (0)	-2.54 (-1)	0 (0)	.0011 (.0027)	0 (0)	-.0026 (-.0066)	.126 (.1127)	.667 (.3412)	.17 (.0460)
7 Lateral bending		5.3 (190.9)	.0121 (0)	-2.54 (-1)	-7.11 (-2.8)	.0026 (.0067)	0 (0)	0 (0)	0 (0)	2.54 (1.0)	.337 (0.6)
8 Engine		7.5 (55.5)	.963.2 .0605 (0)	-2.54 (-1)	0 (0)	0 (0)	0 (0)	0 (0)	0 (0)	0 (0)	0 (0)
9 2nd lateral bending		10.0 (144.2)	.25253 .02779 (0)	-2.54 (-1)	0 (0)	0 (0)	0 (0)	0 (0)	0 (0)	1.27 (.05)	0 (0)
10 Transmission roll		12.6 (19.23)	.3367.7 .147 (0)	-2.54 (-1)	-20.3 (-.08)	.003 (0.0333)	0 (0)	0 (0)	0 (0)	0 (0)	.795 (.313)
11 Vertical bending		6.1 (26.74)	.4682.9 .0914 (1)	0 (0)	-.19 (-.75)	0 (0)	.00026 (.0007)	0 (0)	0 (0)	0 (0)	.668 (-.631)
12 Transmission pitch		10.1 (5.92)	.1036.8 .0546 (1)	2.54 (0)	.33 (.13)	0 (0)	.0053 (.0134)	0 (0)	0 (0)	0 (0)	.785 (-.309)
13 Tall cone vertical		10.9 (7.29)	.1276.7 .0507 (1)	2.54 (0)	-.58 (-.23)	0 (0)	.0056 (.0143)	0 (0)	0 (0)	0 (0)	.363 (-.43)
10.1 Transmission roll - ABS locked		13.6 (10.06)	.1761.8 .0605 (0)	-2.54 (-1)	.203 (.08)	.013 (.0333)	0 (0)	0 (0)	0 (0)	0 (0)	.95 (.313)
12.1 Transmission pitch - ABS locked		13.1 (14.4)	.2521.8 .0257 (1)	2.54 (0)	.33 (.13)	0 (0)	.0053 (.034)	0 (0)	0 (0)	0 (0)	.363 (-.43)

TABLE 18. RSRA NATURAL MODE PROPERTIES

UH-60A ROTOR ON RSRA

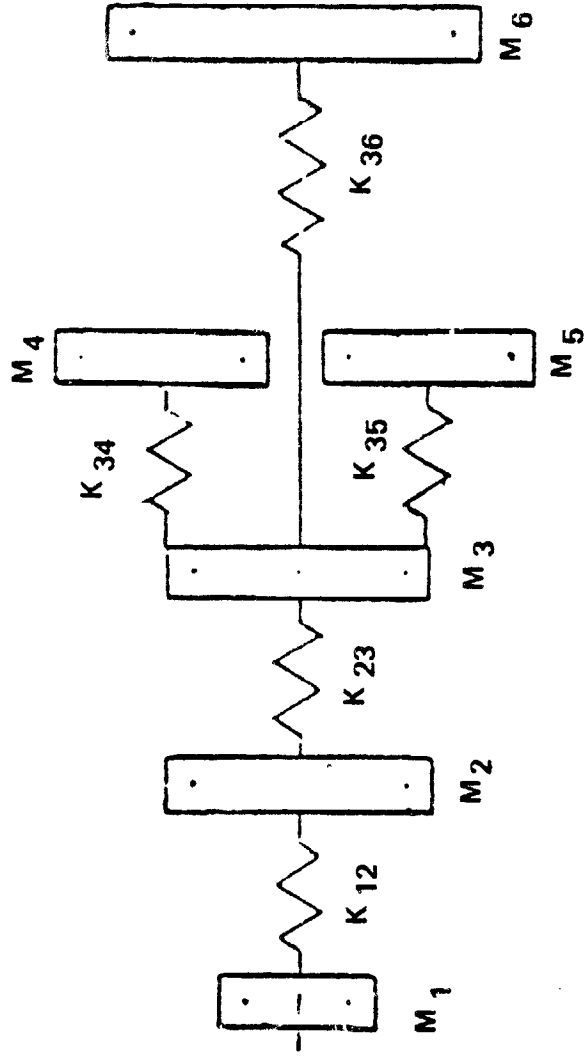
MAIN ROTOR CONTROL SYSTEM DATA

DESCRIPTION	UNITS	VALUE
Radius of Pushrod Connection on Swashplate	cm (in)	44.20 (17.40)
Radius of Servo Connection on Swashplate	cm (in)	40.01 (15.75)
Pushrod Horn Length Normal to Feathering Axis	cm (in)	18.42 (7.25)
Swashplate Mass	kg (lb-sec ² /in)	90.54 (.517)
Swashplate Diametrical Mass Moment of Inertia	kg-m ² (in-lb-sec ²)	2.054 (18.2)
Mass at Pushrod	kg (lb-sec ² /in)	3.397 (.0194)
Pushrod Horn Stiffness	N/m (lb/in)	8.758×10^6 (50,000.)
Forward Servo Stiffness	N/m (lb/in)	18.603×10^6 (106,200.)
Aft Servo Stiffness	N/m (lb/in)	18.603×10^6 (106,200.)
Lateral Servo Stiffness	N/m (lb/in)	18.603×10^6 (106,200.)
Radius of Pushrod Station Along Feathering Axis	cm (in)	38.43 (15.13)
Flap-Lag Hinge Offset	cm (in)	38.1 (15.00)

ORIGINALLY
OF POOR QUALITY

TABLE 19. UH-60A ROTOR ON RSRA MAIN ROTOR CONTROL SYSTEM DATA

**ORIGINAL DESIGN
OF POOR QUALITY**



DESCRIPTION	UNITS	SYMBOL	VALUE*
Rotor Hub	kg-m^2	M_1	8.47 (75)
Transmission	kg-m^2	M_2	102.6 (909)
Coupling Gear Box	kg-m^2	M_3	117.8 (1044)
Power Turbine	kg-m^2	M_4	732.9 (6494)
Power Turbine	kg-m^2	M_5	732.9 (6494)
Tail Rotor	kg-m^2	M_6	533.2 (4724)
Main Rotor Shaft	N.m	K_{12}	$4.853 + E06 (42.95 + E06)$
Transmission,	N.m	K_{23}	$189.7 + E06 (1679 + E06)$
Coupling Shaft	N.m	K_{34}	$133.8 + E06 (1184 + E06)$
Engine Shaft	N.m	K_{35}	$133.8 + E06 (1184 + E06)$
Engine Shaft	N.m	K_{36}	$541.9 + E06 (4797 + E06)$

*Normalized to Rotor Speed: (Actual Value) \times (RPM/Rotor RPM)²

TABLE 20 RSRA DRIVE SYSTEM DATA

ORIGINAL
OF POC

CM	R (IN)	CHORD (IN)		STRUCTURAL TWIST		AERODYNAMIC TWIST		CM (IN)	CL (IN)	CM (IN)	CL (IN)	LATERAL MODE SHAPE CM	LA (IN)
		CM	AC	CM	AC	CM	AC						
0	(0, 0)	0	(0, 0)	-9, 50000	-9, 50000	0	(0, 0)	0	(0, 0)	0	(0, 0)	0	(0, 0)
38.1	(15, 00000)	0	(0, 0)	-9, 50000	-9, 50000	0	(0, 0)	0	(0, 0)	0	(0, 0)	0	(0, 0)
38.19	(15, 03825)	21.08	(8, 30000)	-9, 50000	-9, 50000	0	(0, 0)	0	(0, 0)	0	(0, 0)	0	(0, 0)
38.42	(15, 12650)	21.08	(8, 30000)	-9, 50000	-9, 50000	0	(0, 0)	18.42	(7, 25000)	0	(0, 0)	-5.271	(-2, 97500)
60.55	(23, 83823)	21.08	(8, 30000)	-9, 50000	-9, 50000	0	(0, 0)	0	(0, 0)	0	(0, 0)	-5.471	(-2, 97500)
104.8	(41, 24997)	21.08	(8, 30000)	-9, 50000	-9, 50000	0	(0, 0)	0	(0, 0)	0	(0, 0)	-5.271	(-2, 07500)
158.8	(62, 4997)	52.73	(20, 75999)	-8, 89205	-8, 89205	.889	(-0, 35000)	-.553	(-0, 22759)	0	(0, 0)	0	(0, 0)
211.8	(83, 39996)	52.73	(20, 75999)	-7, 87555	-7, 87555	-.889	(-0, 35000)	-2.088	(-0, 82200)	0	(0, 0)	-13.18	(-2, 19600)
254.3	(100, 19997)	52.73	(20, 75999)	-7, 05846	-7, 05846	-.889	(-0, 35000)	-2.088	(-0, 82200)	0	(0, 0)	-13.18	(-5, 19000)
296.9	(116, 99997)	52.73	(20, 75999)	-6, 24137	-6, 24137	-.889	(-0, 35000)	-2.088	(-0, 82200)	0	(0, 0)	-13.18	(-5, 19000)
339.9	(133, 79997)	52.73	(20, 75999)	-5, 42427	-5, 42427	-.889	(-0, 35000)	-2.088	(-0, 82200)	0	(0, 0)	-13.18	(-5, 19000)
382.5	(150, 59998)	52.73	(20, 75999)	-4, 60713	-4, 60713	-.889	(-0, 35000)	-2.088	(-0, 82200)	0	(0, 0)	-13.18	(-5, 19000)
425.9	(167, 74498)	52.73	(20, 75999)	-3, 77331	-3, 77331	-.889	(-0, 35000)	-1.694	(-0, 66700)	0	(0, 0)	-13.18	(-5, 30000)
470.4	(185, 23499)	52.73	(20, 75999)	-2, 92266	-2, 92266	-.889	(-0, 35000)	-1.694	(-0, 66700)	0	(0, 0)	-13.18	(-5, 19000)
514.9	(202, 72499)	52.73	(20, 75999)	-2, 07201	-2, 07201	-.889	(-0, 35000)	-1.190	(-0, 66850)	0	(0, 0)	-13.18	(-5, 19000)
559.3	(220, 21500)	52.73	(20, 75999)	-1, 22136	-1, 22136	-.889	(-0, 35000)	-1.774	(-0, 69851)	0	(0, 0)	-13.18	(-5, 19000)
601.8	(236, 90999)	56.69	(22, 31700)	-0, 40938	0	(0, 0)	(0, 0)	.745	(0, 29348)	0	(0, 0)	-13.18	(-5, 80000)
642.1	(252, 80998)	56.69	(22, 31700)	0, 36394	0	(0, 0)	(0, 0)	.772	(0, 30385)	0	(0, 0)	-14.17	(-5, 80000)
682.5	(268, 70996)	56.69	(22, 31700)	1, 13726	0	(0, 0)	(0, 0)	.786	(0, 30962)	0	(0, 0)	-14.17	(-5, 80000)
719.18	(283, 14478)	52.73	(20, 75999)	2, 25158	2, 25158	-.889	(-0, 35000)	.935	(0, 36800)	0	(0, 0)	-13.18	(-5, 19000)
752.1	(296, 11475)	52.73	(20, 75999)	3, 20765	3, 20765	-.889	(-0, 35000)	5.331	(2, 09900)	0	(0, 0)	-13.18	(-5, 19000)
778.4	(306, 44971)	52.73	(20, 75999)	3, 51006	3, 51006	-.448	(-1, 75114)	.981	(0, 38613)	0	(0, 0)	-13.18	(-5, 19000)
797.9	(314, 14966)	52.73	(20, 75999)	1, 97007	1, 97007	-11.566	(-4, 5570)	-8.081	(-3, 18142)	0	(0, 0)	-13.18	(-5, 19000)
817.8	(319, 99951)	52.73	(20, 75999)	1, 20000	1, 20000	-16.975	(-6, 68288)	-14.549	(-5, 72782)	0	(0, 0)	-13.18	(-5, 19000)

TABLE 21. UH-60A BLADE GEOMETRIC DATA

BLADE MASS kg/m (lb. SEC**2/IN.**)²	DEFLAR CM (IN.)	BLADE EDGEWISE M. OF I. ABOUT C.G. kg.m (LB. IN. SEC**2/IN.)	BLADE TORSIONAL M. OF I. ABOUT C.G. kg.m (LB. IN. SEC**2/IN.)		DEFLAR CM (IN.)	BLADE TORSIONAL M. OF I. ABOUT HINGE kg.m (LB. IN. SEC**2/IN.)
			DEFLAR CM (IN.)	DEFLAR CM (IN.)		
0 (0.0) (0.01604)	38.10 (15.00000)	0 (0.07650)	(0.0) (0.00269)	38.10 (15.0000)	0 (0.0)	38.10 (15.0000)
110.59 (0.19410)	.1943 .2540	.01195 (0.16000)	.01195 (0.00479)	.21.08 .1112	.01195 (8.300)	21.08 (8.300)
1338.3 (0.00695)	44.002 (17.32349)	.02128 (0.00823)	.03657 (0.01842)	.02128 .1112	.02128 (0.00479)	.02128 (2.800)
47.92 (0.00436)	44.45 (17.50000)	.08185 (0.01842)	.08185 (0.02398)	9.91 .0185	.03657 (0.00823)	9.91 (3.900)
30.06 (0.00150)	63.50 (25.00000)	.10656 (0.02398)	.10656 (0.02398)	.40.21 .0185	.08185 (0.01842)	.40.21 (15.830)
10.34 (0.00149)	42.67 (16.80000)	.14131 (0.03180)	.14131 (0.03180)	.74.09 .0185	.10656 (0.02398)	.74.09 (29.170)
10.27 (0.00149)	42.67 (16.80000)	.15437 (0.03474)	.15437 (0.03474)	.213.4 .0185	.213.4 (64.000)	.213.4 (64.000)
10.20 (0.00149)	42.67 (16.80000)	.17645 (0.03971)	.17645 (0.04650)	.154.9 .0185	.154.9 (61.000)	.154.9 (61.000)
10.34 (0.00149)	42.67 (16.80000)	.20663 (0.04650)	.20663 (0.04650)	.22.76 .0185	.17645 (8.960)	.22.76 (8.960)
10.34 (0.00149)	42.67 (16.80000)	.20663 (0.04650)	.20663 (0.04650)	.28.04 .0185	.20663 (11.040)	.28.04 (11.040)
10.34 (0.00149)	42.67 (16.80000)	.19347 (0.04354)	.19347 (0.04354)	.93.12 .0185	.19347 (36.660)	.93.12 (36.660)
10.62 (0.00154)	44.42 (17.49001)	.15024 (0.03381)	.15024 (0.03381)	.19347 .0185	.19347 (12.340)	.19347 (12.340)
10.41 (0.00151)	44.42 (17.49001)	.3043 (0.06848)	.3043 (0.06848)	.31.34 .0185	.15024 (2.000)	.31.34 (2.000)
10.55 (0.00153)	44.42 (17.49001)	.2604 (0.05861)	.2604 (0.05861)	.5.08 .0185	.3043 (8.000)	.5.08 (8.000)
11.65 (0.00169)	44.42 (17.49001)	.2543 (0.05723)	.2543 (0.05723)	.20.32 .0185	.2604 (9.500)	.20.32 (9.500)
13.17 (0.00191)	40.39 (15.90000)	.16908 (0.03805)	.16908 (0.03805)	.24.13 .0185	.2543 (13.500)	.24.13 (13.500)
13.1 (0.00190)	40.39 (15.90000)	.16.03 (0.03805)	.16.03 (0.03805)	.34.29 .0185	.16908 (0.03805)	.34.29 (13.500)
13.03 (0.00189)	40.39 (15.90000)	.16.27 (0.00236)	.16.27 (0.00236)	.34.29 .0185	.16908 (0.03805)	.34.29 (13.500)
17.79 (0.00258)	32.94 (12.97000)	.17.79 (0.00258)	.17.79 (0.00258)	.34.29 .0185	.16908 (0.03805)	.34.29 (13.500)
16.75 (0.00243)	19.56 (7.70000)	.16.75 (0.00182)	.16.75 (0.00182)	.34.29 .0185	.16908 (0.03805)	.34.29 (13.500)
12.55 (0.000658)	19.56 (7.70000)	.3.99 (4.00000)	.10.16 (4.00000)	.34.29 .0185	.16908 (0.03805)	.34.29 (13.500)

BLADE RIGID BODY PROPERTIES

FLAPPING MASS	=	118.82 (.679362) kg (LB SEC**2/IN.)
1ST MOM ABOUT HINGE	=	39.39 (86.8380) kg-sec ² (LB SEC ²)
FLAPPING INERTIA	=	2053.2 (18191.0) kg-m ² (LB SEC ²)
FLAP FREQUENCY	=	.267531 CYCLES/REV
PITCH INERTIA	=	1.173 (10.3949) kg-m ² (LB IN SEC ²)

TABLE 22 UH-60A BLADE MASS DATA

BLADE FLATWIST SECOND MOMENT OF AREA cm ⁴	BLADE FLATWIST DELTA R cm (IN.)	SECOND MOMENT OF AREA cm ⁴ (IN. ⁴)		BLADE TORSIONAL STIFFNESS N.m ² (LB-IN.* ²)		BLADE TORSIONAL STIFFNESS LM (IN.)	
		cm	(IN.)	cm	(IN.)	cm	(IN.)
2290. (0.55020E+02)	-194.3 (0.07650)	2290. (0.55020E+02)	-194.3 (0.07650)	.1943 (0.07650)	.28698E+06 (0.10000E+09)	38.1 (15.00000)	
2290. (0.55020E+02)	.254 (0.10000)	2290. (0.55020E+02)	.254 (0.10000)	.254 (0.10000)	.2018E+05 (0.70320E+08)	55.1 (21.69853)	
3710. (0.89141E+02)	44.00 (17.32349)	3680. (0.88423E+02)	44.00 (17.32349)	44.00 (17.32349)	.1429E+05 (0.49798E+08)	55.1 (21.69853)	
15792. (0.37941E+03)	44.45 (17.50000)	3900. (0.91696E+02)	44.45 (17.50000)	44.45 (17.50000)	.7428E+05 (0.25885E+08)	55.1 (21.69853)	
19523. (0.46903E+03)	63.5 (25.00000)	1149. (0.21593E+02)	63.5 (25.00000)	63.5 (25.00000)	.6926E+05 (0.24310E+08)	55.1 (21.69853)	
34755. (0.83500E+03)	42.67 (16.80000)	924. (0.22200E+02)	42.67 (16.80000)	42.67 (16.80000)	.6976E+05 (0.24310E+08)	55.1 (21.69853)	
34755. (0.83500E+03)	42.67 (16.80000)	924. (0.22200E+02)	42.67 (16.80000)	42.67 (16.80000)	.6976E+05 (0.24310E+08)	55.1 (21.69853)	
34755. (0.83500E+03)	42.67 (16.80000)	924. (0.22200E+02)	42.67 (16.80000)	42.67 (16.80000)	.6976E+05 (0.24310E+08)	55.1 (21.69853)	
34755. (0.83500E+03)	42.67 (16.80000)	924. (0.22200E+02)	42.67 (16.80000)	42.67 (16.80000)	.6976E+05 (0.24310E+08)	55.1 (21.69853)	
34822. (0.83660E+03)	42.67 (16.80000)	933. (0.22408E+02)	42.67 (16.80000)	42.67 (16.80000)	.7111E+05 (0.24780E+08)	55.1 (21.69853)	
34994. (0.84073E+03)	44.42 (17.49001)	961. (0.23100E+02)	44.42 (17.49001)	44.42 (17.49001)	.7111E+05 (0.24780E+08)	55.1 (21.69853)	
35000. (0.84090E+03)	44.42 (17.49001)	961. (0.23100E+02)	44.42 (17.49001)	44.42 (17.49001)	.7111E+05 (0.24780E+08)	55.1 (21.69853)	
33645. (0.80832E+03)	44.42 (17.49001)	964. (0.23167E+02)	44.42 (17.49001)	44.42 (17.49001)	.7077E+05 (0.24661E+08)	55.1 (21.69853)	
29030. (0.69745E+03)	44.42 (17.49001)	978. (0.23500E+02)	44.42 (17.49001)	44.42 (17.49001)	.6916E+05 (0.24310E+08)	55.1 (21.69853)	
29681. (0.71308E+03)	40.39 (15.90000)	978. (0.23500E+02)	40.39 (15.90000)	40.39 (15.90000)	.6916E+05 (0.24310E+08)	55.1 (21.69853)	
29053. (0.69800E+03)	40.39 (15.90000)	978. (0.23500E+02)	40.39 (15.90000)	40.39 (15.90000)	.6916E+05 (0.24310E+08)	55.1 (21.69853)	
27319. (0.65779E+03)	40.39 (12.90000)	945. (0.22710E+02)	40.39 (12.90000)	40.39 (12.90000)	.6916E+05 (0.24310E+08)	55.1 (21.69853)	
21586. (0.51860E+03)	32.94 (12.90000)	929. (0.22330E+02)	32.94 (12.90000)	32.94 (12.90000)	.6916E+05 (0.24310E+08)	55.1 (21.69853)	
19521. (0.46901E+03)	32.94 (12.90000)	826. (0.19843E+02)	32.94 (12.90000)	32.94 (12.90000)	.6916E+05 (0.24310E+08)	55.1 (21.69853)	
16198. (0.38891E+03)	19.56 (7.70000)	614. (0.14760E+02)	19.56 (7.70000)	19.56 (7.70000)	.6916E+05 (0.24310E+08)	55.1 (21.69853)	
16232. (0.38998E+03)	19.56 (7.70000)	370. (0.89007E+01)	19.56 (7.70000)	19.56 (7.70000)	.6916E+05 (0.24310E+08)	55.1 (21.69853)	
18522. (0.44500E+03)	10.16 (4.00000)	308. (0.74000E+01)	10.16 (4.00000)	10.16 (4.00000)	.6916E+05 (0.24310E+08)	55.1 (21.69853)	

Young's Modulus E = 10⁶

OPTIMUM CONSTRUCTION

TABLE 23. UH-60A BLADE STIFFNESS DATA

ORIGINAL
OF FLOOR PLAN

POTENTIAL V_{TIP} /RPM OPERATING CONDITIONS

<u>% N_R</u>	<u>RPM</u>	<u>V_{TIP} m/sec (FPS)</u>	
92	236.44	202.5	(664.31)
95	244.15	209.1	(685.97)
100	257	220.1	(722.08)
110	282.7	242.1	(794.28)

TABLE 24. POTENTIAL V_{TIP} /RPM OPERATING CONDITIONS

~~ORIGINAL DESIGN
OF POOR QUALITY~~

SUMMARY OF TIP CAP STUDY

<u>Items</u>		<u>Production Tip</u>	<u>Proposed Extended Tip</u>
Weight	kg (lb)	1.565 (3.45)	2.72 (6)
C.G. - Spanwise	cm (in)	790.2 (311.1)	806.6 (317.54)
C.G. - Chordwise (Aft of F.A.)	cm (in)	12.98 (5.11)	21.69 (8.54)
Minimum Ultimate Margin of Safety (Analytical):			
Static		1.09*	0.41**
Fatigue		0.56*	1.02**

* Reference UTTAS Rotor Blade Analysis, SER-70512

** Based on Geometry of Figure 45.

TABLE 25. COMPARISON OF PRODUCTION AND EXTENDED TIP CAP CHARACTERISTICS

**CRITICAL MEASUREMENTS
OF PCON QUALITY**

ROTOR BLADE MEASUREMENTS

(1) MASTER BLADE MEASUREMENTS

8 Normal Bending Moment*
4 Edgewise Bending Moment*
7 Trailing Edge Strain*
2 Torsion Moment
2 Cuff Total Stress
2 Bottom Rear Stress
1 Top Rear Stress
1 Trailing Edge Weld Stress
2 Tip Fitting Stress

Pitch Link Load
Damper Load
Damper Position

Blade Root Flapping
Blade Root Lag
Balde Root Pitch

(4) ROTOR SHAFT MEASUREMENTS

Shaft Bending Moments - 2 Stations
2 Orthogonal Directions Each (Total of 4 Measurements)
Shaft Torque

(5) ROTOR HUB MEASUREMENTS

Flapwise Load on Each of 4 Barrels
Edgewise Load on Each of 4 Barrels
Tensile Load in Each of 4 Barrels

(6) BIFILAR ABSORBER MEASUREMENTS

Tangential Acceleration on Each of 4 Masses
Tangential Acceleration on Each of 4 Bifilar Arms
Hub Acceleration Near Centerline - 3 Orthogonal Directions

*See Figure 49 For Location.

(2) MEASUREMENTS ON EACH OF 3 ADDITIONAL BLADES

3 Outboard Normal Bending
3 Outboard Edgewise Bending
2 Torsion Moment
1 Blade Root Normal Bending
1 Blade Root Edgewise Bending
Damper Load
Pitch Link Load

(7) ACTIVE ISOLATOR/BALANCE SYSTEM MEASUREMENTS

4 Main Rotor Transmission Load Cells
4 Isolator Mount Motions
4 Isolator Axial Loads
Transmission Torque Link Load
4 Isolator Force Pressures

(8) ROTOR BLADE PRESSURE MEASUREMENTS

Detailed in Separate Sections.

(3) ROTOR CONTROL SYSTEM MEASUREMENTS

Rotating Scissors Load
3 Swashplate Link/Servo Loads
1 Swashplate Guide Bending
1 Stationary Scissors Load

TABLE 26. INSTRUMENTATION LIST

ORIGINAL DRAWING
OF POOR QUALITY

% N _r	C _T /σ	Level Flight Speed Change, km/hr (knots)					
		Double Swept	Mini-Anhedral	10% Tip			
110	.062	7.04 (3.8)	7.04 (3.8)	3.34 (1.8)			
100	.075	2.22 (1.2)	2.22 (1.2)	1.67 (.9)			
92	.088	(-1.67) (-.9)	-1.67 (-.9)	- .927 (-.5)			

TABLE 27. CALCULATED FORWARD FLIGHT ENVELOPE CHANGES WITH ADVANCED TIPS - GROSS WEIGHT = 8709 kg (19,000 lb) SEA LEVEL STANDARD DAY CONDITIONS, TRANSMISSION TORQUE LIMITED POWER

**ORIGIN
OF POOR**

W.B.'s.	item	Year/Quarter	1				2				3				4				Initial
			1	2	3	4	5	6	7	8	9	10	11	12	13	14	15	16	
1.1.1.1.1	Mechanical Flight Controls Modification	37.0	37.0	156.0	237.0	110.0	157.0												134
1.1.1.1.1.1	RSRA Transmission Modifications	15.0	37.0	97.0	70.0	307.0	164.0	40.0											130
1.1.1.1.1.1.1	Rotor Hub Adaptation	15.0	15.0	69.0	52.0	52.0													203
1.1.1.1.1.1.2	Rotor Blade Adaptation (Blade Severence)	42.0	42.0	22.0	428.0	180.0	42.0												156
1.1.1.1.1.1.3	Airfoil Leading Edge Contour Modification	15.0	15.0	55.0	90.0	65.0													240
1.1.1.1.1.1.4	Blade Tip Modifications	15.0	20.0	24.0	58.0	78.0													110
1.1.1.1.1.1.5	Blade Fabrication			201.0	19.0														660
1.1.1.1.1.1.6	Alternate Rotor Mast Extender	15.0	15.0	48.0	48.0	8.0	8.0												142
1.1.1.1.1.1.7	Rotor Blade Instrumentation		270.0	97.0	60.0	16.0													443
1.1.1.1.1.1.8	Rotor System Test Program				860.0	828.0													1088
1.1.1.1.1.1.9	Contractor Test Support (2 yrs)																		6766.0
TOTAL 1981 DOLLARS (1000's \$)		154.0	176.0	613.0	1229.0	960.0	566.0	900.0	828.0	84.0	84.0	84.0	84.0	84.0	84.0	84.0	84.0	84.0	6036.0

TABLE 28. RSRA/BLACK HAWK ROTOR - PLANNING ESTIMATE (COST)

ORIGINAL ~~REPRODUCTION~~
OF POOR QUALITY

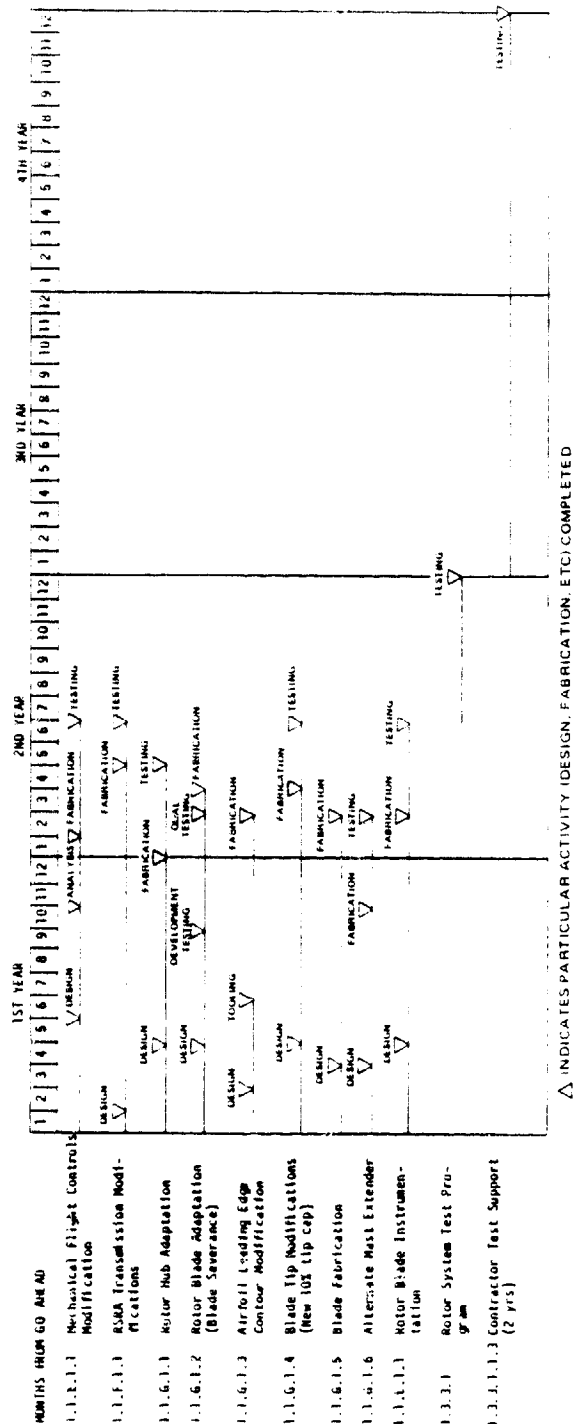
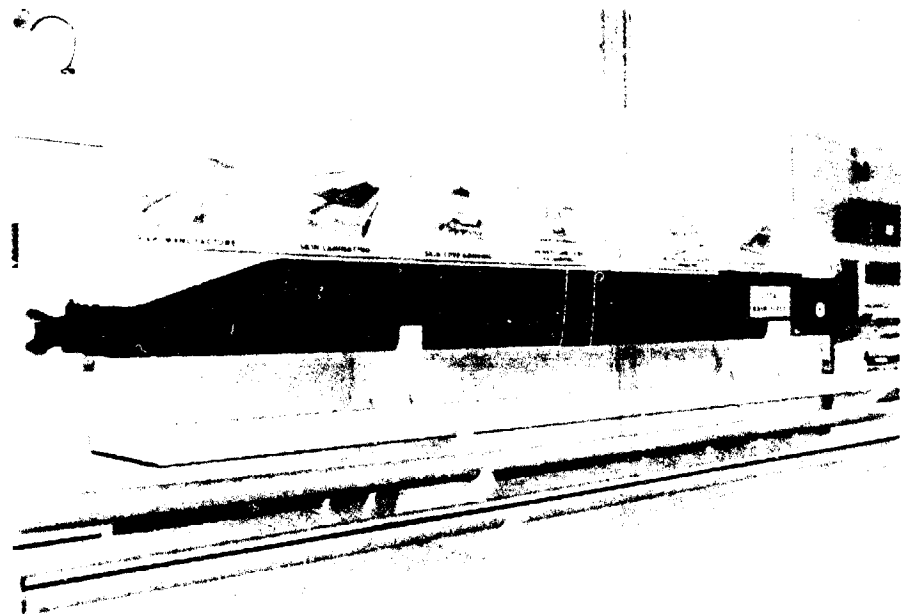
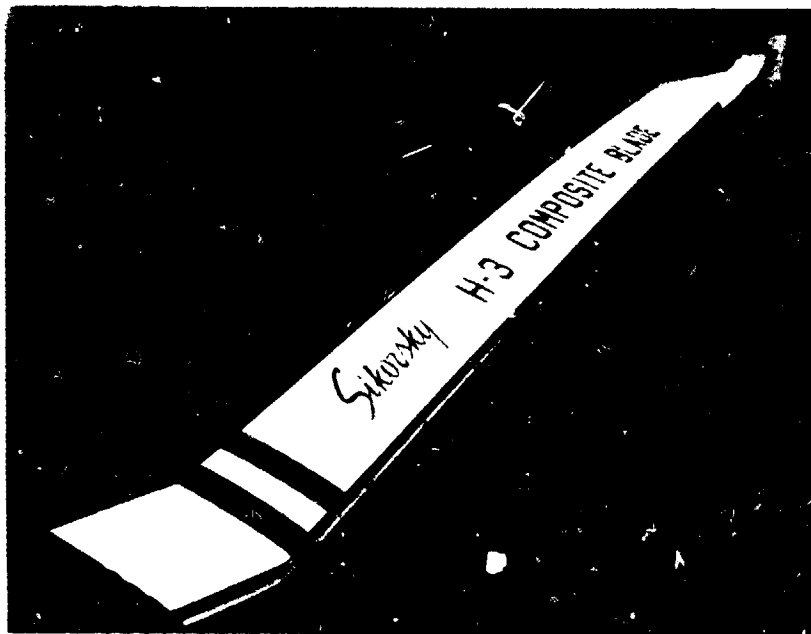


TABLE 29. RSRA/BLACK HAWK ROTOR PLANNING SCHEDULE

ORIGINAL PAGE IS
OF POOR QUALITY



BLACK HAWK

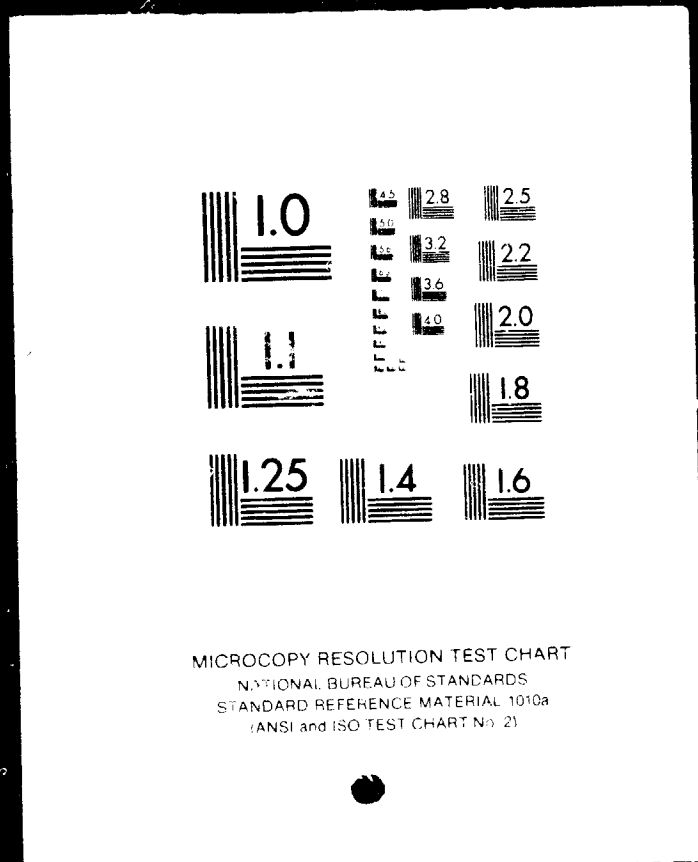


H-3 COMPOSITE

FIGURE 1. PHOTOGRAPH OF BLACK HAWK AND H-3 COMPOSITE BLADES

20F2

N83-13065 UNCLAS



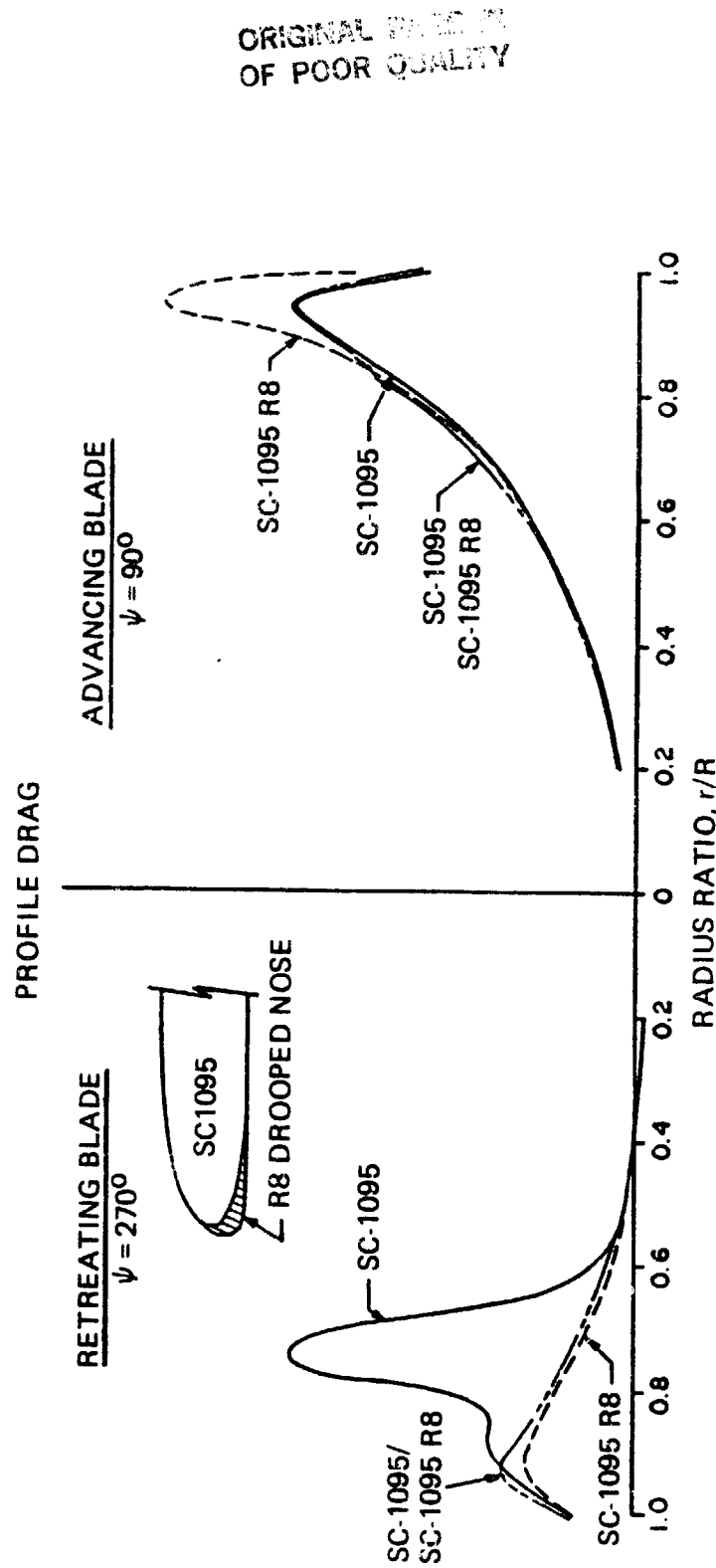


FIGURE 2. PROFILE POWER LOSSES FOR SINGLE AND DUAL AIRFOIL CONFIGURATIONS.

ORIGIN
OF POOL VOLUME

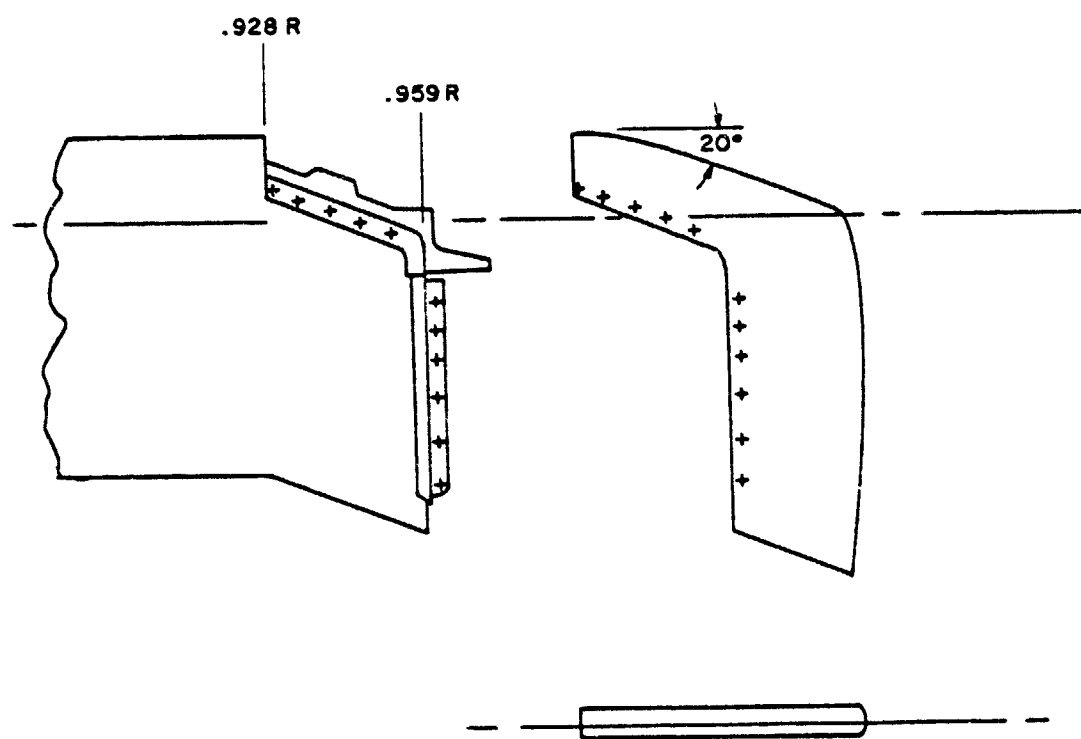


FIGURE 3. BLACK HAWK STANDARD TIP

ON THE OTHER
OF POOR

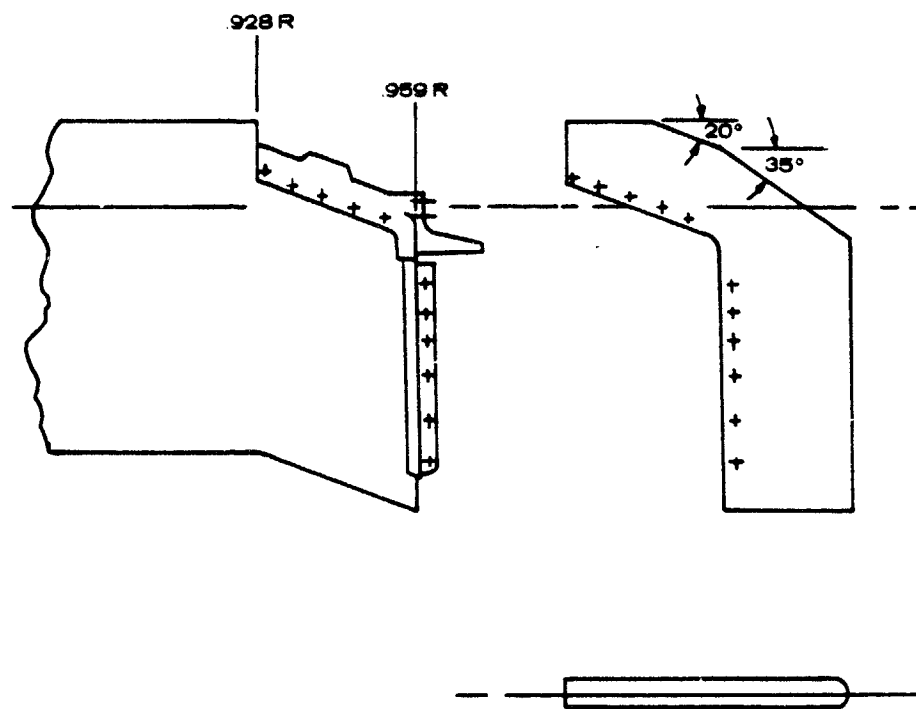
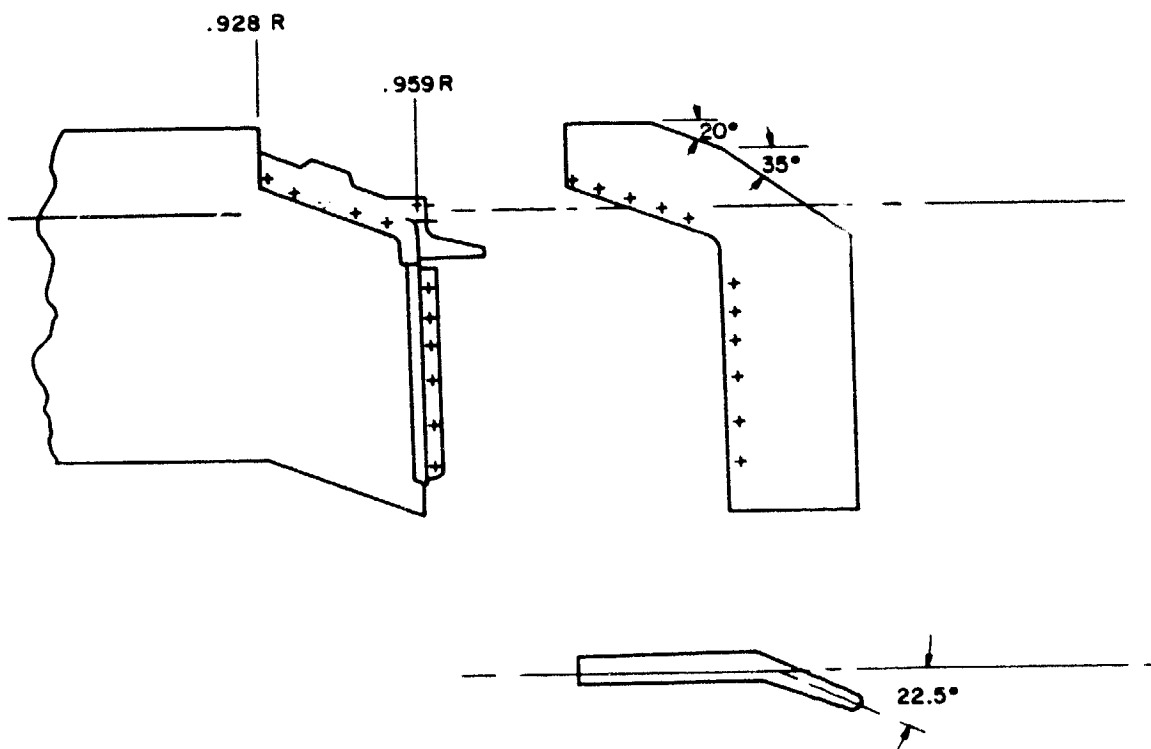


FIGURE 4. SWEPT TAPERED TIP.

ORIGINAL DRAWING
OF POOR QUALITY



LIMITED RIGHTS NOTICE

This data is a trade secret of Sikorsky Aircraft and is submitted in confidence under NASA contract No. NAS 2-10691 on 11/19/60. It may be duplicated and used by the Government with the express limitation that it will not, without permission of the Contractor, be disclosed outside the Government, or used for purposes of manufacture. However, the Government may disclose this data for use by onsite employees of support service contractors, providing such Contractors have agreed in writing to protect this data from unauthorized use or disclosure. These restrictions shall terminate seven (7) years from the submittal date specified in this notice. This notice shall be marked on any reproduction of this data, in whole or in part.

FIGURE 5. SWEPT/TAPERED TIP WITH ANHEDRAL.

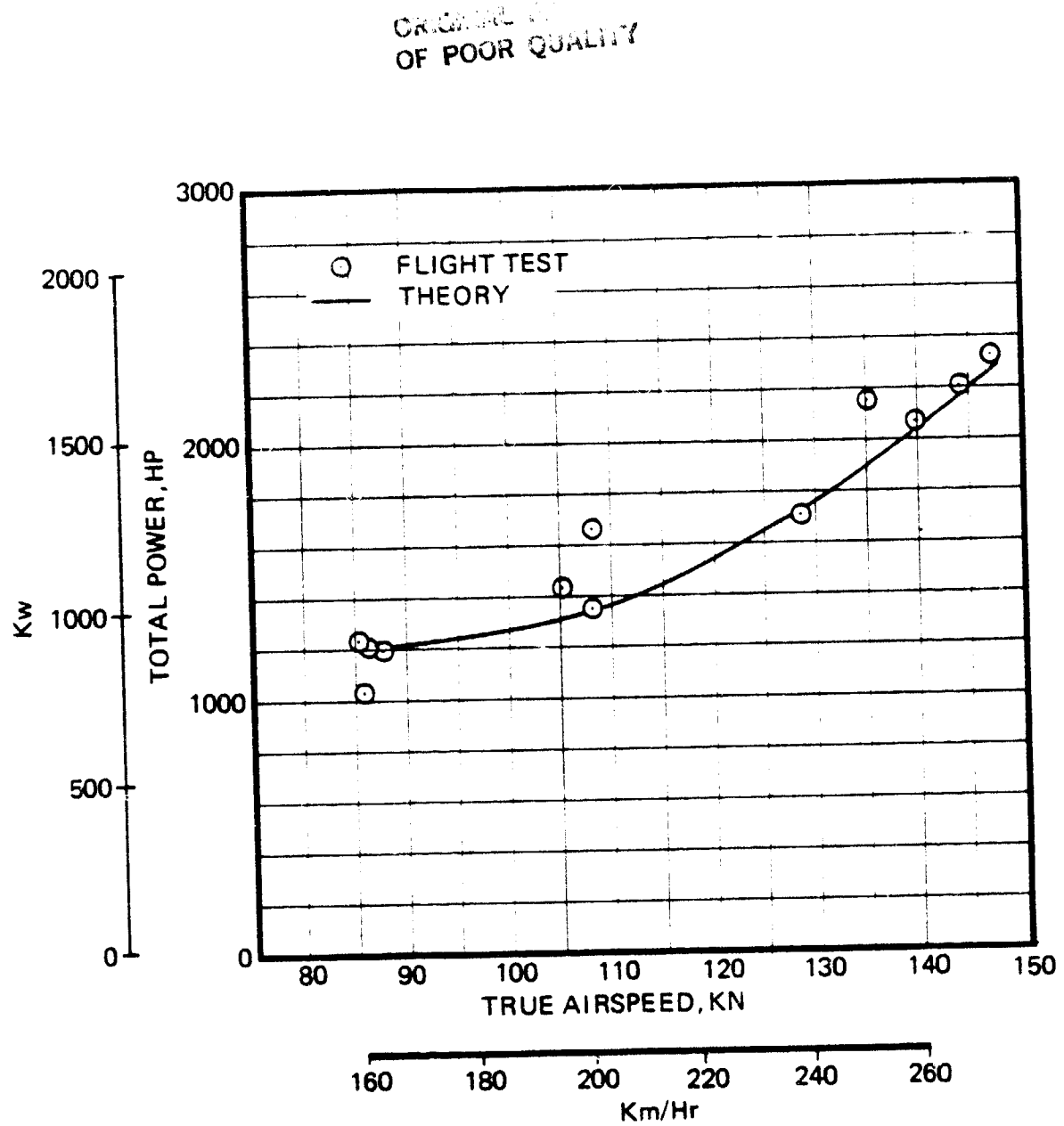


FIGURE 6. RSRA HELICOPTER CRUISE PERFORMANCE CORRELATION

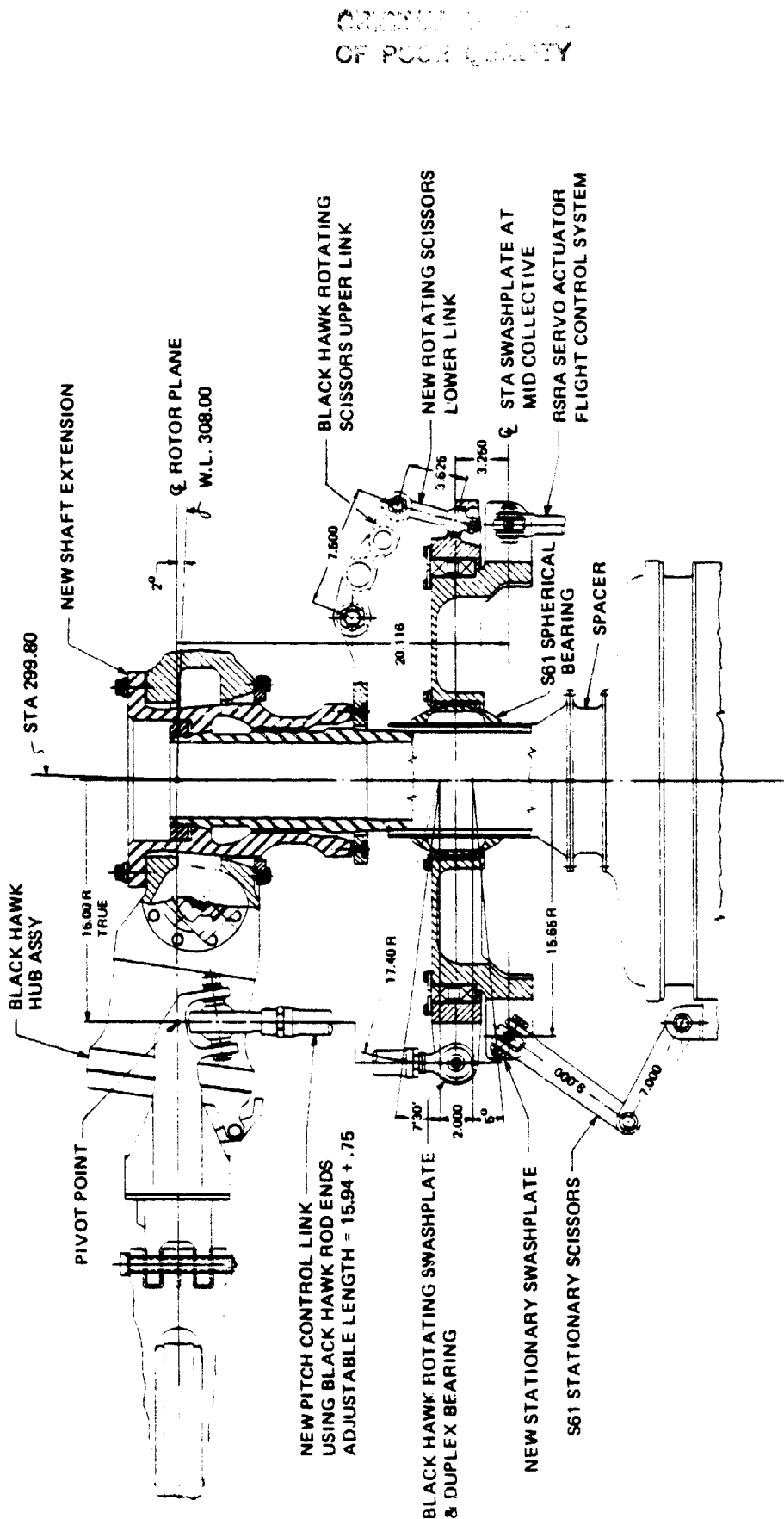


FIGURE 7. 4 – BLADED ROTOR HEAD INSTALLATION

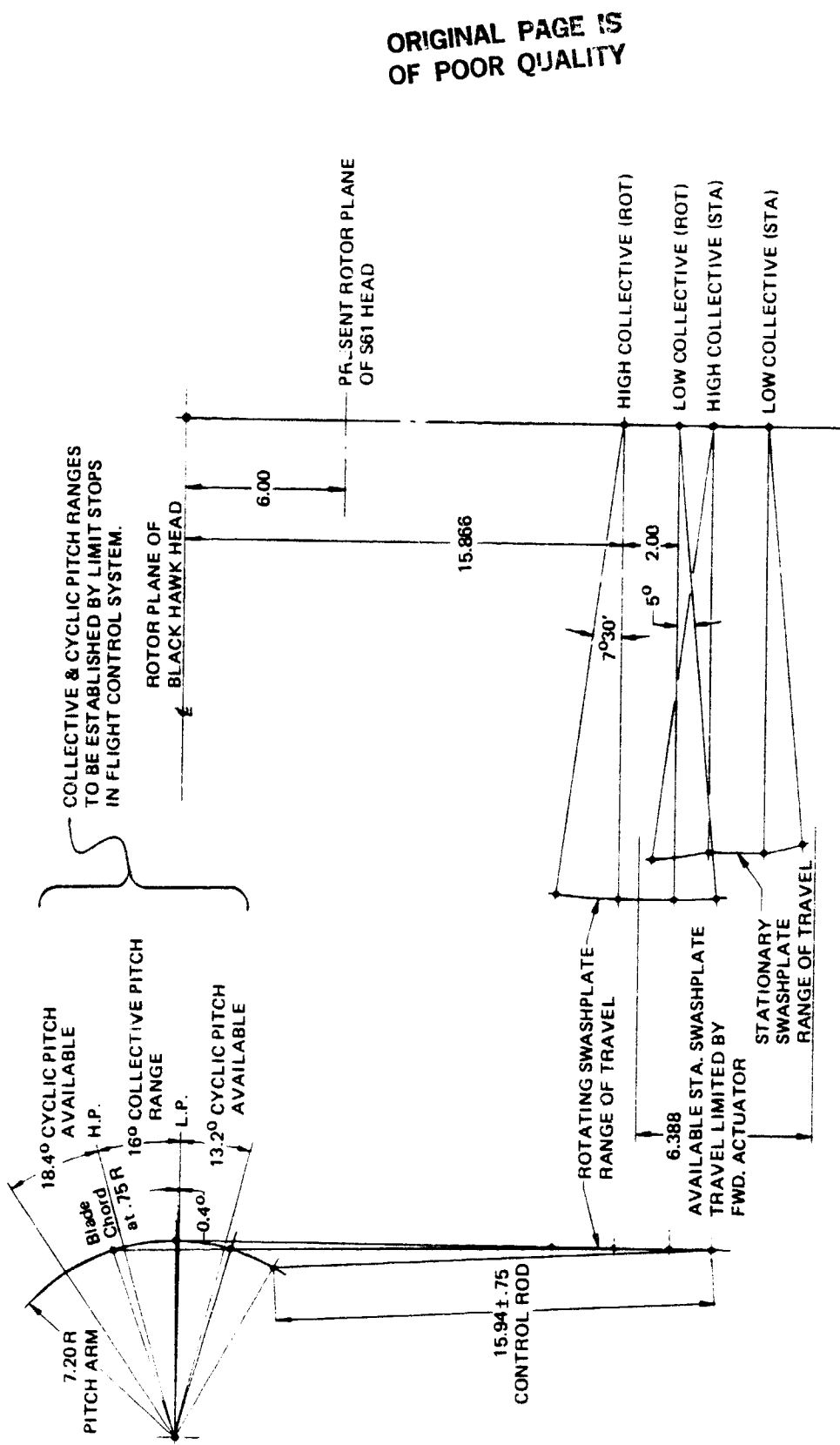


FIGURE 8. 4-BLADED ROTOR HEAD CONTROL SCHEMATIC

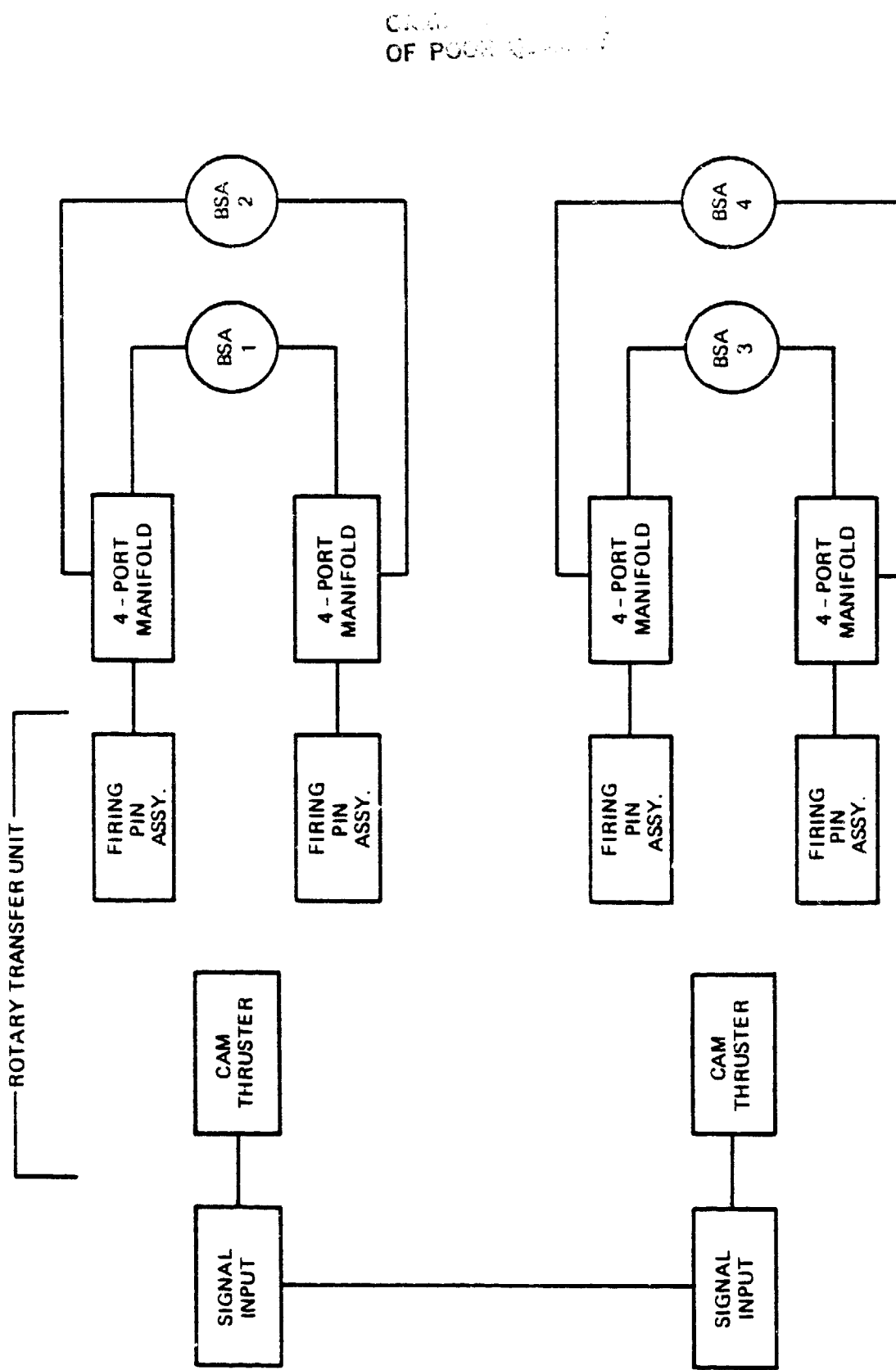


FIGURE 9. SCHEMATIC DIAGRAM – BLADE SEVERANCE SYSTEM

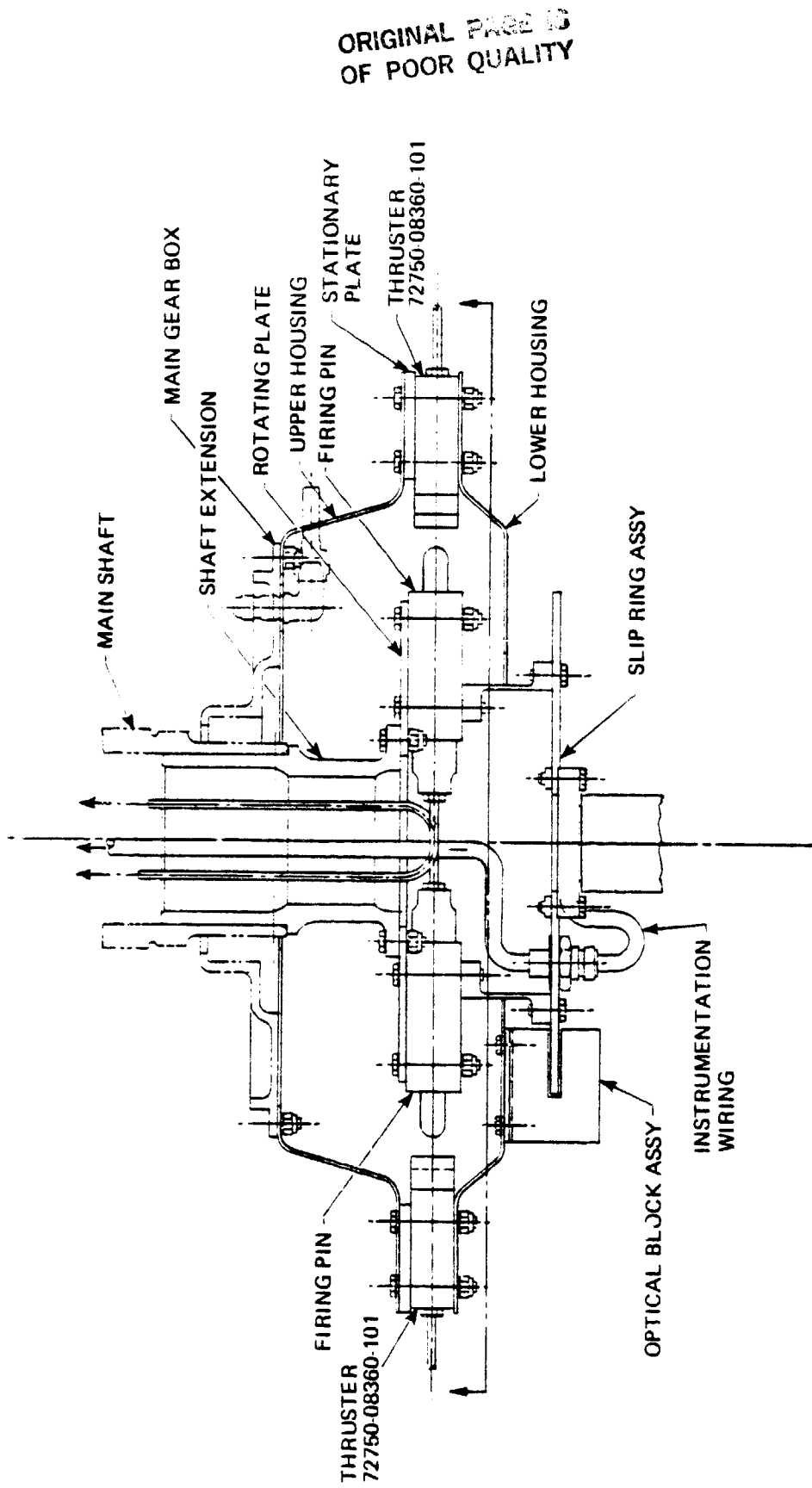


FIGURE 10. 4-BLADED ROTOR — MAIN ROTOR DRIVE SHAFT (LOWER PORTION)

ORIGINAL PAGE IS
OF POOR QUALITY

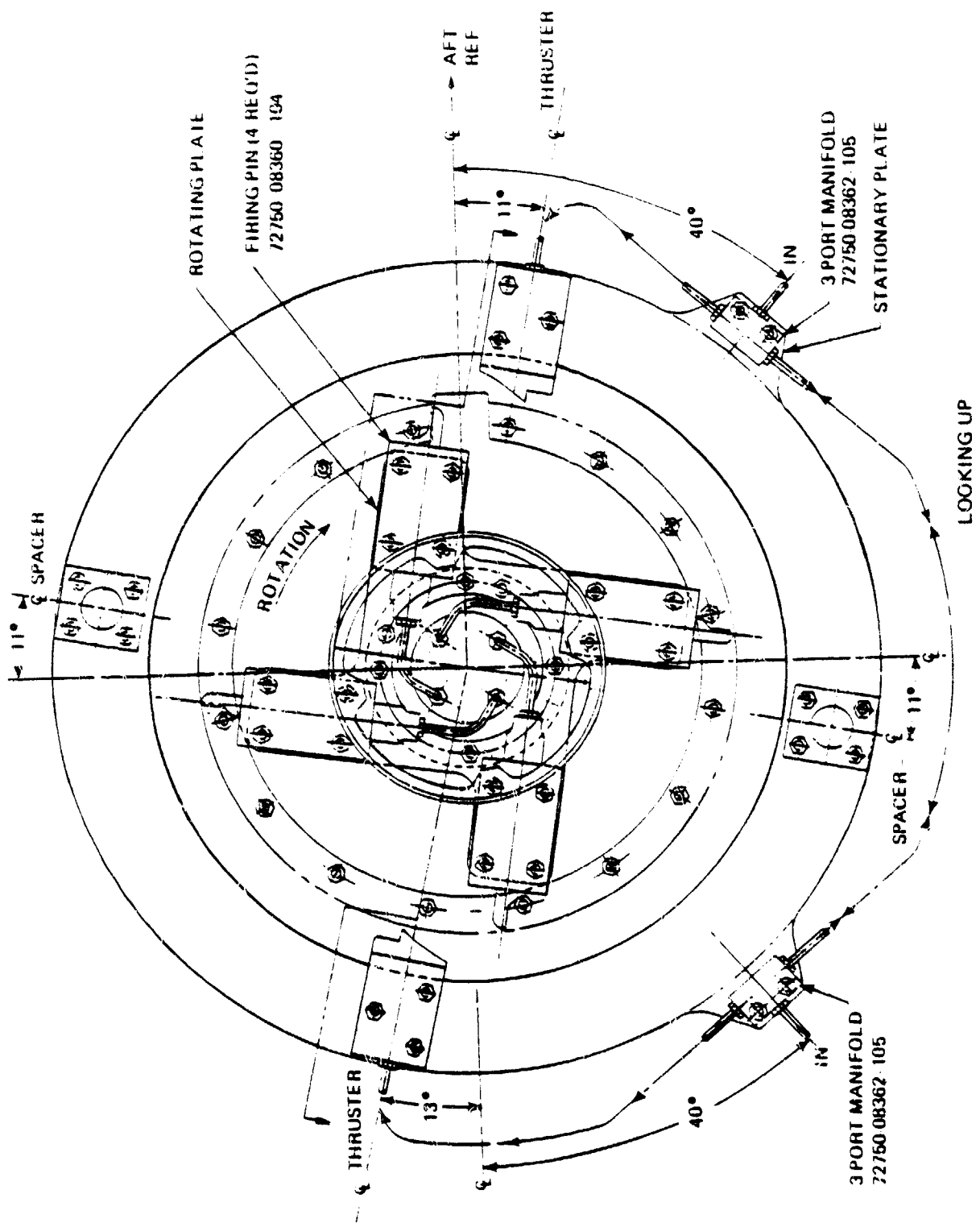


FIGURE 10. (CONTINUED)

ORIGINAL PHOTO A
OF POOR QUALITY

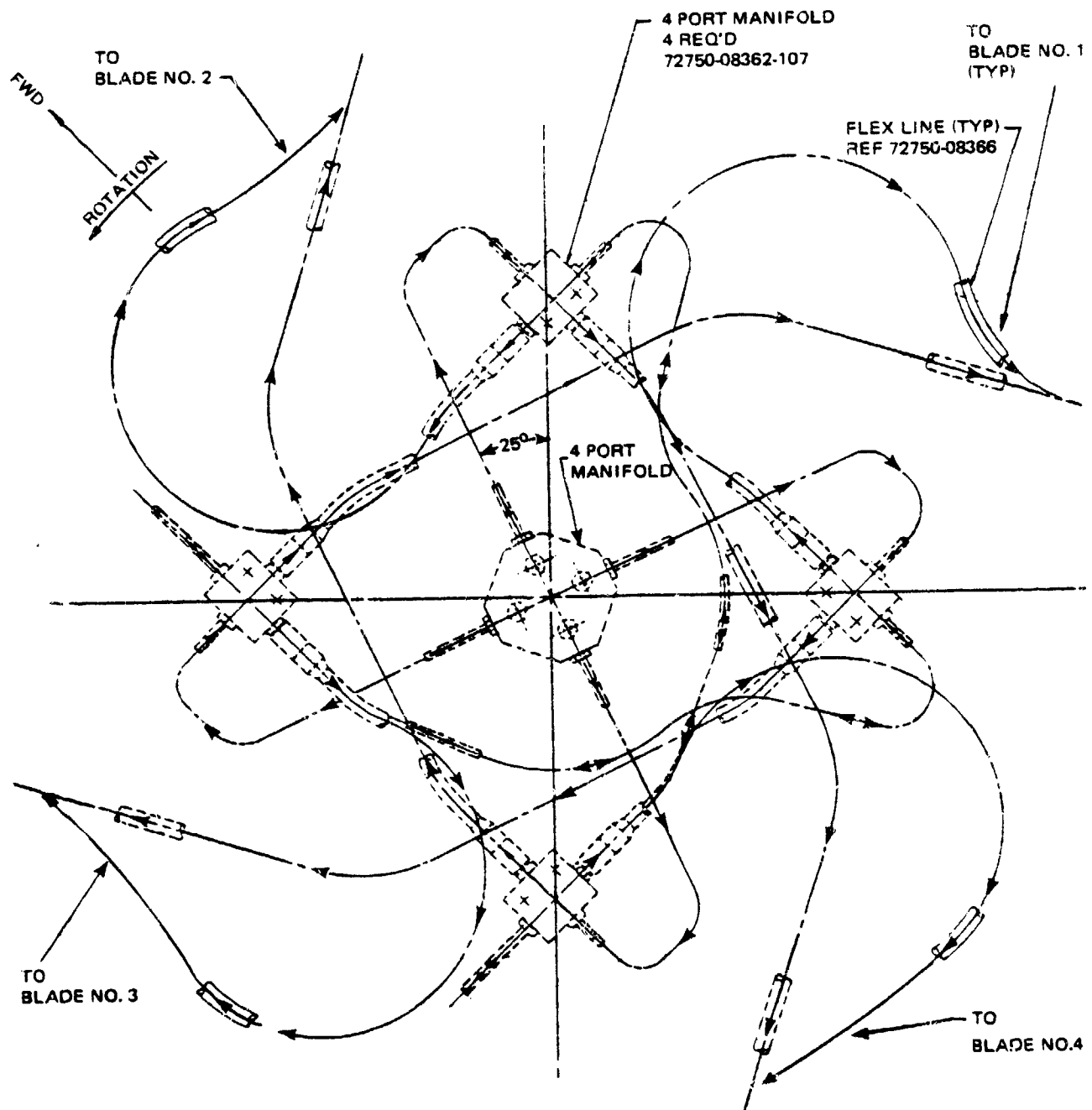


FIGURE 11. 4-BLADED ROTOR – PYROTECHNIC HARDWARE
AT THE ROTOR HEAD

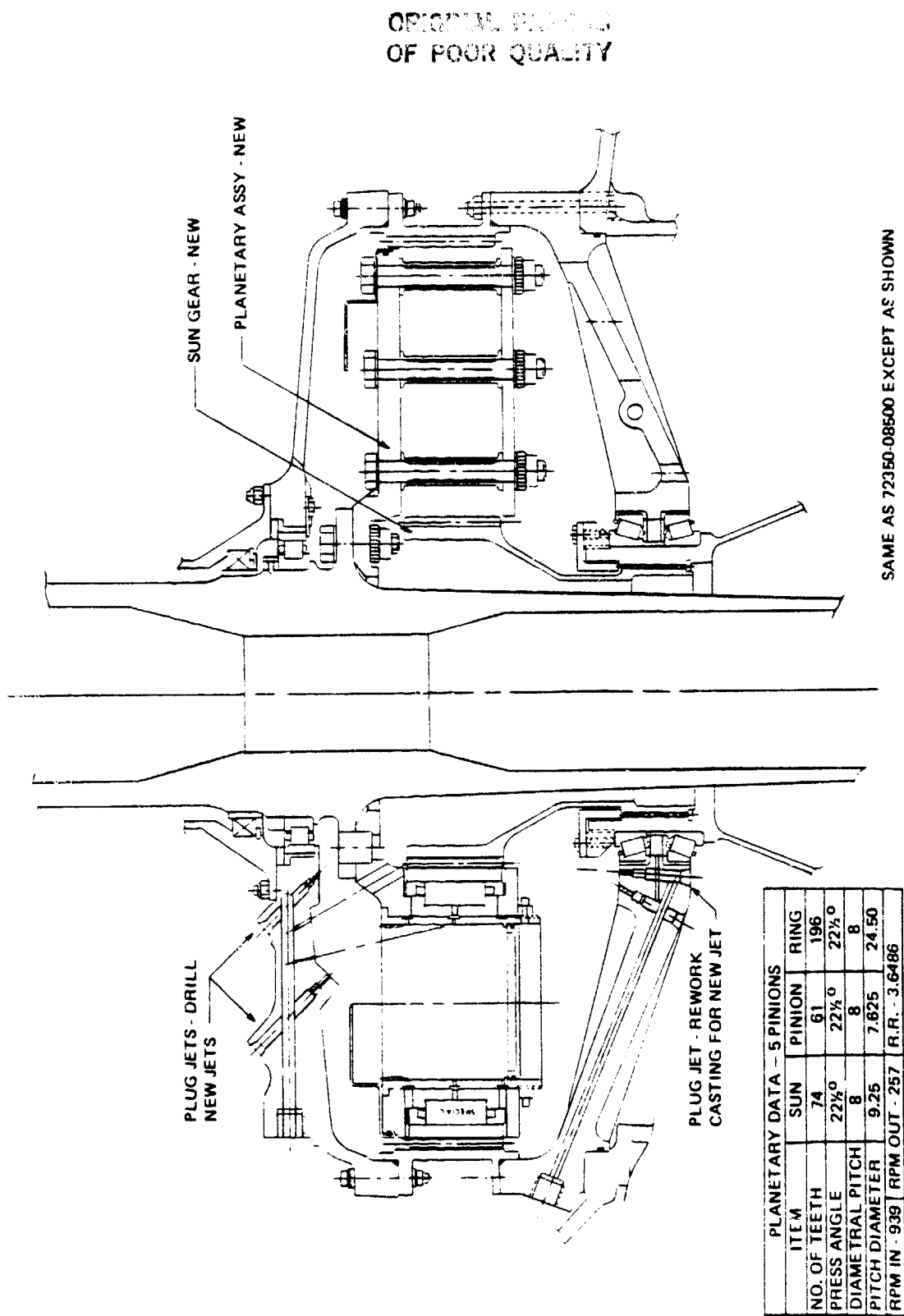


FIGURE 12. CROSS SECTION OF MODIFIED RRA TRANSMISSION.

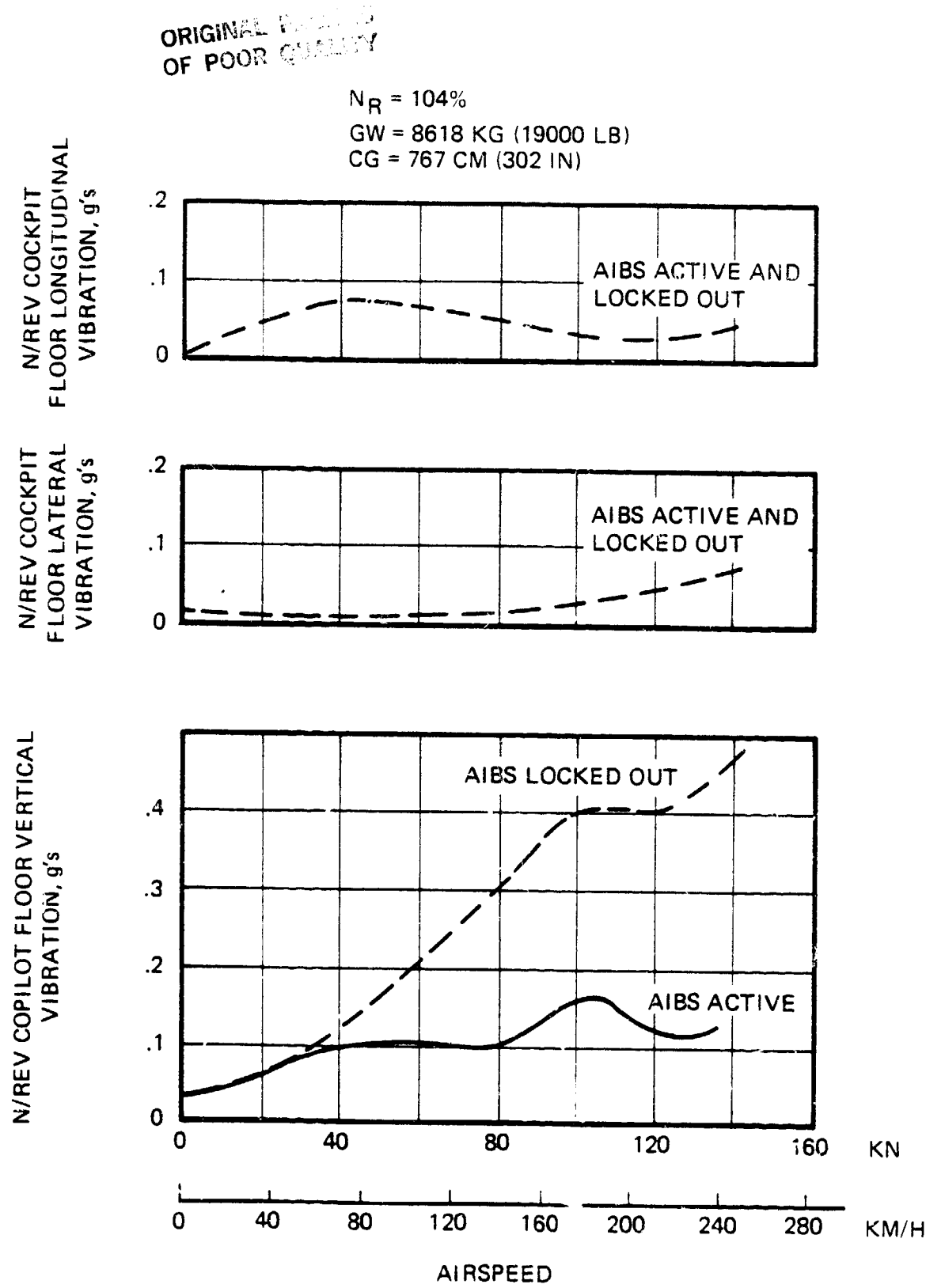


FIGURE 13. RSRA COCKPIT VIBRATION WITH ACTIVE ISOLATION SYSTEM, S-61 ROTOR

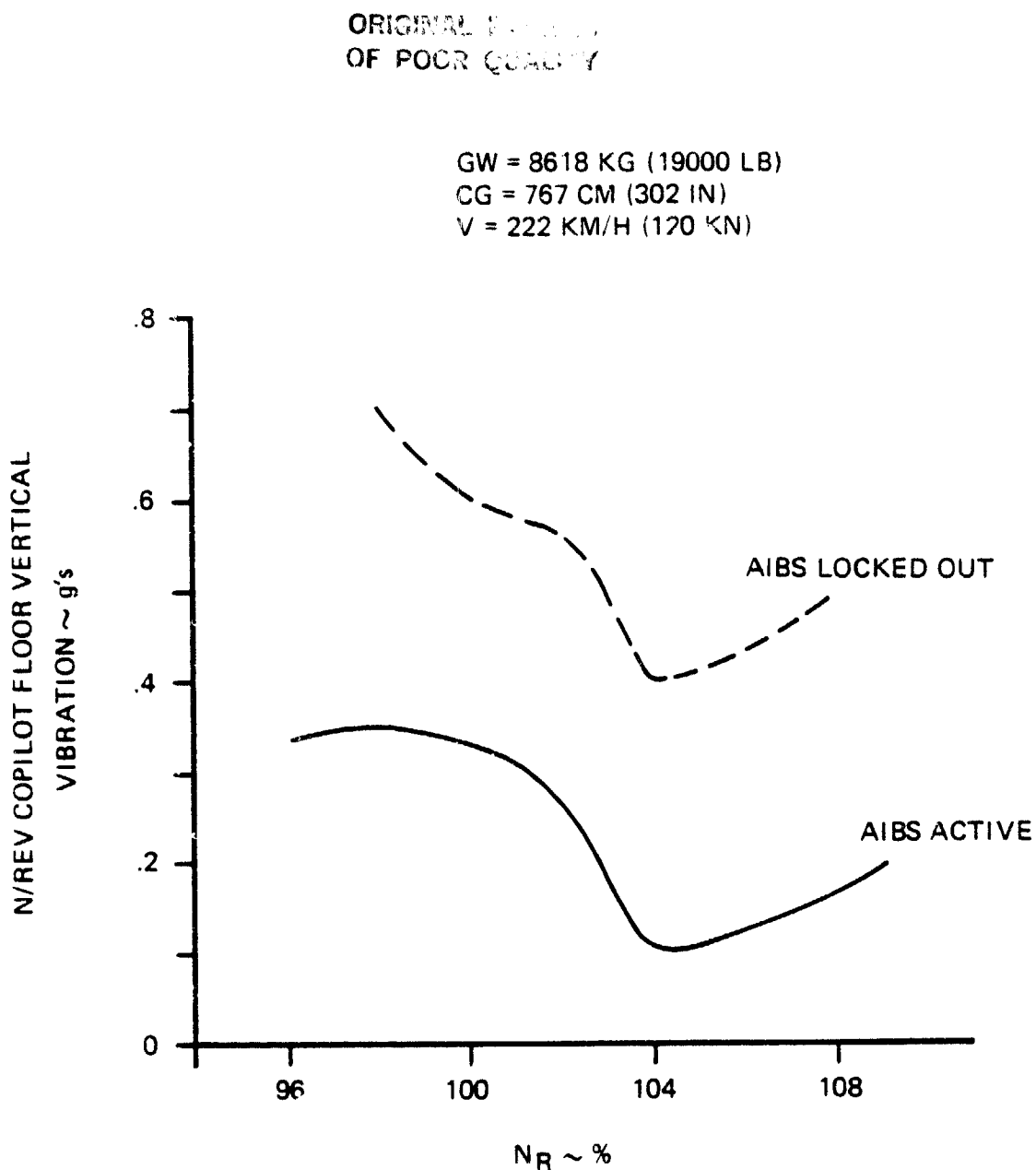


FIGURE 14. ACTIVE ISOLATION SYSTEM EFFECTIVENESS WITH RPM VARIATIONS, S-61 ROTOR

ORIGINAL PAGE IS
OF POOR QUALITY

GW = 12338 KG (27,200 LB)

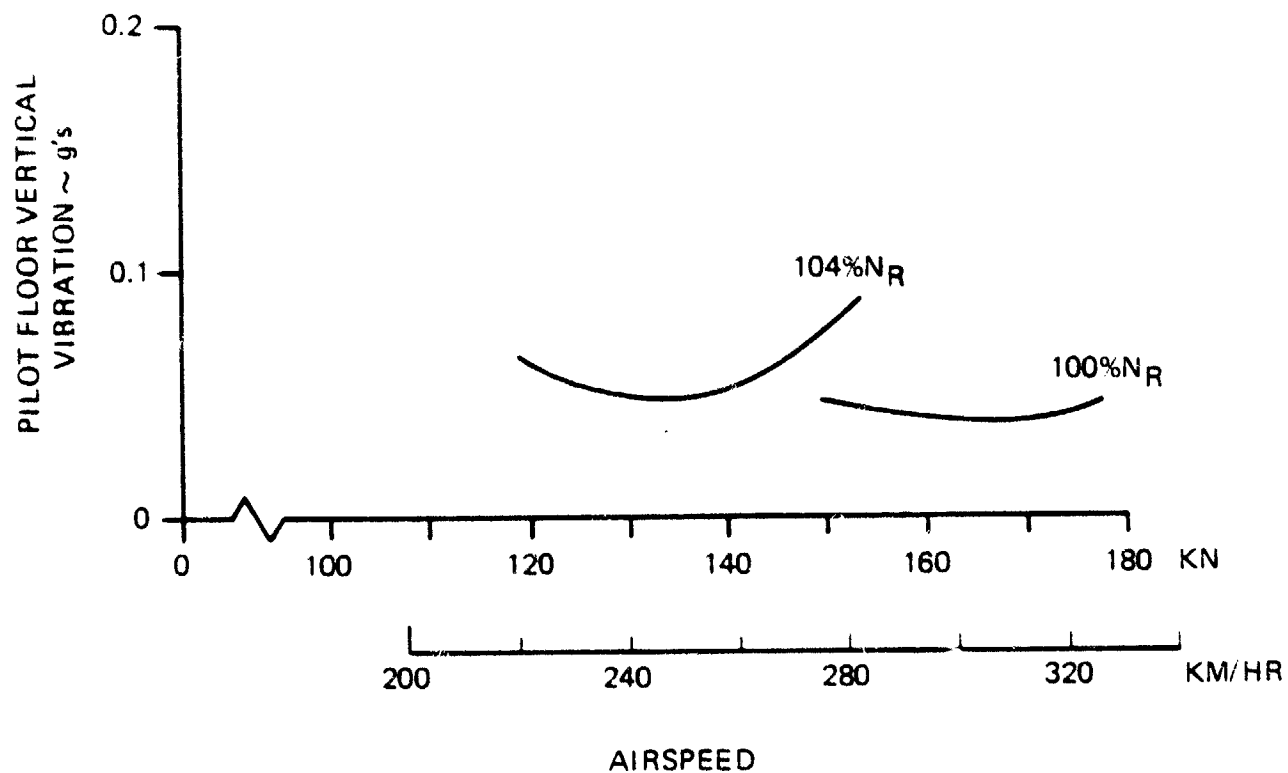


FIGURE 15. RSRA COMPOUND CONFIGURATION N/REV VIBRATION
Vs AIRSPEED AND RPM; S-61 ROTOR; VIBRATION
BY MEANS OF A ROTORHEAD BIFILAR ABSORBER

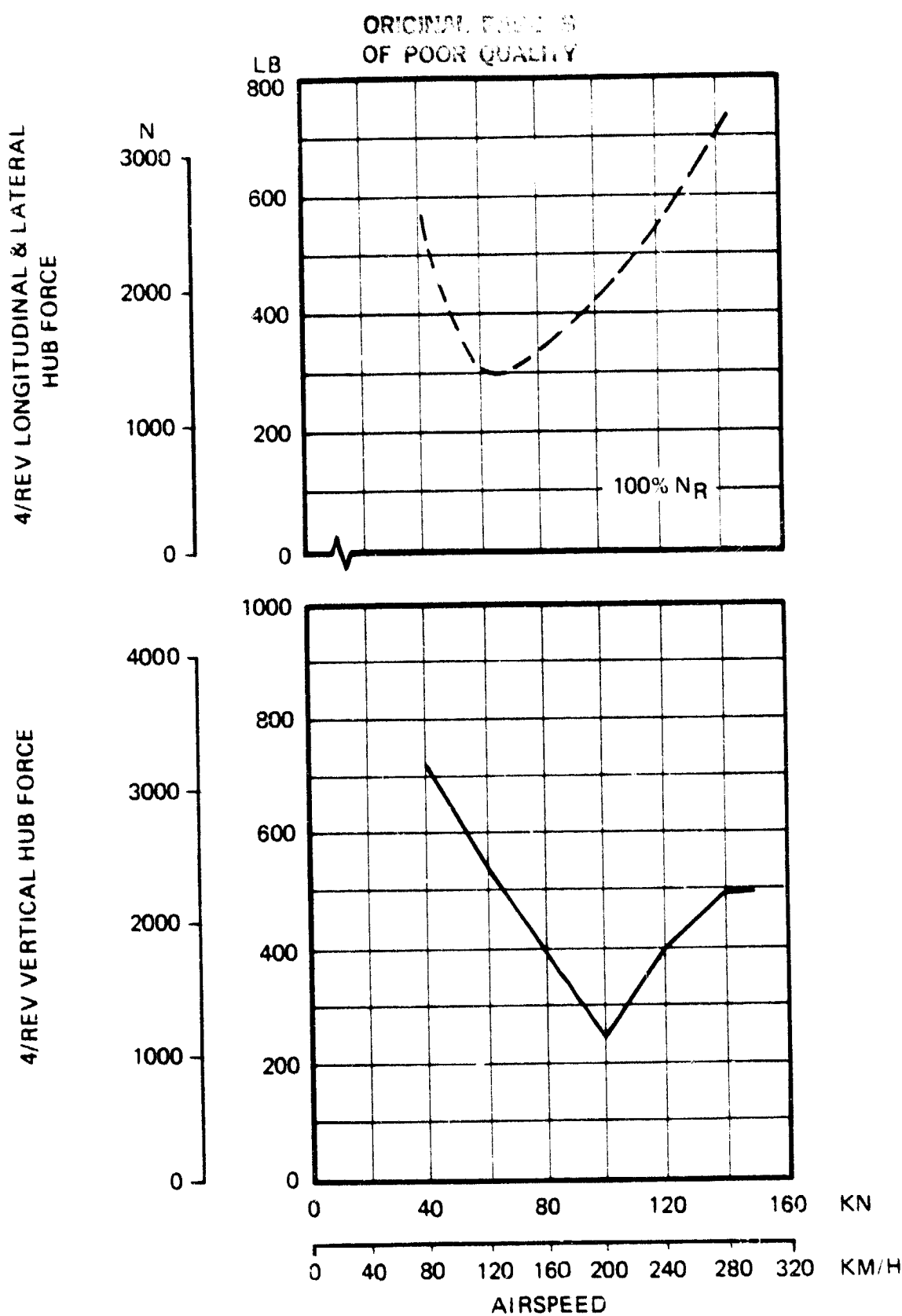


FIGURE 16. BLACK HAWK HELICOPTER 4P HUB VIBRATORY LOADS

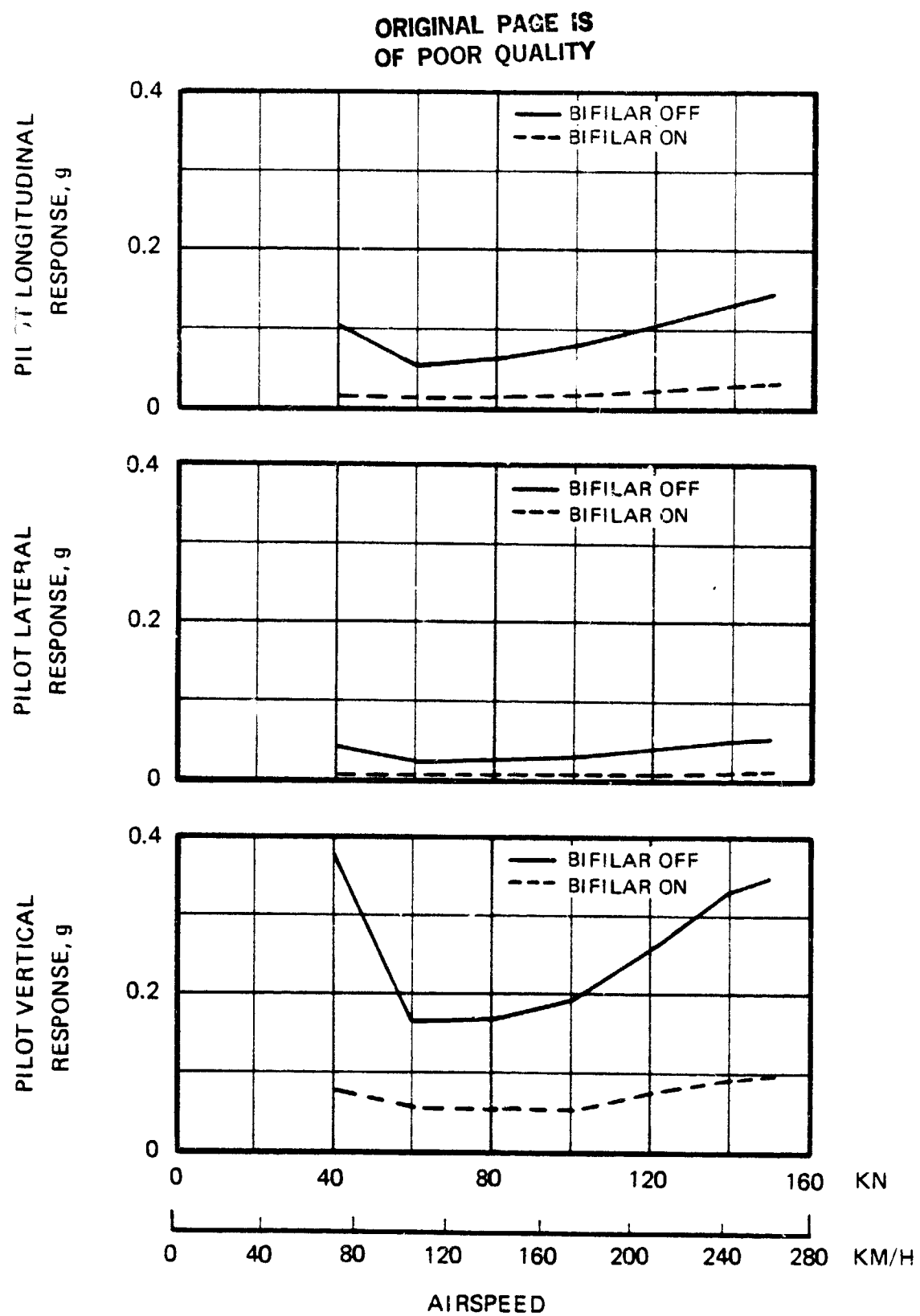


FIGURE 17. EFFECT OF BIFILAR ON RSRA COCKPIT WITH BLACK HAWK ROTOR, (AIBS LOCKED OUT)

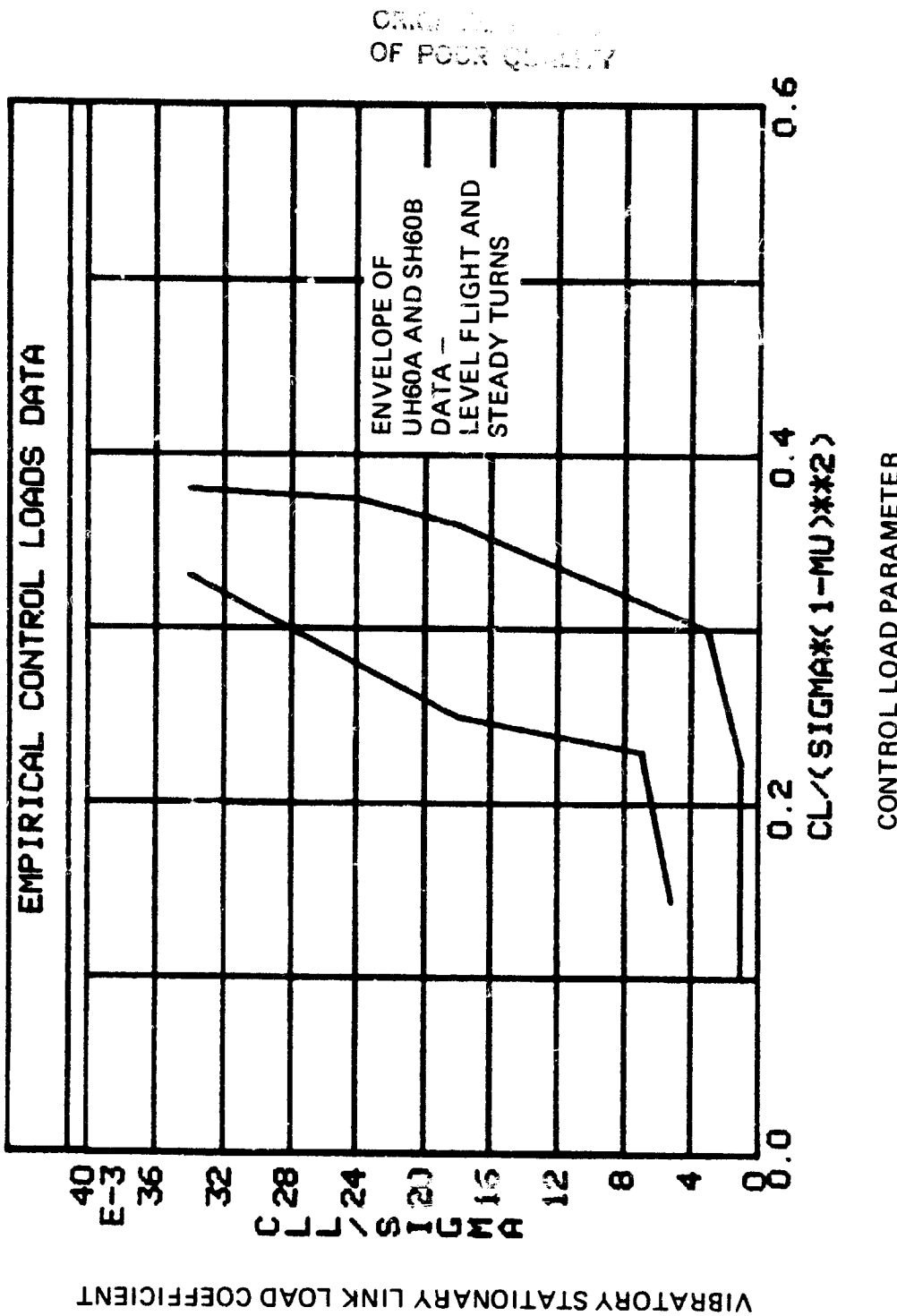


FIGURE 18. EMPIRICAL CONTROL LOADS DATA

ORIGINAL PAGE IS
OF POOR QUALITY

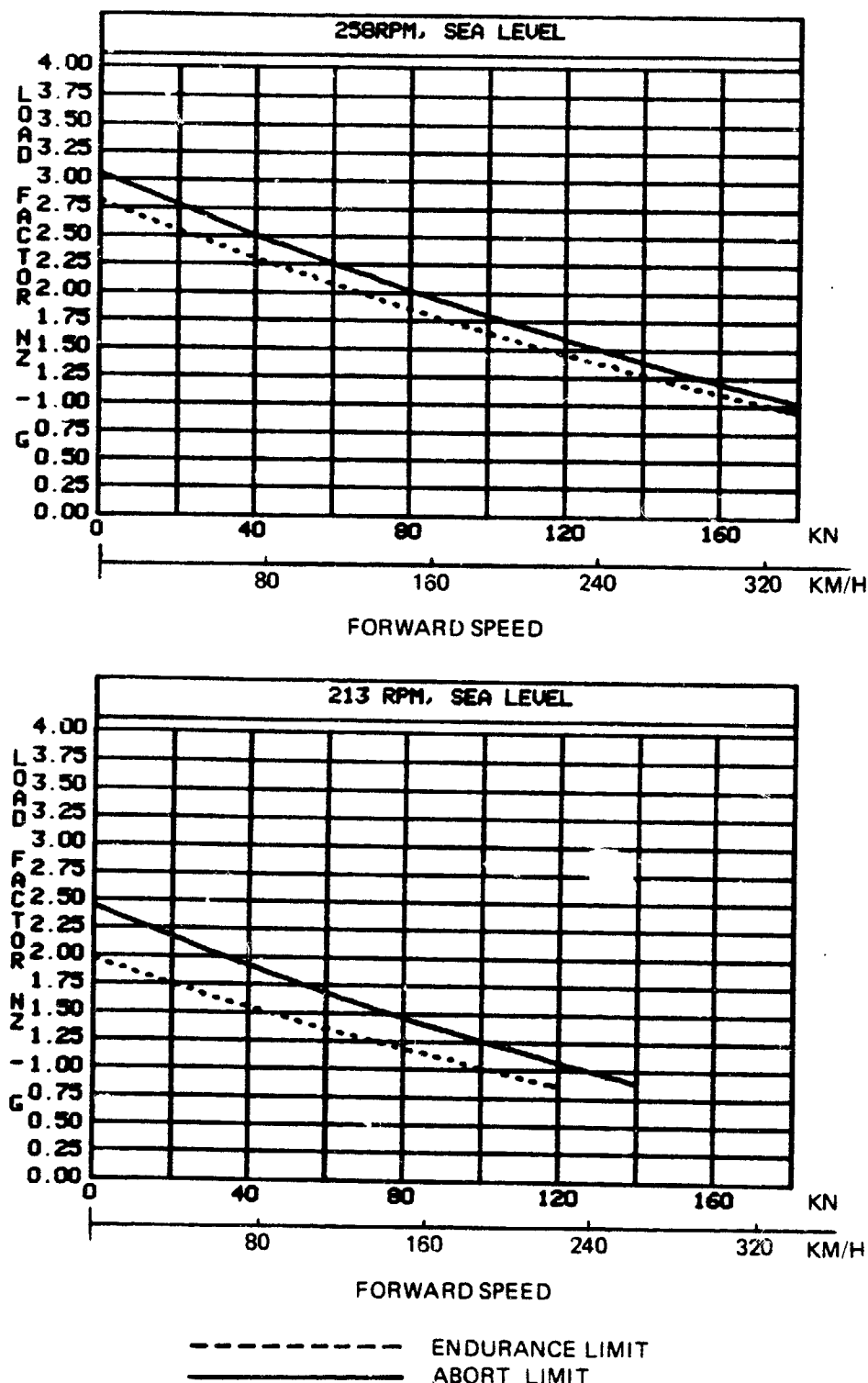


FIGURE 19. CONTROL LOADS LIMITS ON FACTOR VERSUS FORWARD SPEED - SLS DAY.

ORIGINAL PART VS
OF POOR QUALITY

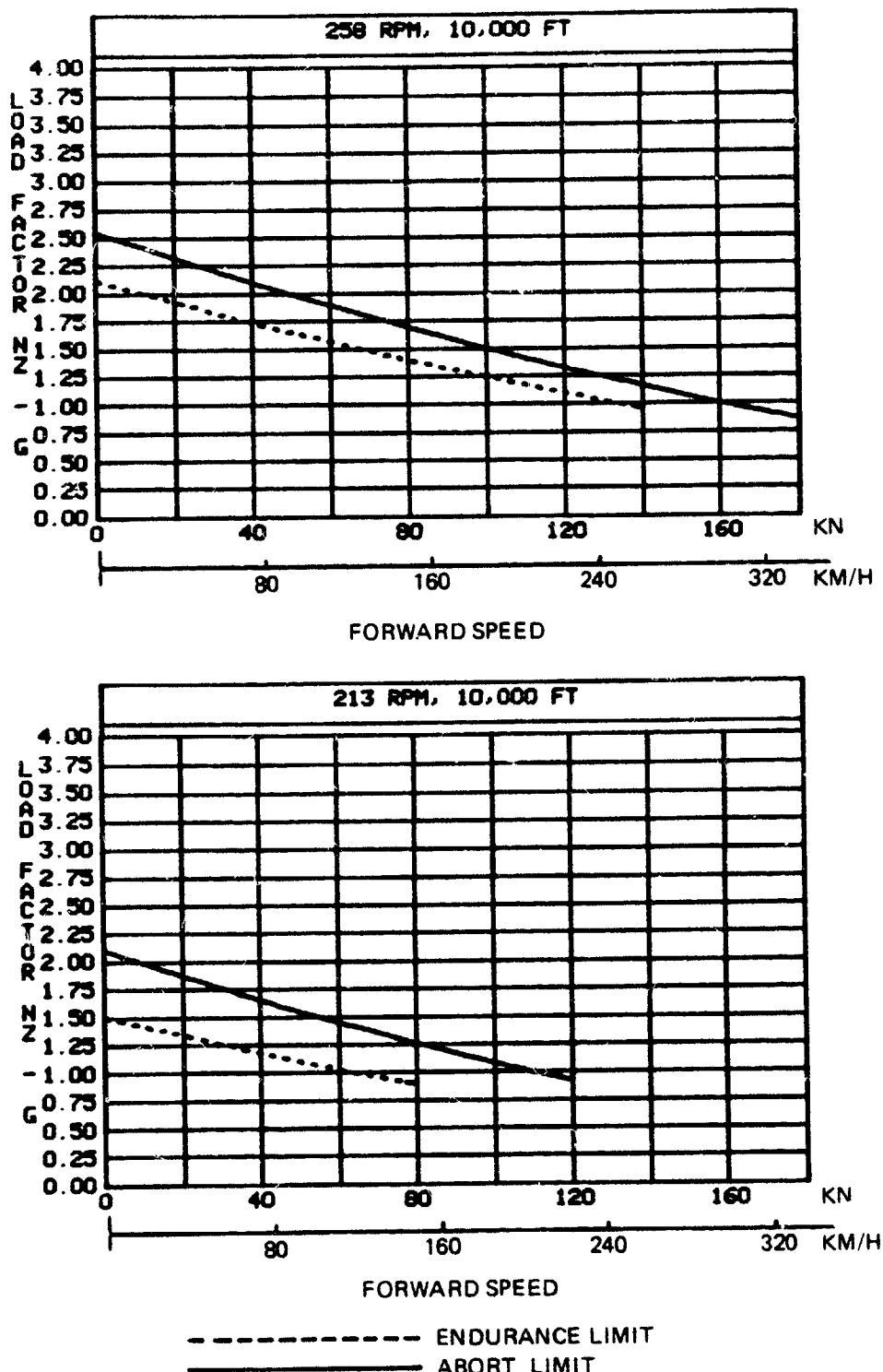


FIGURE 20. CONTROL LOAD LIMITS ON LOAD FACTOR VERSUS FORWARD SPEED - 10,000 FT, STANDARD DAY.

ORIGINAL PAGE IS
OF POOR QUALITY

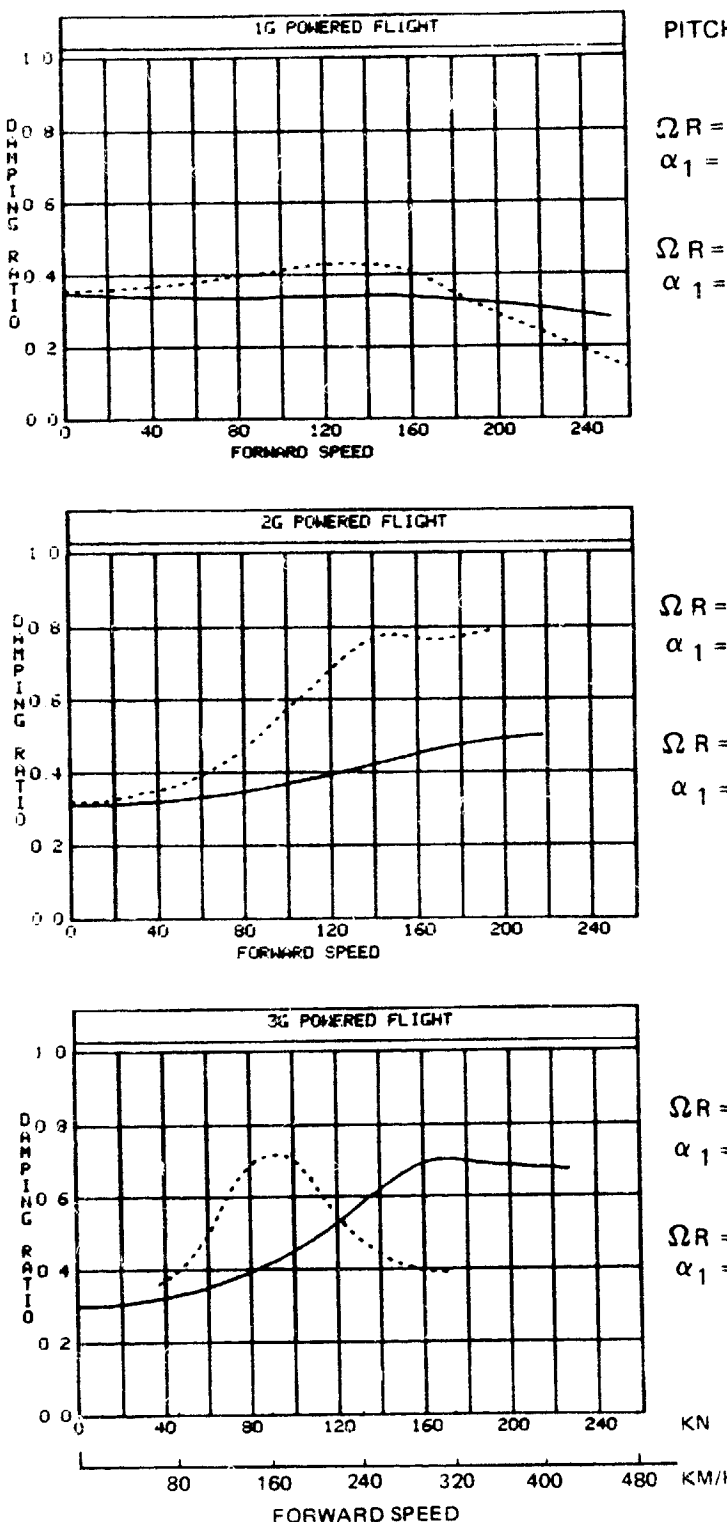


FIGURE 21. BLADE LAG MODE DAMPING RATIO VERSUS AIRSPEED FOR POWERED FLIGHT.

ORIGINAL PAGE VS
OF POOR QUALITY

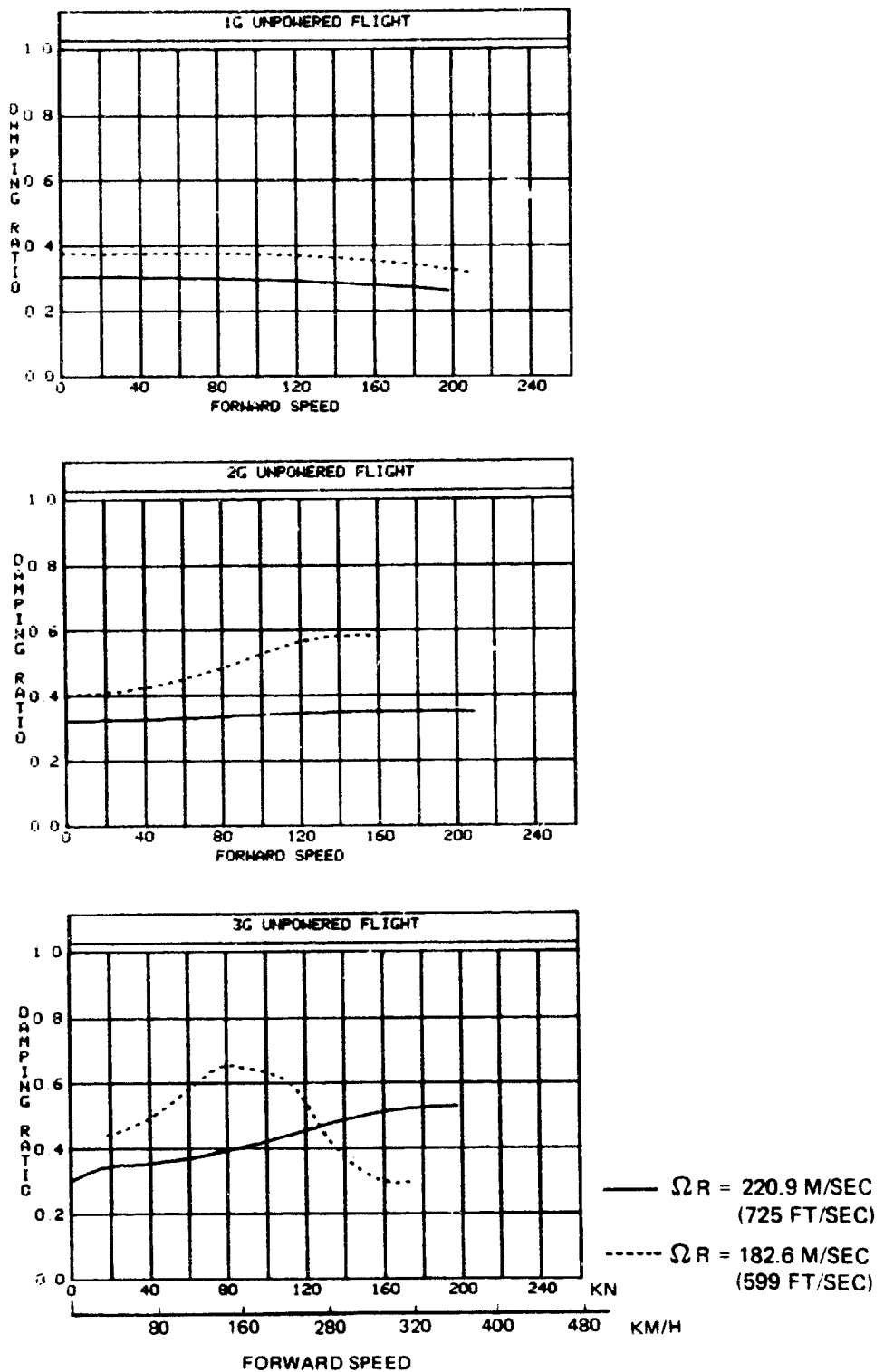


FIGURE 22. BLADE LAG MODE DAMPING RATIO VERSUS
AIRSPEED FOR UNPOWERED FLIGHT
PITCH-LAG COUPLING $\alpha_1 = .1$

ORIGINAL MODE IS
OF POOR QUALITY

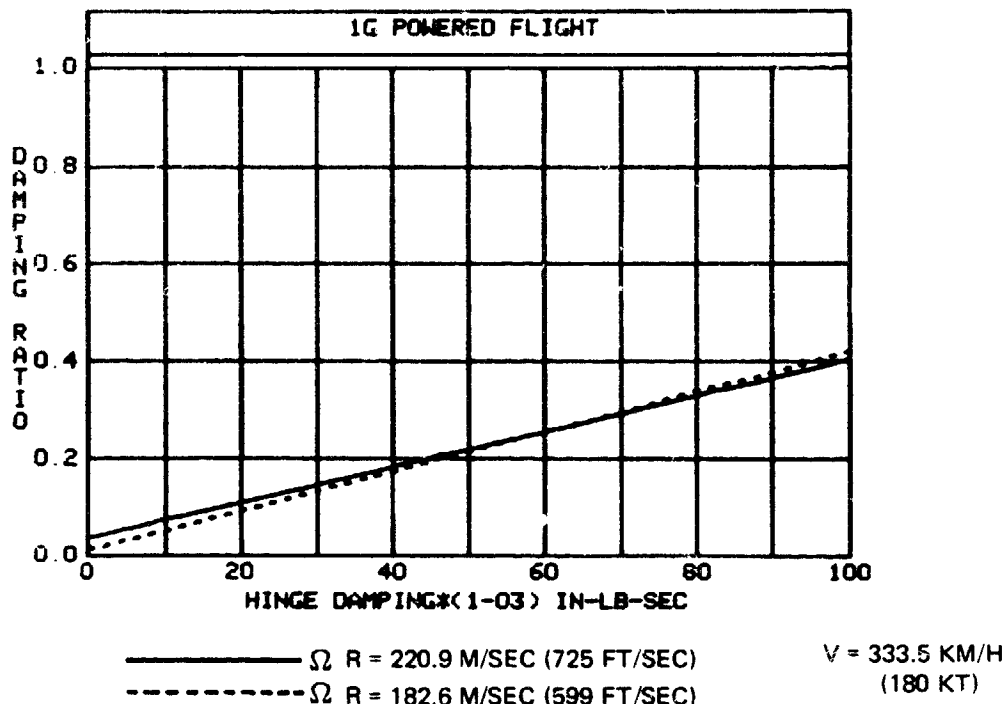


FIGURE 23. EFFECT OF BLADE LAG DAMPING VARIATION ON BLADE LAG MODE DAMPING RATIO.

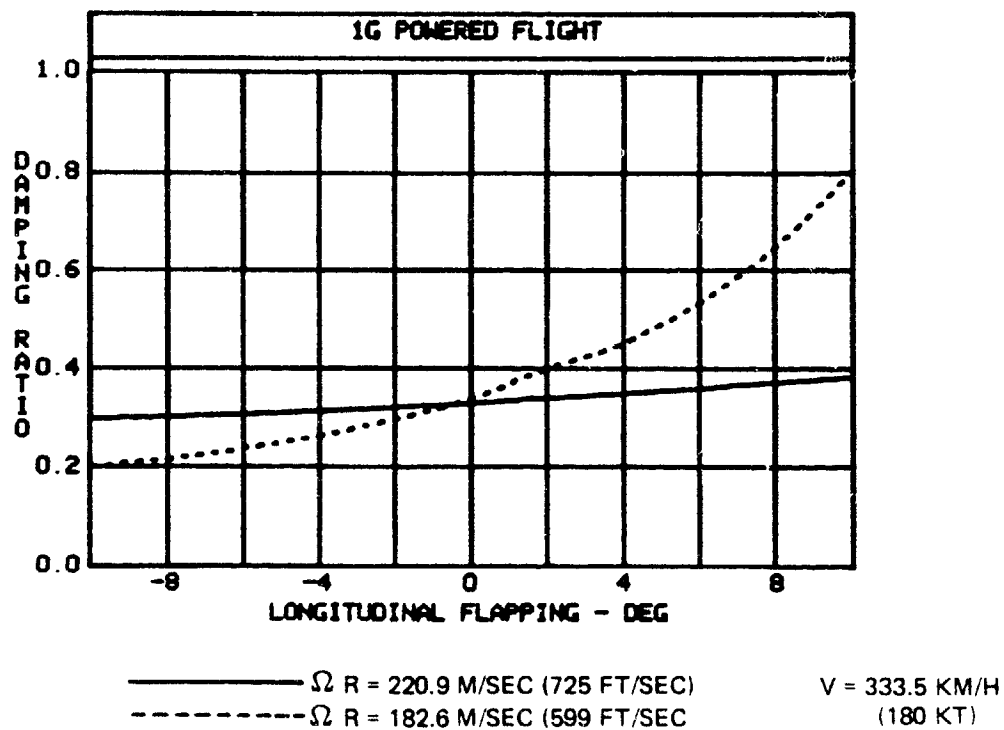


FIGURE 24. EFFECT OF LONGITUDINAL FLAPPING VARIATION ON BLADE LAG MODE DAMPING RATIO.

**OPERATING POINTS
OF POOR QUALITY**

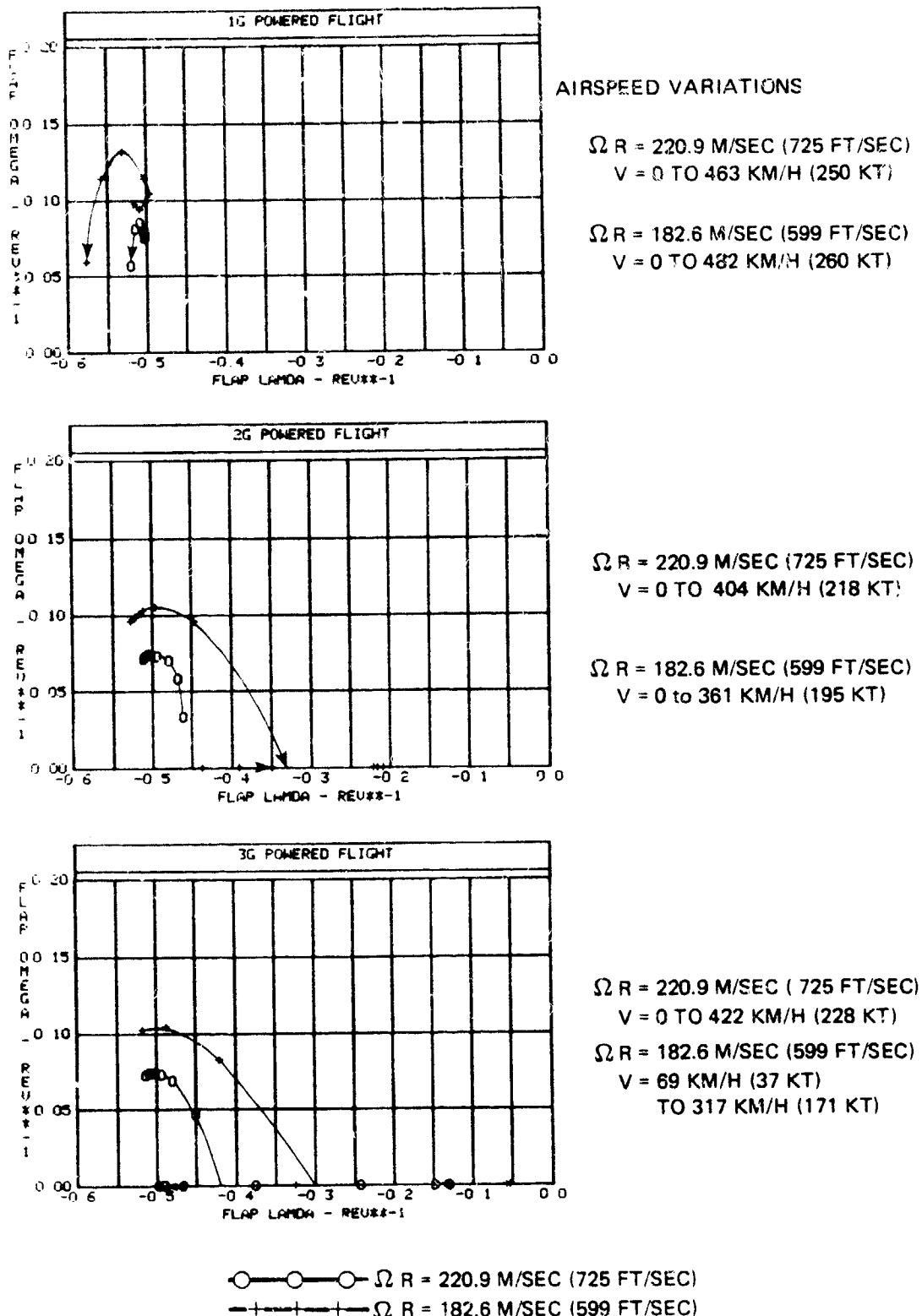


FIGURE 25. ROOT LOCUS FOR FLAP AND LAG MODES WITH AIRSPEED VARIATION IN POWERED FLIGHT.

ORIGINAL EQUATIONS
OF POOR QUALITY

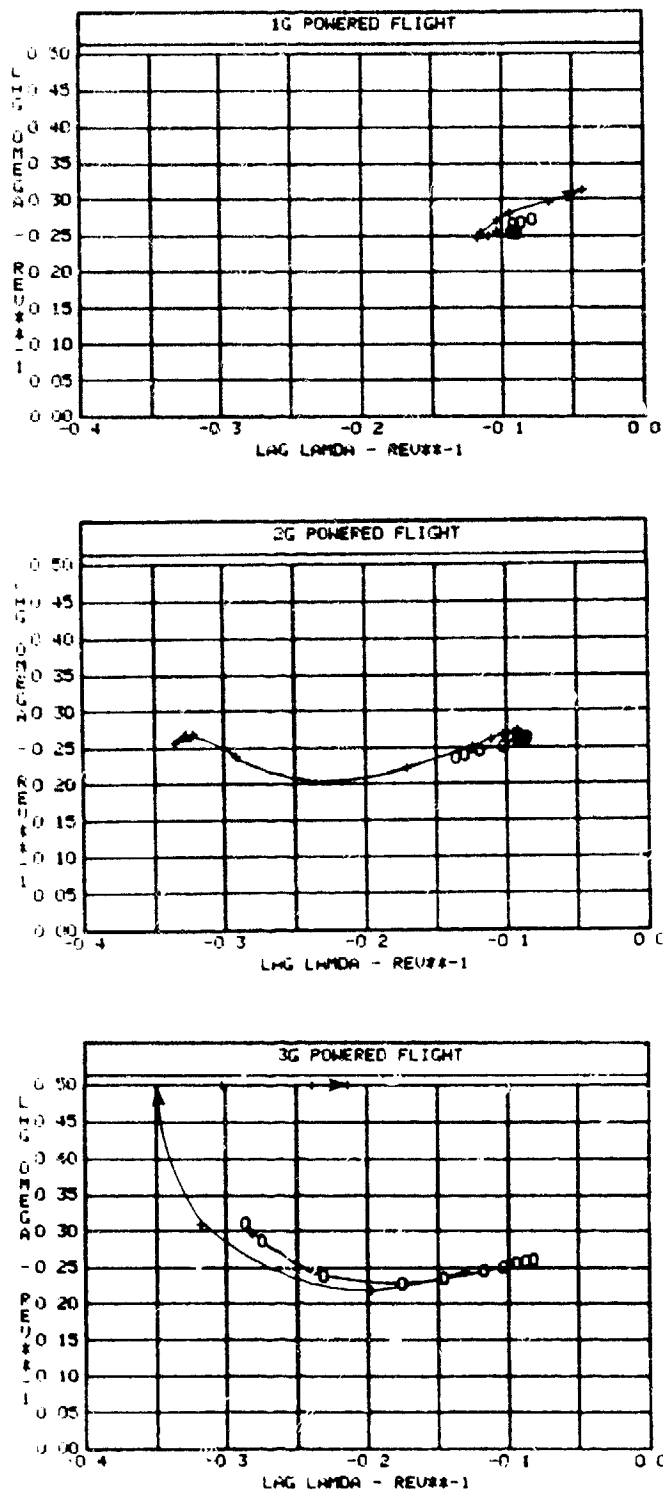
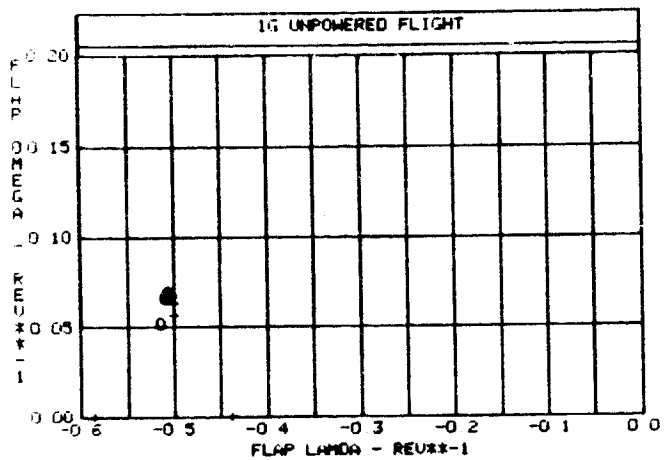


FIGURE 25. (CONCLUDED)

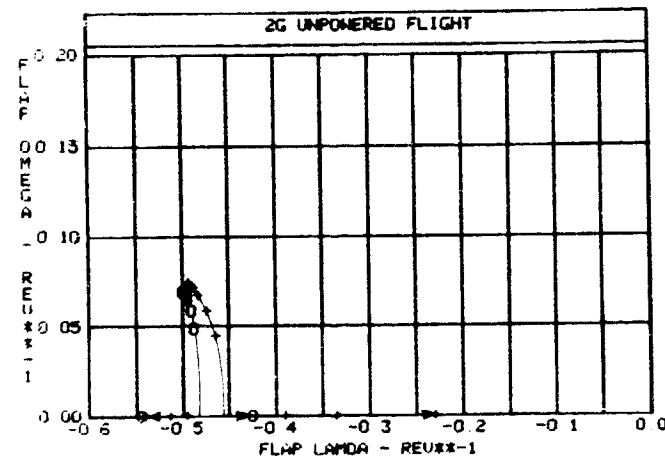
ORIGIN
OF POOR STABILITY



AIRSPEED VARIATIONS

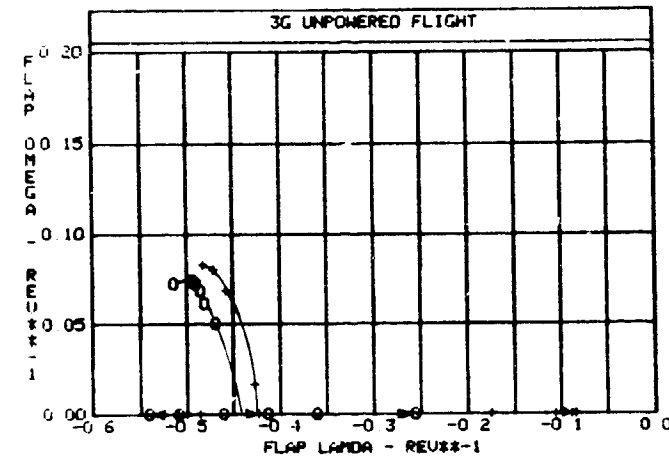
$\Omega R = 220.9 \text{ M/SEC (725 FT/SEC)}$
 $V = 0 \text{ TO } 367 \text{ KM/H (198 KT)}$

$\Omega R = 182.6 \text{ M/SEC (599 FT/SEC)}$
 $V = 0 \text{ TO } 389 \text{ KM/H (210 KT)}$



$\Omega R = 220.9 \text{ M/SEC (725 FT/SEC)}$
 $V = 0 \text{ TO } 387 \text{ KM/H (209 KT)}$

$\Omega R = 182.6 \text{ M/SEC (599 FT/SEC)}$
 $V = 0 \text{ TO } 304 \text{ KM/H (164 KT)}$



$\Omega R = 220.9 \text{ M/SEC (725 FT/SEC)}$
 $V = 0 \text{ to } 367 \text{ KM/H (198 KT)}$

$\Omega R = 182.6 \text{ M/SEC (599 FT/SEC)}$
 $V = 33.4 \text{ KM/H (18 KT)}$
 $\text{TO } 324 \text{ KM/H (175 KT)}$

○—○ $\Omega R = 220.9 \text{ M/SEC (725 FT/SEC)}$
 + + + $\Omega R = 182.6 \text{ M/SEC (599 FT/SEC)}$

FIGURE 26. ROOT LOCUS PLOTS FOR FLAP AND LAG MODES
 WITH AIRSPEED VARIATION IN UNPOWERED FLIGHT

ORIGIN OF POOR STABILITY

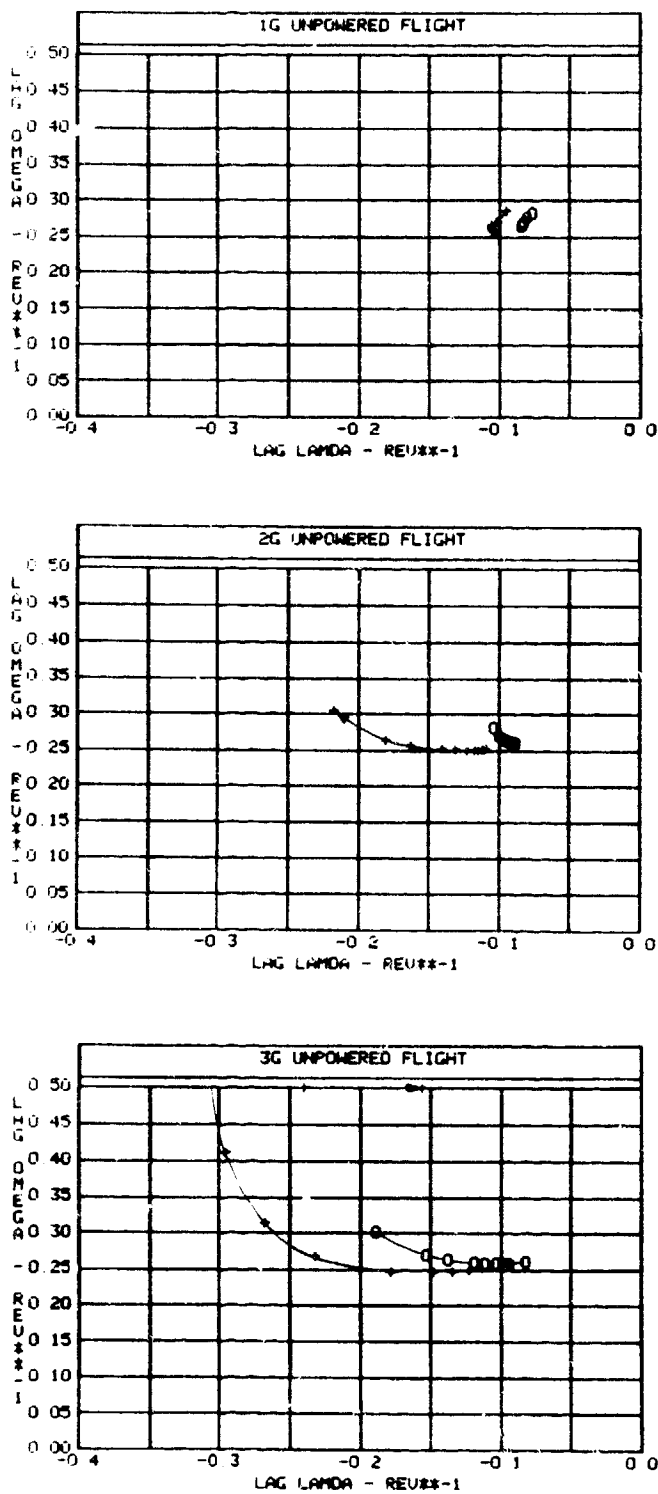
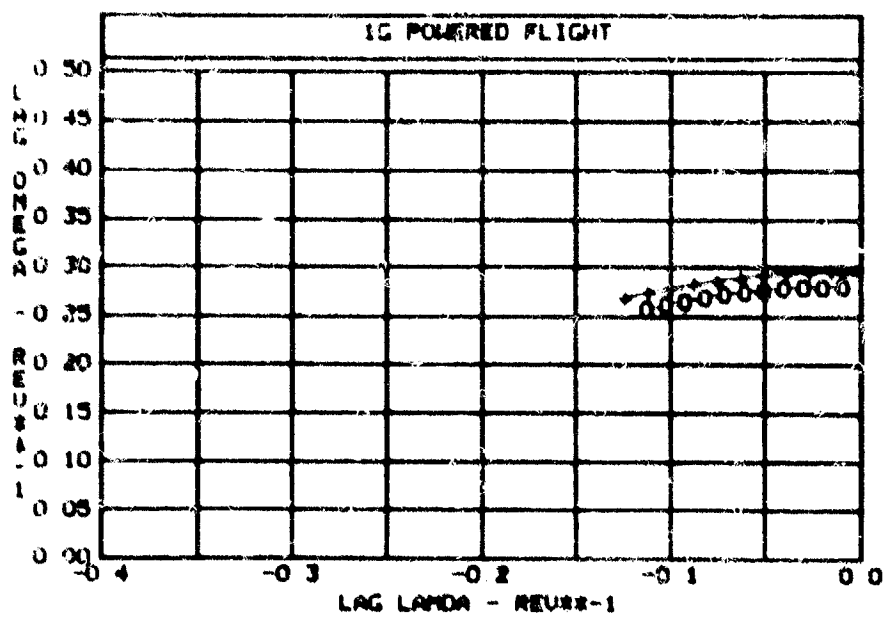
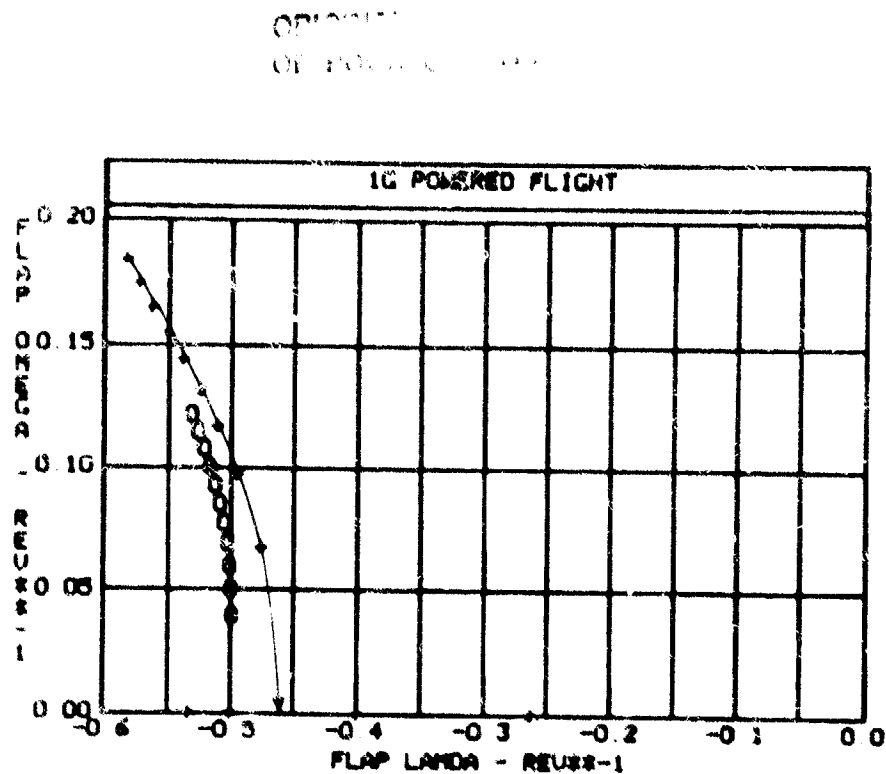


FIGURE 26. (CONCLUDED)



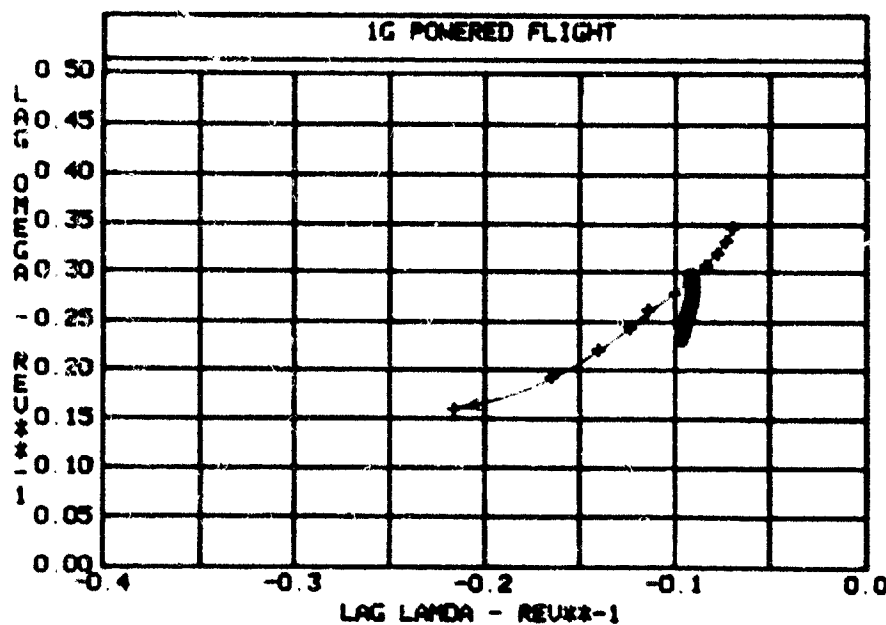
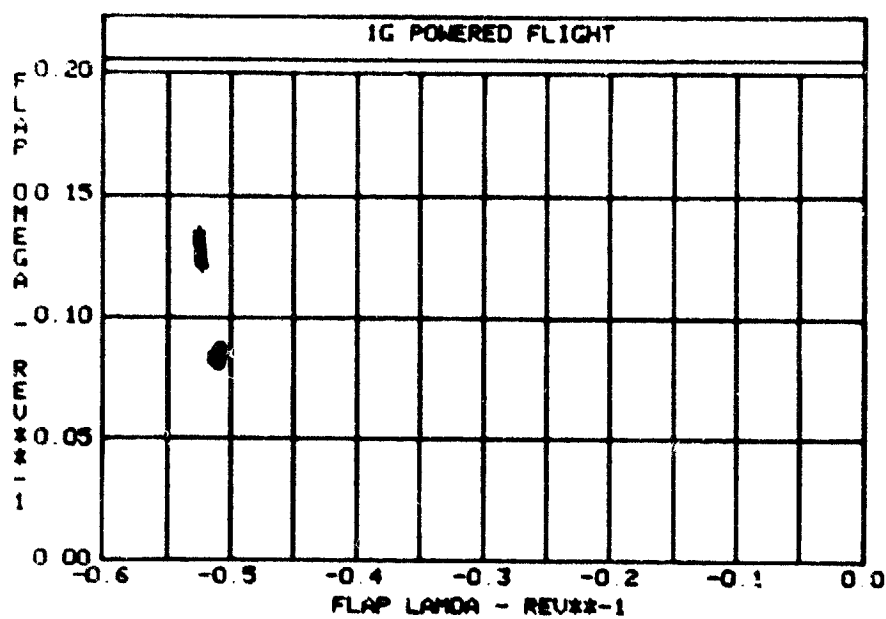
AIRSPED V = 333.6 KM/H (180 KT)

—(—) S2R = 220.9 M/SEC (726 FT/SEC)
-+---+---+--- S2R = 182.6 M/SEC (599 FT/SEC)

VARIATION OF HINGE DAMPING COEFFICIENT
 $C_{DH} = 11298 \text{ N}\cdot\text{M}\cdot\text{SEC}$ (100,000 IN-LB-SEC) TO 0

FIGURE 27. ROOT LOCUS PLOTS FOR FLAP AND LAG MODES WITH LAG DAMPING VARIATION.

ORIGINAL PAGE IS
OF POOR QUALITY



—○— $\Omega R = 220.9 \text{ M/SEC (725 FT/SEC)}$
-+---+-- $\Omega R = 182.6 \text{ M/SEC (599 FT/SEC)}$
VARIATION OF LONGITUDINAL L FLAPPING
 $a_1 s = -10^\circ \text{ TO } +10^\circ$

FIGURE 28. ROOT LOCUS PLOTS FOR FLAP AND LAG MODES WITH LONGITUDINAL FLAPPING VARIATION.

ORIGINAL PAGE IS
OF POOR QUALITY

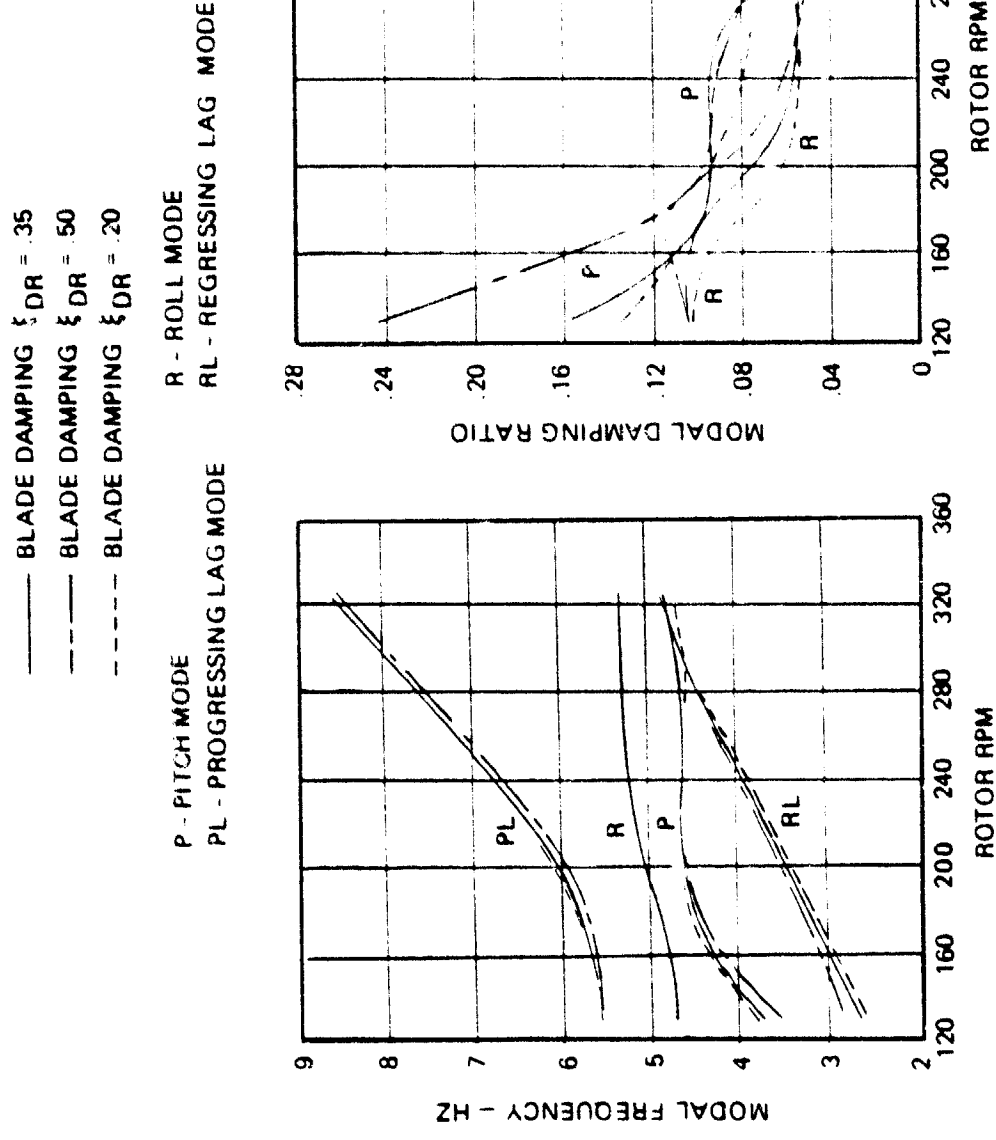


FIGURE 29. MECHANICAL STABILITY VARIATION WITH RPM AND BLADE DAMPING AT 0% AIRBORNE

ORIGINAL PAGE IS
OF POOR QUALITY

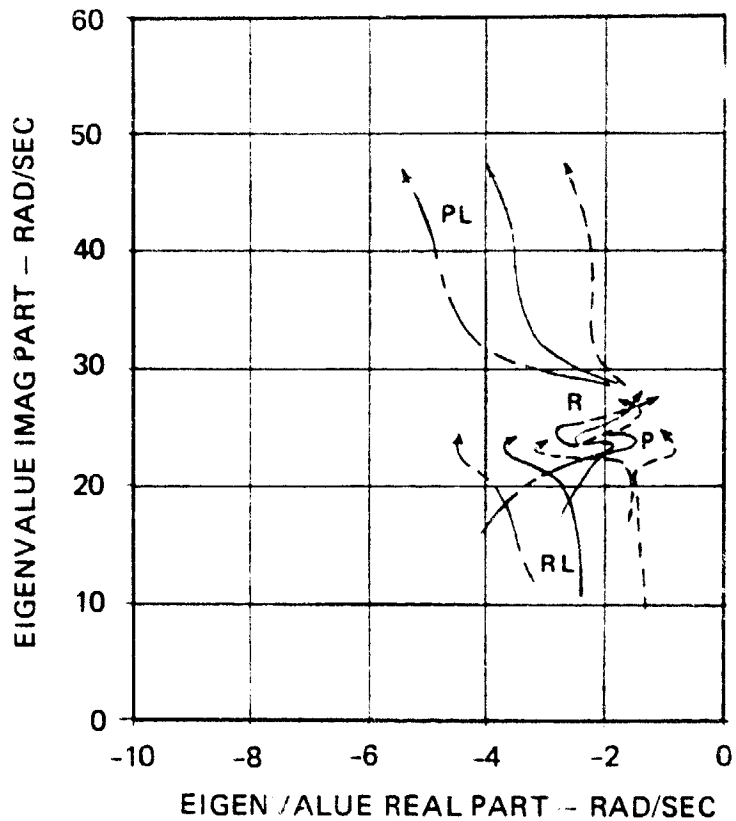


FIGURE 29. (CONCLUDED)

ORIGINAL PAGE IS
OF POOR QUALITY

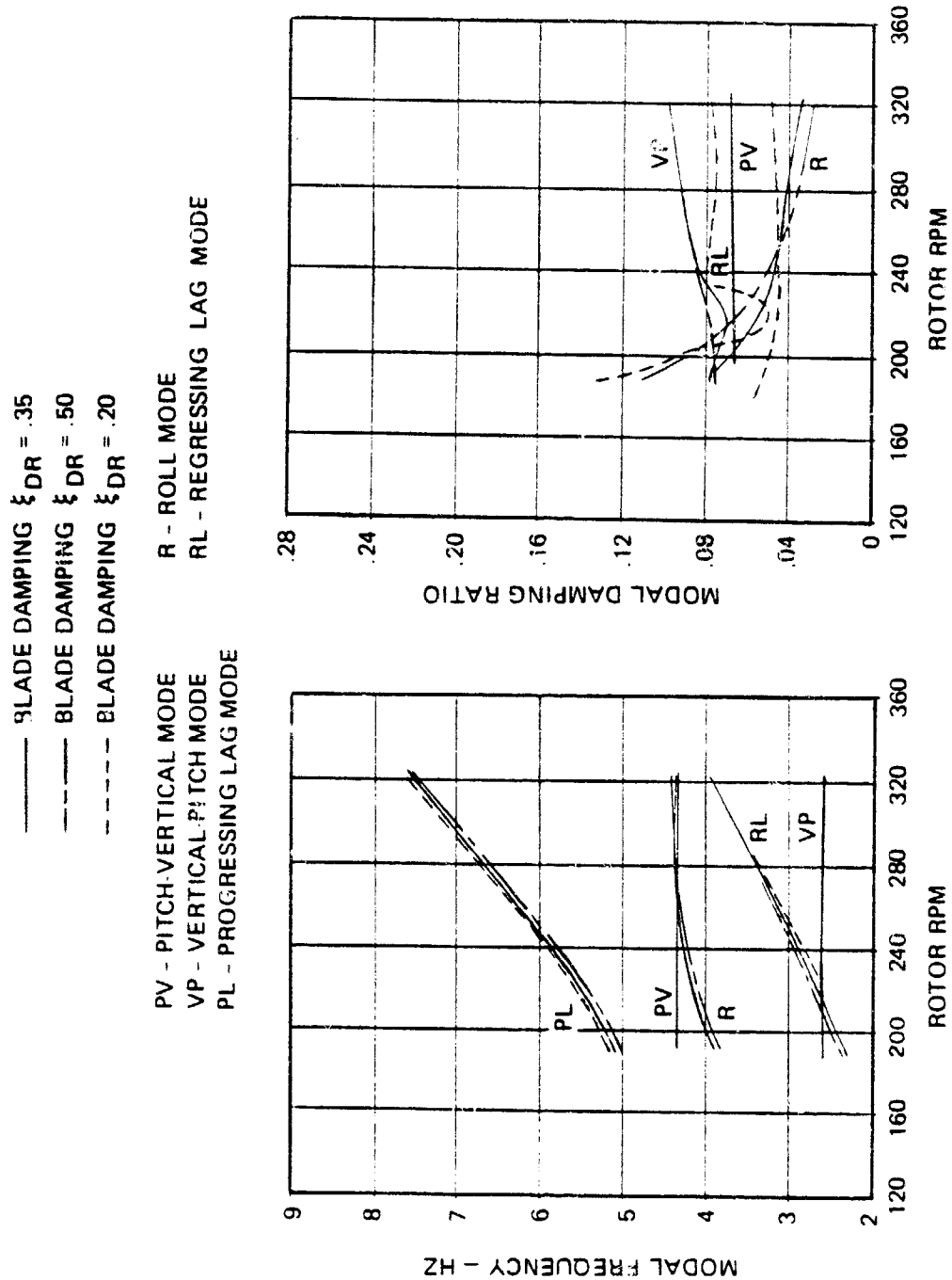


FIGURE 30. MECHANICAL STABILITY VARIATION WITH RPM AND BLADE DAMPING AT 80% AIRBORNE

ORIGINAL PAPER
OF POOR QUALITY

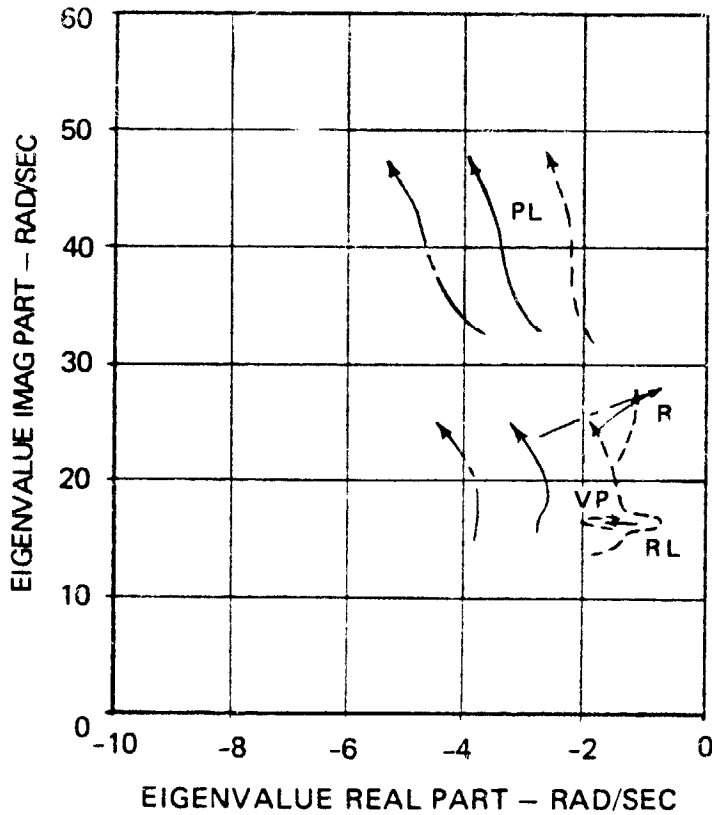


FIGURE 30. (CONCLUDED)

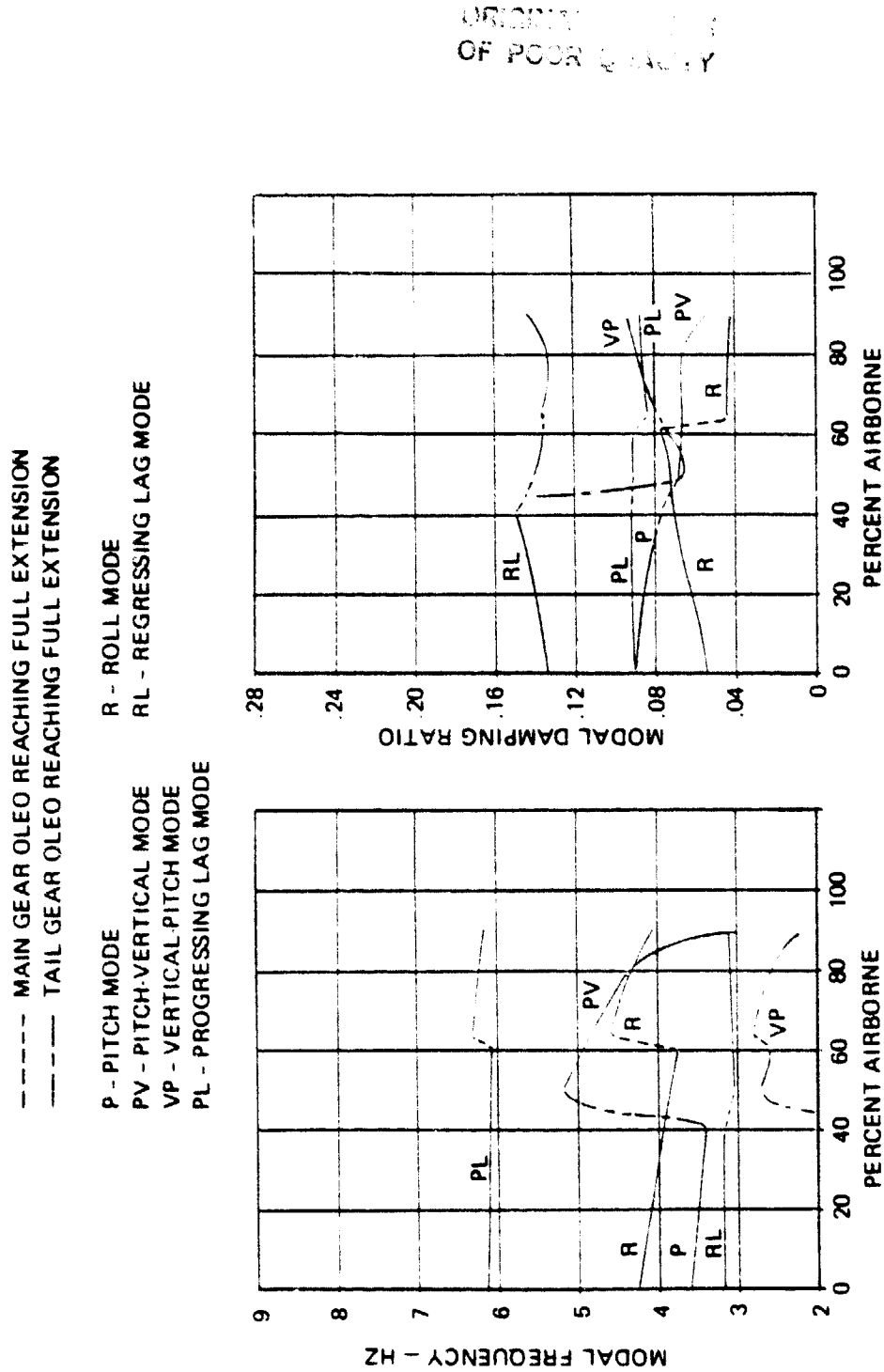


FIGURE 31. MECHANICAL STABILITY VARIATION WITH PERCENT AIRBORNE AT 258 RPM. $\xi_{DR} = .35$

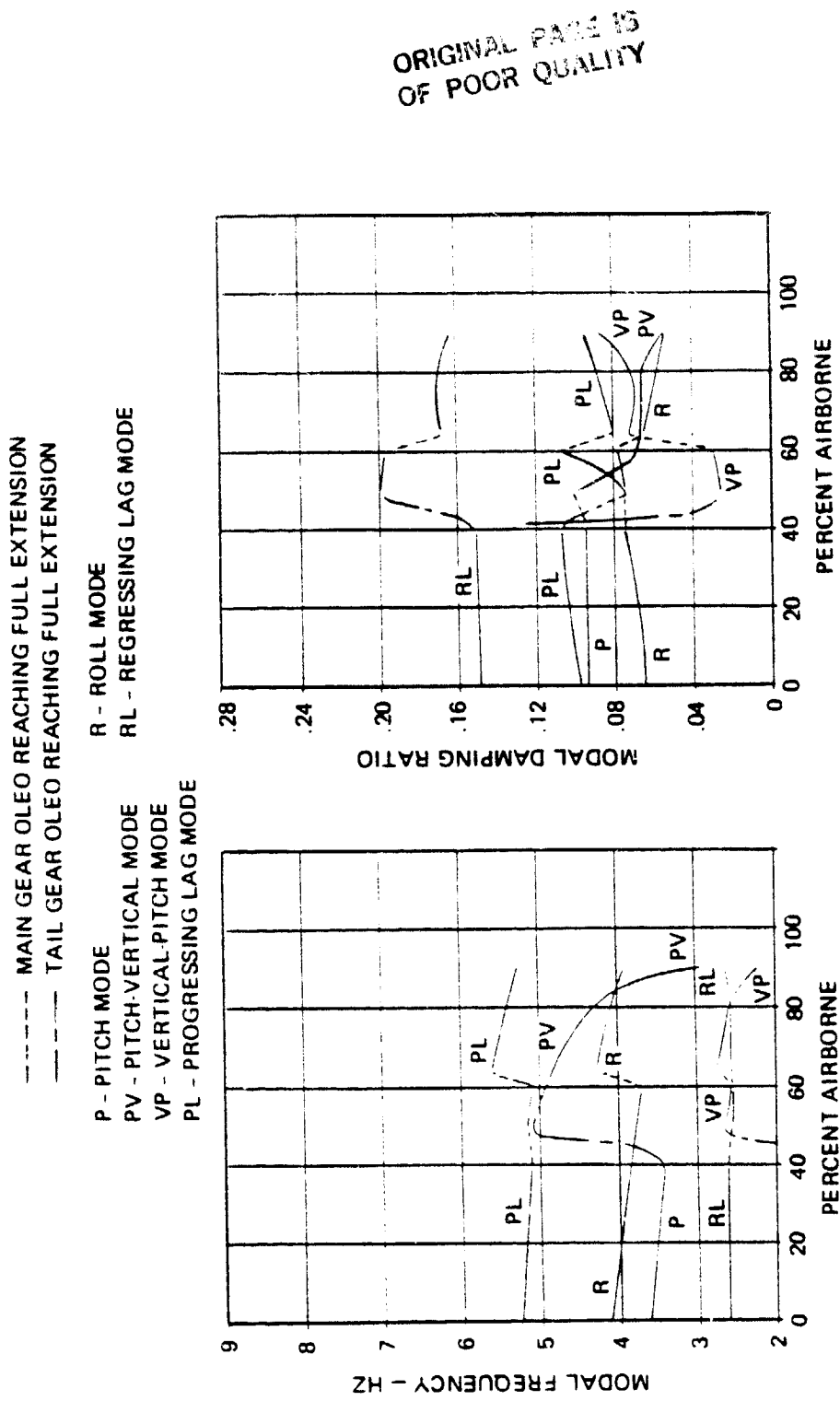


FIGURE 32. MECHANICAL STABILITY VARIATION WITH PERCENT AIRBORNE AT 213 RPM; $\xi_{DR} = .35$

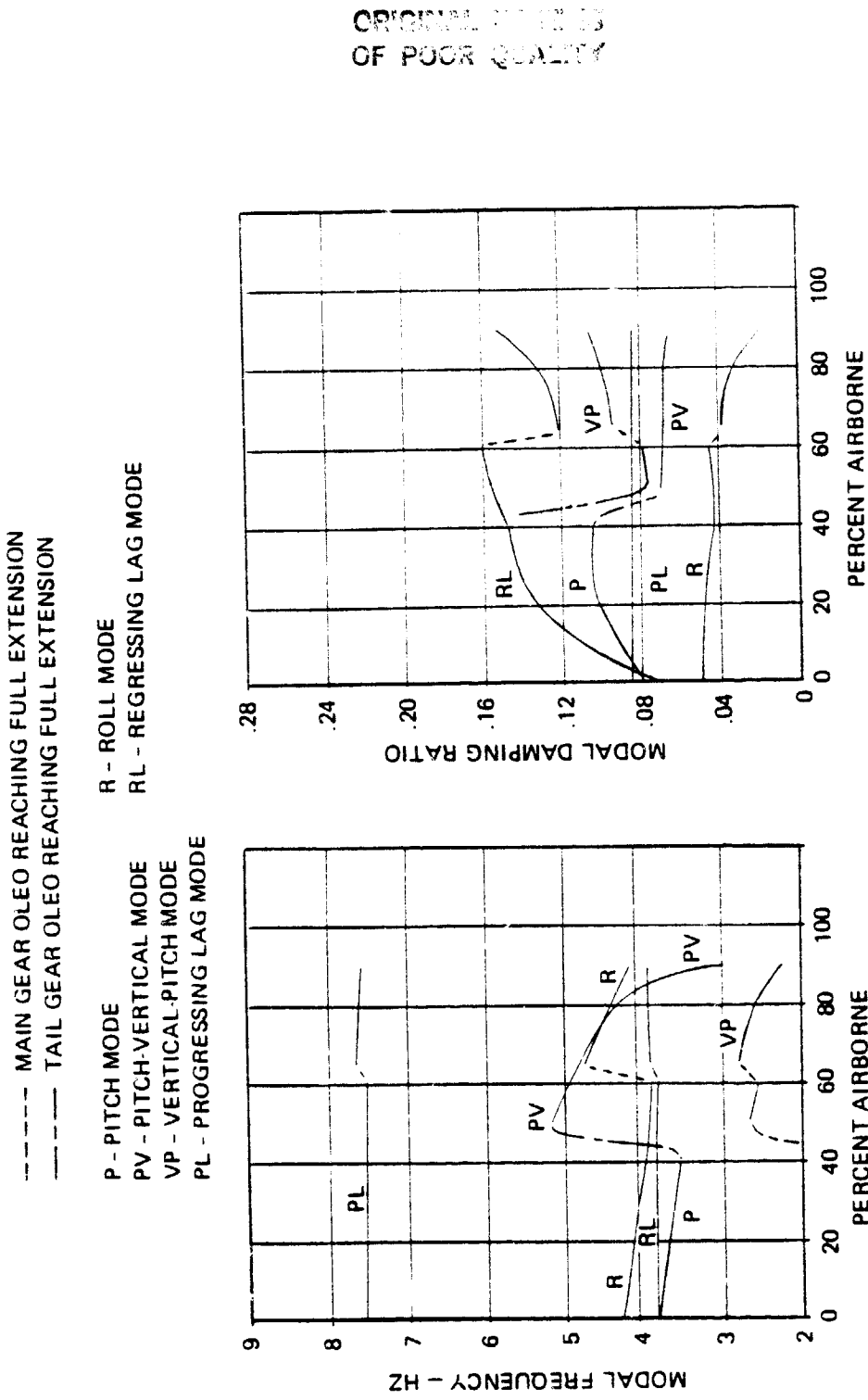


FIGURE 33. MECHANICAL STABILITY VARIATION WITH PERCENT AIRBORNE AT 322.5 RPM; $\zeta DR = .35$

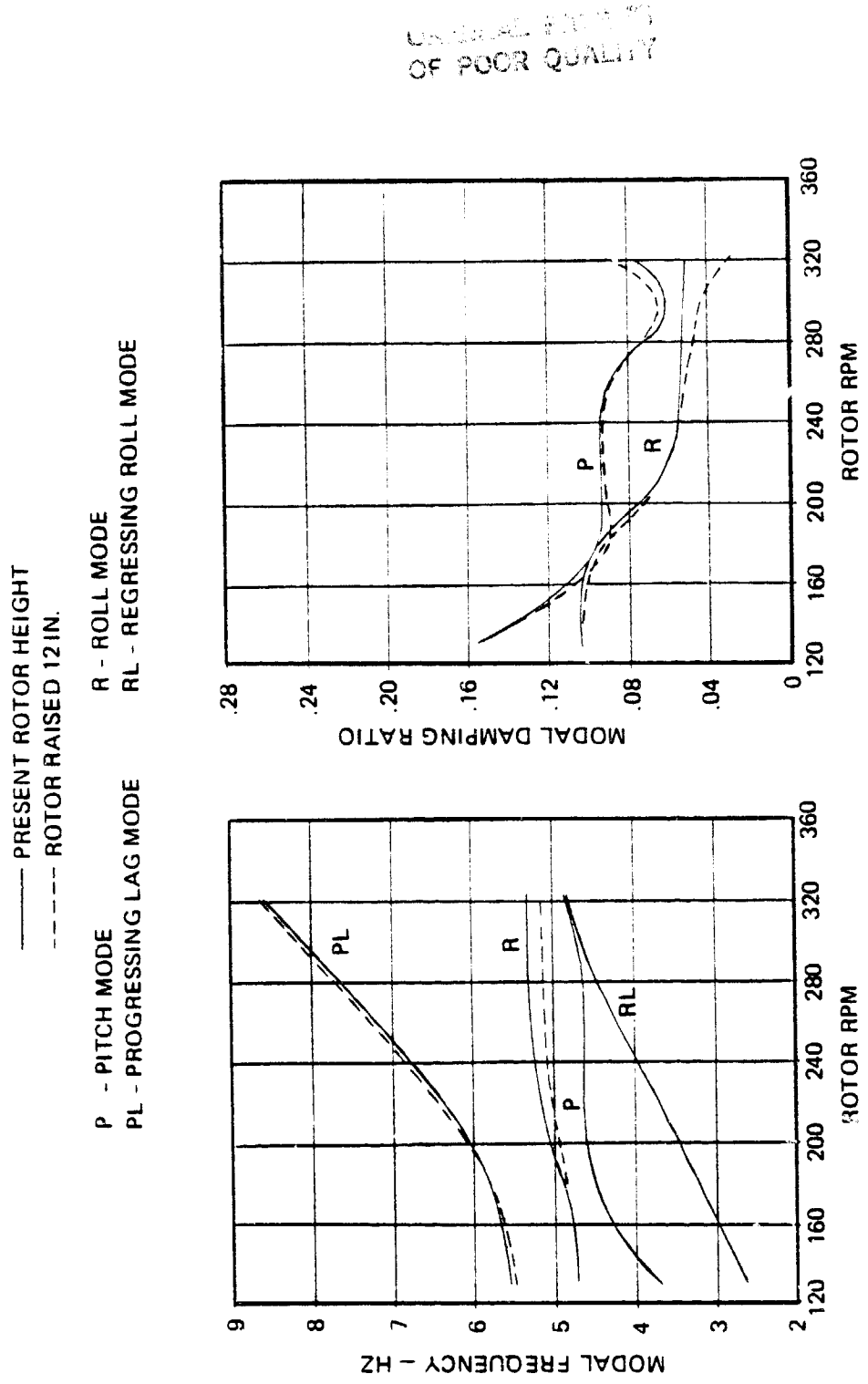


FIGURE 34. MECHANICAL STABILITY VARIATION WITH RPM AND ROTOR HEIGHT AT 0% AIRBORNE; $\xi_{DR} = .35$

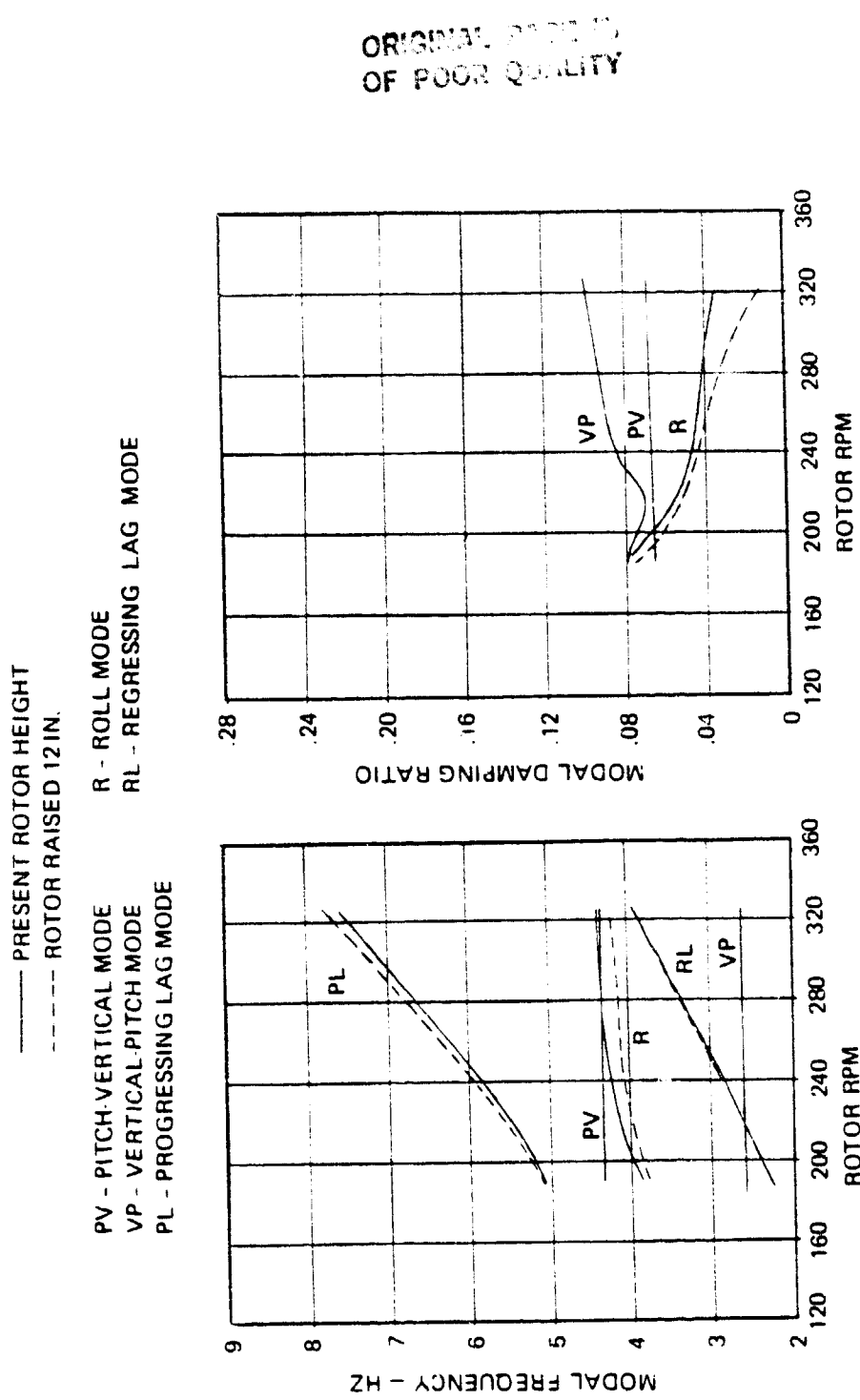


FIGURE 35. MECHANICAL STABILITY VARIATION WITH RPM AND ROTOR HEIGHT AT 80% AIRBORNE; $\xi_{DR} = .35$

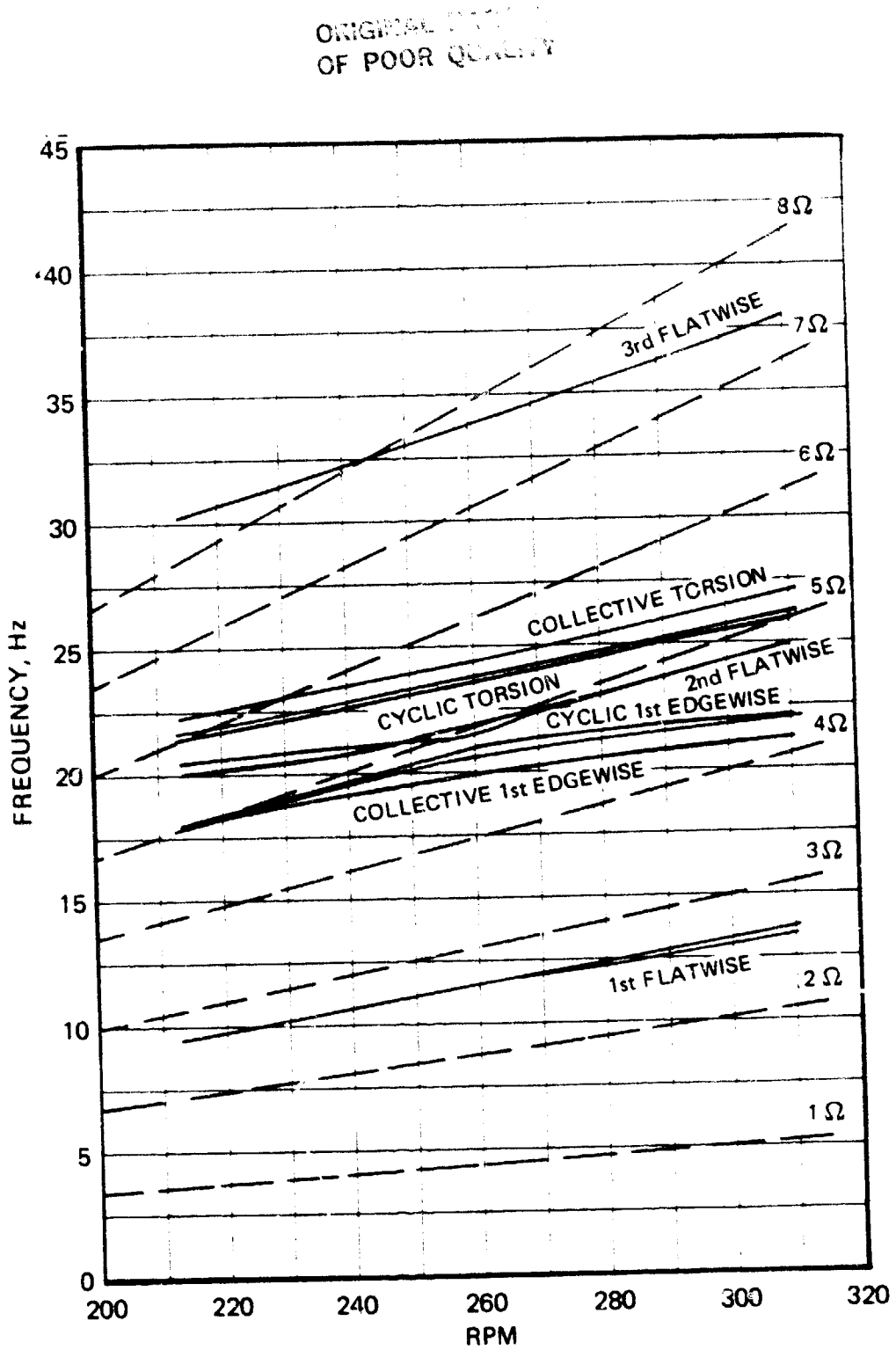


FIGURE 36. COUPLED BLADE BENDING MODE ROTATING SYSTEM
FREQUENCY VERSUS ROTOR SPEED - AIBS ACTIVE

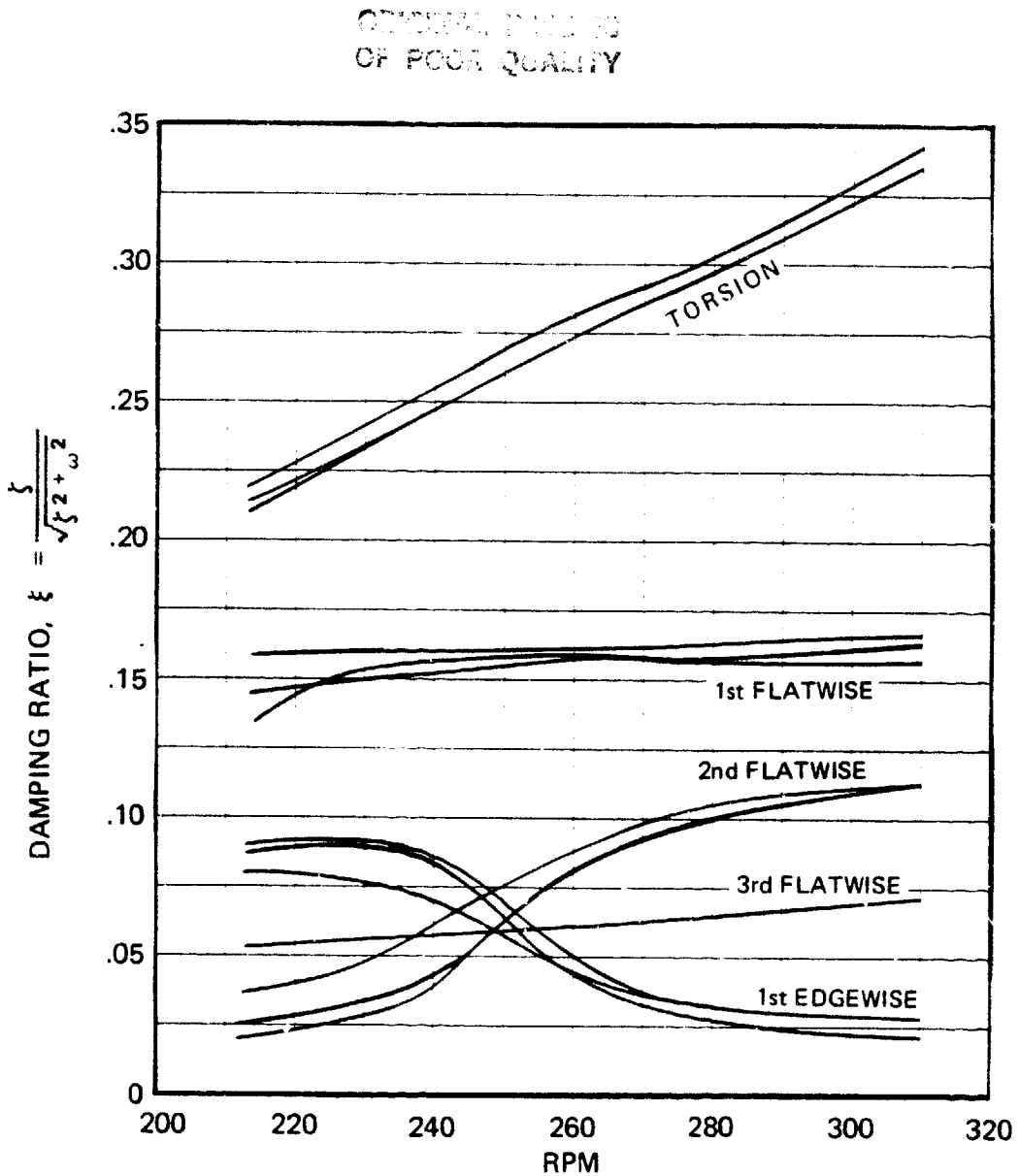


FIGURE 37. COUPLED BLADE BENDING MODE ROTATING SYSTEM
DAMPING RATIO VERSUS ROTOR SPEED - AIBS ACTIVE

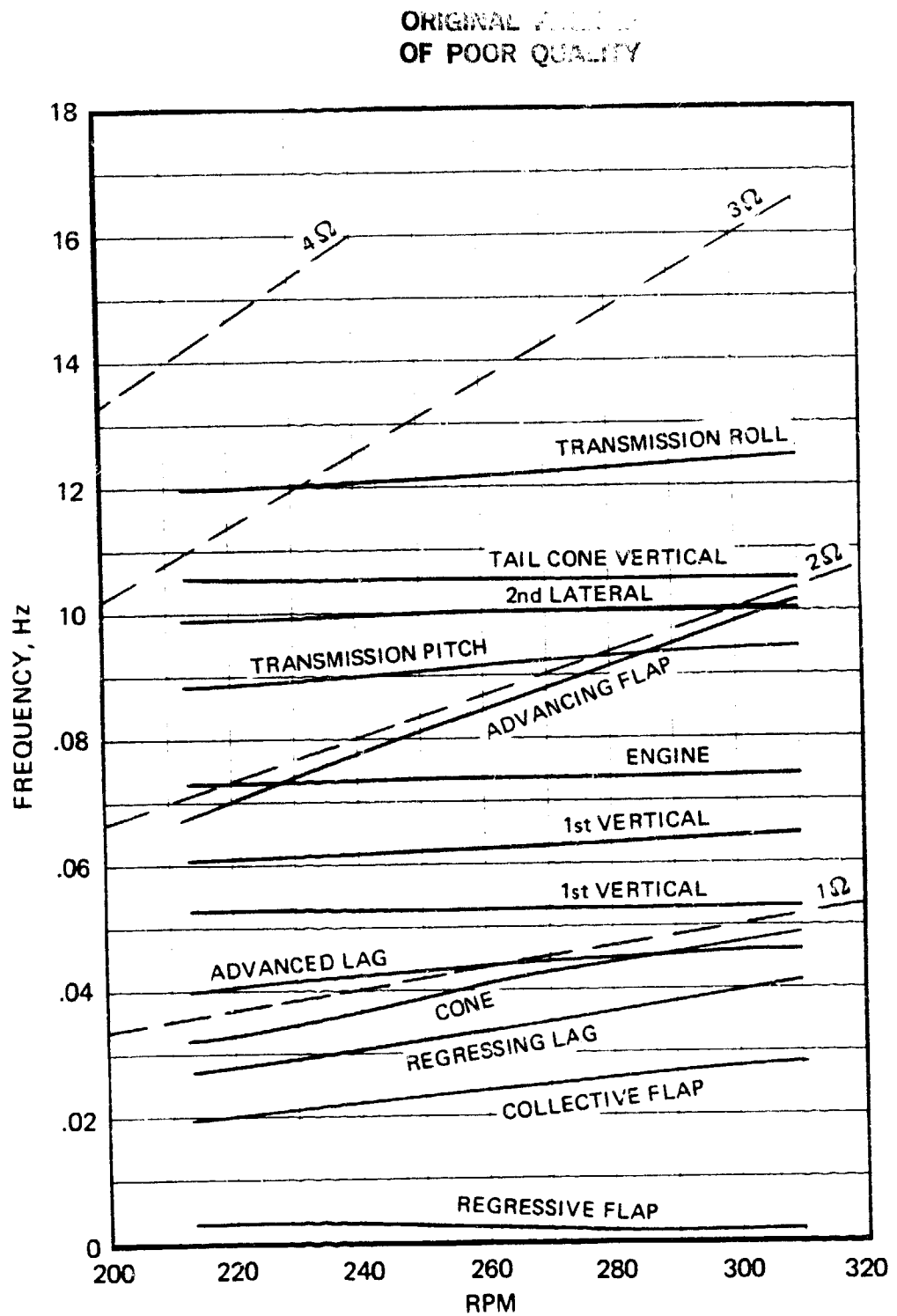


FIGURE 38. FUSELAGE MODE AND FLAP - LAG MODE COUPLED FREQUENCY VERSUS ROTOR SPEED - AIBS ACTIVE

CHART NO. 39
OF POOR QUALITY

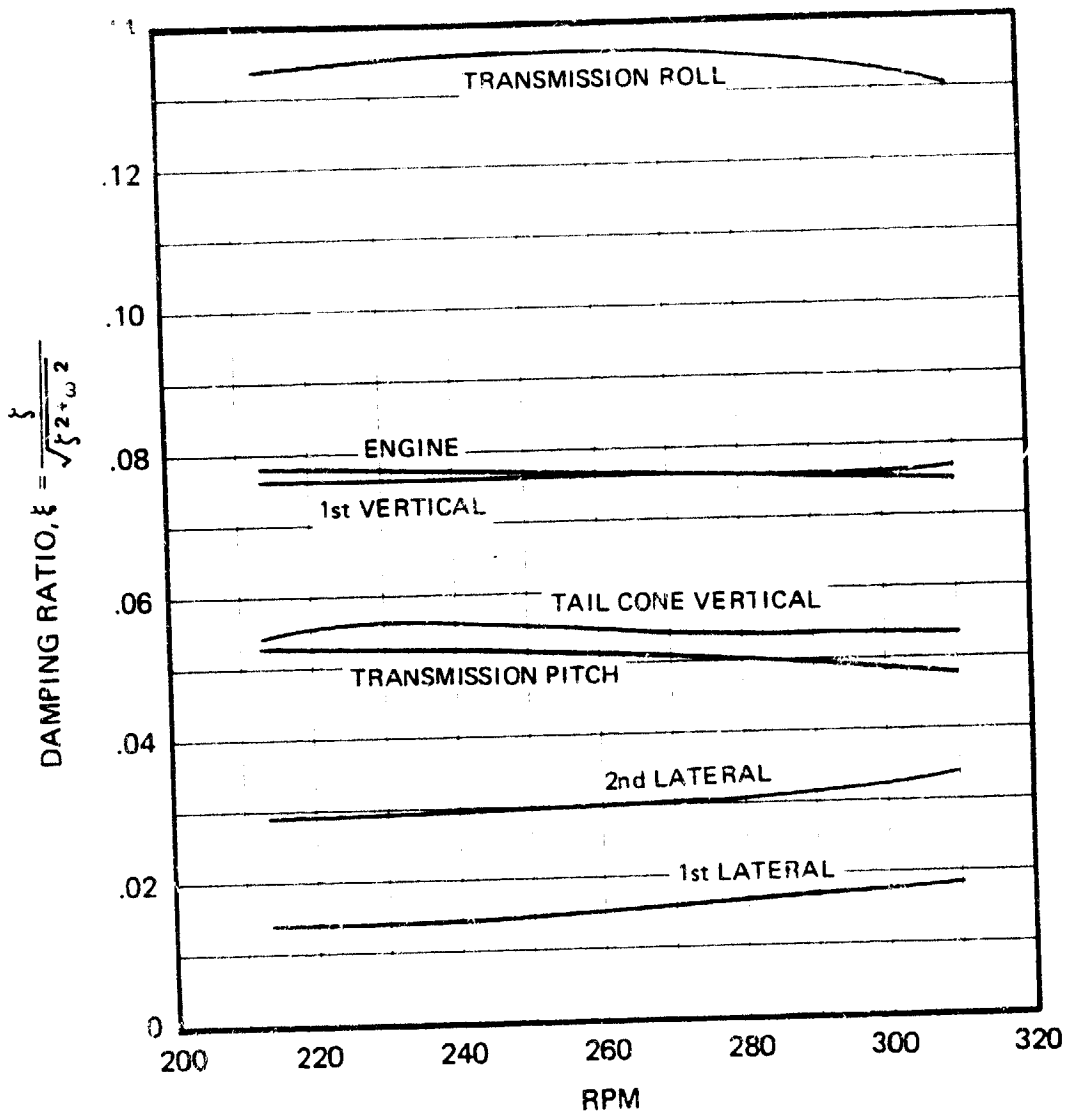


FIGURE 39. COUPLED FUSELAGE MODE DAMPING RATIO VERSUS ROTOR SPEED - AIBS ACTIVE

ORIGINAL FROM AIAA
OF POOR QUALITY

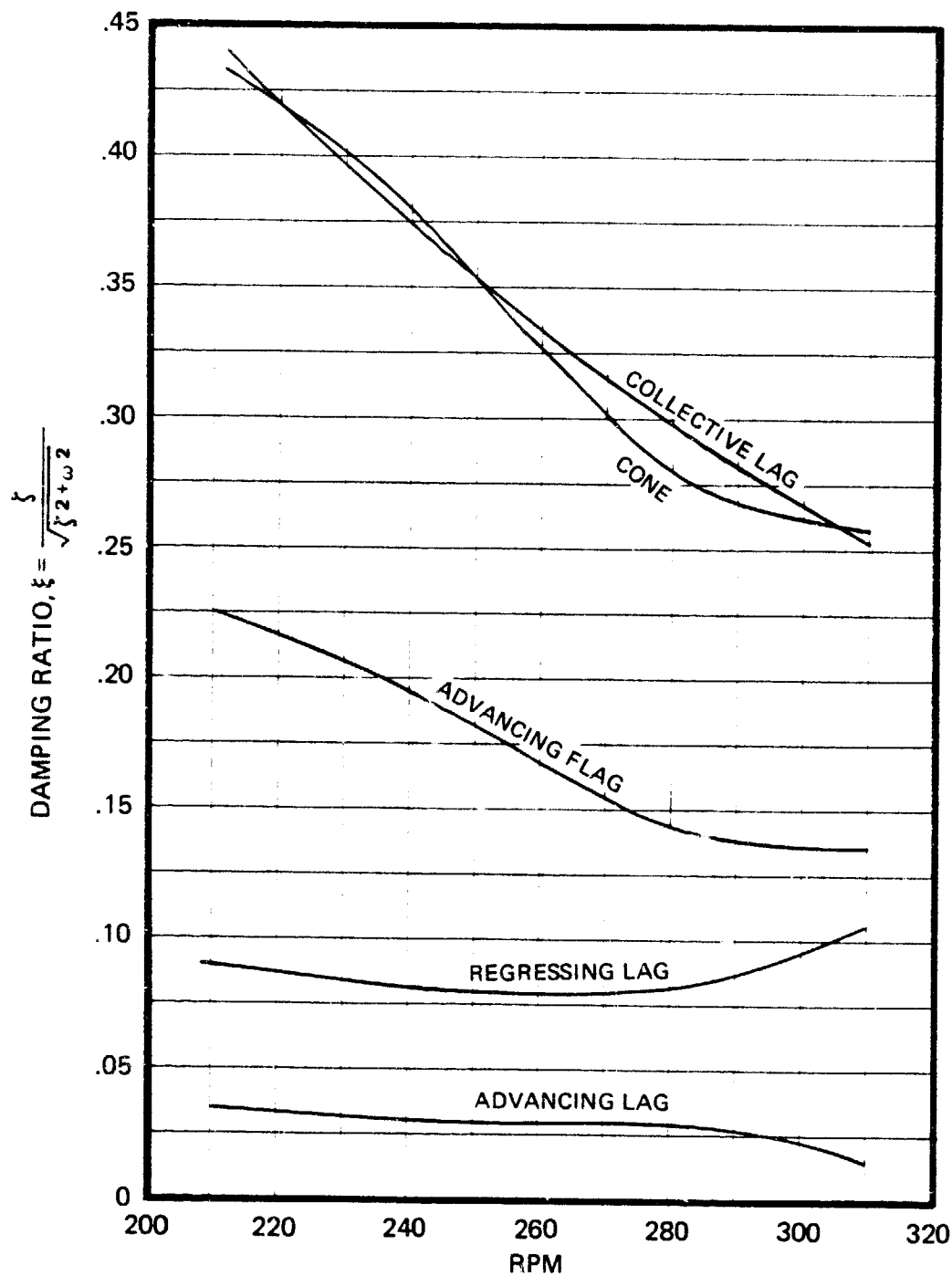


FIGURE 40. COUPLED FLAP - LAG MODE DAMPING RATIO VERSUS ROTOR SPEED - AIBS ACTIVE

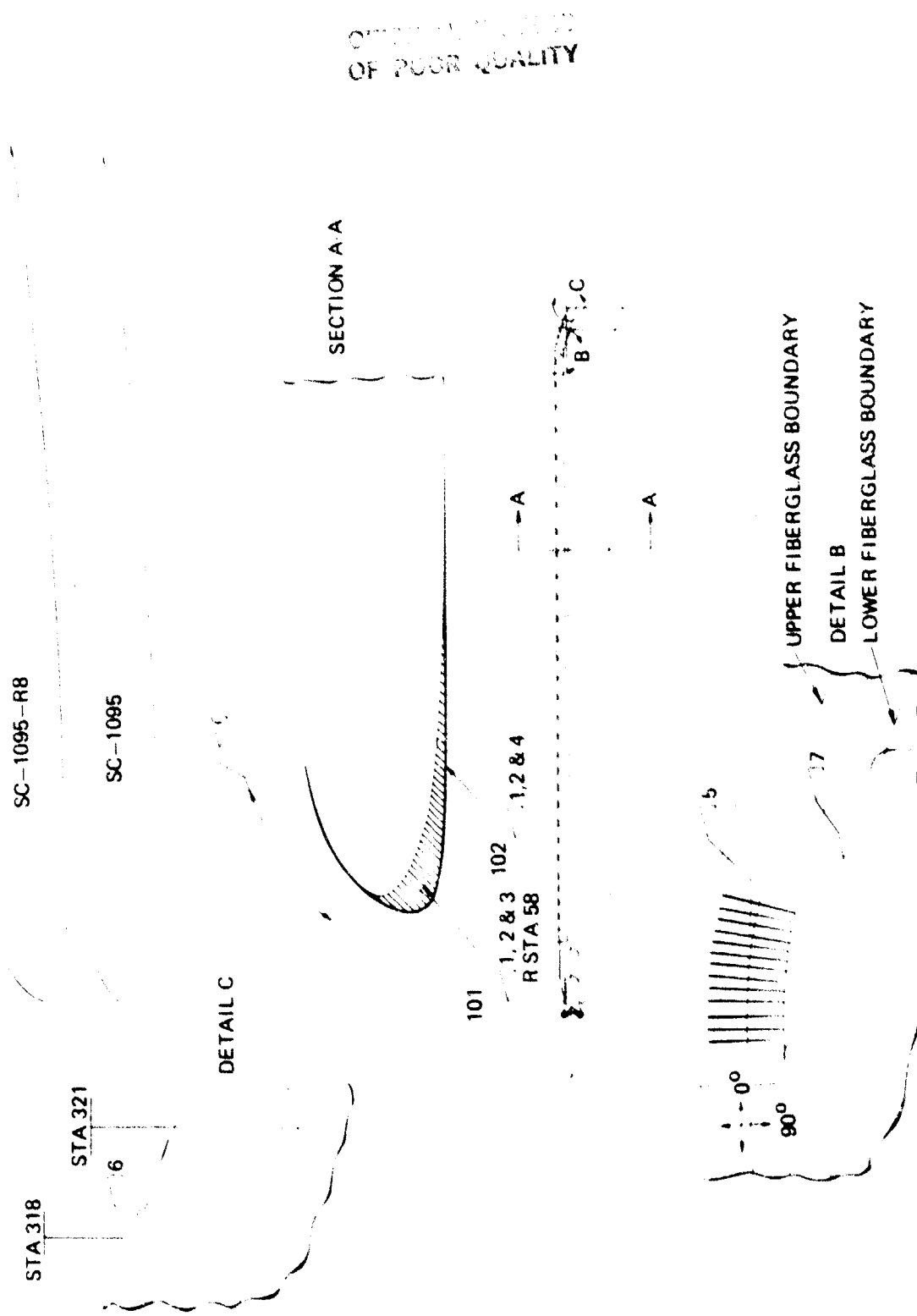


FIGURE 41. LAYOUT DRAWING – RSRA 4 BLADED ROTOR LEADING EDGE MODIFICATION

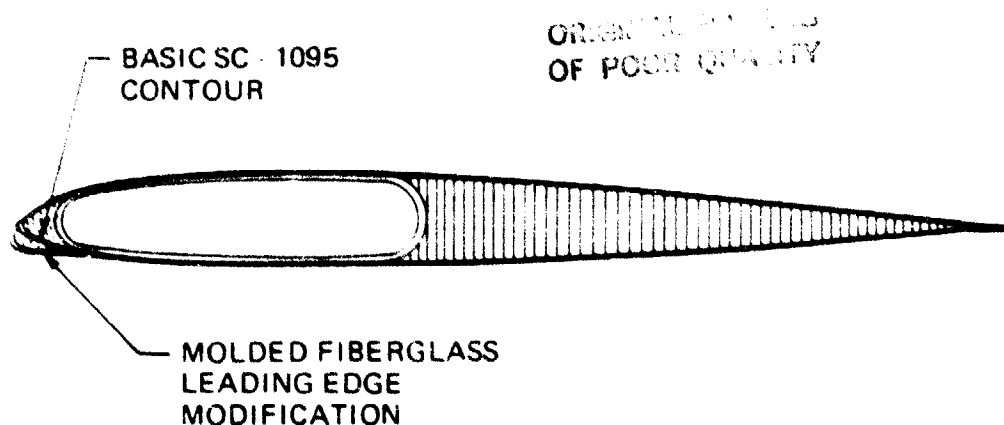


FIGURE 42. BONDED LEADING EDGE MODIFICATION TO BASIC SC-1095 AIRFOIL

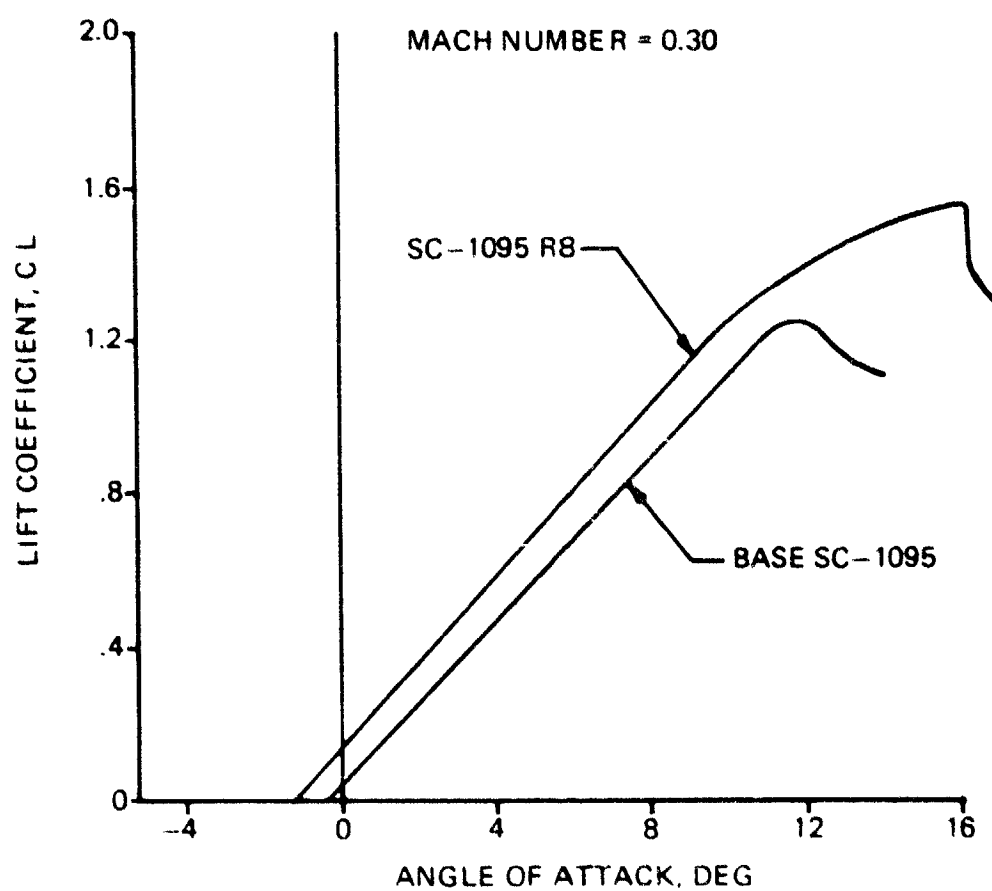


FIGURE 43. EFFECT OF NOSE EXTENSION ON SC-1095 LIFT CHARACTERISTICS

CRITICAL
OF POOR QUALITY

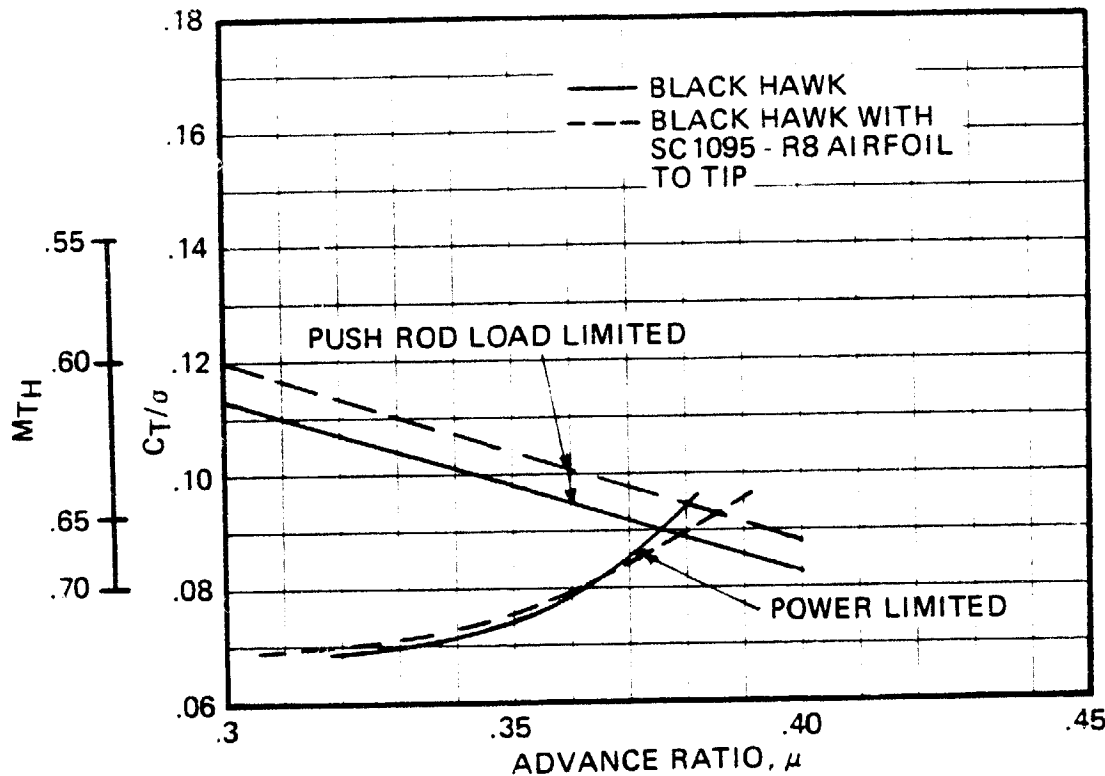
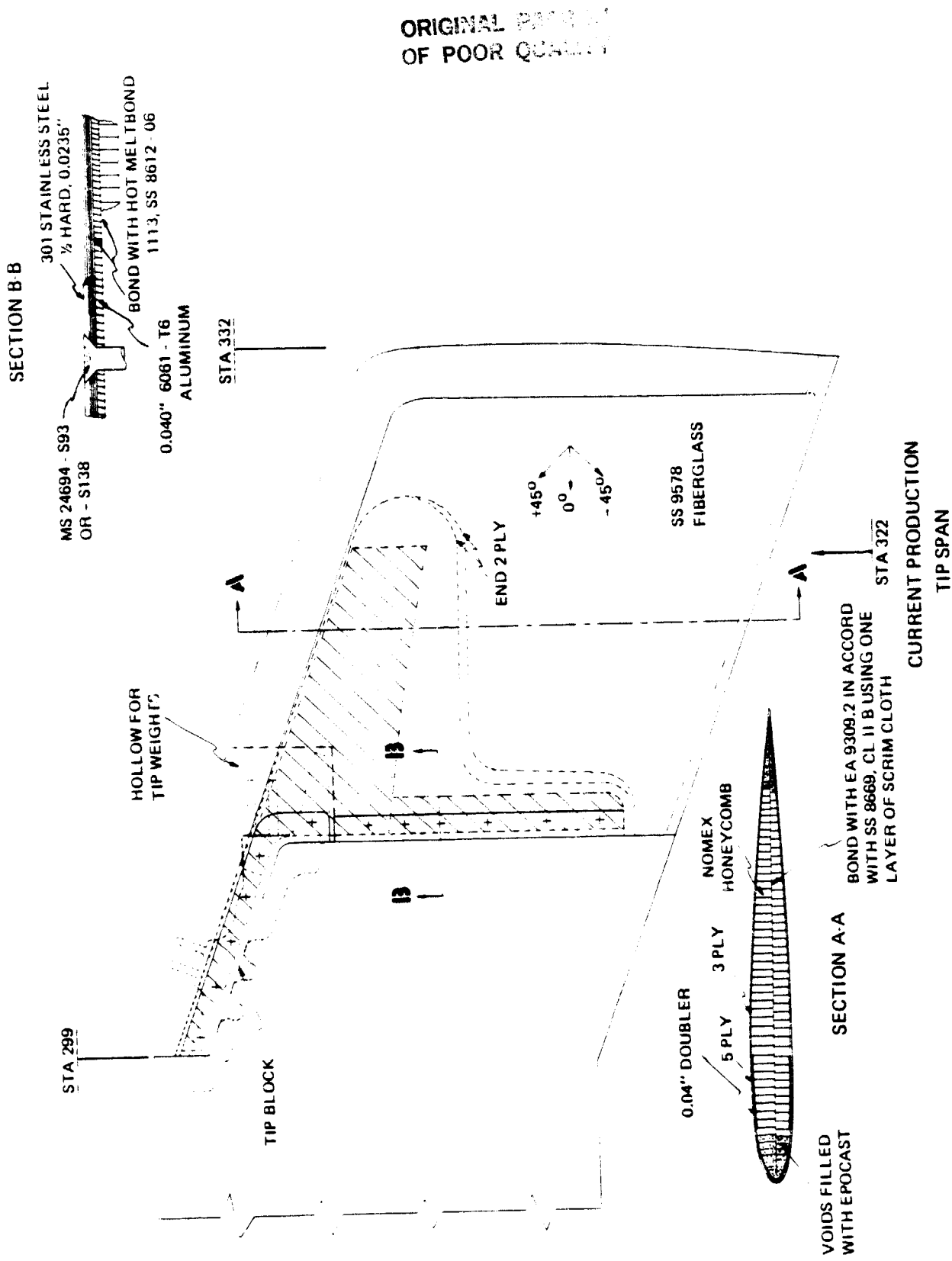
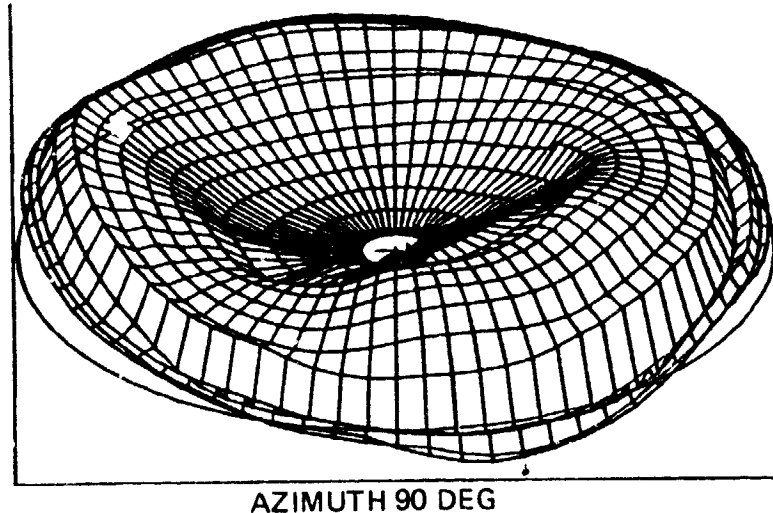


FIGURE 44. EFFECT OF INBOARD AIRFOIL EXTENSION ON FORWARD FLIGHT RESEARCH LIMITS

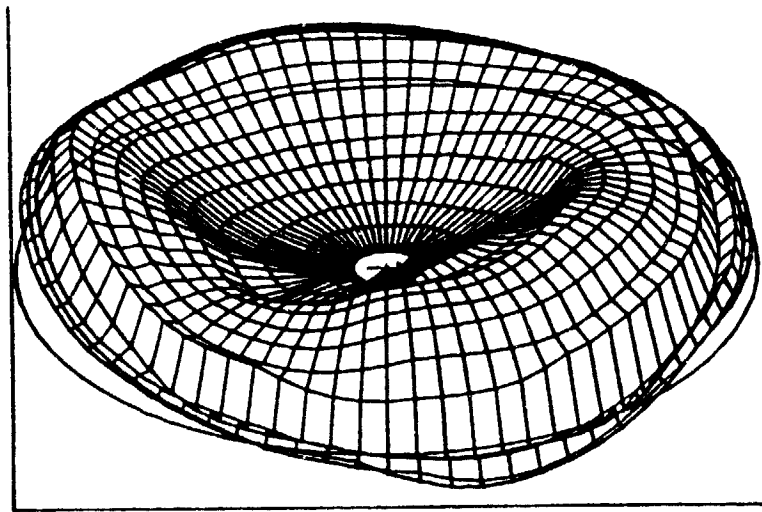


GRAPHS OF
OF POOR QUALITY



AZIMUTH 90 DEG

(a) 6 IN.



AZIMUTH 90 DEG

(b) 18 IN.

FIGURE 46. AZIMUTHAL AND RADIAL DISTRIBUTIONS OF THE VIBRATORY FLATWISE STRESSES PREDICTED FOR TWO MAST HEIGHTS

ORIGINAL PAGE
OF POOR QUALITY

GW = 8618 KG (19000 LB)
AIRSPEED = 268.7 KM/H (145 KN)

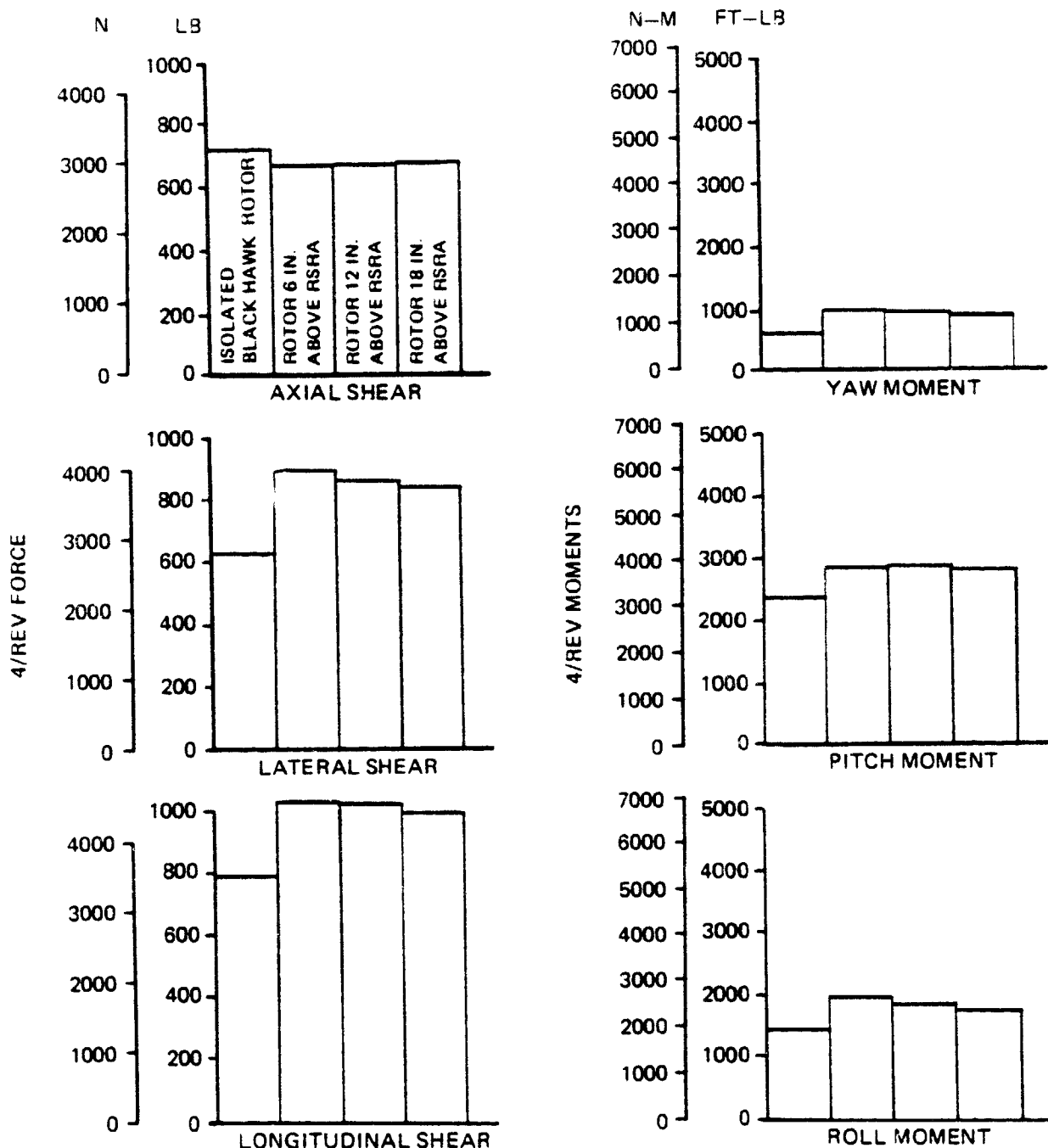
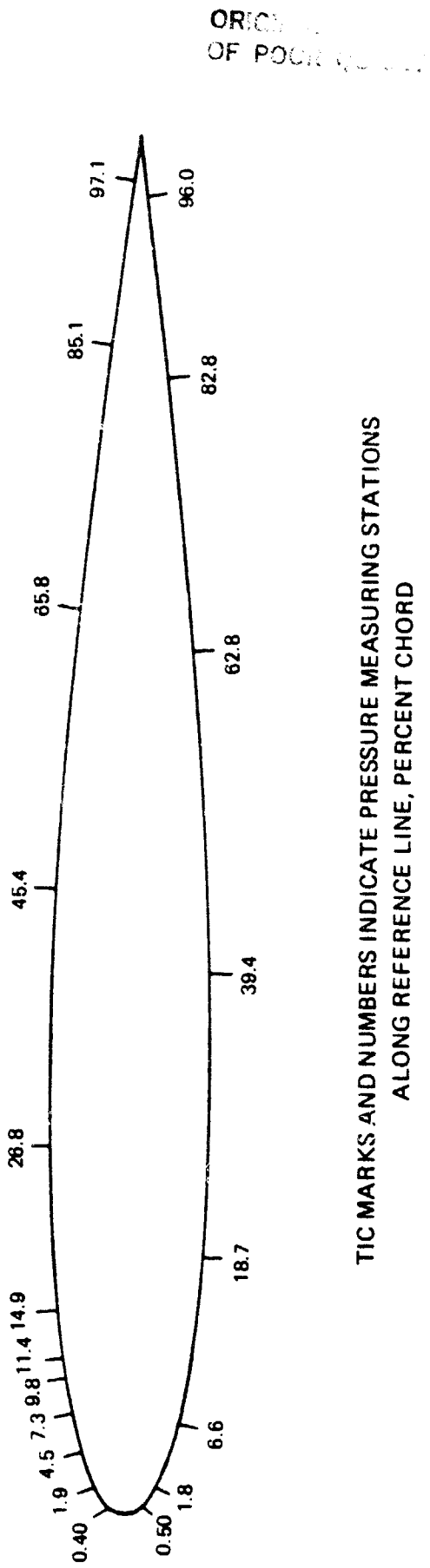


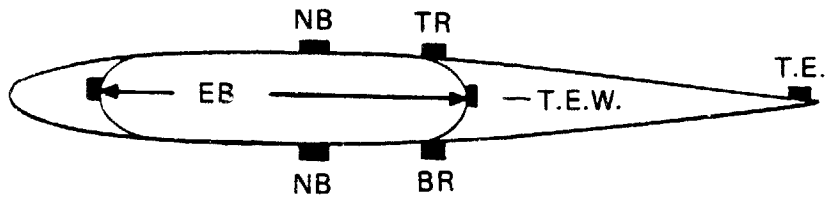
FIGURE 47. EFFECT OF MAST HEIGHT ON CALCULATED 4P FORCES AND MOMENTS



TIC MARKS AND NUMBERS INDICATE PRESSURE MEASURING STATIONS
ALONG REFERENCE LINE, PERCENT CHORD

FIGURE 48. AIRFOIL CROSS SECTION SHOWING CHORDWISE MEASURING STATIONS

ORIGINAL PAGE IS
OF POOR QUALITY



BLADE STATION

<u>N/R</u>	<u>NB</u>	<u>EB</u>	<u>T.E.</u>
.10	✓		
.20	✓		
.30	✓		
.40	✓		
.50	✓	✓	
.60	✓	✓	
.70	✓	✓	
.80	✓	✓	

DAMPER TOTAL STRESS, LOAD

PITCH LINK TOTAL STRESS, LOAD

CUFF (2) TOTAL STRESS

BR (2)

TR(1)

T.E.W. (1)

TIP FITTING (2)

SINGLE ACTIVE

NOTES:

NB - NORMAL BENDING

EB - EDGEWISE BENDING

BR - BOTTOM REAR

TR - TOP REAR

TE - TRAILING EDGE

TEW - TRAILING EDGE WELL

FIGURE 49. FOUR-BLADED RSRA INSTRUMENTATION – ONE BLADE

ORIGINAL SHEET
OF POOR QUALITY

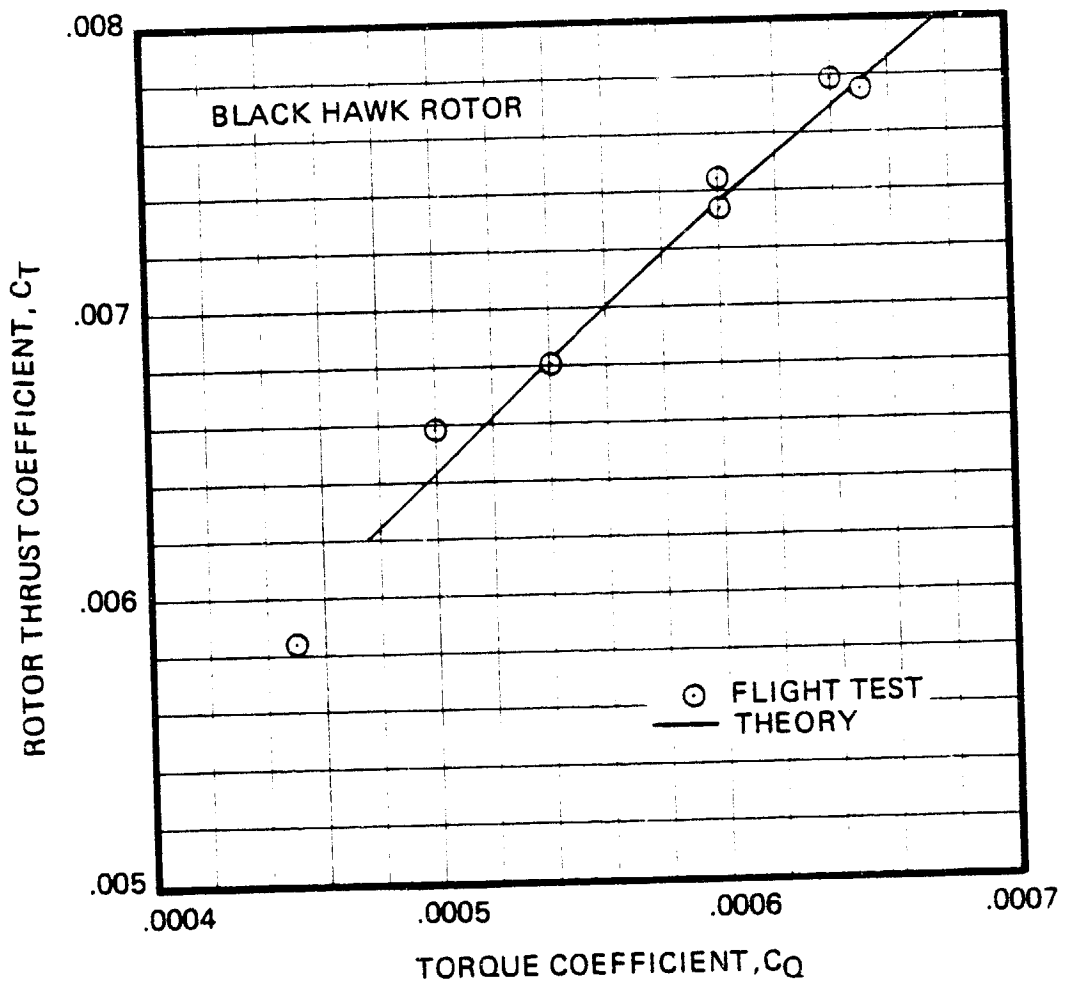


FIGURE 50. HOVER THEORY CORRELATION WITH
WHIRLSTAND TEST DATA - BLACK HAWK ROTOR

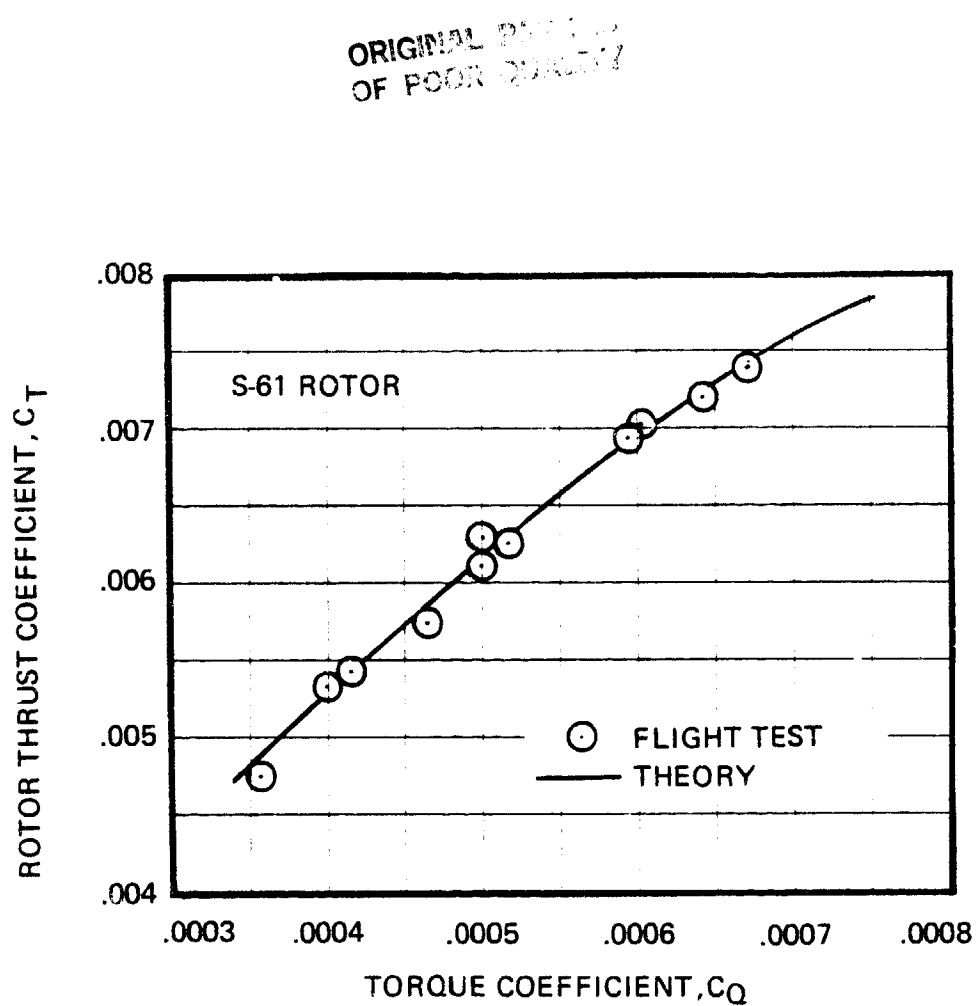


FIGURE 51. HOVER THEORY CORRELATION WITH WHIRLSTAND TEST DATA - S-61 ROTOR.

CHART OF RSRA HOVER PERFORMANCE
OF PROBABILITY

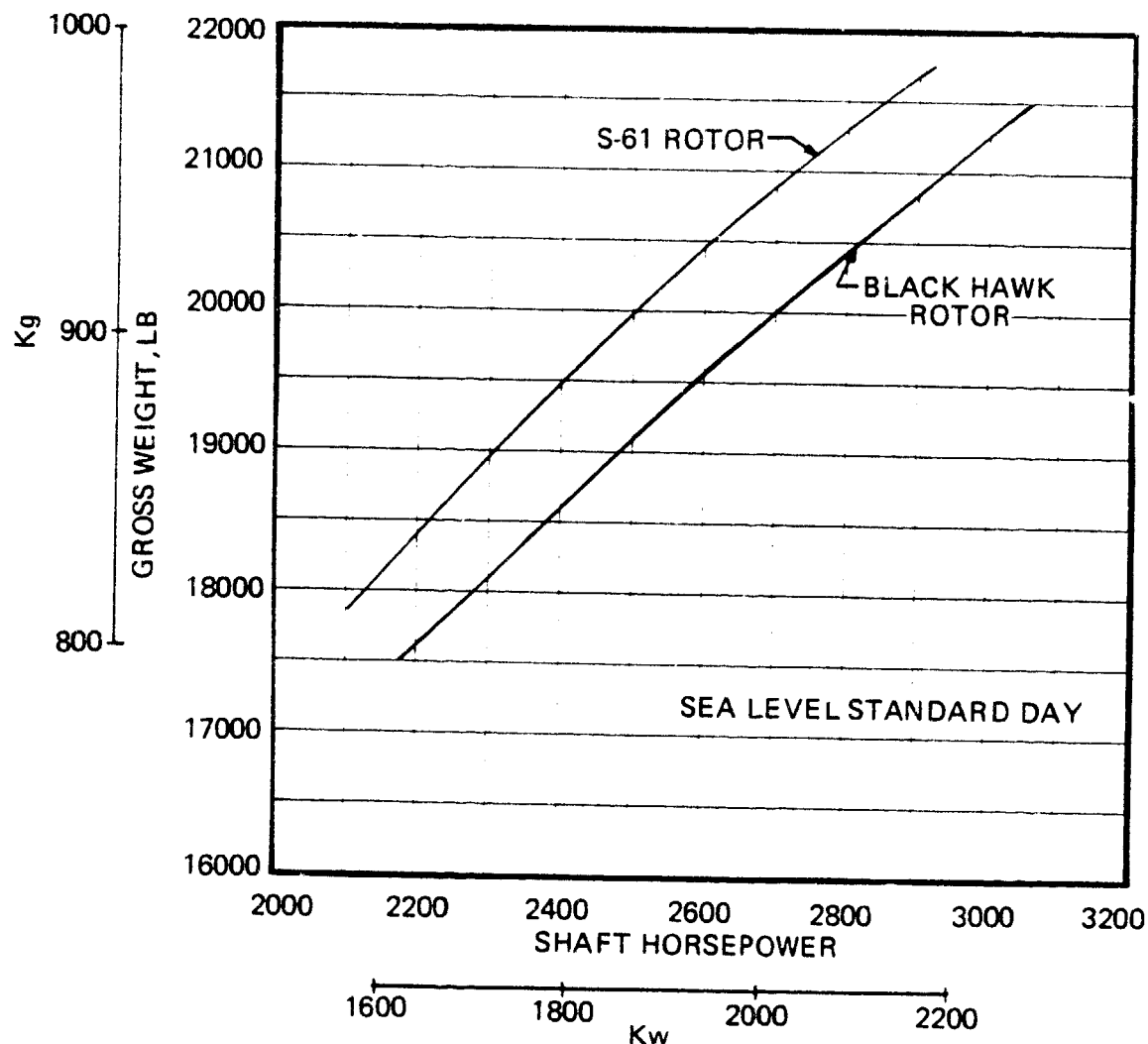


FIGURE 52. DIMENSIONAL RSRA HOVER PERFORMANCE – SEA LEVEL STANDARD DAY

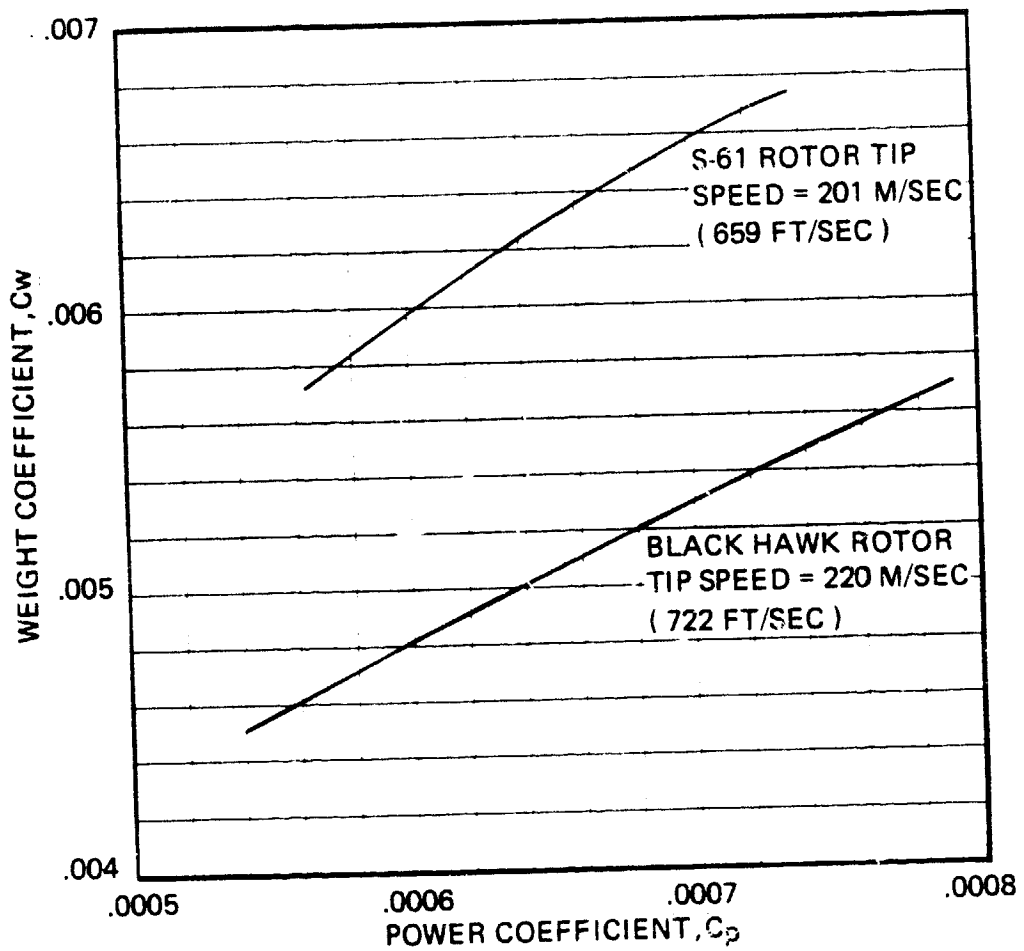


FIGURE 53. NON-DIMENSIONAL RSRA HOVER PERFORMANCE –
SEA LEVEL STANDARD DAY.

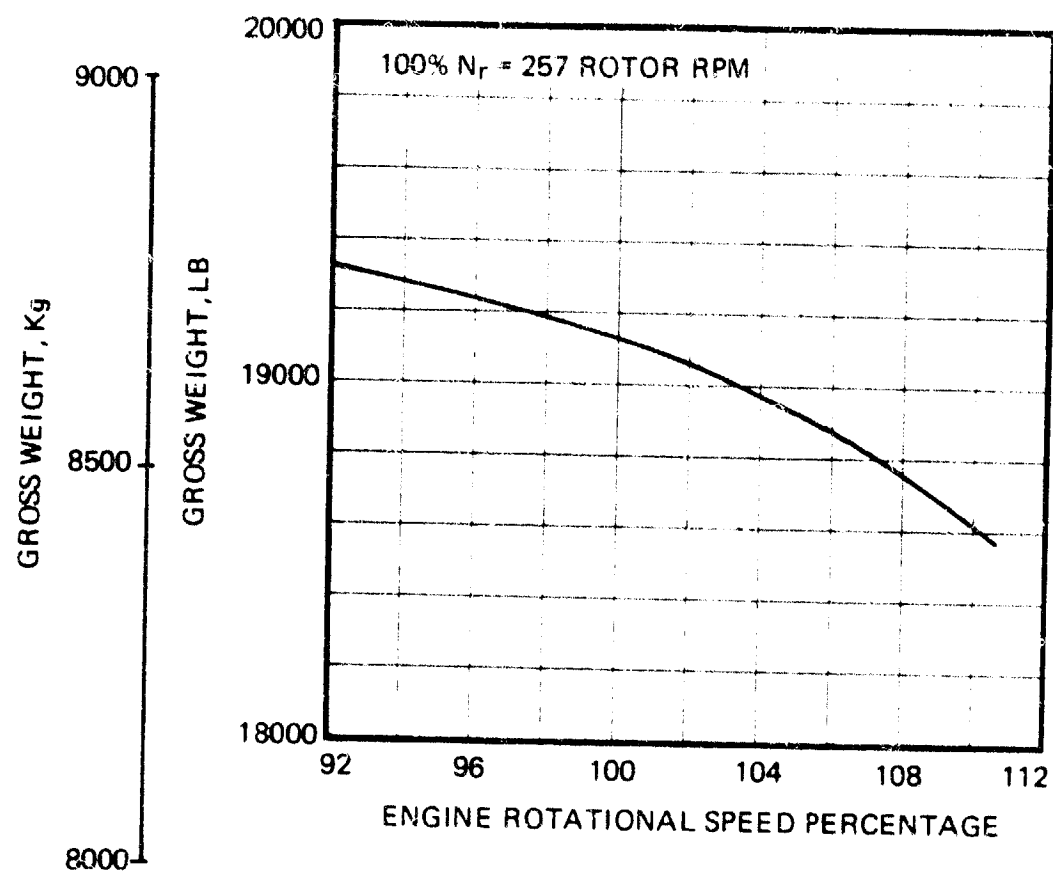


FIGURE 54. EFFECT OF ROTOR RPM ON SEA LEVEL STANDARD HOVER CAPABILITY

ORIGINAL PAGE IS
OF POOR QUALITY

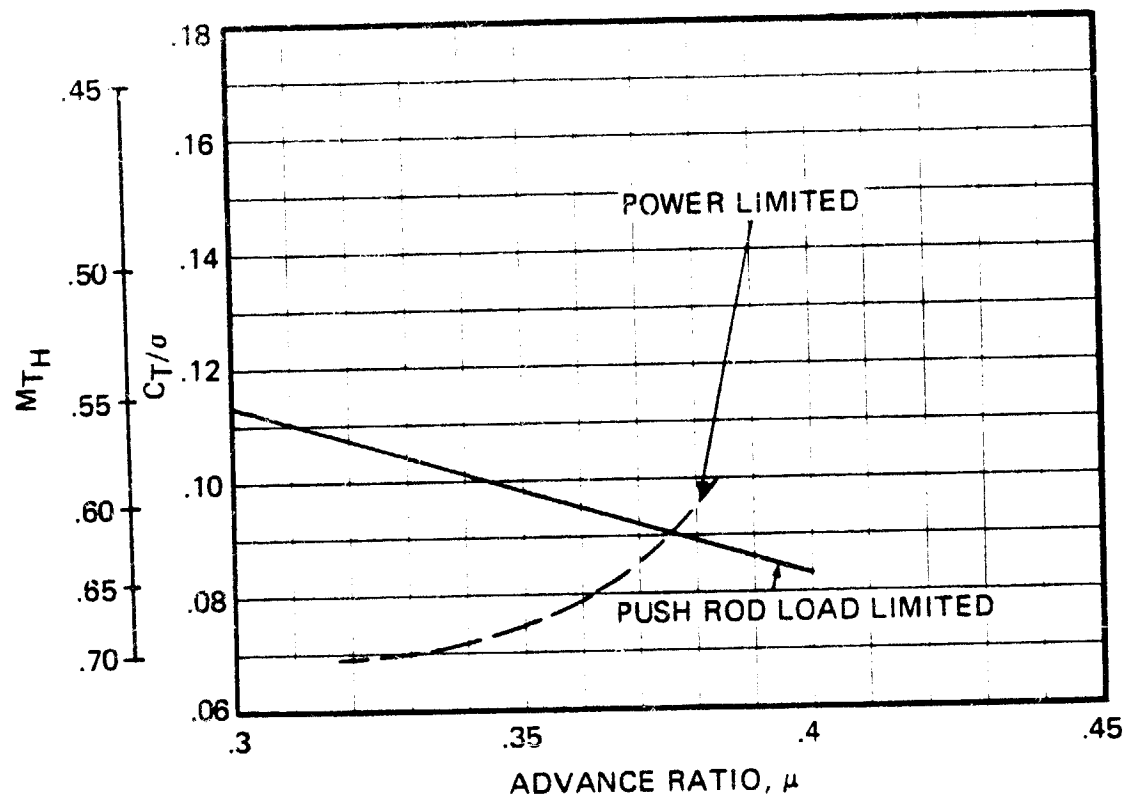


FIGURE 55. BLACK HAWK ROTOR LIMITS - SEA LEVEL STANDARD DAY

ORIGINAL PAGE IS
OF POOR QUALITY

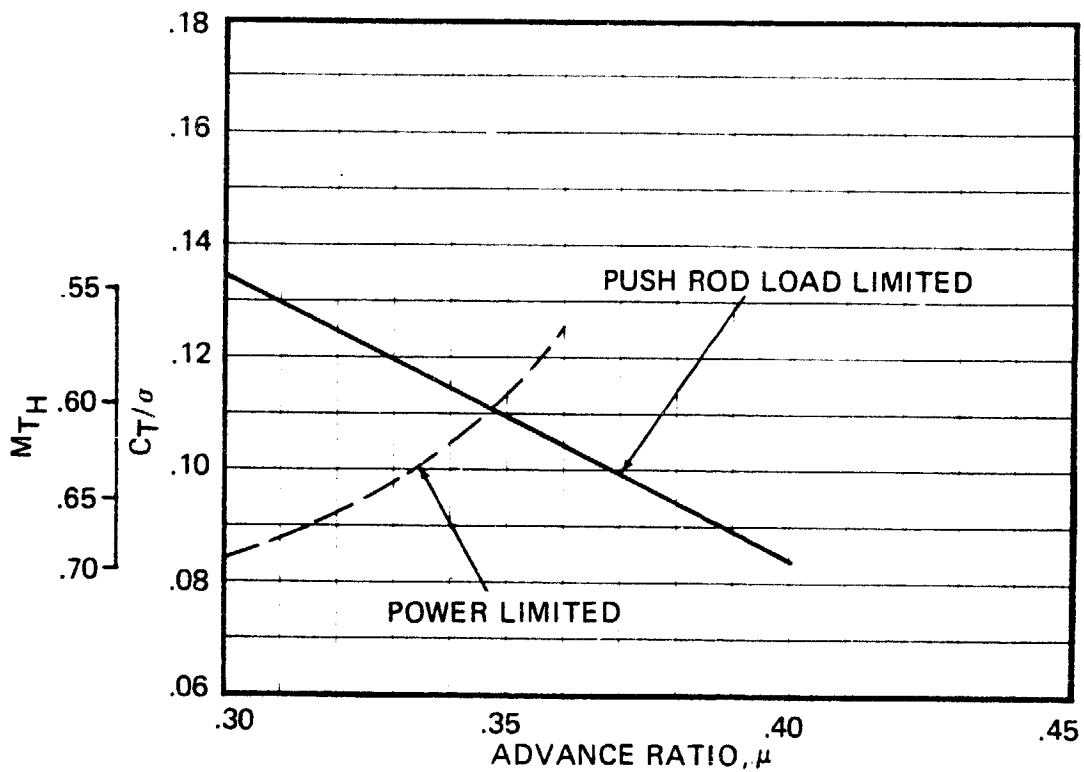
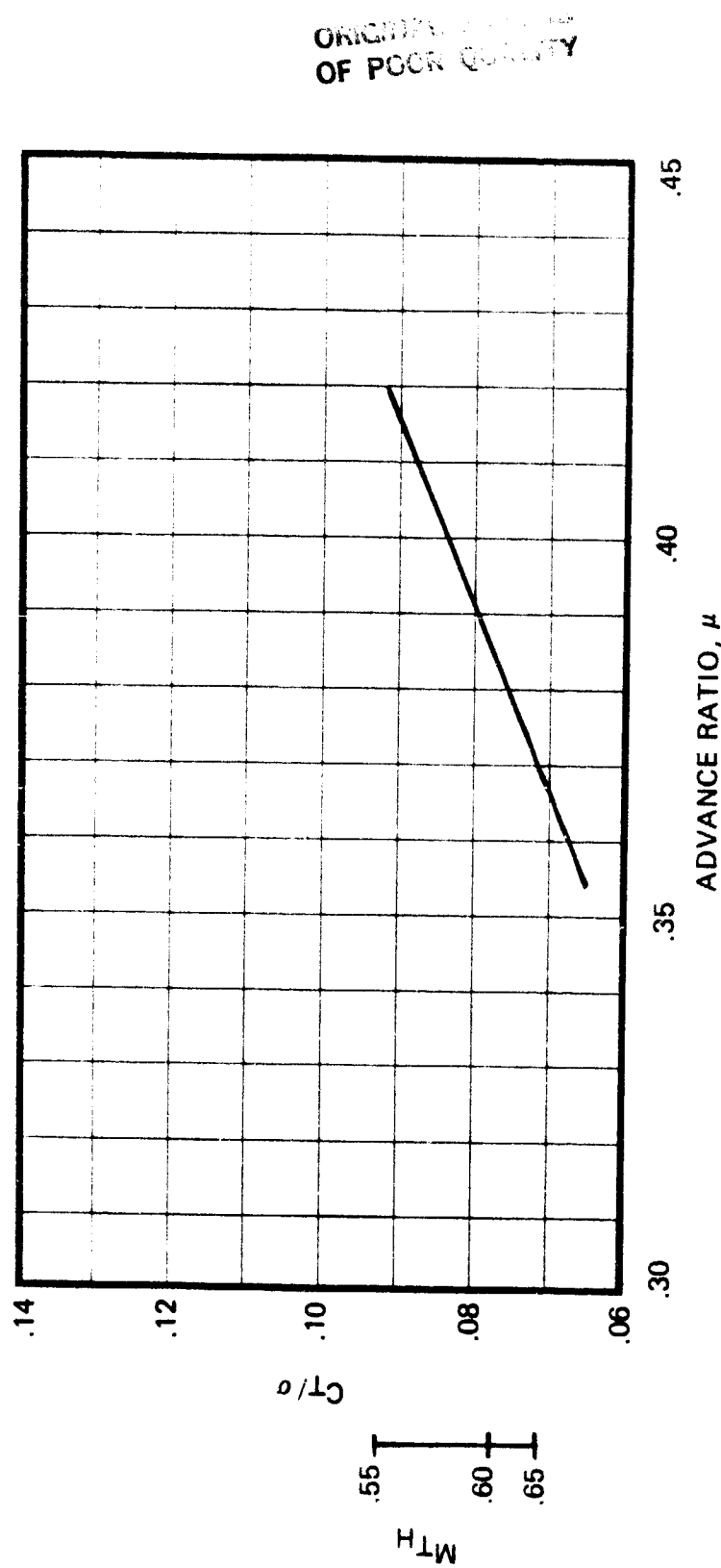


FIGURE 56. BLACK HAWK ROTOR LIMITS - 4000 FT, 95°F DAY

FIGURE 57. S-61 ROTOR LIMITS - SEA LEVEL STANDARD DAY



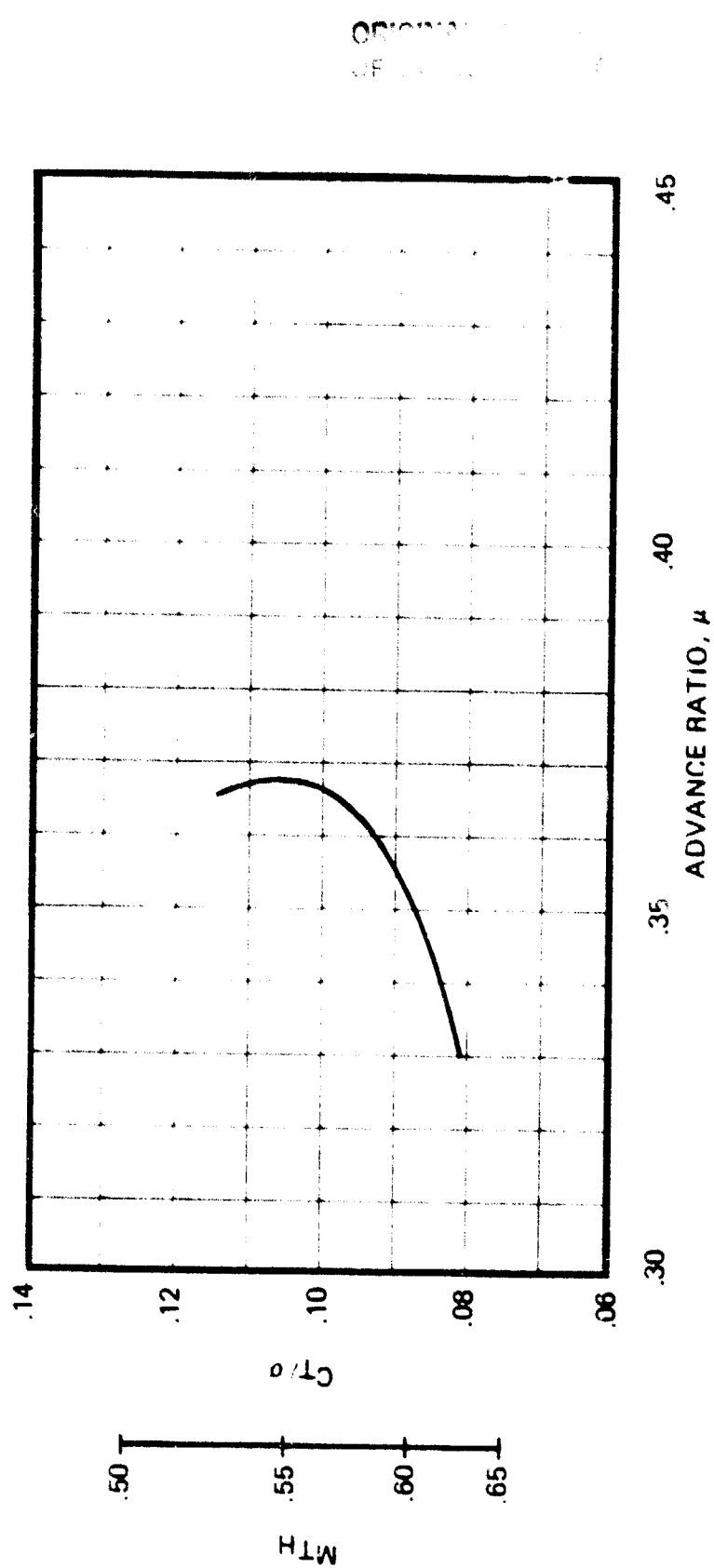


FIGURE 58. S-61 ROTOR LIMITS - 4000 FT, 950 F DAY

ORIGINAL PAGE IS
OF POOR QUALITY

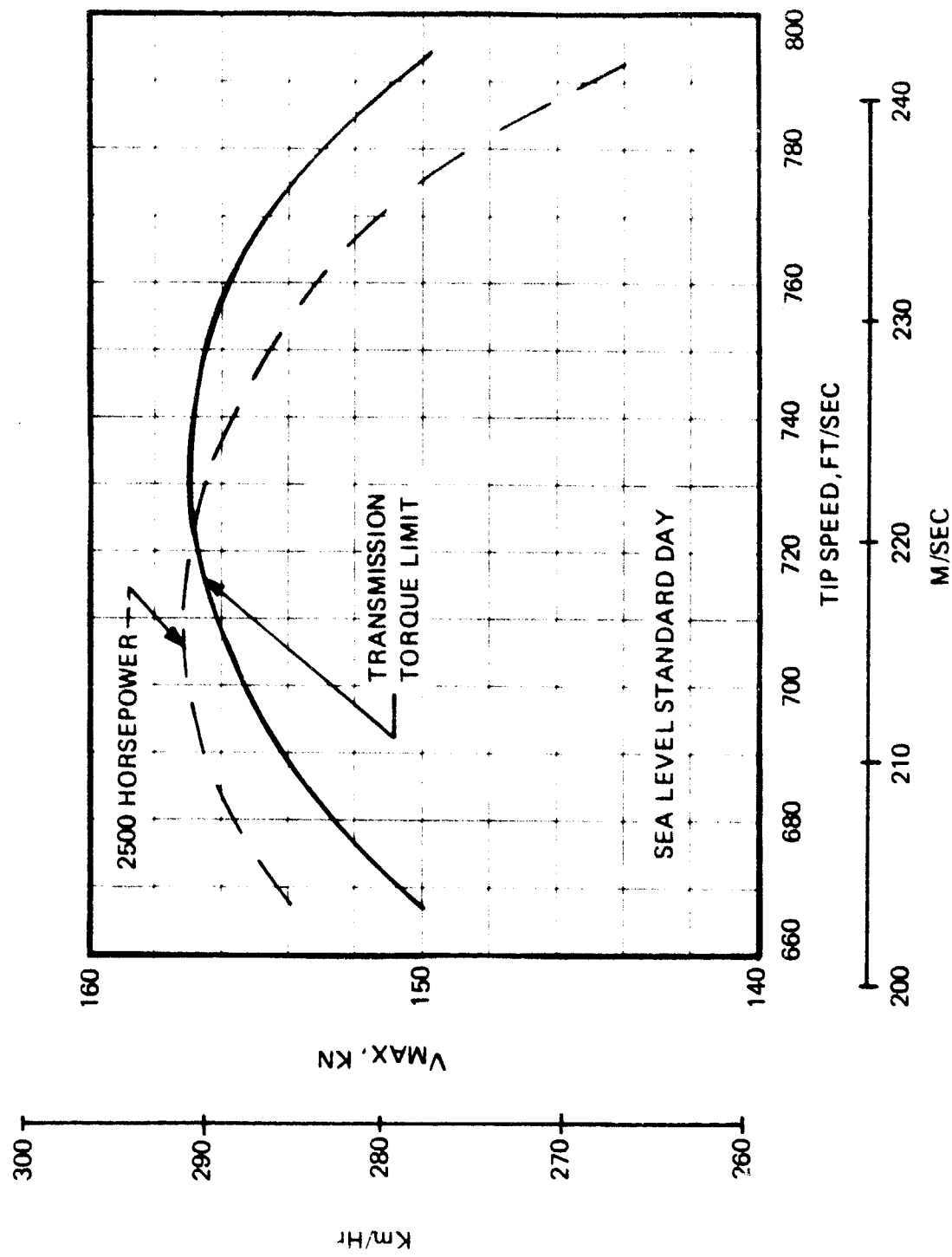


FIGURE 59. EFFECT OF TIP SPEED ON MAXIMUM LEVEL FLIGHT SPEED - SEA LEVEL STANDARD DAY

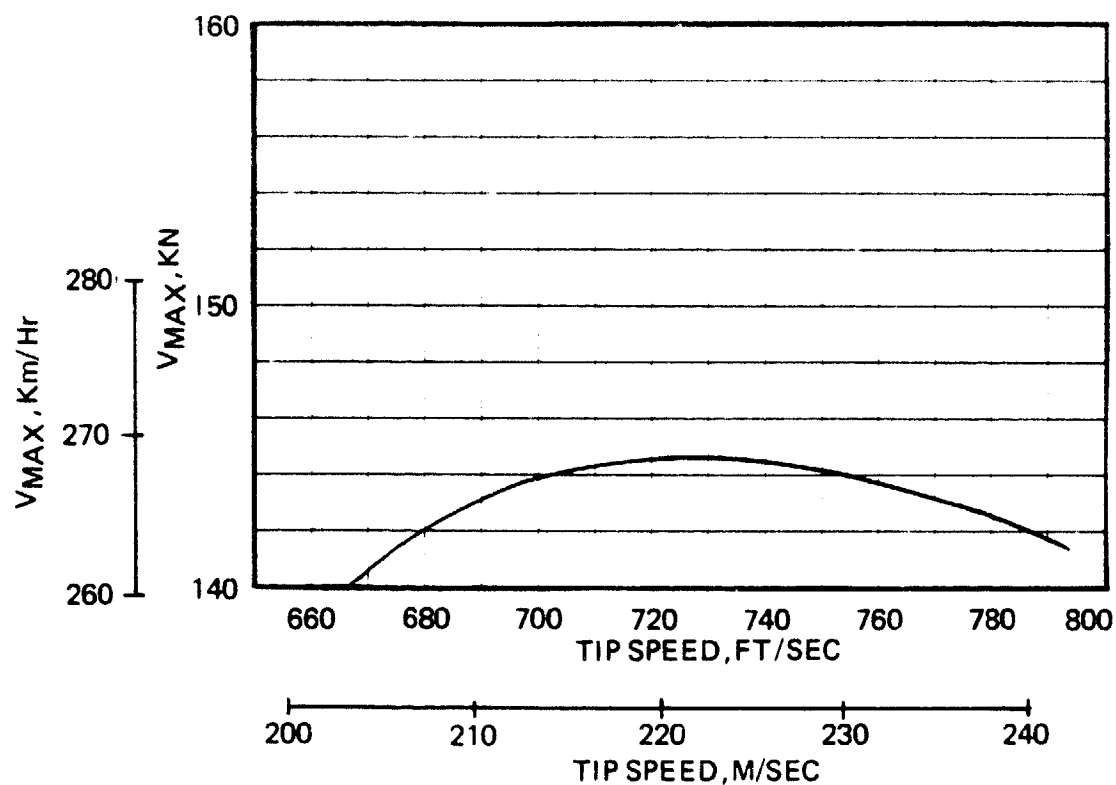


FIGURE 60. EFFECT OF TIP SPEED ON MAXIMUM LEVEL FLIGHT SPEED
— 4000 FT, 95°F DAY.

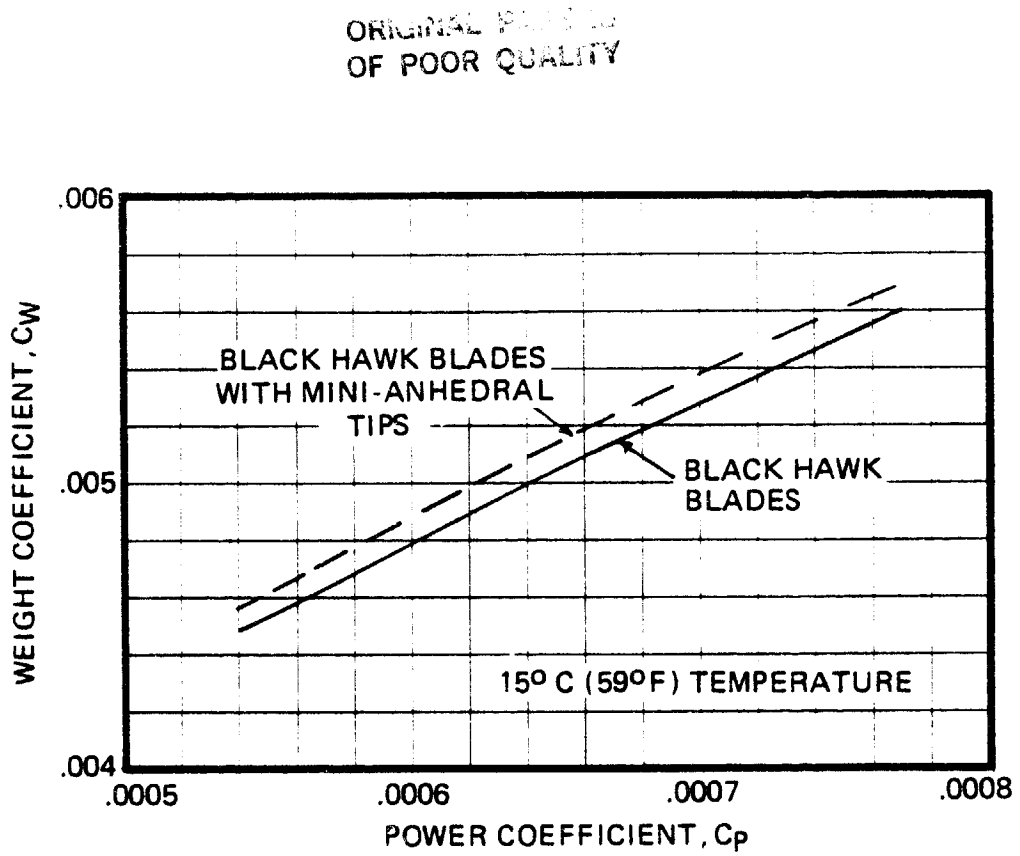


FIGURE 61. EFFECT OF MINI-ANHEDRAL TIP ON OGE HOVER PERFORMANCE

ORIGINAL PAGE IS
OF POOR QUALITY

(1/6 SCALE MODEL H-60 ROTOR BLADES)

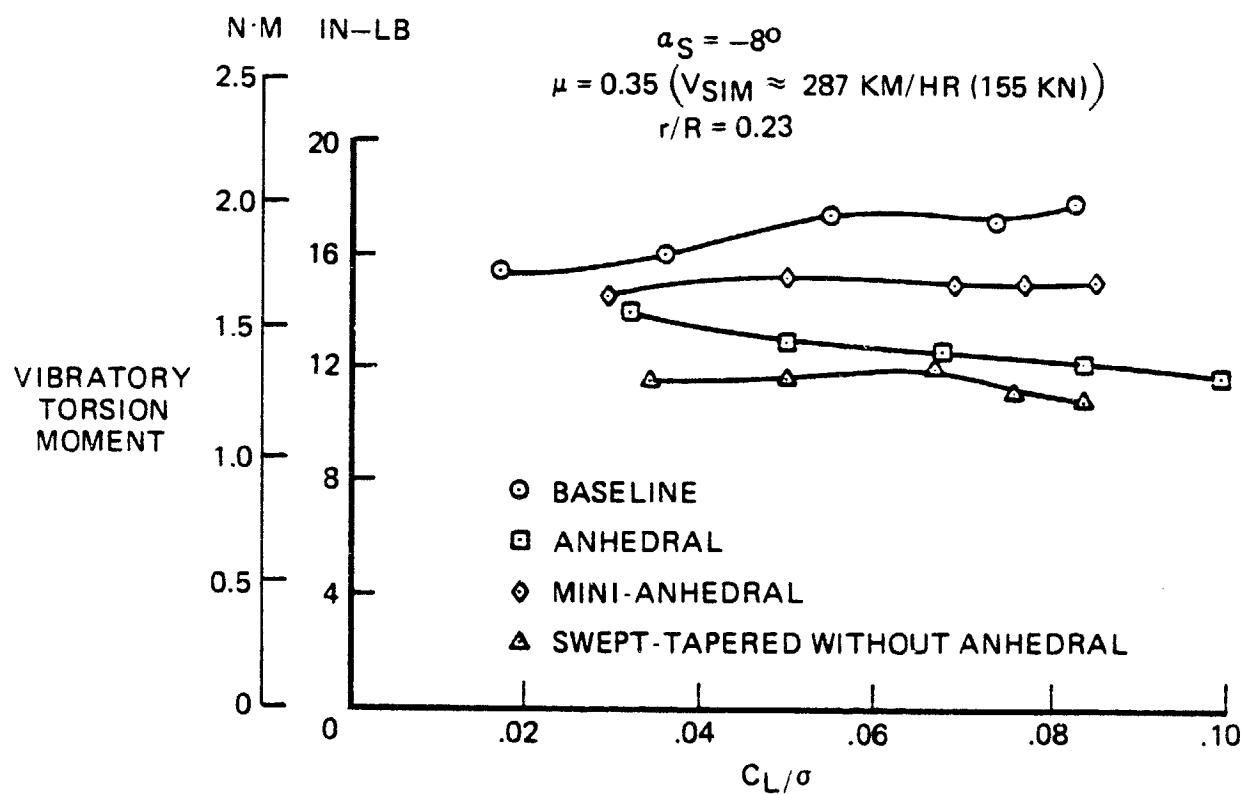


FIGURE 62. EFFECT OF VARIOUS TIP CONFIGURATIONS ON MAXIMUM VIBRATORY TORSION MOMENTS.

ORIGINAL PAGE IS
OF POOR QUALITY

(1/6 SCALE MODEL H-60 ROTOR BLADES)

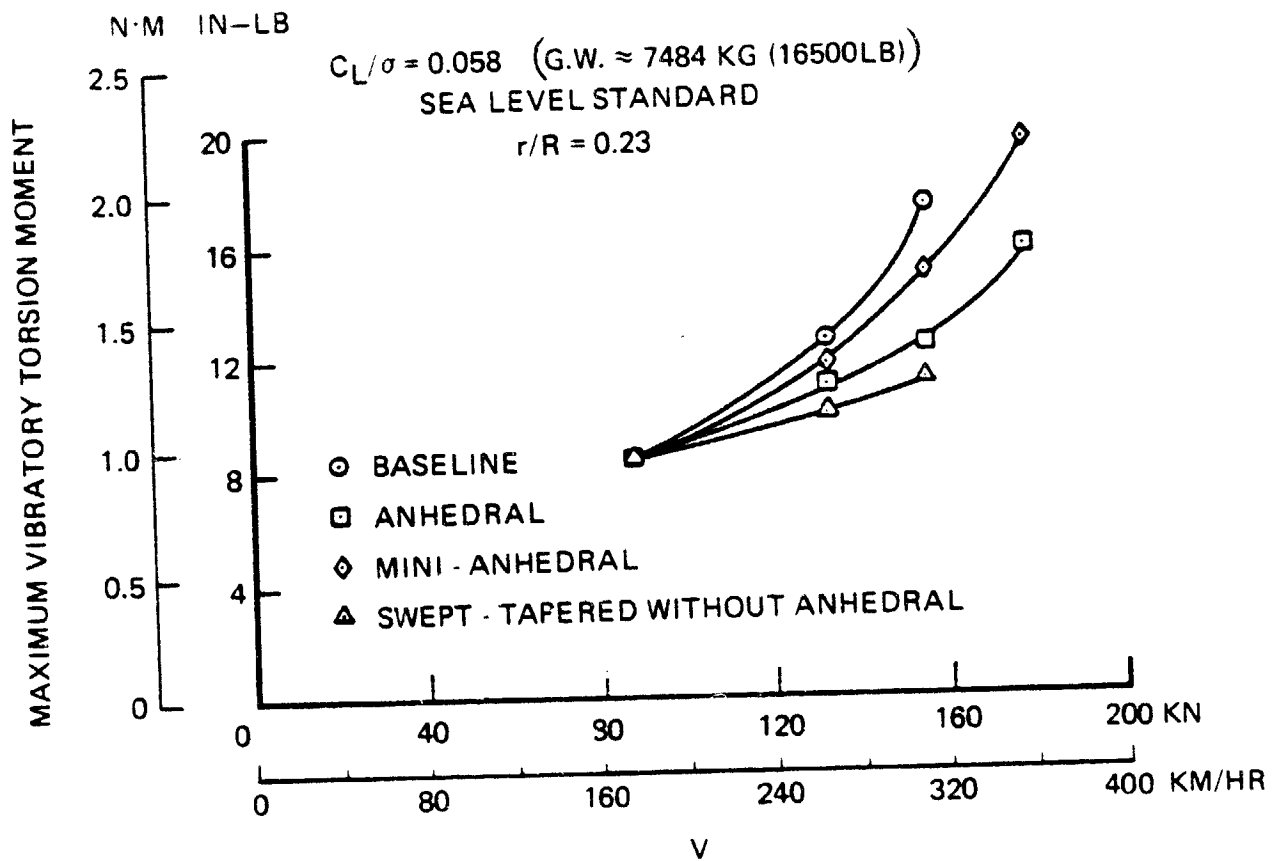


FIGURE 63. EFFECT OF VARIOUS TIP CONFIGURATIONS ON MAXIMUM VIBRATORY TORSION MOMENTS

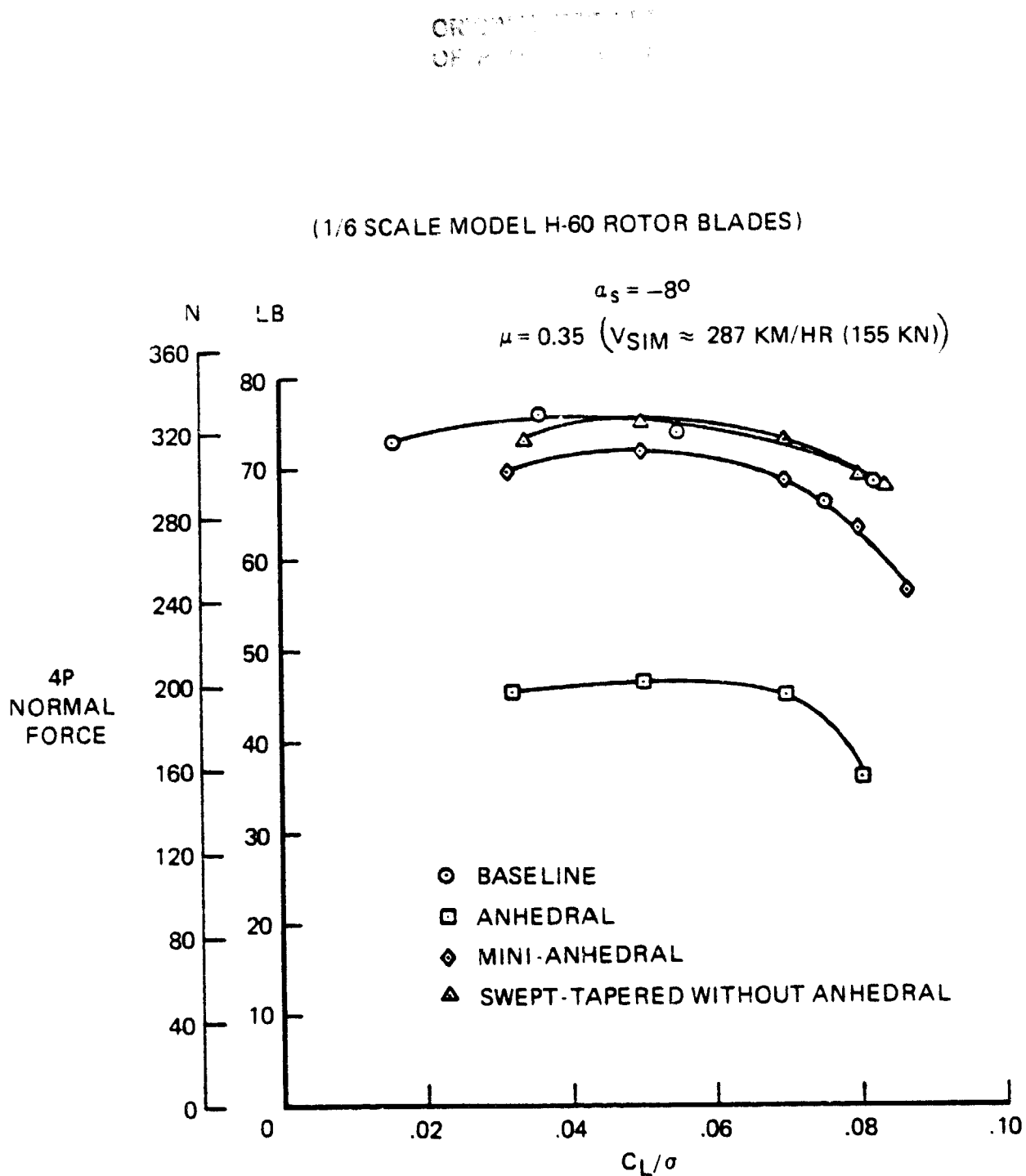


FIGURE 64. EFFECT OF VARIOUS TIP CONFIGURATIONS ON 4P FIXED SYSTEM VERTICAL FORCE

APPENDIX

BLACK HAWK ROTOR SYSTEM

Sikorsky Aircraft has developed the titanium spar BLACK HAWK rotor blade through an extensive manufacturing technology program that started with the RH-53D, progressed to the YCH-53E, and finally culminated with the prototype UH-60 UTTAS and the production BLACK HAWK. These titanium spar blades have reached C_T/σ vs. advance ratio limits beyond those of any other blades. This performance achievement provides a proven blade technology, off the shelf, as a candidate for meeting the four-bladed RSRA replacement rotor requirements.

The high specific fatigue strength of the titanium D-spar and the fiberglass skin provides the BLACK HAWK rotor blade with the high-performance high speed capability required for the ambitious mission spectrum of this advanced helicopter. The D-spar is fabricated of ground titanium, sheet, which is the lowest cost form of wrought titanium. The sheet is plasma-arc seam-welded into a tube and hat formed into a D-shape, with the weld head positioned in a non-critical stress region. A continuous fiberglass skin forms the outer periphery of the airfoil and is supported by Nomex honeycomb aft of the spar. A reinforced trailing edge provides additional chordwise stiffening. The blade is made of wholly non-corrosive materials.

The D-spar carries most of the torsional and flapwise loading. The Sikorsky blade crack detection system BIM^R is incorporated in the spar structure. High hover and forward flight performance is achieved by high twist rate, high performance airfoils, and a swept tip. Figure A-1 illustrates the fabrication technique. Figures A-2 thru A-6 present aerodynamic and structural design details.

ORIGINAL PAGE IS
OF POOR QUALITY

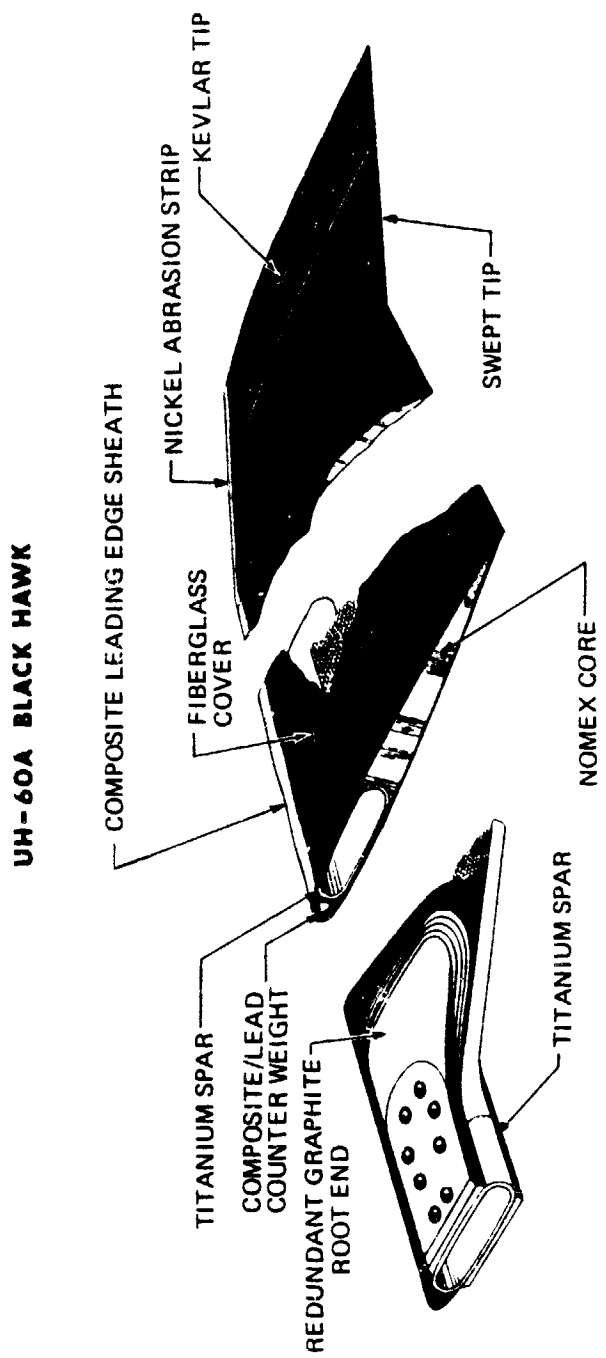


FIGURE A - 1. BLACK HAWK BLADE CONSTRUCTION TECHNIQUE

ORIGINAL FUSE IS
OF POOR QUALITY

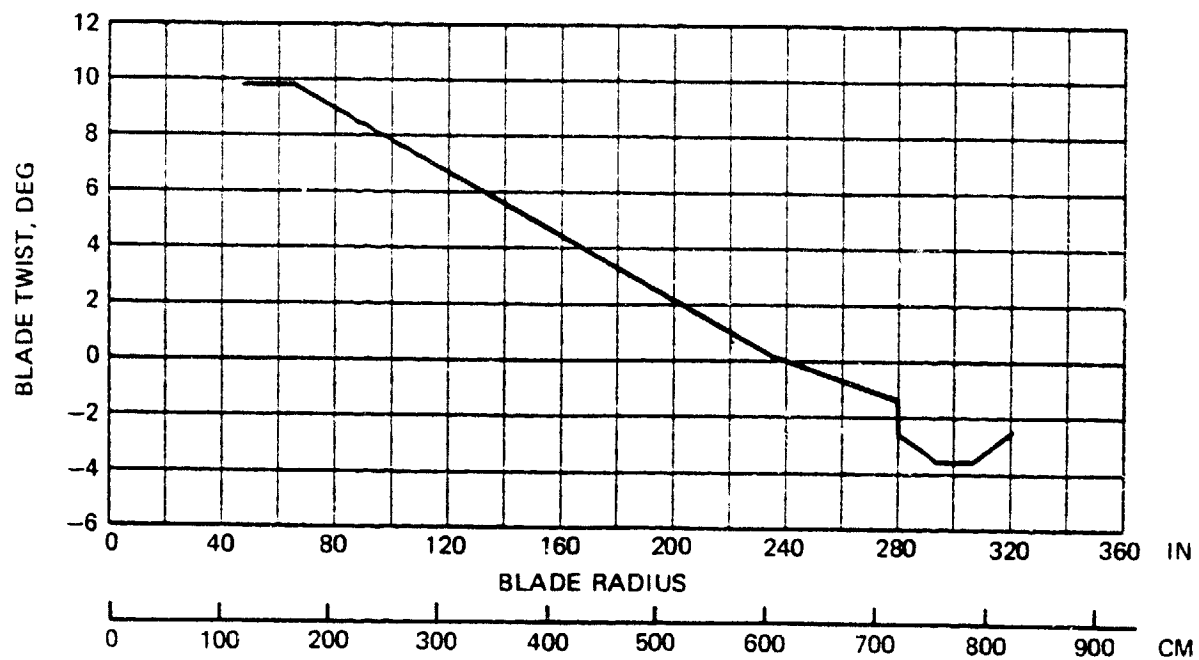


FIGURE A - 2. BLACK HAWK BLADE TWIST DISTRIBUTION

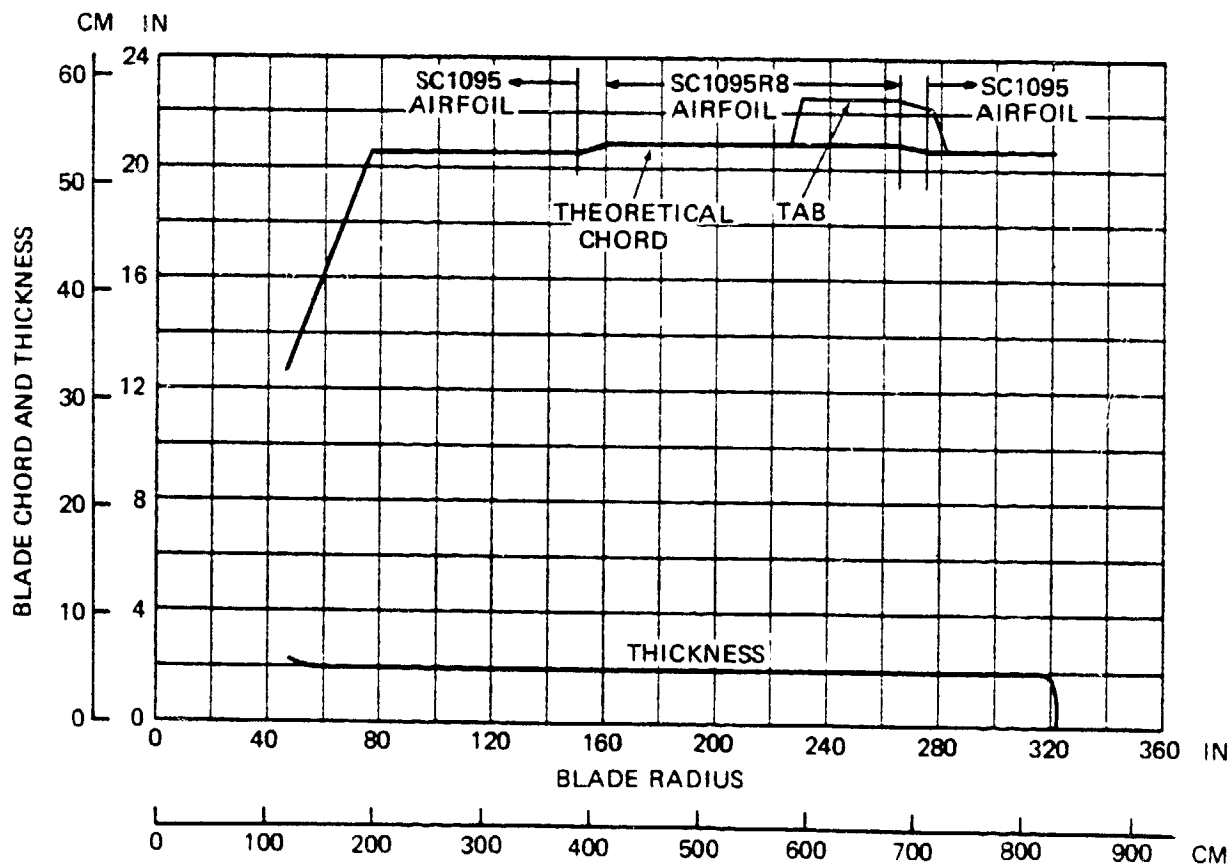


FIGURE A - 3. BLACK HAWK BLADE CHORD AND THICKNESS DISTRIBUTIONS

ORIGINAL PAGE IS
OF POOR QUALITY

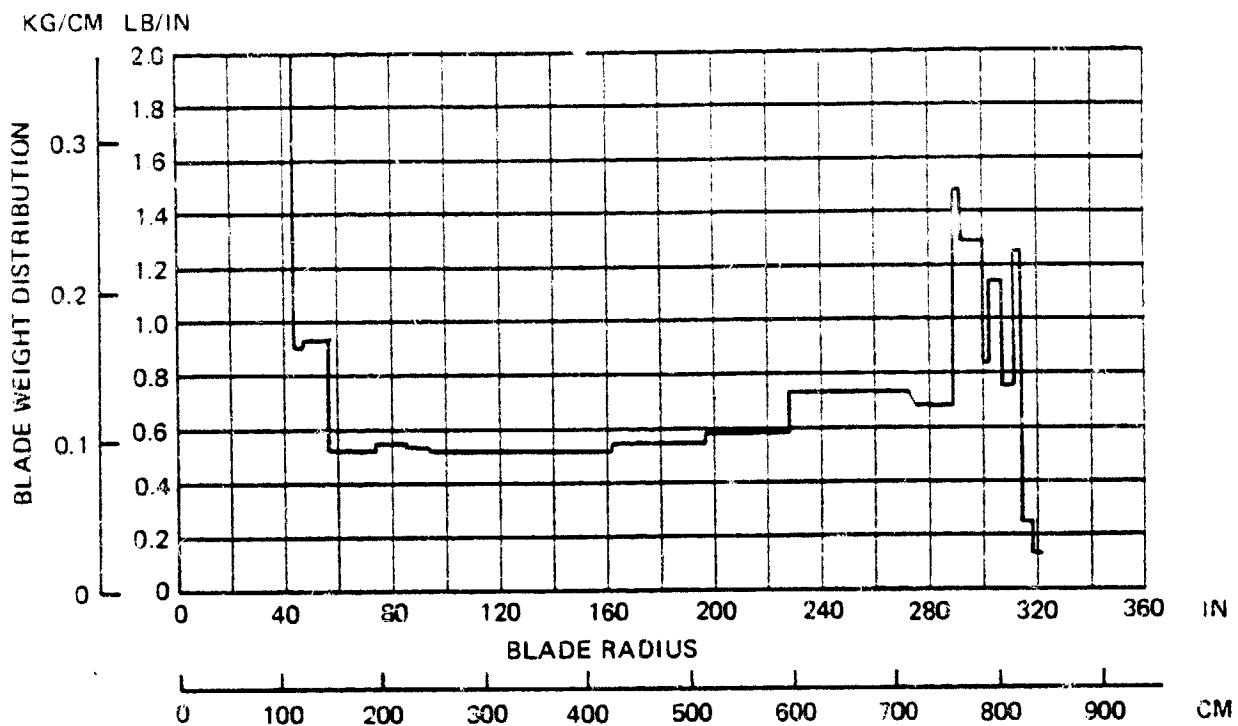


FIGURE A - 4. BLACK HAWK BLADE WEIGHT DISTRIBUTION

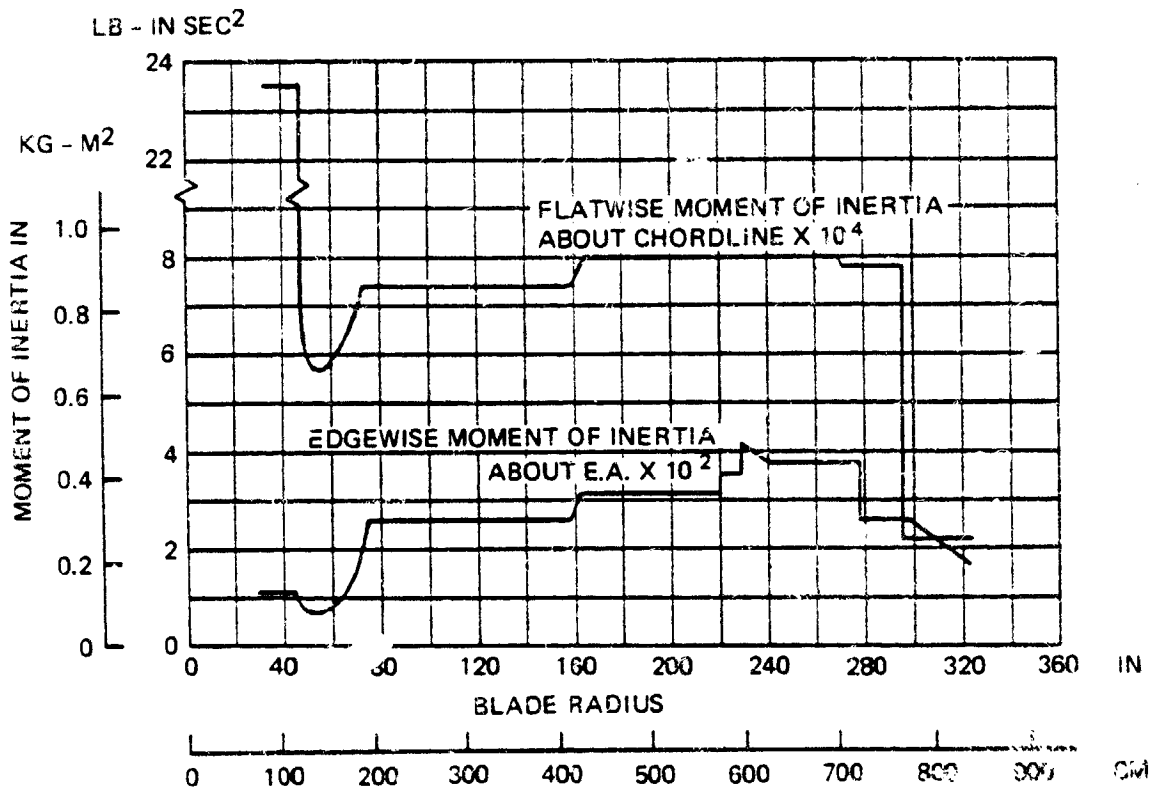


FIGURE A - 5. BLACK HAWK BLADE MOMENT OF INERTIA

ORIGINAL PAGE IS
OF POOR QUALITY

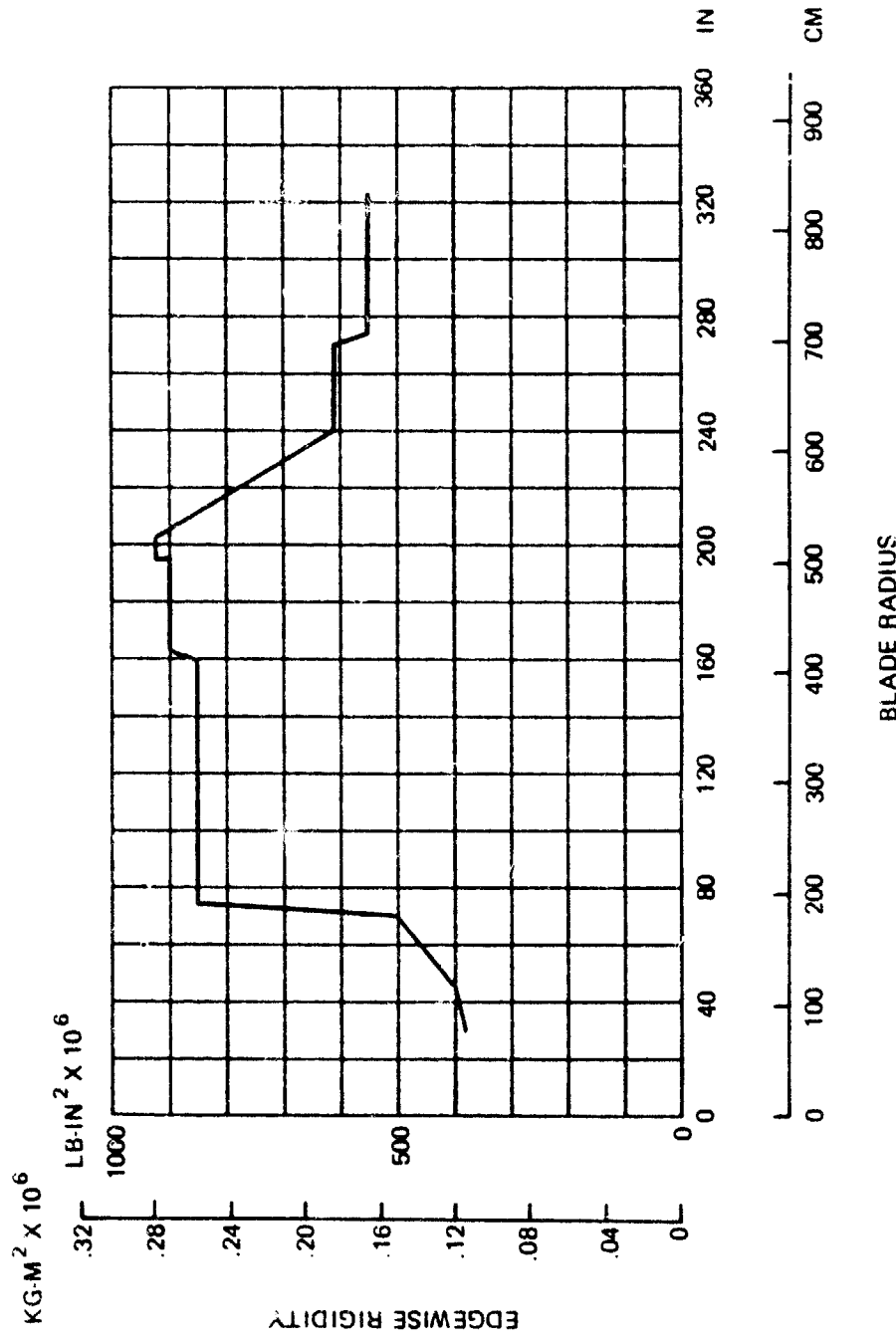


FIGURE A - 6. BLACK HAWK BLADE FLATWISE, EDGEWISE AND TORSION TORSIONAL RIGIDITY

H-3 COMPOSITE BLADE

The Sikorsky twin beam H-3 composite blade was originally designed and fabricated under Navy Contract N00019-73-C-0319 as a high technology replacement rotor blade for the H-3 aircraft. The contract involved design, development, manufacture, fatigue test, and flight test of the full scale blades.

The twin beam concept uses graphite and fiberglass epoxy structure, coupled with a unique assembly procedure that results in full compaction of the composite structure during curing and true fidelity of aerodynamic contour. The structure consists of a C-spar member with a structured honeycomb web to form an efficient lay-up that generates the required torsional stiffness in the thin, high performance airfoil section. A continuous fiberglass skin forms the outer contour of the airfoil. Nomex honeycomb stabilizes the skin behind the C-spar and provides a shear path between the upper and lower skins.

A unidirectional graphite strip in the trailing edge provides the required chordwise stiffness. In-board, the C-spar and skin transition into a constant thickness closed member. A bolt attachment provides the primary structural coupling to a titanium cuff. The blade contains both abrasion and lighting protection systems.

The fabrication technique lends itself to low-cost ease of manufacture and minimizes complicated and expensive contour machining of the honeycomb core. The composite material is layed up and cured separately for the upper and lower airfoil halves. The open halves permit complete inspection of the cured composite structure. Production plans call for automated broad goods lay-up of pre-cut laminates, which are placed in the easily accessible open mold. Honeycomb is bonded to the internal structure and machined to the chord line, so chordwise machining is strictly planar. Finally the halves are bonded together at the chord line. A splice bonded to the leading edge provides redundancy in the torsional shear capacity at the bonded joint.

The high fatigue strain allowables of the graphite and fiberglass materials have permitted the use of high built-in twist to improve the hover performance, yet they allow the structure to operate under the resulting increased forward flight vibratory strains. This in conjunction with a high-performance SC1095 airfoil and a swept tip (which is easily designed into this type of composite structure), has provided a significant increase in the figure of merit over the original H-3 aluminum blades.

Figures A-7 thru A-13 summarize aerodynamic and structural blade properties.

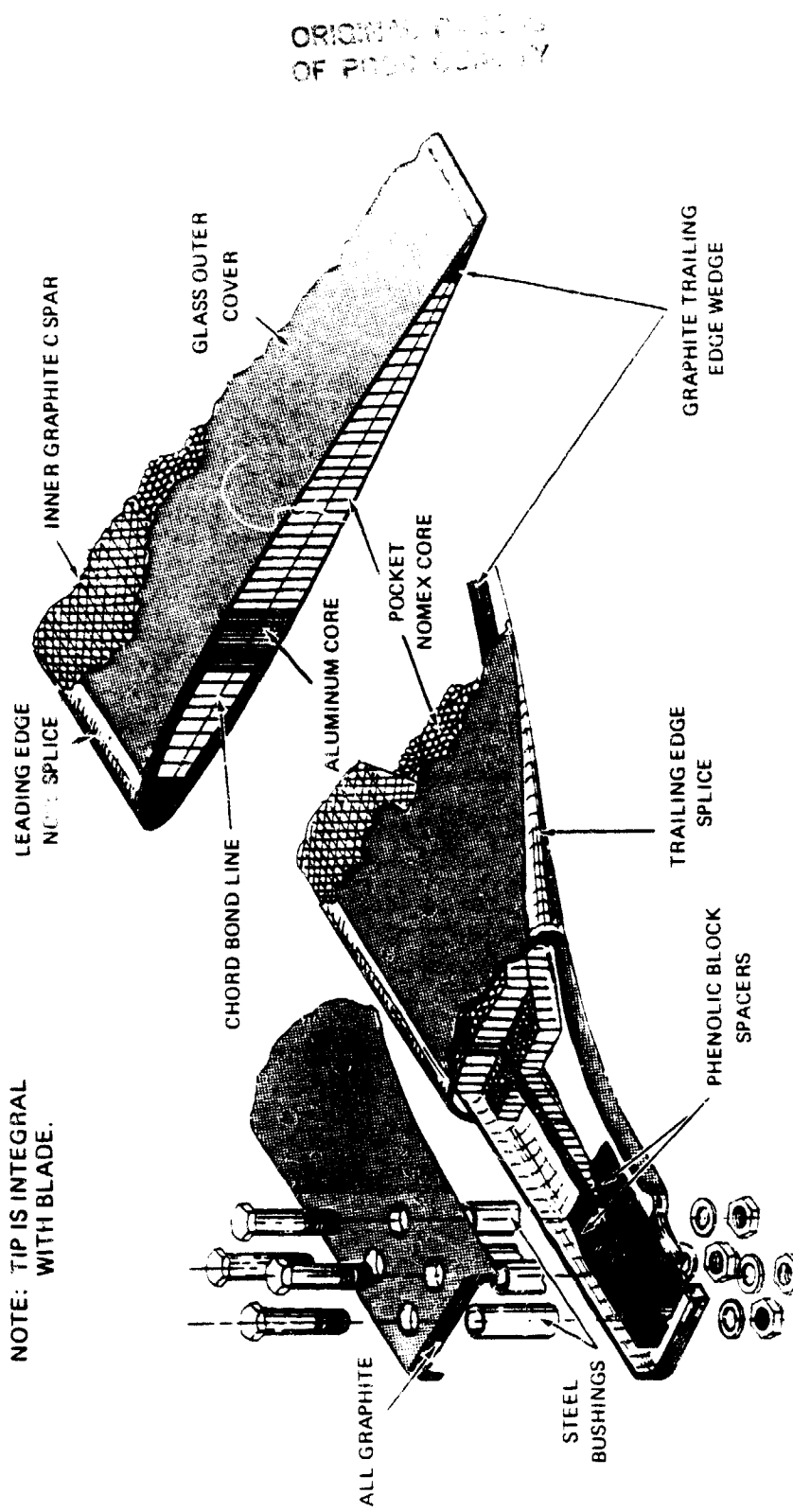


FIGURE A - 7. COMPOSITE BLADE DESCRIPTION

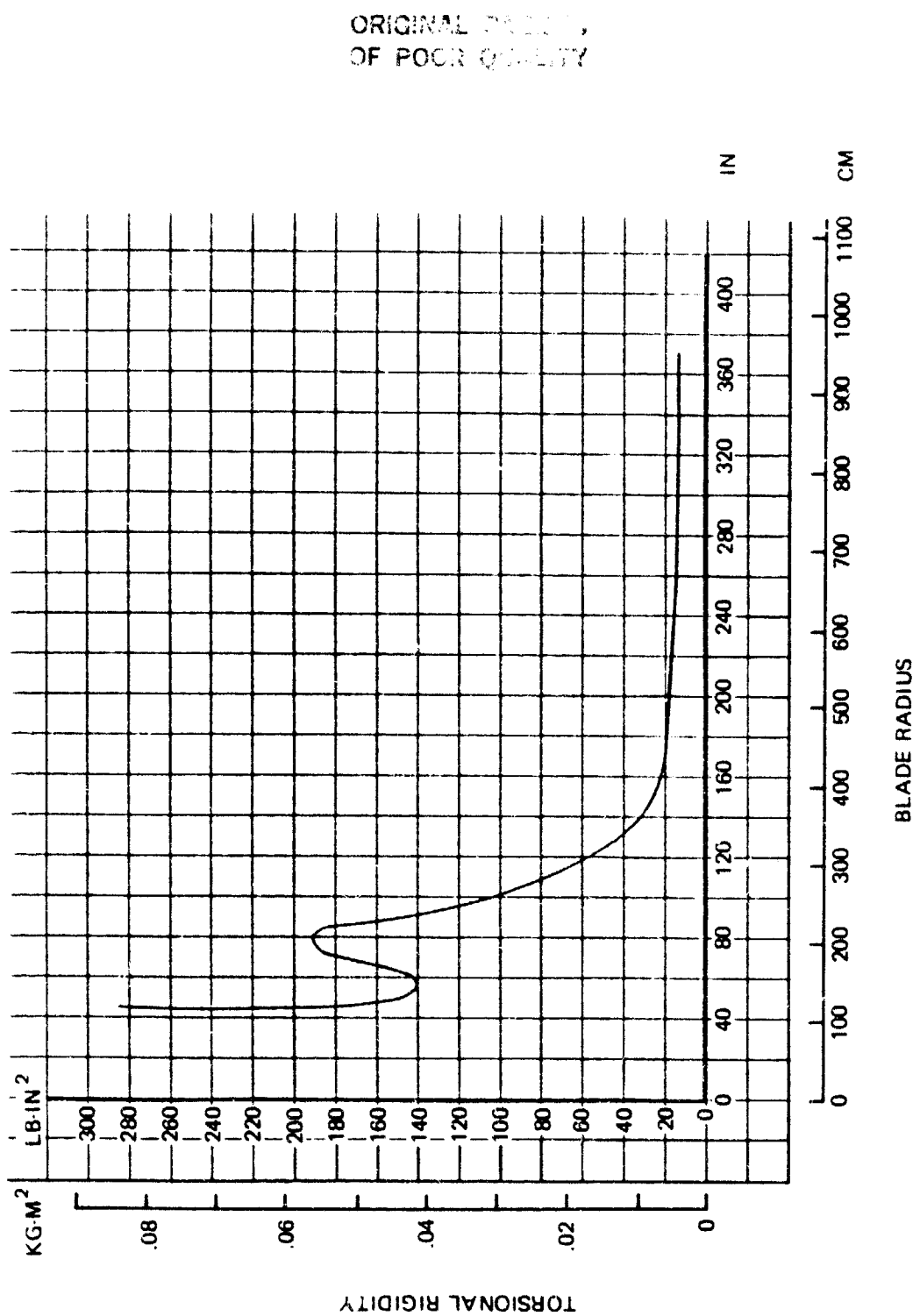


FIGURE A - 8. H-3 COMPOSITE BLADE TORSIONAL RIGIDITY

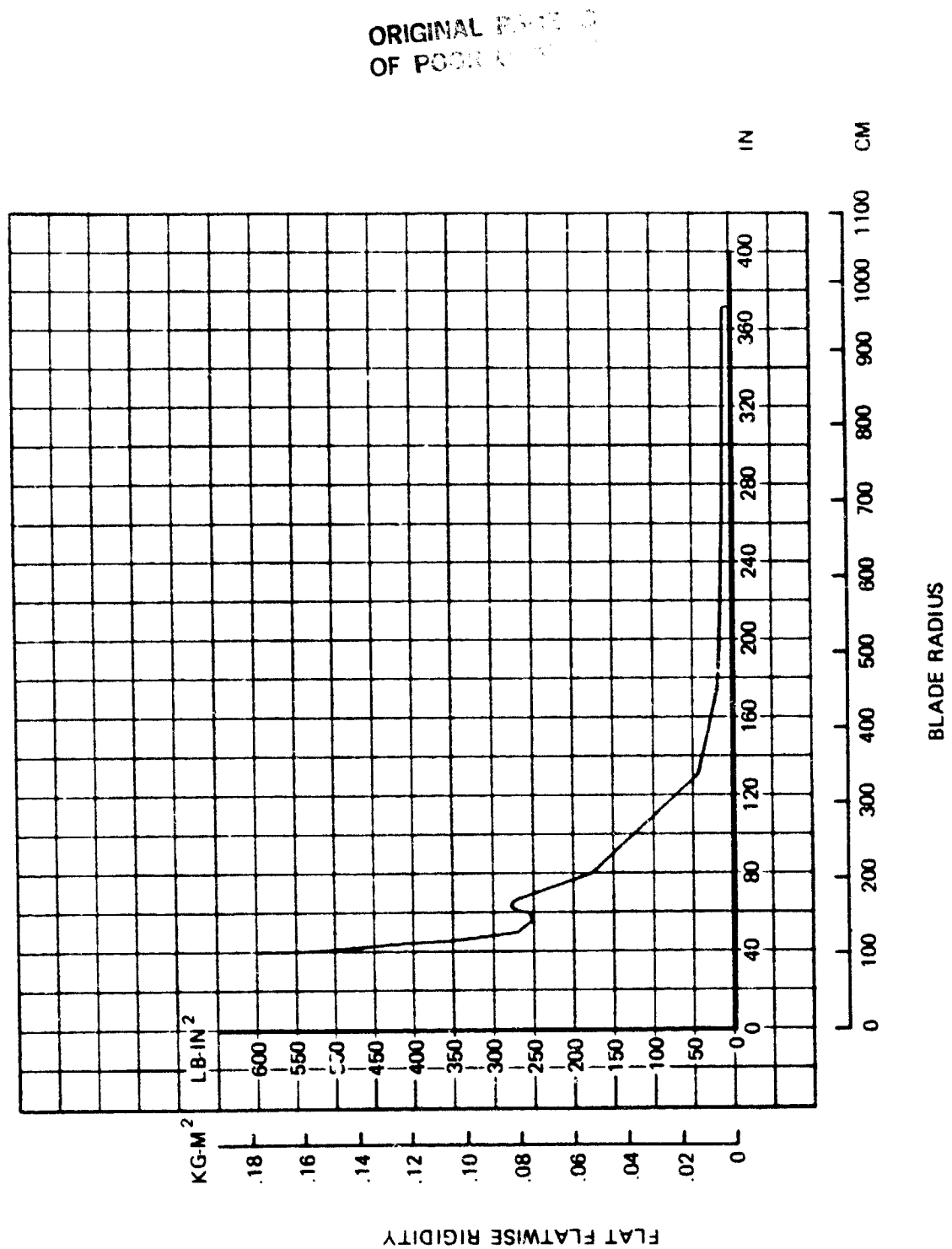


FIGURE A - 9. H-3 COMPOSITE BLADE FLATWISE RIGIDITY

CRITICAL RIGIDITY
OF POOR QUALITY

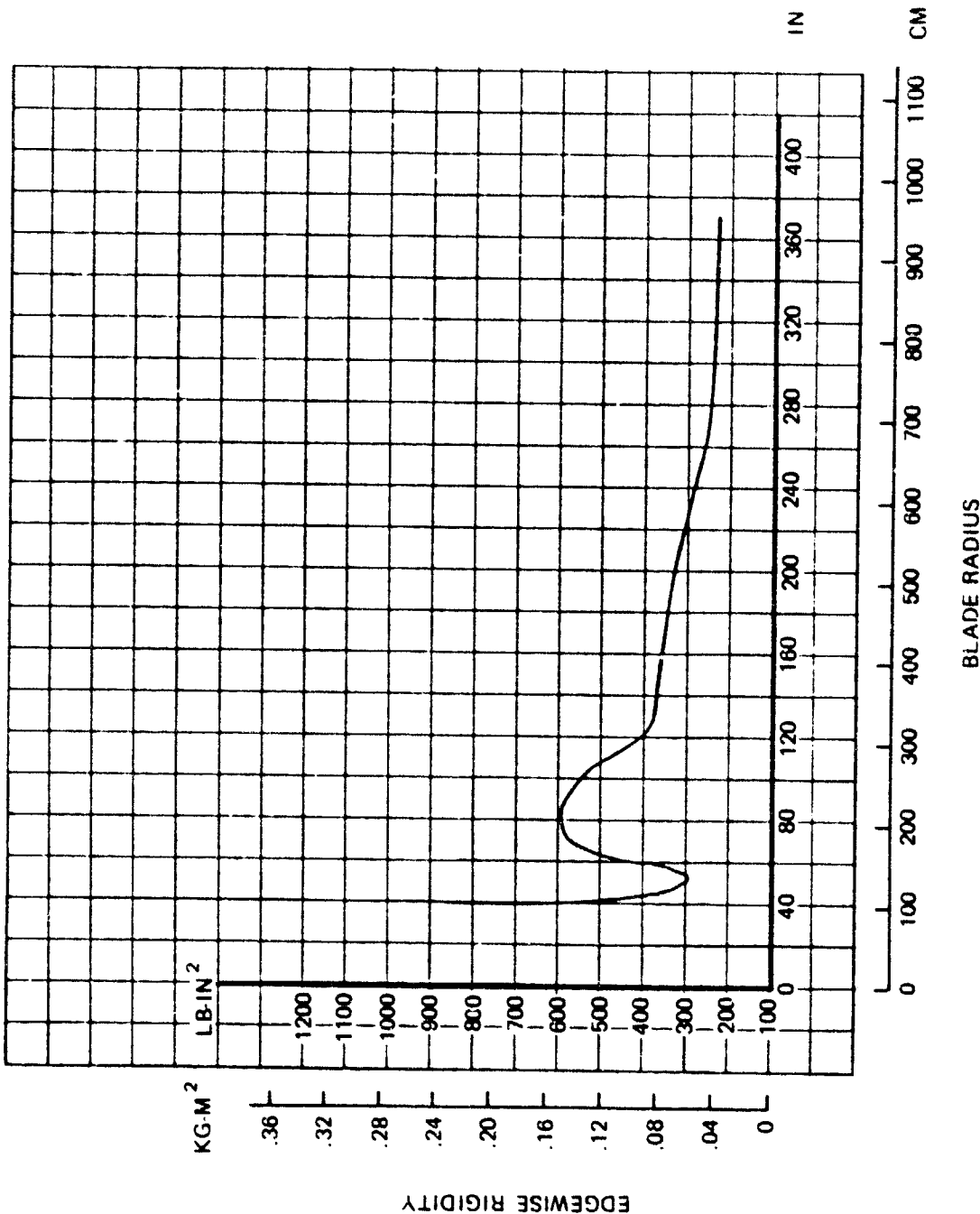


FIGURE A - 10. H-3 COMPOSITE BLADE EDGEWISE RIGIDITY

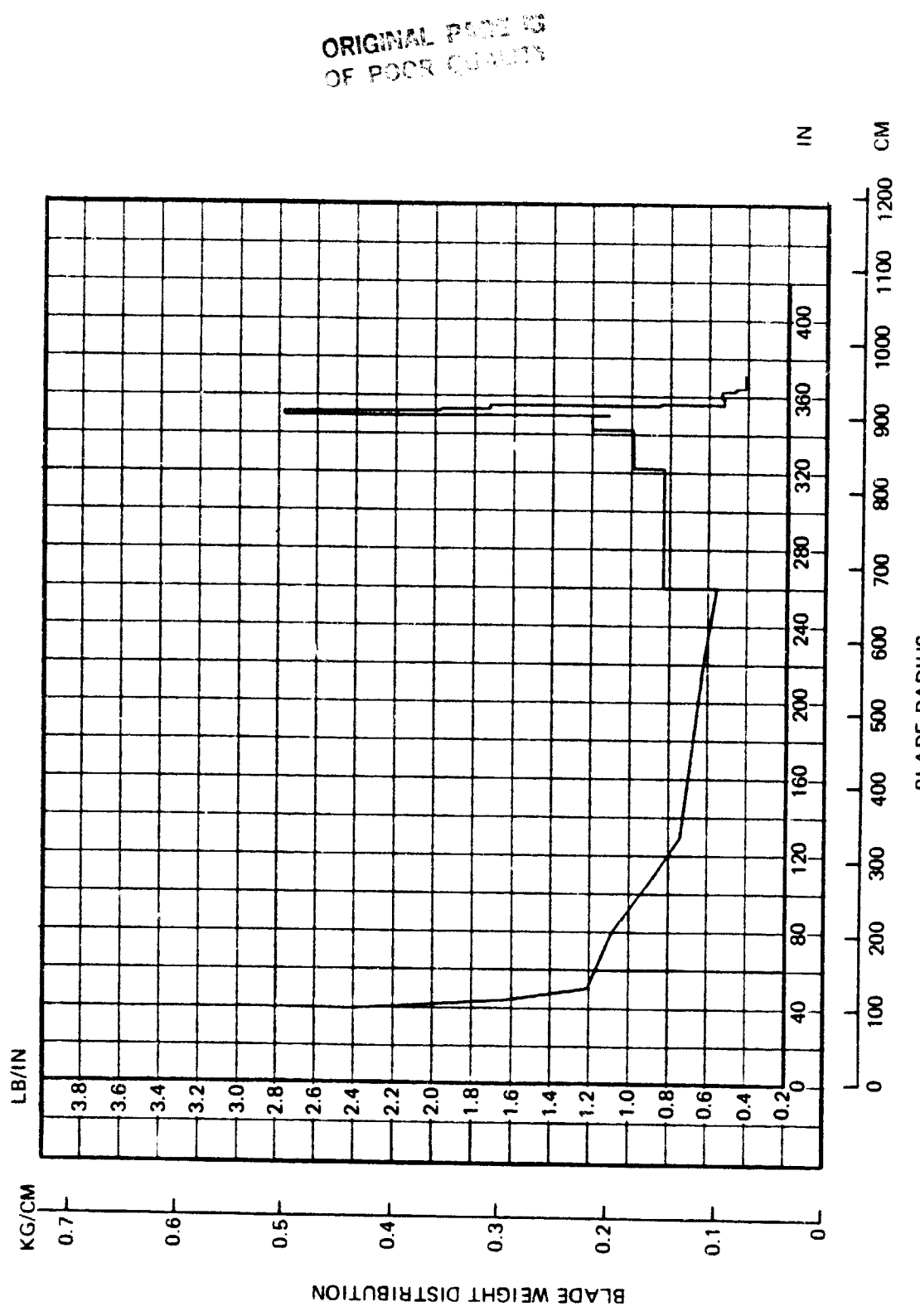


FIGURE A - 11. H-3 COMPOSITE BLADE WEIGHT DISTRIBUTION

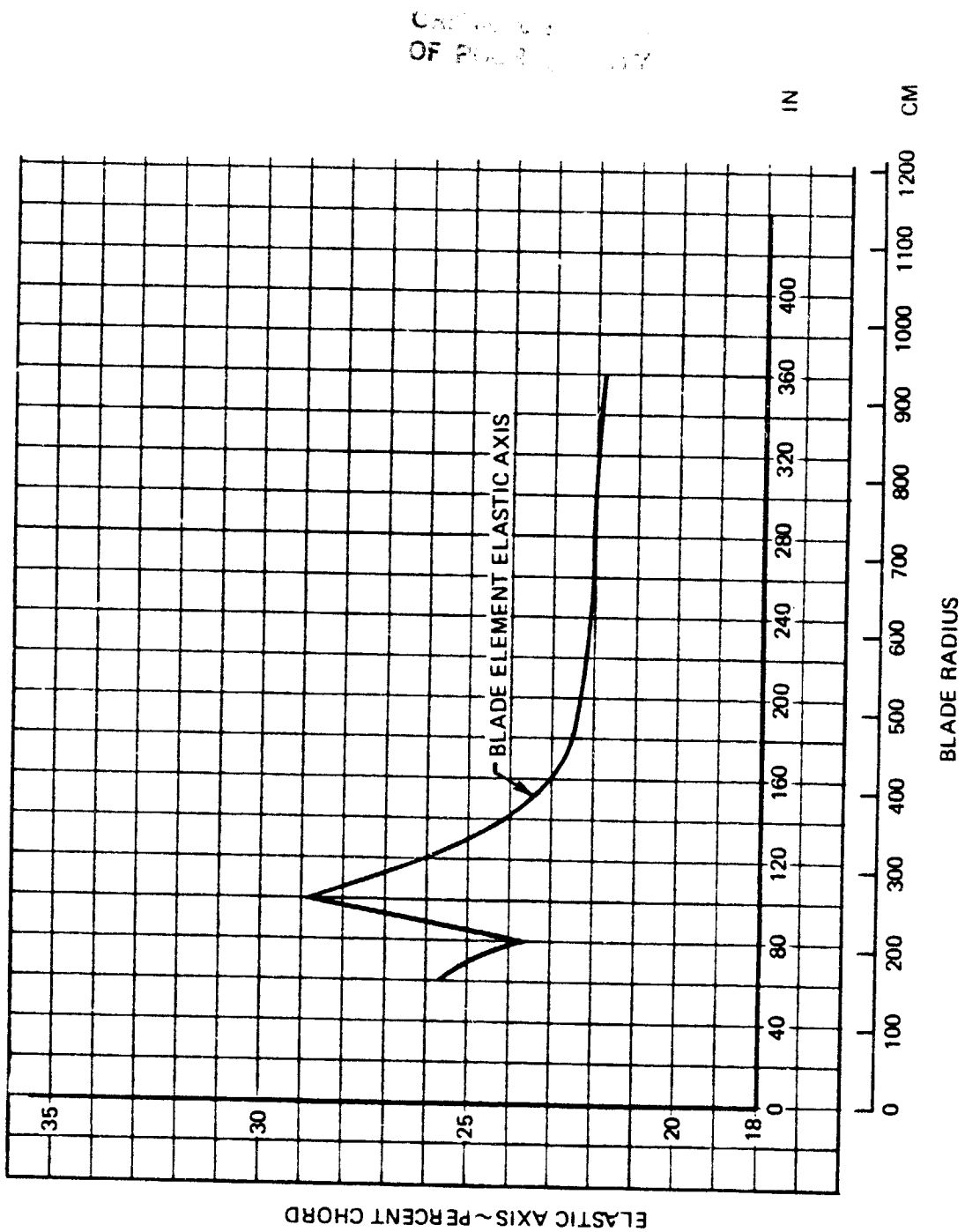


FIGURE A - 12. H-3 COMPOSITE BLADE ELASTIC AXIS POSITION

ORIGINAL PAGE IS
OF POOR QUALITY

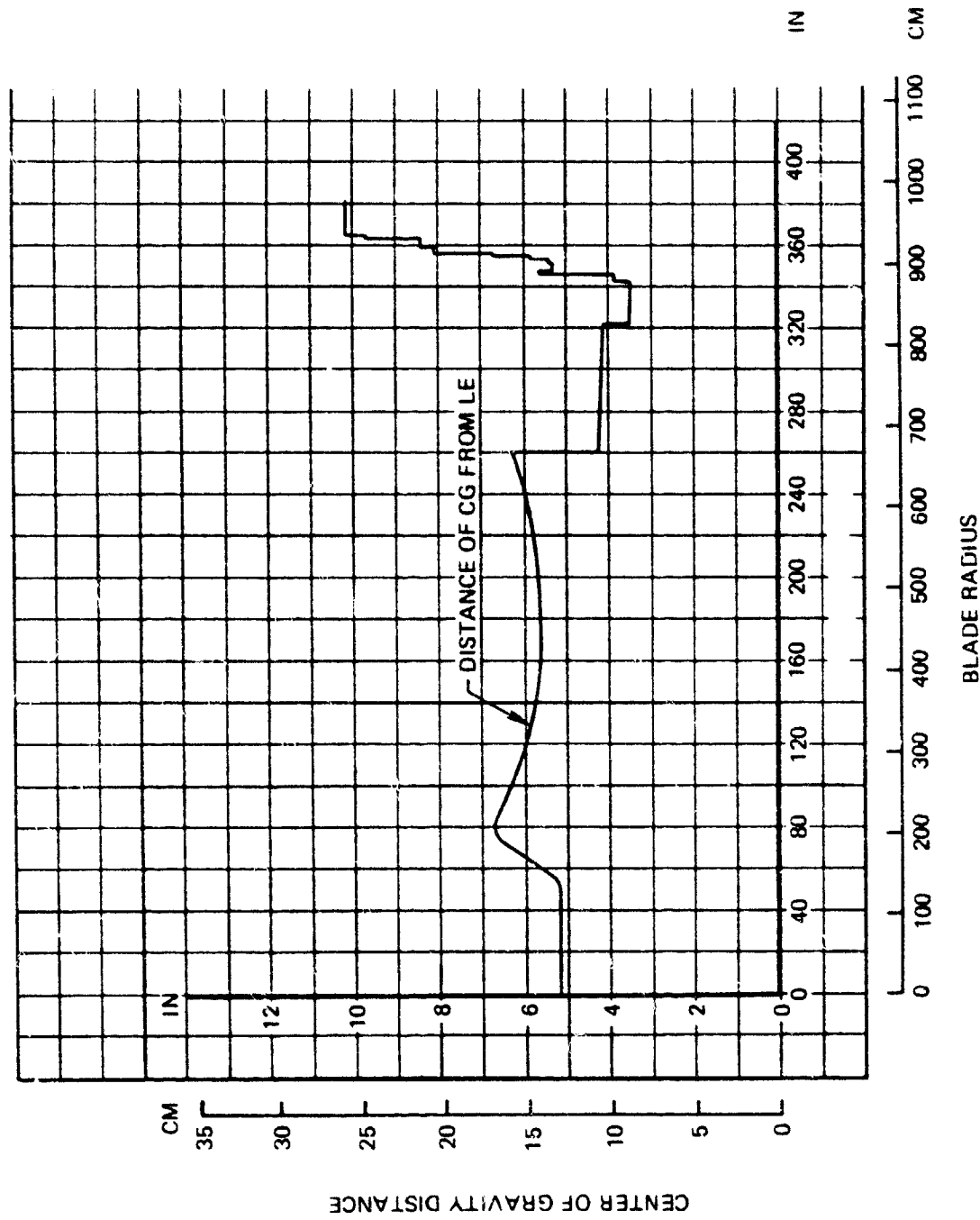


FIGURE A - 13. H-3 COMPOSITE BLADE CENTER OF GRAVITY POSITION

END

DATE

FILMED

FEB 8 1983